BNIP3L/Nix-induced mitochondrial fission, mitophagy, and impaired myocyte glucose uptake are abrogated by PRKA/PKA phosphorylation

by

Simone Cristina da Silva Rosa

A thesis submitted to the Faculty of Graduate Studies, University of Manitoba, in partial fulfillment of the requirements for the degree of

DOCTOR OF PHILOSOPHY

Department of Human Anatomy & Cell Science
University of Manitoba
Winnipeg

Abstract

Lipotoxicity is a form of cellular stress caused by the accumulation of lipids resulting in mitochondrial dysfunction and muscle insulin resistance. Interestingly, mitophagy genes, such as BNIP3L/Nix, has also been linked to lipid metabolism. BNIP3L is an outer mitochondrial pro-apoptotic protein that plays an important role in serving as a mitochondrial autophagy receptor and an indispensable regulator of erythropoiesis. Recent studies from our group demonstrated that BNIP3L is elevated in response to lipid-induced stress leading to mitochondrial dysfunction and impaired insulin signalling. However, the precise mechanisms of BNIP3L activation of such responses are not entirely known.

Given BNIP3L's role in mitochondrial autophagy, also known as mitophagy, in my thesis, I investigate aberrant mitochondrial turnover as a mechanism leading to impaired myocyte insulin signalling. In a series of gain-of-function and loss-of-function experiments in rodent and human myotubes, I demonstrate that BNIP3L accumulation triggers a series of cellular events, ultimately resulting in dysfunctional mitochondria. I also demonstrate mechanistically how BNIP3L can inhibit insulin signalling via mTOR activation. Finally, I provide evidence that BNIP3L-induced mitophagy and impaired glucose uptake can be reversed by pharmacologically targeting BNIP3L with PRKA activating agents, leading to BNIP3L's translocation from the mitochondria and sarcoplasmic reticulum to the cytosol, therefore blunting BNIP3L function.

Collectively, the data presented here emphasize the crucial role of proper mitochondrial quality control in maintaining myocyte glucose homeostasis. Furthermore, disruption of mitochondrial quality control pathways, such as under lipotoxicity stress, may lead to pathological conditions, whereby mitophagy becomes a maladaptive response to nutrient storage stress. Therefore, understanding BNIP3L's role in mitophagy and how it impairs muscle insulin signalling *in vitro* is essential to further investigate and delineate its importance in both *in vivo* and human studies, with the ultimate goal being to avert early-onset insulin resistance.

Acknowledgements

Firstly, I would like to start by thanking my supervisor, Dr. Joseph Gordon, for his constant support, mentorship, and guidance throughout these years. I initially came to his lab as a summer student through the Brazilian exchange program Science Without Borders, and I am extremely grateful for him taking a chance on me and giving me the opportunity to pursue a master's degree after my undergraduate program, which subsequently turned into a Ph.D. Secondly, I would like to express my sincere gratitude to my graduate advisory committee: Dr. Sari Hannila, Dr. Vernon Dolinsky, and Dr. Jonathan McGavock, for their constant feedback over these last 6 years, which has tremendously contributed to my academic growth, and also Dr. Mary-Ellen Harper for her very kind and enthusiast feedback to improve my thesis.

I also would like to acknowledge the various funding support and awards I received over the years, including scholarships, poster awards, travel awards, and excellence in research awards, which aided my research studies and my attendance at various scientific meetings nationally and abroad. Thank you: Research Manitoba, CHRIM, DREAM, DEVOTION, Ralph A. Mann Memorial Award, Faculty of Graduate Studies, Human Anatomy and Cell Science Department, and the University of Manitoba.

This journey has not been made alone, and I would like to acknowledge the individuals from my lab who immensely contributed to my work: Mr. Donald Chapman, Dr. Wajihah Mughal, Dr. Lucas Nguyen, Dr. William Diehl-Jones, Dr. Yan Hai, Mr. Matthew Martens, Mr. Jared Field, Dr. Adel Moghadem, Mr. Philip Kawalec, Ms. Nichole Nayak, and Mr. Andrei Caymo. I would like to especially thank Donald and Yan for their invaluable support with various laboratory techniques, which allowed me to complete my project. I also would like to acknowledge all the collaborators, especially Dr. Vernon Dolinsky, for providing the animal tissues for my studies; and Dr. Saeid Ghavami, for his mentorship, critical feedback on my experimental approaches, and for opportunities of collaboration with his lab, culminating in many co-authored publications. Further, I would like to acknowledge all the graduate community members and friends I made along the way from University of Manitoba, including from the CHRIM, DREAM, DEVOTION, HACS, HSGSA, and UMGSA. Thank you.

I also would like to thank my friends outside academia (including from Church and French school) who made me feel at home while thousands of miles away from family. Next, from the bottom of my heart, I would like to thank all my friends and family in Brazil, who unconditionally supported me all steps of the way despite the distance, especially my parents Cleire and Nelson, and my brothers Pedro and Tiago. Finally, I thank God for the gift of life and for the willingness to pursue a scientific career, a beautiful profession that will contribute and be a blessing to many lives through my work. My trust is in Him and all glory is to Him. As my dear mother always says to me:

"Uns confiam em carros e outros em cavalos, mas nós faremos menção do nome do Senhor nosso Deus." (Salmos 20:7)

Dedication

This thesis is dedicated

to all patients, families, and friends of those affected by diabetes, a metabolic disorder that has impacted many worldwide**.** In particular, I dedicate it in memory of my great-grandmother Adelaide, one of the people responsible for my upbringing, who taught me fundamental moral values and helped shape my character as a human being; someone who was taken away from our lives rather too soon as a consequence of Type 2 Diabetes.

Table of Contents

List of Tables

CHAPTER I: Literature Review

CHAPTER III: Manuscript

List of Figures

CHAPTER I: Literature Review

CHAPTER II: Thesis Rationale and Specific Aims

CHAPTER III: Manuscript

CHAPTER IV: Dissertation Discussion

List of Abbreviations

AC:	adenylyl cyclase
α-MHC:	alpha myosin heavy chain
AKAP:	A-kinase anchoring proteins
Akt:	protein kinase B
AMPK:	5'adenosine monophosphate-activated protein kinase
APS:	adaptor protein
ATP:	adenosine triphosphate
ATF6:	activating transcription factor 6
ATM:	adipose tissue macrophages
β2-AR:	β2-adrenergic receptor
BCAA:	circulating branched-chain amino acids
Bcl2:	B-cell leukemia/lymphoma 2
BH:	Bcl-2 homology
bHLH:	muscle-specific basic helix-loop-helix
BNIP3L/Nix:	BCL2/adenovirus E1B interacting protein 3-like
cAMP:	cyclic adenosine monophosphate
CFCM:	cross-fiber connection mitochondria
COPD:	chronic obstructive pulmonary disease
COOH:	carboxyl terminal
DAG :	diacylglycerol
DPP-4:	dipeptidyl peptidase-4
DNM1L/DRP1:	dynamin 1-like
DNL:	*de novo* lipogenesis
ER:	endoplasmic reticulum
FDA:	Food and Drug Administration
FPM:	fiber parallel mitochondria
FOXO1:	transcription factor forkhead box 01
FUNDC1:	FUN14 domain containing 1
GIP:	glucose-dependent insulinotropic polypeptide

GLP-1:	glucagon-like peptide-1 agonist
GLUT4:	glucose transporter 4
G6P:	glucose-6-phosphate
GRB10:	growth factor receptor-bound protein 10
GRB14:	growth factor receptor-bound protein 14
GSV:	GLUT4 containing storage vesicles
GSK3:	glycogen synthase kinase 3
GPCR:	G protein-coupled receptor
GTPase:	guanosine triphosphatase
HGP:	hepatic glucose production
HSL:	hormone-sensitive lipase
IHTG:	intrahepatic triglycerides
IL-1β:	interleukin-1 beta
IL-6:	interleukin-6
KO:	knockout
LIR:	LC3 interacting region
IMCL:	intramyocellular lipid
INSR:	insulin receptor
IRE-1:	inositol requiring enzyme 1
IRS1:	insulin receptor substrate 1
IRS2:	insulin receptor substrate 2
IMF:	intermyofibrillar
JNK1:	c-Jun N-terminal kinase 1
MAM:	mitochondria-associated ER membrane
MAPK:	mitogen activated protein kinase
MAP1LC3A/LC3:	microtubule-associated protein 1 light chain 3 alpha
MAP1LC3B:	microtubule-associated proteins 1A/1B light chain 3B
MCAT:	mitochondrial-target catalase
MEF:	myocyte enhancer factor
Mfn1:	mitofusin 1
Mfn2:	mitofusin 2

MHC: myosin heavy chain

MRF: muscle regulatory factor

mTORC1: mammalian target of rapamycin

MTOR-RPS6KB/p70S6K: mechanistic target of rapamycin kinase-ribosomal protein S6 kinase

NAFLD: non-alcoholic fatty liver disease

NEFA: non-esterified fatty acid

NH2: amino terminal

NOX4: NAD(P)H oxidase 4

OMM: outer mitochondrial membrane

OPA1: OPA1 mitochondrial dynamin like GTPase

PDE: phosphodiesterase

PDE3B: phosphodiesterase 3B

PDE4i: phosphodiesterase 4 inhibitor

PDK1: phosphoinositide-dependent kinase

PERK: PKR-like ER kinase

PH: pleckstrin homology domain

PLIN: perilipin

PLD6: phospholipase D family member 6

PI3K: phosphoinositide 3 kinase

PIP2: phosphatidylinositol-4, 5 biphosphate

PIP3: phosphatidylinositol-3, 4, 5 triphosphate

PGC1α : proliferator-activated receptor γ co-activator 1α

PKA: protein kinase A

PKA-C: protein kinase A catalytic subunit

PKA-R: protein kinase A regulatory subunit

PKC: protein kinase C

PRKA/PKA: A kinase anchor protein

PRKCD/PKC: protein kinase C, delta

PRKCQ/PKC: protein kinase C, theta

PVM: paravascular mitochondria

PTP: phosphotyrosine phosphatase

RAC1:	Ras-related C3 botulinum toxin substrate 1
RHEB:	Ras homolog enriched in brain
ROS:	reactive oxygen species
SLiM:	short linear motif
Ser:	serine
SS:	subsarcolemmal
SH2:	Src homology 2 domains
SR:	sarcoplasmic reticulum
Src:	Src homology collagen
SREBP-1c:	sterol regulatory element-binding protein-1c
S6K:	S6 kinase
SQSTM1/p62:	sequestosome 1
TBC1D1:	TBC1 domain family member 1
TBC1D4:	TBC1 domain family member 4
TCA:	tricarboxylic acid
T2D:	type 2 diabetes
TM:	transmembrane domain
TNF-α:	tumor necrosis factor alpha
Tyr:	tyrosine
UPR:	unfolded protein response
WAT:	white adipose tissue
WT:	wild type
YWHAB/14-3-3:	tyrosine 3-monooxygenase/tryptophan 5-monooxygenase activation protein beta

CHAPTER I: Literature Review

1.1 Muscle Biology

Skeletal muscle is abundant throughout the body, performing essential anatomical and physiological functions, such as locomotion, helping to maintain posture, stabilizing bones and joints, controlling internal movement, and generating heat. There are three major muscle tissues in the body. First, cardiac muscle, which primarily functions to pump blood in the heart; failure of its basal contractility role is severely detrimental to general health and survival. Second, the smooth muscle, present in the vasculature, i.e. veins and arteries as well as other visceral organs, serves as a luminal wall covering for such organs as the gut, bladder and esophagus. Finally, the skeletal muscle, attached to the skeleton, holds the bones, organs and vascular system together. Functional skeletal muscle is tasked with producing both aerobic and anaerobic respiration in order to generate adenosine triphosphate (ATP), the primary energy source for muscle essential to force generation. To that end, skeletal muscle highly relies on the mitochondria, described as the powerhouse of the cell. Some of its fuel sources are fat, glucose, and protein oxidation. It is crucial to maintain basal physiological mitochondrial function properties for skeletal muscle homeostasis. Importantly, disruption in the mitochondrial system is associated with pathological conditions, such as muscular atrophy, diabetes, cancer, Alzheimer's, and Parkinson's disease among others. Therefore, there is an absolute necessity to comprehensively understand the underlying mechanisms behind dysfunctional mitochondria and their role in the development of certain metabolic disorders. Knowledge obtained in these studies may decrease the burden of disease and lead to better treatment options.

1.1.1 Skeletal muscle and mitochondrial aspects

As previously mentioned, there are three major types of human muscles, categorized as striated (cardiac and skeletal) and smooth. The striated skeletal muscle is the most abundant type, representing nearly 40% of total body weight (1). The smooth muscle mainly controls non-voluntary muscular contraction (2); similarly, the cardiac muscle is also not voluntarily controlled (3). All three aforementioned muscle types possess structured parallel individual muscle fibers that allow for contraction. In particular, the skeletal striated muscle structure is organized in several bundles of tubular muscle cells, known as fibers or myofibers, which contain several myofibrils. Every myofiber represents a muscle cell containing its own cellular unit: the sarcomere, where contraction occurs at the cellular level (4). The cardiac muscle is somewhat structurally similar to skeletal muscle, also striated, containing sarcomeres. In contrast, the smooth muscle lacks the striations that skeletal muscle has, forming a fusiform shape (5).

The skeletal muscle is well known for its remarkable capacity to adapt to various mechanical or physical challenges by altering its phenotypic size, fiber type, capillarization levels and even aerobic capacity (6). Accordingly, a highly specialized mitochondrial system in the skeletal muscle has evolved for this reason. The skeletal muscle mitochondria are generally classified based on their subcellular location, as subsarcolemmal (SS) and intermyofibrillar (IMF) (7). A distinguishing characteristic of SS mitochondria is their large lamellar shape, located under the sarcomere, while the IMF mitochondria are considerably smaller and located between contractile myofilaments (7). Moreover, using a three-dimensional approach, recent studies have further classified skeletal muscle mitochondria as paravascular mitochondria (PVM), I-band mitochondria (IBM), fiber parallel mitochondria (FPM), and cross-fiber connection mitochondria (CFCM) (8). These four newly identified mitochondrial populations are highly interconnected forming a network capable of fast energy distribution throughout the myofibers (8).

Collectively, skeletal muscle mitochondria are dynamic organelles constantly adapting in response to physiological and pathophysiological stresses to meet the energy and contraction demands of the muscle. Further details about the role of mitochondria in skeletal muscle and their role in disease will be discussed in the following sections of Chapter I of this literature review.

1.1.2 Fiber types

Muscle fibers are formed during myogenesis, a tightly controlled process that allows skeletal muscle differentiation (Figure 1.1). Briefly, the differentiation process starts when progenitor cells, containing transcription factors Pax3 and Pax7, begin to express myogenic regulatory factors Myf5 or MyoD as committed myoblasts (9). Next, these myoblasts slowly start to express myogenin (MyoG), giving rise to single-nucleated myotubes with myosin heavy chain (MHC) (10), leading to terminal differentiation of myoblasts into multinucleated myotubes. (11).

Figure 1.1. Brief overview of *in vitro* skeletal muscle differentiation.

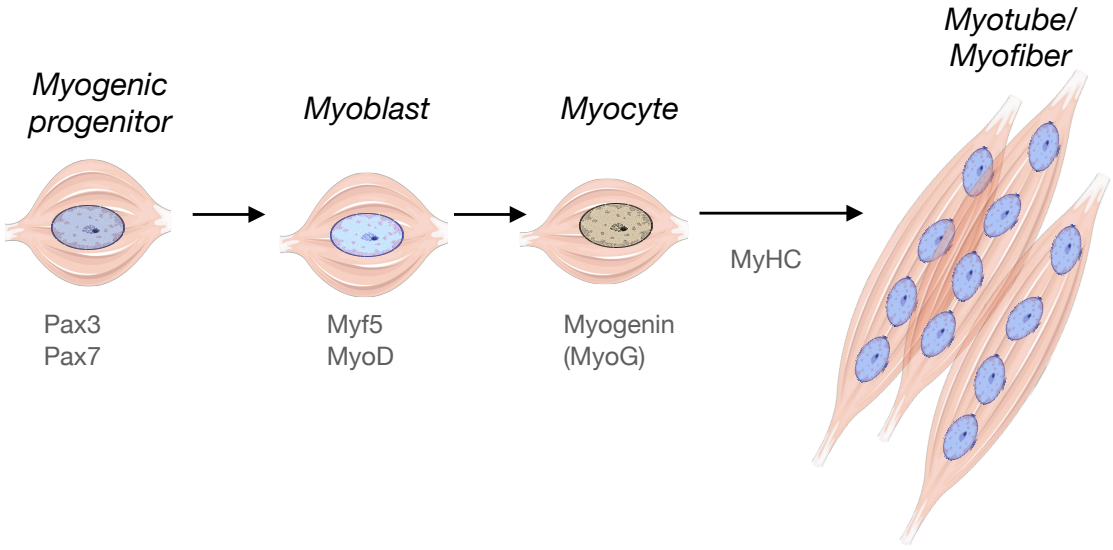

Skeletal muscle fibers are further categorized into four major types that are present in rodent muscles: one type of slow-twitch fiber (type I) and three types of fast-twitch fiber (type IIa, IIx/d, and IIb) (12). Type I and type IIa fibers are more oxidative, presenting higher mitochondrial content and are more resistant to fatigue, while type IIx and IIb are more glycolytic, presenting lower mitochondrial content, and are less resistant to fatigue (13). Furthermore, postural muscles (often called red muscles) are also known to be richer in slow fibers, highly vascularized and dependent on oxidative metabolism. On the other hand, muscles used for movement and repeated contraction (white muscles) are richer in fast fibers, largely dependent on glycolytic metabolism (14). These fiber types are well distributed throughout mammal's body muscles, including in the

limb, trunk, and head. For instance, in rodents, the leg muscle is the most studied in the body with abundant slow type I fibers, especially in the posterior compartment where the soleus muscle is located. In most species, type II fibers are more abundant in forelimbs than in hindlimbs, as they are the fastest muscles; similarly, in humans, they are more concentrated in upper limb muscles (15, 16).

As mentioned above, mitochondrial energetics highly contributes to regulation of muscle fiber-specific function. Furthermore, other mitochondrial aspects, such as mitochondrial dynamics (fusion and fission) are also important features of proper muscle function. For instance, genetic ablation of mitofusin Mfn1 and Mfn2, proteins that facilitate fusion of the outer mitochondrial membrane, have been noted to result in severe myopathies, such as muscle atrophy (17). Recently, it has been shown that mitochondrial fusion rates correlate with oxidative capacity at the fiber level, according to the fiber type (18). Mishra et al. demonstrated that rates of mitochondrial fusion are higher in type I and IIA fibers, which also present elongated mitochondria, while type IIX and IIB glycolytic fibers have lower mitochondrial fusion rates, becoming more punctate (18). Furthermore, elongated mitochondria have been previously associated with increased metabolic states facilitating the maintenance of ATP levels in oxidative muscle fibers that rely on long-term energy production (19). Consequently, Mishra et al. suggests that mitochondrial morphology may be capable of adapting to the specific functional needs of the individual fiber.

Other studies have suggested that each muscle fiber type may play a different role on insulin-stimulated glucose metabolism (12, 20). On a physiological level, slow-twitch (type I) fibers have higher amounts of glucose transporter (GLUT)4 and hexokinase II, among others, but lower protein kinase B (Akt)2, TBC1 domain family member (TBC1D)4 and (TBC1D)1 amounts compared to type II fibers (21). These studies concluded that type I fibers have better glucose-handling capacity, but similar insulin phospho-regulation sensitivity (21). Furthermore, in other reports, obese and type 2 diabetes (T2D) patients presented a lower proportion of type I fibers, which is rich in mitochondria, compared to type II fibers, concurrent with reduced oxidative metabolism (22).

In obesity and insulin resistance, the skeletal muscle capillary network is compromised, impairing insulin-mediated capillary recruitment. A study by Umek and colleagues (2019) investigated the possibility that the anatomical changes in the capillary network could be linked to

fiber-type specific differences. Capillary density was found to be increased in small muscle fibers (type I) compared to large fibers (type II) and is attributed to increased capillarization selectiveness towards more insulin-sensitive oxidative muscle fibers (23). Their findings suggest that the selective increase in capillarization surrounding more insulin-sensitive oxidative muscle fibers act to alleviate obesity-related insulin resistance (23). Obese insulin-resistant humans and mice present muscle fiber type transformation, which provides a possible mechanism related to impaired glucose metabolism and T2D. Although intriguing in the context of diabetic microangiopathy, further studies are required to more fully appreciate these observations (21, 23).

Collectively, skeletal muscle function is highly dependent on mitochondrial activity, which is influenced according to fiber location, summarized in Table 1.1.

Table 1.1. Summary of skeletal muscle fiber type phenotype.

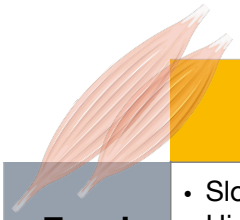

	Oxidative or slow- twitch	Glycolytic or fast-twitch	Mitochondrial aspects
Type I Type IIA	• Slow contraction • High resistance to fatigue • Red/postural muscles • Higher GLUT4 amounts	———	• High content • Elongated • Increased fusion rates
Type IIx Type IIB	———	• Rapid contraction • Low resistance to fatigue • White/moviment muscles • Lower GLUT4 amounts	• Low content • Punctate • Decreased fusion rates

1.1.3 Muscle metabolism

The skeletal muscle is the predominant site of insulin-mediated glucose uptake in a postprandial state (25). Approximately 80% of glucose uptake occurs in the skeletal muscle under euglycemic hyperinsulinemic conditions (24). As previously mentioned, skeletal muscle plays an essential role in metabolic homeostasis and its positive effects are amplified with exercise (25). During exercise, skeletal muscle ATP consumption increases, accumulating intracellular AMP concentrations, resulting of adenylate kinase reaction (26). Therefore, the increased cellular AMP/ATP and ADP/ATP ratios lead to activation of AMP-activated protein kinase (AMPK) (26). AMPK enhances glucose utilization through the increased expression of glucose transporters (GLUT)4, which are translocated to the plasma membrane in an insulin-independent manner (27). Notably, disruption in normal muscle physiology and lack of exercise has been linked to metabolic diseases such as T2D.

Moreover, skeletal muscle greatly relies on the uptake and mitochondrial β-oxidation of fatty acids to meet its energy demand and sustain contractile function, especially during physical activity (28). In human studies, it has been demonstrated that failure to increase reliance upon fat oxidation is associated with the pathogenesis of insulin resistance in the muscle. For instance, Ukropcova *et al*. (29) examined the fat oxidation capacity from a muscle biopsy of human vastus lateralis and found that insulin sensitivity is increased in lean and aerobic fitness individuals. Furthermore, exercise training also enhances muscle sensitivity to insulin-stimulated glucose uptake. Therefore, an imbalance between fatty acid uptake and oxidation promotes lipid accumulation, contributing to insulin resistance in T2D, ultimately impairing various steps in the insulin signalling cascade (30).

Various factors underly the molecular mechanisms of the progression of this pathological condition, including skeletal muscle mitochondrial dysfunction and insulin resistance. Further details on the possible mechanisms by which mitochondrial dysfunction arises will be discussed in more depth in the following sections.

1.2 Type 2 Diabetes

1.2.1 Insulin overview: cell biology and physiology

For nearly 100 years, the regulation of insulin secretion and its actions on peripheral tissues have been at the forefront of cell biology and physiological research. Frederick Banting and Charles Best are credited with the discovery of insulin in 1921 while working at the University of Toronto in Canada. Soon after its discovery, insulin was purified by James Collip, making its commercialization possible (31)**.** In 1923, Banting received the Nobel Prize for the insulin discovery, and it was shared with his supervisor John Macleod. Although many excellent reviews of insulin function and T2D have been recently published (32, 33), Tokarz et al. (2018) have uniquely summarized the 'journey' of insulin in five main steps, starting with its biosynthesis in the pancreas to its final degradation by the kidney (33).

Arguably the most studied hormone in history, the study of insulin is embedded within most major cell biology discoveries (33). Some major areas of insulin investigation range from pro-hormone production and trafficking, membrane biology, exocytosis, receptor tyrosine kinases, Src homology 2 (SH2) domains, GLUT4 trafficking, and the regulation of carbohydrate, lipid, and protein metabolism (32), to name a few. More recently, the study of mitochondrial function, autophagy, and mitophagy in the peripheral tissues has provided insight into how muscle, liver, and adipose tissues regulate their sensitivity to insulin function, and to how these key target tissues of insulin communicate with each other to control whole body metabolism (34).

Primarily in myofibers and adipocytes, insulin binds to receptors on the plasma membrane and coordinates anabolic responses to nutrient availability (32). Upon insulin binding to its receptor, a signalling cascade of events are activated, ultimately promoting glucose uptake. Additionally, insulin action impacts fatty acid, amino acid, and potassium uptake in muscle and fat tissues (35). If this system becomes disrupted, it gives rise to insulin resistance, which affects virtually every tissue in the body, but has a dominant effect on muscle, adipose, and liver tissues (36). However, despite the growing body of literature highlighting various aspects of insulin signalling impairment leading to insulin resistance and later T2D, the underlying molecular mechanism is yet to be fully understood.

1.2.2 Pathophysiology

T2D is a fast-growing epidemic affecting over 425 million people globally, according to the World Health Organization in 2020. Previously known to be more prevalent in older adults, this trend has shifted over the past two decades with an alarming increase in T2D diagnoses among children and young adults (37). Moreover, diabetes in youth was historically thought to be exclusively type 1 diabetes (T1D), a chronic autoimmune disease characterized by insulin deficiency followed by increased circulating levels of blood glucose (38). Importantly, the progression of T1D results from a highly complex interaction between the pancreatic β-cell and the immune system (39), while T2D is associated with some risk factors such as physical inactivity, obesity and unhealthy diet (40). The leading causes of T2D are not completely clear; however, a growing body of literature has highlighted multiple aspects of mitochondrial dysfunction and insulin resistance involved in the etiology of T2D (40–42).

T2D is characterized by insulin insensitivity or overt insulin resistance (41)**.** As a result, glucose transport into the liver, muscle and adipose cells are compromised (43)**.** In the early stages of the disease, the pancreas attempts to compensate by increasing insulin secretion into the bloodstream to overcome defects in peripheral insulin target tissues (42). As a consequence, this increased demand for insulin production cause β-cell hypertrophy (42). However, when β-cells fail to secrete insulin to compensate for a falling insulin sensitivity it leads impaired glucose disposal, following a meal or glucose challenge (impaired glucose tolerance), contributing to the further development of T2D (44). The relationship between insulin secretion and insulin sensitivity is referred as the disposition index (DI), an important marker of β-cell function, and lower DI predicts conversion of insulin resistance to T2D (44).

Historically, it is debatable whether insulin resistance is the cause of T2D or a consequence of the altered upstream factors. Moreover, obesity is thought to play a central role in the development of insulin resistance and T2D (45). For instance, in obesity, sustained mitochondrial dysfunction, characterized as lower mitochondrial content and reduced mitochondrial gene expression, is deemed a pivotal contributor to this phenomenon (46–49). The mechanisms that connect obesity and T2D are closely associated, with evidence of impaired skeletal muscle glucose disposal and elevated fasting insulin (49–51)**.** In obesity, adipose tissue cannot store excess lipids, resulting in ectopic lipid accumulation, for instance, in muscle (intramyocellular triglycerides) (52,

53). As a result, impaired or inefficient FA oxidation in skeletal muscle can lead to further accumulation of lipid intermediates, contributing to disturbances in mitochondrial function and insulin signalling. Lipid species, such as acylcarnitines, FA, DAG and ceramides have been shown to impair insulin signalling (52, 53).

Detailed insulin resistance mechanisms will be further discussed in the insulin resistance section of this literature review.

1.2.3 Glucose management and therapy

Exercise training is one of the best strategies to prevent as well as treat T2D by promoting increased muscle oxidative capacity (41). It has been demonstrated in numerous studies that mitochondrial function is improved in T2D patients after a short bouts of high-intensity training (41, 54). Additionally, vigorous physical activity has been demonstrated to be more effective in improving insulin sensitivity as compared to low-intensity exercise. Other therapies have also been shown to be effective, such as bariatric surgery (gastric bypass, gastric banding) to treat severe obesity associated with T2D (55). Whether its cost-benefit represents an optimal approach to prevent T2D, it still remains unclear. Therefore, more research is needed to recommend bariatric surgery as part of T2D prevention routine (56).

Ultimately, the goal in the management of T2D patients is focused on glucose control, in order to prevent acute and chronic complications (57). Considering the cost and affordability of many medications, the World Health Organization has listed some medications as essential to meeting the healthcare needs of the population. Among these drugs are short-acting and, intermediate-acting insulin formulations, metformin, gliclazide and glucagon (to treat episodes of hypoglycemia) (IDF, 2017). It should be noted that some of these medications are used for both T2D as well as type 1 diabetes.

Currently, there are twelve available classes of medications to treat T2D and they are classified into three main categories: drugs targeting β-cell dysfunction (sulphonylureas, biguanides, glinides, α-glucosidase inhibitors, thiazolidinediones, GLP-1 agonists, DPP-4 inhibitors, amylin analogues, and insulin); drugs targeting non-insulin dependent pathways (SGLT-2 inhibitors); and drugs with unknown mechanisms (dopamine D2-receptor agonists and

bile acid sequestrants) (55, 57, 59). The most commonly used medications to treat T2D are metformin (biguanide), sulfonylureas, GLP-1 analogue and DPP4 inhibitors (59). Their central mechanism of the action revolves around increasing the body's response to carbohydrate intake and reducing post-prandial glucose levels.

In particular, the sulfonylureas, developed in the 1950's, bind to a specific sulfonylurea receptor in the β-cell linked to an ATP-K^+ channel and inhibit it. Once this channel is inhibited, it blocks K^+ efflux, which depolarizes the cell membrane leading to the opening of voltage-gated Ca^+ channels. This series of events ultimately results in the exocytosis of insulin from the cell (60). Upon insulin secretion, glucose production is normalized, peripheral glucose disposal is enhanced, and glucagon levels are decreased (57). The expected efficacy of sulfonylureas is shown by a decrease in glycated hemoglobin (HbA1c) by 1.5 to 1.7%, as well as a reduction in fasting plasma glucose. They are relatively safe and inexpensive, therefore highly used.

Metformin is a glucose-lowering agent belonging to the class of antidiabetic drugs known as biguanides. It was first approved by the FDA in 1994 to be in the market, since then metformin is still considered the first-line of defense in treating T2D (61, 62). Metformin activates the AMPK pathway, which is an essential regulator of glucose and lipid metabolism. AMPK inhibits acetyl-CoA carboxylase resulting in a reduction of lipid synthesis and increase in fatty acid oxidation (43, 57). Metformin is not associated with hypoglycemia, which can occur with the use of sulfonylureas, and may also promote weight loss. Additionally, has been noted to reduce HbA1c levels by 1.5 to 1.7% and a decrease in fasting plasma glucose levels by 50 to 70 mg/dL (62).

The incretin-based therapy glucagon-like peptide-1 agonists (GLP-1) were first introduced to the market in 2005 and are a part of a new line of therapies gaining popularity for the treatment of T2D. Incretins are insulinotropic hormones, which are secreted from neuroendocrine cells in response to carbohydrate ingestion and absorption. Two incretin hormones are the GIP (glucose-dependent insulinotropic polypeptide) and GLP-1. Both hormones induce glucose-dependent β-cell insulin secretion, inhibit glucagon secretion from α-cells, and inhibit hepatic glucose production (59). Incretin mimetics also promote a decrease in HbA1c by 0.5% to 1.0% (62).

Finally, the dipeptidyl peptidase-4 (DPP-4) inhibitors are used as an adjunctive therapy to sulfonylureas, biguanides, thiazolidinediones, and insulin, or as monotherapy. The dipeptidyl peptidase-4 inhibitors, or DPP-4 inhibitors, inhibit degradation of GIP or GLP-1 once entered

gastrointestinal circulation, enhancing endogenous GLP-1 as a result (55, 63). The efficacy with this agent is presented by a reduction in HbA1c ranging from 0.5 to 0.8% (62). Some advantages include having a low risk of causing hypoglycemia, and having a minimal effect on weight.

1.2.4 Emerging therapies

More recently, a new class of drug has emerged as a potential therapeutic approach to treat T2D. The phosphodiesterase 4 inhibitor (PDE4i) roflumilast is an FDA-approved therapy to treat chronic obstructive pulmonary disease (COPD) and asthma since 2011 (64). A 12-week randomized controlled trial investigated the effects of roflumilast on glucose homeostasis and body weight in patients newly diagnosed with T2D. It was found that HbA1c was significantly reduced by 0.79% in patients that received roflumilast as compared to a placebo (64). This suggests that roflumilast contributes to minimizing postprandial hyperglycemia. However, the precise mechanism has yet to be investigated (64). In a parallel animal model study, it was found that roflumilast potentially improves glycemic levels by promoting GLP-1 release following food intake (65).

As briefly mentioned above, roflumilast has been found to promote weight loss in humans (66, 67), which can often be beneficial if the affected patient is also overweight. In an animal study, mice fed with high-fat diet, roflumilast treatment significantly reduced fasting plasma glucose and body weight through increased energy expenditure (68). The mechanism proposed suggests that roflumilast increases cyclic adenosine monophosphate (cAMP) levels intracellularly by inhibiting phosphodiesterase enzymes. As a result, protein kinase A (PRKA) downstream signalling pathway is activated leading to mitochondrial biogenesis and mitochondrial activity, which promotes higher insulin sensitivity and weight loss (68). Though this may represent a novel therapeutic target to treat T2D, more research is needed to elucidate the precise molecular mechanisms by which PDE4i improves glucose homeostasis. Taking this into consideration, in our studies we have further investigated how PRKA signalling may be involved in muscle insulin resistance, using cilomilast, another PDE4i, as proof of concept to modulate this pathway. Please refer to the manuscript described in Chapter III of this thesis for further details.

1.3 Insulin Signalling

1.3.1 Insulin receptors and substrates

The first report describing how insulin interacted with cell membranes was published in 1949, by Levine and colleagues (69). Following, in 1970, the Australians House and Weidemann described for the first time the radio-labeled insulin binding to the membrane of liver cells (70). Since then, many discoveries have been made that have allowed for a deeper understanding of insulin's action and kinetics. For instance, De Meyts and Lawrence summarize over 30 years of insulin research since its discovery in a review (69, 71).

Insulin performs its function when it binds to the insulin receptor (INSR) (32). INSR is composed of both alpha (α) and beta (β) subunits (72). In the β subunit, tyrosine phosphorylation is more specific to insulin (72), and this subunit is mostly expressed in differentiated liver, muscle, and white adipose tissue (WAT) (73, 74). When β subunits present conformational changes, it initiates trans-autophosphorylation of tyrosines, for instance, Tyr1162, Tyr1158, Tyr1163, and later Tyr972 (75). The binding events are an essential step for INSR substrate recruitment and activation, resulting in downstream mitogenic and metabolic signalling (76). These signal activations are dependent on insulin concentrations. While induction of the metabolic response requires lower insulin amounts, the mitogenic response requires more (77).

Upon insulin binding to INSR, complex cascades of downstream signalling events are activated, allowing insulin to perform its action in insulin-target tissues. In all cell types, activation of INSR is mediated upon the recruitment of phosphotyrosines-binding scaffold proteins (PTB), initiating a cascade of cellular phosphorylation (78). The INSR receptor substrates are IRS1 and IRS2, Src homology collagen (Src), and adaptor protein (APS), with a pleckstrin homology (PH) and SH2 domain. Once phosphorylated, these substrates bind and activate kinases, mediating the initiation of insulin action in the cell (76). The SH2B1, SH2B2/APS, GRB10 (growth factor receptor-bound protein 10), and GRB14 are known to interact via their SH2 domain. These substrates play a critical role in cellular function. For instance, GRB10 is phosphorylated by the mammalian target of rapamycin (mTORC1) and activated by insulin signalling, contributing to negative feedback inhibition of INSR (79). While the GRB2 is involved in the mitogenic arm of insulin signalling, the SH2B2/APS initiates the metabolic insulin response, depending on the cell

type (77). Phosphotyrosine phosphatases (PTPases), mostly PTP1B, has the potential to inhibit INSR by causing its dephosphorylation. However, this is prevented by INSR activation of NAD(P)H oxidase 4 (NOX4), which inhibits PTP1B and amplifies insulin signalling (80). Collectively, proper activation of these substrates, proteins, and kinases are crucial in the regulation of insulin function within the cell.

The insulin receptor substrate (IRS) is the best-described class of the INSR scaffold. Though six IRS isoforms have been described in the literature, IRS1 and IRS2 are responsible for mediating most of the metabolic effects of INSR (81, 82). The IRS contains an amino (NH2) and a carboxyl (COOH) terminal, full of tyrosine and serine/threonine phosphorylation sites (83). IRS PTB domain bind to INSR pTyr972 to phosphorylate IRS tyrosine residues. Then, downstream signalling effectors are recruited to propagate and amplify insulin response (78). The S6 kinase (S6K) is the predominant inhibitor of insulin signalling, mediated by serine phosphorylation of IRS (79). Furthermore, IRS serine phosphorylation is one of the major events leading to insulin resistance.

IRS mediates insulin-stimulated glucose uptake upon IRS tyrosine phosphorylation and recruitment of phosphoinositide 3 kinase (PI3K). PI3K has been intensely investigated, and inhibition of it results in impairment of insulin-stimulated glucose uptake (84, 85). One of the critical roles of PI3K is to catalyze phosphatidylinositol-4,5 biphosphate (PIP2) into phosphatidylinositol-3,4,5 triphosphate (PIP3) (86). Following the reaction, PIP3 recruits proteins with the PH domain to the plasma membrane and activates downstream effectors, such as phosphoinositide-dependent kinase (PDK1) and AKT (87). AKT1 activation is either mediated by PDK1 Thr308 phosphorylation or by mTORC2 ser473 phosphorylation (88). The AKT1 ser473 phosphorylation is one of the most commonly used markers of insulin action; however, the precise mechanisms that link INSR activation to AKT ser473 are not fully understood.

In summary, insulin binds to INSR and it auto-phosphorylates, initiating recruitment of various substrates upon phosphorylation. The significant arms of insulin signalling are mitogenic and metabolic functions. In the mitogenic arm, GRB2 and SHC are activated and initiates the downstream signalling activations (77), while the metabolic arm is activated by IRS and SH2/APS (89). Insulin performs both positive and negative feedback mechanisms. In the positive feedback, there is an increase of PI3K-AKT axis, phosphatase inhibition by Nox4 derived H_2O_2. Moreover,

in the negative feedback, there is stabilization and recruitment of GRB10 to INSR, as well as activation of S6K1 to phosphorylate and inhibit IRS1 (79, 90).

1.3.2 Muscle glucose uptake

The skeletal muscle accounts for approximately 80% of postprandial glucose disposal in humans, and proper insulin action is crucial to maintain glucose homeostasis (91–93). The primary role of glucose in the skeletal muscle is to promote glycolysis or glycogen synthesis, where the latter represents approximately 75% of all glucose disposal (91).

Elevated levels of blood glucose trigger pancreatic insulin release, which subsequently binds to INSR to promote glucose uptake and glycogen storage in skeletal muscle (33). Moreover, INSR stimulation triggers a phosphorylation-dephosphorylation cascade that is mediated by various kinases such as S6K, Akt, PDK-1, and isoforms of protein kinase C (PKC) (94). These proteins function to regulate numerous pathways in the skeletal muscle that contribute to glucose metabolism (94). One signalling pathway involves the translocation of GLUT4 containing storage vesicles (GSVs) to the plasma membrane, which is regulated by Akt2 (91, 95). Other downstream effects result in an increase in glucose-6-phosphate (G6P), dephosphorylation of glycogen metabolic proteins, and glycogen synthesis (91). In order to sustain normal insulin-stimulated glucose uptake in the muscle, it is crucial to maintain the IRS1/PI3K/Akt pathway (91).

Tyrosine phosphorylation of IRS mediates PI3K recruitment and insulin stimulated glucose uptake. Conversely, serine and threonine phosphorylation of IRS has an opposite effect (96). Continuous exposure to high insulin levels were found to induce phosphorylation of either serine or threonine, which consequently inhibited IRS1 and decreased GLUT4 translocation to the plasma membrane (96). Skeletal muscle uses IRS1 as the primary substrate for INSR during insulin-mediated glucose metabolism (94). Although IRS2 is also expressed, it is unnecessary for insulin-stimulated glucose transport in the muscle (97). In the presence of high amounts of phosphatidylinositol (3,4,5)-trisphosphate (PIP3) in the cellular membrane, kinases with a PH domain such as PDK1 and Akt are recruited (98). While both Akt1 and Akt2 are present in skeletal muscle, Akt2 is more critical for insulin-stimulated glucose uptake. Studies on mice have indicated that Akt2 knockouts are extremely glucose intolerant (99), whereas Akt1 knockouts exhibit normal glucose tolerance, along with growth and metabolic defects (100).

PI3K regulates GLUT4 translocation to the plasma membrane (101), mediated by Akt2 phosphorylation and the activity of a Rho family of small guanosine triphosphatases (GTPase) Ras-related C3 botulinum toxin substrate 1 (RAC1) (102, 103). Studies on muscle-specific RAC1 knockouts in mice have indicated that Rho GTPases may likely be involved in insulin-stimulated glucose uptake regulation in the muscle via PI3K dependent signalling (104). Further, Sylow and colleagues (2013) observed that even in the presence of activated Akt, these knockout mutations resulted in impaired insulin-stimulated glucose uptake (105). Despite its relevance to insulin-stimulated glucose uptake signalling, the precise mechanisms of RAC1 induced GLUT4 translocation is still not entirely known.

In summary, GLUT4 translocation to the plasma membrane in a fed state is an important step in normal blood glucose disposal in the skeletal muscle and is characteristic of normal insulin physiology. However, the failure of this event in response to insulin may indicate an early stage of insulin resistance and T2D (89).

1.4 Insulin Resistance

1.4.1 Causes

The hallmark of insulin resistance is unresponsive target tissues, resulting in insulin's failure to adequately dispose of glucose from the blood, inhibit lipolysis, and stimulate glycogen synthesis (32). Traditionally viewed as a compensatory response, insulin secretion is enhanced leading to hyperinsulinemia. These defects may be reversible by weight loss, exercise, and proper nutritional diets; however, if left unopposed insulin resistance is a precursor event that likely contributes to β-cell dysfunction. The most widely reported consequences of insulin resistance include the onset of T2D, with corresponding fasting and postprandial hyperglycemia, elevated HbA1c, and non-alcoholic fatty liver disease, which are accompanied by increased fasting plasma insulin. However, more recent evidence using genetically engineered mouse models, have challenged the idea that insulin resistance is a direct cause of T2D, and instead posits that basal hyperinsulinemia caused by β-cell gluco/lipotoxicity drives obesity and resistance in peripheral tissues (106, 107)**.** Collectively, these insights support the notion of a feed-forward system where insulin resistance stimulates hyperinsulinemia, and hyperinsulinemia worsens obesity and insulin resistance until β-cells fail, marking the onset of T2D.

As insulin has different roles in various tissue types, this has ramifications in the concept of insulin resistance. In other words, the pathogenesis of insulin resistance may be distinct in each target tissue (i.e. muscle, adipose, or liver). Among the leading etiological factors in the pathogenesis of insulin resistance is the effect of lipotoxicity (108). Additionally, cellular nutrient stress, for instance, the effect of the endoplasmic reticulum (ER), mitochondrial dynamics and energetics, and oxidative stress, are also emerging areas of investigation (Figure 1.2). Finally, integrated physiological mechanisms, such as the relationship between macrophages and adipocytes during inflammation and circulating branched-chain amino acids (BCAAs), are possible mechanisms that may also contribute to the onset of insulin resistance (32).

Figure 1.2. Impaired mitochondrial function and insulin resistance.

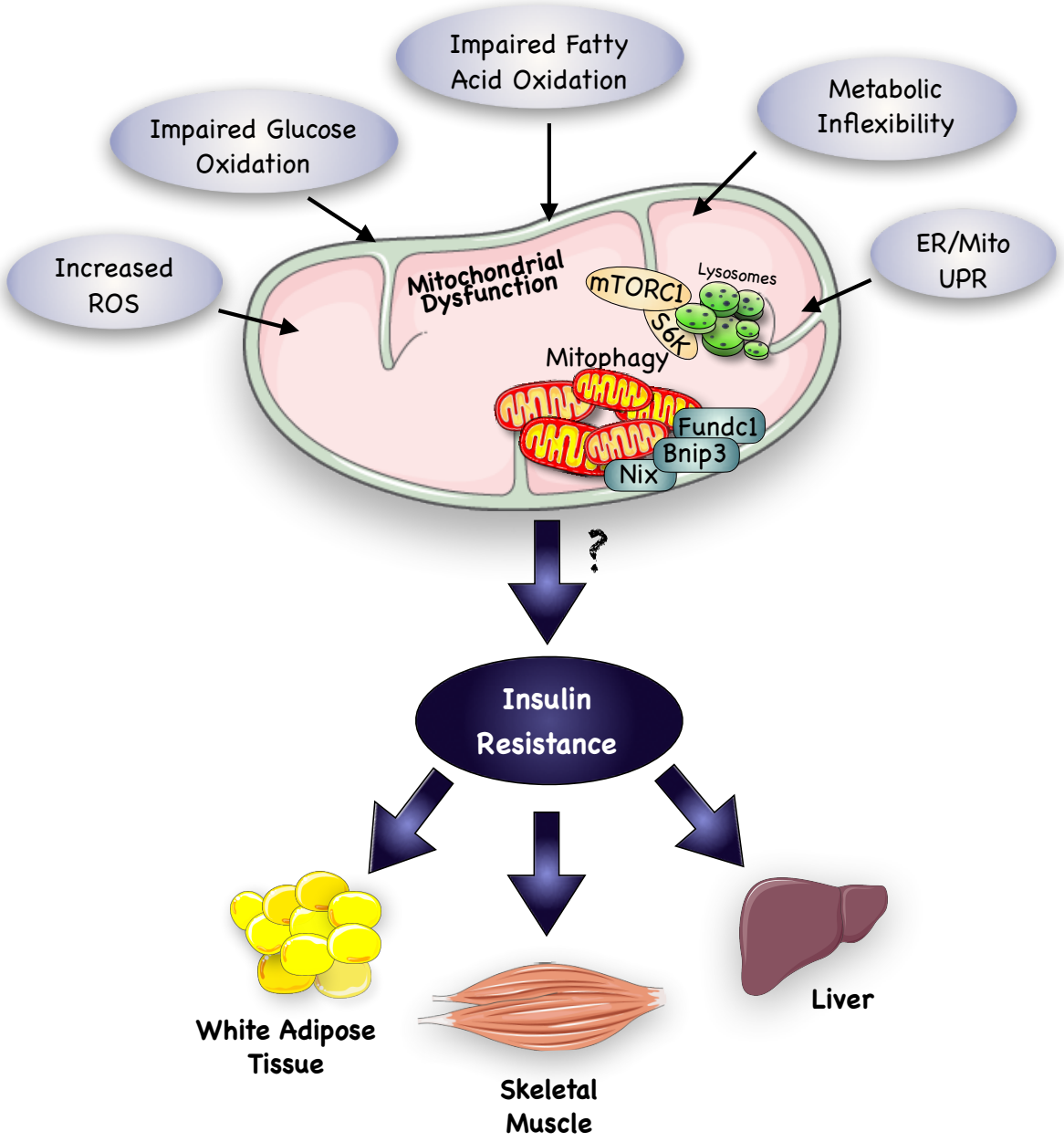

Impaired mitochondrial functioning is a suggested mechanism through which insulin resistance develops. Several factors have been implicated in the development of mitochondrial dysfunction. Some of the most reported factors include increased ROS production, impaired glucose and fatty acid oxidation, metabolic inflexibility, ectopic lipid accumulation and mitochondrial damage, leading to insulin resistance in major insulin target tissues, such as muscle, adipose tissue, and liver.

1.4.1.1 Lipotoxicity

Contemporary theories regarding insulin resistance outline different mechanisms by which it arises (40, 42, 53). Lipotoxicity is a type of cellular stress induced by the accumulation of lipid intermediates such as diacylglycerols (DAGs), ceramides, and triglycerides that facilitate the development of insulin resistance in muscle, liver, and adipose tissue (32, 40, 109, 110). Moreover, in skeletal muscle, the overabundance of fatty acid intermediates impedes insulin signalling via the reduction of GLUT4 transporters on the myocyte membrane surface (111–113). In other tissues such as the liver, intrahepatic triglycerides (IHTG) accumulation and DAG-PKC-ε axis have been hypothesized to be implicated in the pathogenesis of hepatic insulin resistance (114). As for adipose tissue, it has been theorized that an increase in lipolysis, governed by a similar cascade to skeletal and liver tissue is the proximal cause of insulin resistance at this site (115).

1.4.1.2 Metabolic inflexibility

Metabolic flexibility is described as the ability of an organism to adapt fuel oxidation to fuel availability (116). Consequently, metabolic inflexibility is characterized by impaired fuel switching and energy dysregulation, concepts that are both closely associated with insulin resistance and cardiometabolic disease (42). Diminished fuel switching capacity can result in the accumulation of intramyocellular lipid (IMCL), as well as DAG-PKCθ activation and impairment of proximal insulin signalling pathways (117). The latter ultimately impairs insulin signalling through different mechanisms, either increased serine phosphorylation of IRS1 at Ser-1101 and/or reduced serine phosphorylation of PKB/Akt (118, 119).

With an excess of fatty acid availability, fatty acid transporters may limit cellular and mitochondrial fatty acid uptake, thereby reducing fat oxidation and increasing the accumulation of lipotoxic lipid metabolites, contributing to the onset of insulin resistance (120). Additionally, myotubes from insulin-sensitive subjects have been reported to be more adaptive to fatty acid exposure *in vitro* (121). Further, palmitate oxidation has also been shown to be lower in myotubes derived from T2D versus matched nondiabetic controls (122, 123). Ultimately, defects in fuel switching can intensify with impaired mitochondrial content and/or function, further contributing to insulin resistance and mitochondrial dysfunction (Figure 1.2).

1.4.1.3 ER stress

The mechanisms of lipid-induced insulin resistance have been well described as an underlying cause of obesity-associated insulin resistance. However, an overload of other nutrients may also be implicated in the etiology of insulin resistance (124), and diabetes (125), for instance, the unfolded protein response (UPR), activated by ER stress (124). The main role of the UPR is to promote an adaptive cellular response that alleviates ER stress through different mechanisms, such as the inhibition of protein synthesis and the enhancement of protein folding and degradation (126). The major arms of UPR activation in mammals are mediated by three ER transmembrane stress sensors: PKR-like ER kinase (PERK), inositol requiring enzyme 1 (IRE-1), and activating transcription factor 6 (ATF6) (127).

Though the precise role of ER stress in muscle insulin resistance remains uncertain, there are two mechanisms proposed in the contexts of obesity and T2D that are well supported by the literature. The first mechanism is the activation of the c-Jun N-terminal kinase (JNK1) pathway via IRE-1, resulting in inhibitory serine phosphorylation of IRS1 (128, 129). Moreover, JNK was proposed to induce insulin resistance in obesity via four different mechanisms, including direct inhibition of IRS1 phosphorylation, induction of metabolic inflammation, increased adipogenesis and metabolic efficiency, and negative regulation of the PPARα-FGF21 axis (129). The second mechanism linking ER stress, obesity and diabetes-induced insulin resistance involves activation of the PERK/eIF2/ATF3 signalling pathway (130). Activation of this pathway leads to increased expression of the tribbles-like protein 3 (TRB3). The TRB3 is an important pseudokinase that highly contributes to insulin resistance by inhibition of Akt activity (131).

1.4.1.4 Mitochondrial dysfunction

Mitochondria are dynamic organelles that adapt to metabolic perturbations by undergoing fusion and fission cycles, rearranging electron transport chain complexes into supercomplexes, and proliferation via peroxisome proliferator-activated receptor γ co-activator 1α (PGC 1α) (132). These normal processes, however, are dysregulated in individuals with T2D and insulin resistance (133, 134). Mechanistic studies have shown that lipotoxicity prompts excessive mitochondrial fission through activation of dynamin related protein 1 (DRP1), resulting in impaired insulin-stimulated glucose uptake (135). Another presumed mechanism connecting mitochondrial

dysfunction to insulin resistance is the generation of reactive oxygen species (ROS) by mitochondria (Figure 1.2). Oxidative stress occurs when ROS production overwhelms cellular antioxidant capacity. In addition to the ability of ROS to induce oxidative damage to nuclear DNA, lipids and protein, they are also signalling molecules that can directly induce insulin resistance (136). The induced oxidative damage caused by the ROS consequently triggers the removal of damaged mitochondria by mitophagy (137). The resultant decrease in mitochondrial function and density compromises overall cellular oxidative capacity, further contributing to ectopic lipid accumulation (138).

1.4.2 Tissue specific insulin resistance

1.4.2.1 Muscle

Human studies examining the mechanisms behind impaired GLUT4 translocation to the plasma membrane in skeletal tissue have suggested that failed INSR signalling activation is likely responsible (139). Additionally, in T2D patients, tyrosine phosphorylation of IRS1 was reported to be severely impaired as a consequence of hyperglycemia (140). Therefore, defects at the proximal level of insulin signalling that involve INSR, IRS1, PI3K, and Akt pathways are more evident in skeletal muscle insulin resistance, resulting in a decrease in insulin-stimulated glucose uptake.

Many theories have been proposed to explain the mechanism of muscle insulin resistance. One of the earliest theories was proposed by Randle and his colleagues in the 1960s. They concluded that an acute increase in muscle fatty acid oxidation leads to the accumulation of citrate, which inhibits phosphofructokinase (PFK), a pivotal enzyme in glycolysis (141). This results in the impairment of glucose utilization (141). Other studies have further elaborated that reduced insulin-stimulated muscle glycogen synthesis and glucose oxidation may drive chronic insulin resistance (92).

Modern theories argue that skeletal muscle lipid exposure is one of the leading causes of muscle insulin resistance. The mechanism of lipid-induced insulin resistance linking DAGs, ceramides and other species have been extensively investigated (32, 142–144). Animals treated

with a high-fat diet and lipid infusion have increased muscle DAG, resulting in activation of PKCθ (145). Similarly, lipid infusions in humans resulted in an increase in DAG and PKCθ signalling, which impairs tyrosine phosphorylation of IRS1 (145, 146). IRS1 is the primary activator of PKB/Akt, inhibition of this pathway blocks insulin signalling cascade events preventing insulin-stimulated glucose uptake in the skeletal muscle (Figure 1.3). In other studies, acute induction of muscle insulin resistance increased DAG content, PKCθ activation, and increased phosphorylation of IRS1 serine 1101, concurrent with inhibition of IRS1 and Akt2 phosphorylation. However, adipokines, ceramides, and acylcarnitine content alterations were not associated with insulin resistance in this study (146).

Figure 1.3. Muscle insulin resistance.

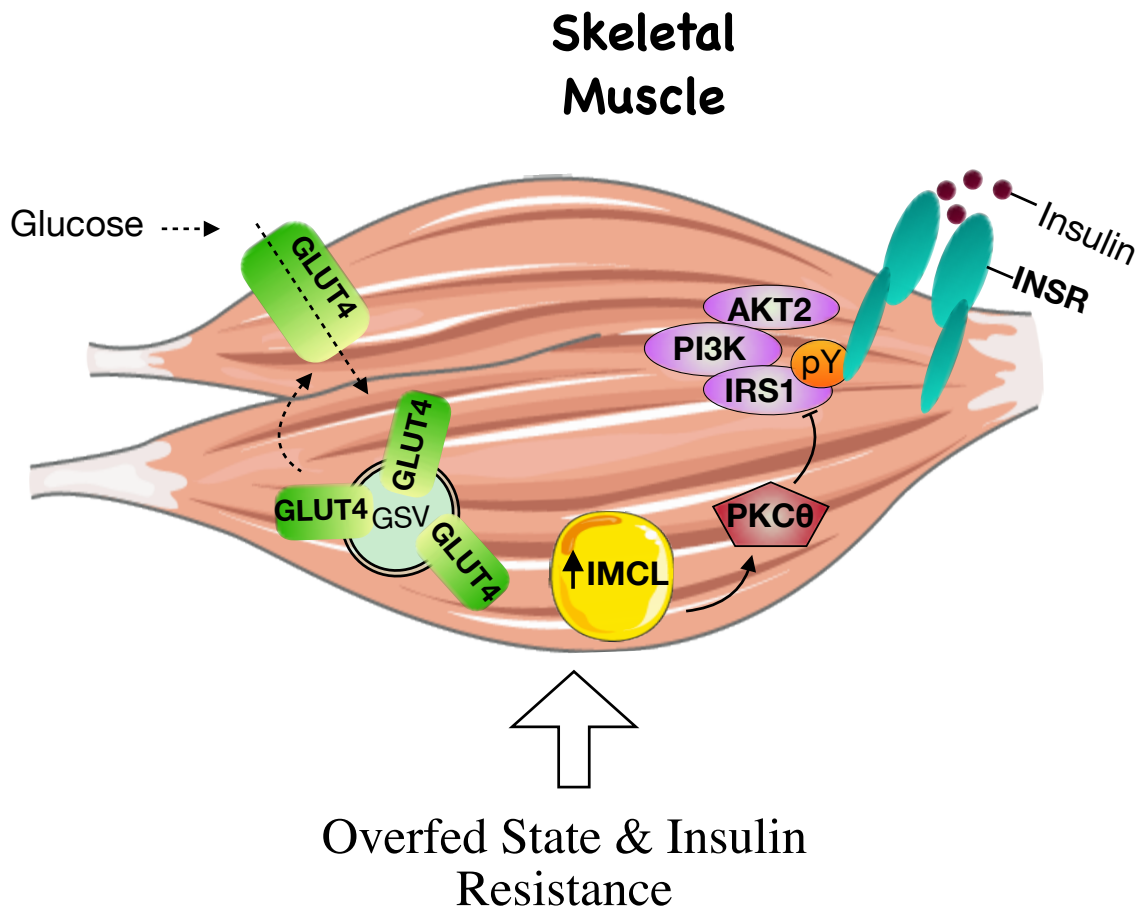

In the skeletal muscle, lipid-induced insulin resistance is initiated upon activation of the DAG-PKCθ axis and inhibition of both PI3k and phosphorylation of IRS1. As a result, insulin signalling is impaired, preventing GLUT4 translocation to the plasma membrane and glucose uptake.

In both skeletal muscle and liver, activation of the nPKCs have been consistently observed. Yu and colleagues (2002) suggested a link between increased DAG content and sustained activation of the PKCθ. In previous studies, rodents were infused with lipid emulsions or glycerol, and it was observed that the nPKCs mediated insulin resistance that results in chronic IMCL accumulation (110, 145). Specifically, in the skeletal muscle, T2D patients present with increased PKCθ (146), and PKCε (147) isoforms, compared to controls. Interestingly, a study conducted on endurance athletes found that IMCL accumulated in athletes who did not have T2D, a phenomenon termed the "Athlete's Paradox" (148). It was discovered that T2D patients and endurance athletes store lipid droplets differently. T2D patients have lipid droplets localized in the subsarcolemmal region of type II muscle fibers while the athlete's lipid droplets were localized in the myofibrillar region of type I muscle fibers. This finding suggests the importance of lipid droplet morphology and storage in the pathogenesis of insulin resistance (148).

As noted above, a multitude of mechanisms have been proposed by which insulin resistance develops in the skeletal muscle. Elevated serum amino acids, particularly BCAAs, were found in obese T2D patients (149). Similarly, animal and human studies have shown that the infusion of amino acids caused impairment of skeletal muscle glucose uptake (150, 151). Recently, pharmacological enhancement of BCAA catabolic activity has been shown to improve insulin resistance and hyperglycemia, at least in an animal model (152). The mechanisms behind how increased BCAAs lead to insulin resistance are still not clear, but it has been linked to an increase in lipotoxicity (153). Other studies have shown that high amounts of BCAA can interfere with insulin signalling via activation of mTOR and S6K1 in a PI3K dependent manner (151). Tremblay et al. (2007) identified in an *in vitro* model that S6K1 directly phosphorylates IRS1 Ser-1101 resulting in suppression of IRS1 tyrosine and Akt phosphorylation, and further, insulin resistance (154).

Recent theories argue that excessive β-oxidation and mitochondria acylcarnitine accumulation are linked to the development of muscle insulin resistance (53). Koves and colleagues (2008) found that concurrent with the upregulation in β-oxidation there was a decrease in tricarboxylic acid (TCA) intermediates. Furthermore, in this imbalanced environment of impaired β-oxidation, the mitochondria become more susceptible to accumulation of acyl-CoAs and acylcarnitine, possibly contributing to mitochondrial failure (53). Mitochondrial dysfunction

has been linked in many ways to impaired insulin sensitivity and T2D (Figure 1.2). This is mostly due to reduced oxidative capacity, impaired mitochondrial biogenesis, and low electron transport chain activity (143). The by-products of incomplete fat oxidation and ROS are accumulated in the mitochondria, leading to activation of serine kinases that ultimately impairs insulin signalling and GLUT4 translocation (155). Importantly, ROS is endogenously produced and have physiological significance at low levels (156), such as enhancing insulin signaling in skeletal muscle (157). Loh and colleagues (2009) demonstrated that mice lacking glutathione peroxidase, an important enzyme in the elimination of physiological ROS, were protected from insulin resistance induced by high fat feeding (157). However, the precise mechanisms are not fully understood as how ROS plays a dual role as both a signal and damaging agent.

Although dysfunctional mitochondria may cause an increase in ROS production in the absence of abundant antioxidants, the increase in ROS production can result in damaged nuclear and mitochondrial DNA, lipid accumulation, and the onset of insulin resistance (158, 159). Hui-Young Lee and colleagues (2017) investigated this hypothesis in mice overexpressing a mitochondrial-target catalase (MCAT) that caused a decrease in mitochondrial ROS, and fed them with a high-fat diet. Findings revealed that these animals were protected from energy imbalances as well as from DAG accumulation and PKCθ activation (149).

Furthermore, gene expression arrays performed on human muscle biopsies found that a series of genes involved in oxidative metabolism were downregulated in T2D patients (41). For instance, the mitochondrial PGC-1α, responsible for promoting mitochondrial biogenesis, is present in the promoter region of these downregulated genes. Therefore, in the absence of such genes regulated by PGC-1α, there was a decrease in muscle oxidative capacity (161, 162). In the absence of functional mitochondria, fatty acids compete with glucose for oxidative degradation (141), resulting in metabolic inflexibility (Figure 1.2). The inability to switch fuel oxidation upon nutrient availability leads to insulin resistance and IMCL accumulation (163). Therefore, these findings emphasize the role of ectopic IMCL accumulation in skeletal muscle insulin resistance as summarized in Figure 1.3.

1.4.2.2 Liver

In the liver, insulin signalling is initiated by INSR trans-autophosphorylation, activation, and recruitment of scaffold signalling proteins (164), such as IRS1 and IRS2. Both isoforms have a similar function; however, IRS1 may have a more significant role in normal glucose homeostasis. Dong et al. 2008 showed that liver-specific Irs-1 knockout animals presented with considerable glucose intolerance, while Irs-2 deletion resulted in mild glucose intolerance; deletion of both isoforms severely weakened insulin stimulation of PI3K-Akt activity (165). The hepatic insulin signalling is distal to Akt activation; however, Akt signalling is central to hepatocellular insulin action. The Akt substrates are glycogen synthase kinase (GSK3), transcription factor forkhead box 01 (FOXO1), and mTORC1. Additional signalling pathways independent of Akt may be involved in metabolic control; however, more studies are needed to describe them (166).

In a fed state, insulin inhibits transcription of gluconeogenic genes, mostly the ones mediated by FOXO transcription factors (167). As previously mentioned, FOXO1 is an Akt target, and its main phosphorylation sites are at Thr24, Ser256, and Ser319 (168). Mice lacking FOXO1 in their liver presented with impaired hepatic glucose production (HGP) (169). Therefore, FOXO1 is a key molecule and highly crucial for HGP. Another critical role of insulin in the liver is its direct effect on lipid metabolism. Insulin regulates genes responsible for *de novo* lipogenesis (DNL), the conversion of sugar into fat (170). The primary transcription factor regulator of this process is the sterol regulatory element-binding protein-1c (SREBP-1c). Insulin regulates activation of SREBP-1c; however, inhibition of the PI3K-Akt-mTORC1 axis is known to also inhibit SREBP-1c via insulin inhibition (171). Finally, insulin also regulates protein synthesis in the hepatocytes in addition to playing a role in glucose and lipid metabolism. The primary mediator of protein synthesis in various insulin-responsive tissues, such as hepatocytes, adipocytes, and myocytes, is mTOR.

Dysregulated hepatic glucose production is associated to the onset of T2D (172). In normal conditions, FOXO1 increases expression of necessary enzymes for gluconeogenesis; therefore, its upregulation results in increased substrate conversion into liver glucose (173). However, in obese mice, upregulation of FOXO1 expression resulted in impaired glucose tolerance and increased hepatic fat accumulation, contributing to the development of diabetes and hepatic steatosis (174). The precise mechanism of overfeeding in the dysregulation of FOXO1 is still under investigation

(174). Conversely, the ablation of hepatic FOXO1 in mice lacking hepatic Irs1 and Irs2 restored glucose and insulin levels close to normal in response to a fasting and fed state (165), and genetic ablation of FOXO1 in mice lacking insulin receptor (LIRFKO) reversed insulin resistance (175). Recent evidence suggests that low hepatic PGC 1α in T2D patients is also associated with hepatic insulin resistance. PGC 1α drives the ratio of IRS1 and IRS2 in hepatocytes, and low levels of it resulted in disruption of IRS1 and 2 expression impacting normal glucose homeostasis (176, 177).

Figure 1.4. Intrahepatic insulin resistance.

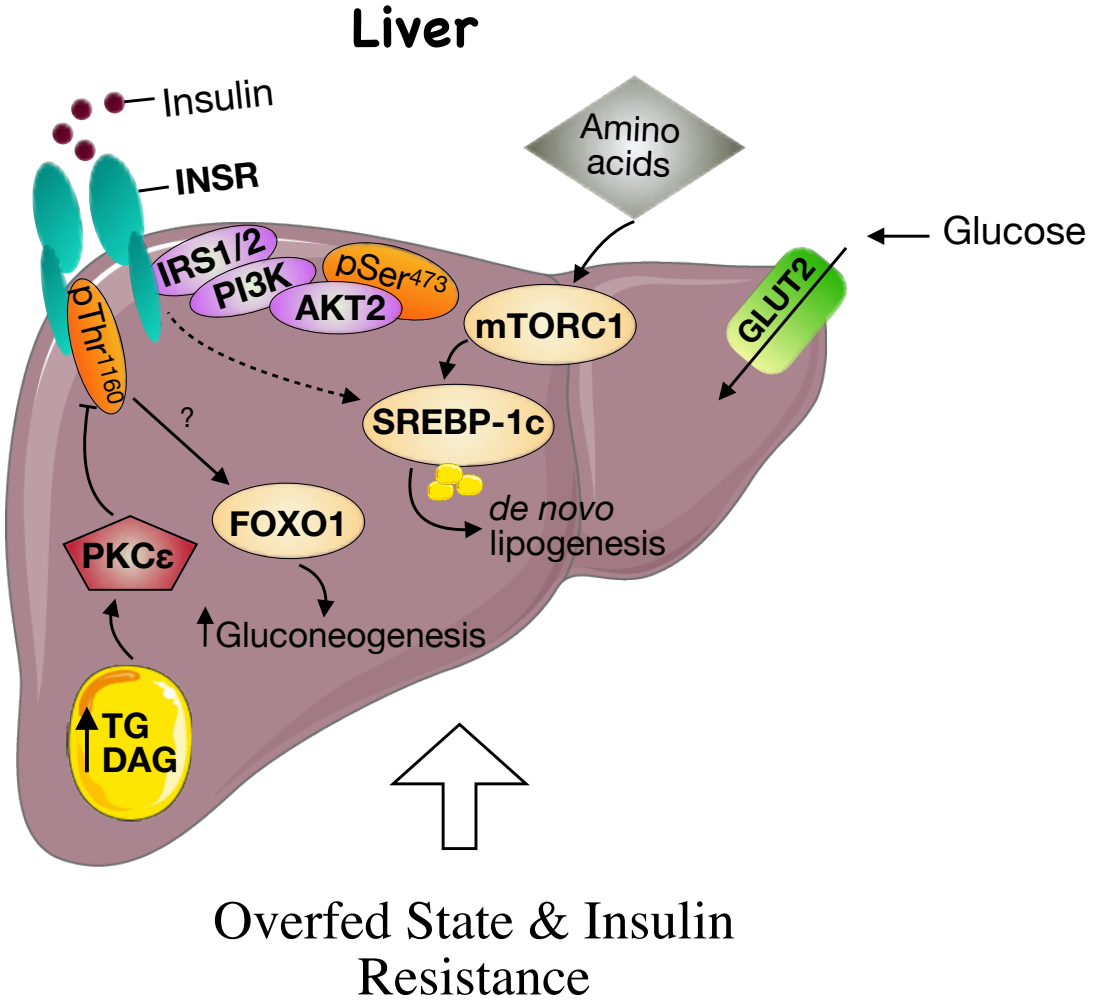

Intrahepatic lipid accumulation triggers activation of the DAG/PKC axis. PKCε directly phosphorylates and inhibits INSR at Thr1160, impairing insulin signalling. As a result, gluconeogenesis is increased, as insulin suppression of gluconeogenesis mediator, FOXO1, is impaired. Furthermore, in a chronic overnutrition state, DNL is increased, concurrent with its mediators mTORC1 and SREBP-1c. Even though activation of SREBP-1c by INSR is impaired in hepatic insulin resistance, other inputs such as amino-acid mediated mTORC1 activation can increase the lipogenic flux. Additionally, a chronic increase in lipolysis contributes to IMCL accumulation and lipid-induced insulin resistance.

As insulin also plays a role in lipid metabolism through SREBP-1C, insulin-resistant people may present with decreased lipogenesis. As shown in animal models of hepatic insulin resistance, there is a decrease in hepatic DNL (178). Several effectors act together and are involved in insulin resistance, for instance, Akt and FOXO1, controlling both glucose and lipid handling (179). In a non-alcoholic fatty liver disease (NAFLD), increased re-esterification of circulating fatty acids supplied by adipose insulin resistant tissue, is a possible leading cause of increased liver triglycerides (180). Furthermore, in insulin-resistant patients, the primary lipogenic flux is re-esterification, and not DNL; DNL is regulated by SREBP-1C, activated by mTORC1 via amino acid stimulation (171).

As shown in Figure 1.3 and 1.4, ectopic lipid accumulation in muscle or liver is a consequence of an overfed state or defective adipocyte fatty acid metabolism. As a result, this leads to activation of DAG-PKCε axis in the liver and subsequent inhibition of INSR signalling via phosphorylation of INSR at Thr1160 (181). Alternatively, ceramides have also been shown to activate an atypical PKCζ (Zeta) isoform and mediate hepatic insulin resistance (182). Therefore, some of the main consequences of this lipotoxicity-induced insulin resistant state are impaired insulin stimulation of hepatic glycogen synthesis, impaired upregulation of transcription factors that regulates DNL, and impaired downregulation of transcription factors that regulates gluconeogenic process. In previous sections of this literature review, the role of impaired mitochondrial function in contributing to insulin resistance in the muscle was discussed. However, in the liver, it has been shown that insulin resistance originating from lipotoxicity has no link with lower mitochondrial capacity. This has been attributed to a mitochondrial adaptation to promote increased lipolysis (183).

More recent literature has highlighted the role of mitochondrial quality control, such as mitophagy in promoting mitochondrial fatty acid oxidation, consequently reducing hepatic fatty acid accumulation and hepatic insulin resistance (184). Studies showed that hepatic fatty acid accumulation resulted in an increase in the accumulation of damaged mitochondria (185); however, through PINK1/Parkin-mediated mitophagy, this phenomenon could be reversed (186, 187).

1.4.2.3 Adipose tissue

Adipose tissue is critically important in influencing both glucose and lipid metabolism (188, 189) through the release of adipokines, proinflammatory cytokines, and free fatty acids (FFAs) (190). Moreover, adipose tissue is an insulin-responsive tissue, whereby insulin prompts the storage of triglycerides by such methods as stimulating the differentiation of preadipocytes to adipocytes, inhibiting lipolysis, and increasing the uptake of fatty acids, and glucose (191). Similar to the mechanisms in the liver and muscle tissues, insulin exerts its biological effects via the IRS-PI3K-Akt2-GLUT4 signalling pathways. However, both IRS1 and IRS2 are involved in adipocyte insulin signalling, in contrast with hepatocytes, where IRS1 has a more significant role in glucose homeostasis as compared to IRS2. In a similar fashion as the skeletal muscle, Rab GAP TBC1D is expressed in adipocytes, though in lower levels, and contributes to the regulation of insulin signalling through vesicle trafficking and translocation of GLUT4 to the plasma membrane (192).

As mentioned above**,** a major role of insulin in adipose tissue is to promote the suppression of lipolysis (191). Lipolysis is a crucial process where lipid triglycerides are hydrolyzed into glycerol and fatty acids and used to provide stored energy during fasting or exercise. The mechanism that regulates lipolysis is highly dependent on PRKA signalling pathway. PRKA phosphorylates the hormone-sensitive lipase (HSL) and perilipin (PLIN) to promote lipolysis (193), where phosphodiesterase 3B (PDE3B) inhibits PRKA through the degradation of cAMP (required for PRKA activation). Consequently, PDE3B impedes the action of the pro-lipolytic hormones HSL and PLIN, inhibiting lipolysis (193). In a fed state, insulin activates Akt2, which through an unknown mechanism, activates PDE3 and inhibits PRKA, thereby suppressing lipolysis. However, with adipose tissue insulin resistance, there is a decrease in Akt2 phosphorylation, resulting in sustained lipolysis activation (115). As a result, non-esterified fatty acid (NEFA) production and circulating fatty acids are increased, which are taken up by the liver and muscle, contributing to ectopic lipid accumulation in both tissues (Figure 1.5).

Figure 1.5. Adipocyte insulin resistance.

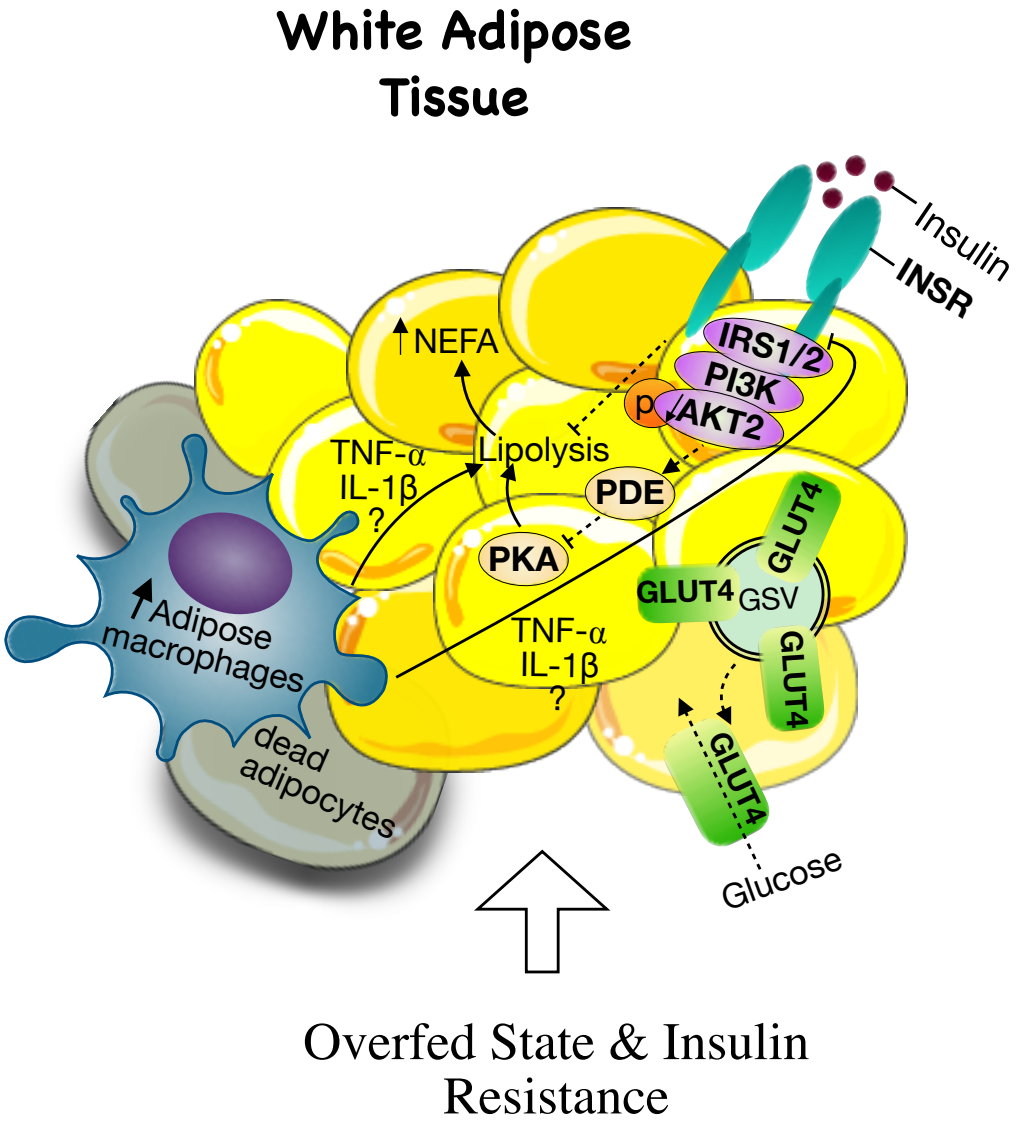

An increase in adipokines causes augmentation in the inflammatory response and recruitment of macrophages and cytokines around dead adipocytes to discard them. The inflammatory mediators, tumor necrosis factor TNFα or IL-1β increase lipolysis and inhibit INSR, therefore, impairing insulin signalling. Lipolysis is regulated by PRKA signalling, and, in a fed state, insulin activates Akt2, which via unknown mechanisms activates PDE3 and inhibits PRKA in order to suppress lipolysis. However, during adipose tissue insulin resistance, there is a decrease in Akt2 phosphorylation, contributing to sustained lipolysis activation and increased NEFAs production and circulation; which are taken up by the liver and muscle, contributing to ectopic lipid accumulation in both tissues.

In the presence of an obesogenic environment, excess energy storage leads to the hypertrophy of adipocytes. Studies investigating the relationship between adipocyte size and adipokine secretion have demonstrated that adipocyte size affects the secretion of many adipokines (194). For instance, TGFβ, a potent anti-adipogenic inflammatory cytokine, is released from hypertrophic and dysfunctional adipocytes of obese mice and humans (195). Therefore, a reduction in anti-inflammatory adipokine secretion, concurrent with an increase in inflammatory cytokine secretion by larger and dysfunctional adipocytes may play an important role in the onset of adipose tissue insulin resistance (32, 194, 196).

Furthermore, inflammatory neutrophil cells are the first to infiltrate white adipose tissue in a high-fat feeding state, which later recruit and activate the adipose tissue macrophages (ATM) (197). Additionally, the mechanisms by which ATM activation leads to insulin resistance is dependent on cytokines activation. Inflammatory cytokines, such as tumor necrosis factor (TNF)-α, interleukin-1 beta and 6 (IL-1β, IL-6), are increased in obese diabetic humans and rodents (198), and neutralization of TNF-α improves insulin sensitivity in obese rodents (199). Further, TNF-α has been shown to induce serine phosphorylation of IRS1, thereby decreasing its association with PI3K and impeding insulin signalling (200). Additionally, the inflammatory mediators, TNFα or IL-1β increase lipolysis and inhibit INSR; therefore, impairing insulin signalling (Figure 1.5). These findings suggest that obesity-induced insulin resistance may partially result from an imbalance in the secretion of pro- and anti-inflammatory adipokines. A recent study suggest that TNF can contribute to insulin resistance, as diet-induced obesity triggers TNF-dependent augmentation of circulating inflammatory monocytes independent of adiposity markers or expansion of adipose tissue (201). Although the exact mechanisms remain unclear, an uncontrolled production and/or secretion of these cytokines from excess adipose tissue can lead to the development of insulin resistance and metabolic disease.

Recent studies suggest that significant events such as mitochondrial dysfunction and mitophagy are also involved in the development of insulin resistant adipose tissue (104). Evidence indicates that mitochondrial content and mitochondrial oxidative capacity are altered in several insulin-responsive tissues (such as adipose tissue), in humans and animal models presenting with obesity and insulin resistance (133). It was identified that Fundc1 acts as an important mitophagy receptor in adipocytes by mediating mitophagy through its interaction with microtubule-associated

proteins 1A/1B light chain 3B (MAP1LC3B) in response to hypoxia (202), and a deficiency in this receptor is linked to insulin insensitivity and metabolic disorders (104). Notably, abnormal Fundc1- mediated mitophagy in adipose tissue resulted in increased oxidative stress and hyperactivation of mitogen activated protein kinase (MAPK) signalling, giving rise to ATMs infiltration and sustained inflammatory response (104).

Collectively, as presented in this section and the sections above, these three major insulin target tissues (muscle, liver and adipose) are intimately related to the development of insulin resistance, where multiple mechanisms interchangeably contribute to its progression (Figure 1.3, 1.4, and 1.5). Furthermore, mitochondrial dysfunction has recently become an attractive area of investigation, due to its possible role on insulin resistance (Figure 1.2). Therefore, the next few sections of this literature review in Chapter I will focus on mitochondrial autophagy (mitophagy) aspects, where I will introduce the key target protein of our investigations, called BNIP3L, a mitophagy receptor, which in our hypothesis is playing a major role in lipotoxicity-induced muscle insulin resistance.

1.5 Autophagy

1.5.1 Autophagy in muscle

In response to the energetic and metabolic demands during periods of cellular stress, cells more frequently undergo autophagy and induced catabolic processes (203–207). As the name implies, autophagy is a self-consuming process that functions to mediate levels of various proteins within the cell. This self-digesting mechanism is imperative in the removal of damaged organelles and proteins by the lysosome. Mammalian autophagy has been identified to primarily involve numerous Atg proteins, autophagy mediators, and conjugation systems that allow for the formation of the autophagosome, which encapsulates the cargo to later be degraded by the lysosomes (205, 208, 209).

Autophagy was initially posited to be a cellular response to prolonged periods of fasting. Studies have suggested that autophagy may potentially play a role in preventing insulin resistance in the fed state (210). Conversely, other studies have argued that autophagy actually contributes to the pathogenesis of insulin resistance (211). The Bcl-2-Beclin-1 complex is an important mediator of autophagy, where phosphorylation of Bcl-2 can release Beclin-1 from this complex, ultimately leading to the induction of autophagy (212). Moreover, rodent models have also shown that acute exercise may play an additive role on autophagy activation in the skeletal muscle (213). Intriguingly, He and colleagues (2012) found that transgenic mice expressing a Bcl-2 mutant that could not inhibit Bcl2-Beclin-1 complex correlated with a decrease in insulin sensitivity and GLUT4 translocation to the membrane surface (214). The authors concluded that the onset of acute exercise can contribute to disruptions in the coupling between the Bc1-2-Beclin-1 complex, which consequently leads to increased autophagy in the skeletal muscle and improved glucose metabolism (214).

Interestingly, Palikaras and colleagues (2018) elucidated a mechanism by which selective mitochondrial autophagy (mitophagy) occurs involving PINK1-Parkin and LC3 interacting regions (LIR) to which the latter can serve as a receptor to induce mitophagy (215). However, mitophagy can also be activated via other mechanisms, which will be further elucidated in the following mitophagy section.

1.6 Muscle Mitochondrial Dynamics

1.6.1 Mitochondrial fragmentation, fusion and fission

Mitochondria dynamically undergo cycles of fission and fusion. These processes, referred to as 'mitochondrial dynamics,' are necessary for appropriately maintaining the mitochondrion's shape, size and distribution in response to changing physiologic conditions (216). For example, in the case of an absolute or relative drop in ATP (owing to either a decrease in supply and/or an increase in demand), there is a shift towards mitochondrial fusion (41). Further, mitochondrial fusion enables content mixing within the mitochondrial population, thereby preventing the loss of essential components (217). Mitochondrial fission is also required to replenish the mitochondrial network (218), as it enables the removal of damaged mitochondria through mitophagy (219, 220). However, aberrant mitochondrial fission can lead to mitochondrial dysfunction and insulin resistance in skeletal muscle (135).

Dysregulated mitochondrial fission is often associated with more severe mitochondrial dysfunction as this morphological state predominates during elevated stress levels and cell death (135). Furthermore, increased mitochondrial fission and subsequent mitochondrial fragmentation have been associated with increased ROS production, mitochondrial depolarization, impaired ATP production and decreased insulin-dependent glucose uptake in C2C12 murine cell line (81), as well as increased mitochondrial ROS and impaired insulin signalling (221). A shift towards fission also negatively impacts on fatty acid β-oxidation (135), which has been described as a crucial metabolic defect in insulin resistance (53). In support of this, a shift towards fusion has been reported to increase fatty acid consumption (222), presumably averting lipotoxicity.

Mitochondrial dynamics can also describe mitochondria-organelle interactions such as the ER, peroxisomes and nucleus (223). In particular, the dysregulation of the interactions between mitochondria and the ER has been stated to be implicated in the pathogenesis of muscle insulin resistance (224). Mitochondria-ER contact points, also known as mitochondria-associated ER membranes (MAMs), are the sites where Ca2+, lipid and metabolite exchange occur, thus representing critical points of interaction for the regulation of oxidative metabolism (225). Additionally, studies have shown that the disruption of the MAMs in the liver promotes insulin resistance (226). Also, studies have shown that an increase in MAMs results in the accumulation

of Ca2+ within the mitochondria, leading to compromised mitochondrial oxidative capacity, an increase in ROS production and impeded insulin signalling (227). Subsequently, MAM formation appears to be an important regulator of mitochondrial function and insulin sensitivity.

Another proposed mechanism offering a causal link between mitochondrial dysfunction and insulin resistance involves the mitochondrial permeability transition pore (mPTP) protein complex. In particular, Taddeo et. al. (2014) showed that genetic deletion of whole body Cyclophilin D, a mPTP gatekeeper protein, protected mice from diet-induced glucose intolerance and increased glucose uptake specifically in skeletal muscle (228). Interestingly, the improved glucose tolerance was only associated with glucose uptake in the skeletal muscle, and the effects did not transfer to adipose and liver tissues. Further, the protective effects of mPTP inhibition on insulin sensitivity did not involve changes to the insulin signalling pathway but rather, it occurred through an unmapped mechanism preventing the formation of GLUT4 vesicles (228), a phenomenon described by other studies (229).

Collectively, the ability of the mitochondria to dynamically respond to metabolic perturbations is essential for healthy cellular bioenergetics, and interference with this delicate process may prompt unregulated mitochondrial biogenesis and mitophagy, thus contributing to insulin resistance (135).

1.7 Mitophagy

1.7.1 Pink and Parkin signalling

The role of mitochondrial dysfunction in the etiology of insulin resistance and T2D is currently an evolving area of research. Various studies are shedding light on the multiple roles of mitochondrial dysfunction in the development of insulin resistance, as briefly discussed in previous sections of Chapter I. In particular, alteration in mitochondrial dynamics and elevated levels of mitophagy have been linked to the onset of insulin resistance in T2D by multiple studies (138, 211, 230). Mitophagy (also known as selective autophagy of the mitochondria) is the process where dysfunctional mitochondria are degraded in a form of organelle turn-over. One of the most well-characterized pathways is the PINK1-Parkin mediated mitophagy (215), stimulated by a decrease in mitochondrial membrane potential and associated with ROS elevations (231). Upon mitochondrial depolarization, the PINK1 kinase accumulates on the outer mitochondrial membrane (OMM) and initiates recruitment of the E3 ubiquitin ligase Parkin. Parkin mediates the ubiquitination of several OMM proteins, leading to the recruitment and degradation of proteases and autophagosomes (232–234). In a human study, T2D patients presented a decrease in various mitophagy-related genes, including PINK1; furthermore, mutations in PINK1 have also been associated with T2D in humans (235).

1.7.2 BNIP3L, Bnip3 and Fundc1

Besides the PINK1-Parkin ubiquitin-dependent mitophagy, mitochondrial proteins also act as mitophagy receptors and target dysfunctional mitochondria for degradation by autophagosomes (215). The mitophagy receptors, such as BCL2L13, FKBP8, Fundc1, Bnip3 and BNIP3L, initiate mitophagy via direct interaction with ATG8 proteins, such as LC3 and GABARAP, on the autophagosome membrane through their LIR motif (236). Fundc1 interacts with the ER calnexin proteins and recruits mitochondrial fission protein DRP1 to activate mitochondrial fission (215). Mitophagy initiated by hypoxia increases the expression of Fundc1, which interacts with and recruits LC3 proteins to dysfunctional mitochondria. A recent study showed that Fundc1 deletion in skeletal muscle resulted in impaired mitochondrial energetics due to LC3-mediated mitophagy defect (237). However, in spite of the reduced muscle mitochondrial energetics and exercise

capacity, these animals interestingly were protected against obesity and insulin resistance elicited by high-fat feeding (237).

Like Fundc1, Bnip3 and BNIP3L are also hypoxia-inducible and regulators of mitophagy. Metabolic stresses such as fatty acid-induced dysfunctional mitochondrial accumulation, hypoxia, and starvation, can all induce Bnip3/BNIP3L mediated mitophagy (238, 239). Recent studies have demonstrated that Bnip3, BNIP3L and Fundc1 mediated mitophagy plays an important role in the treatment of lipid metabolism and various hepatic dysfunctions (Figure 1.2) (238, 240–242). Furthermore, in previous study by our group, BNIP3L was demonstrated to become elevated in insulin-resistant rodents (243). These preliminary findings prompted us to further investigate how BNIP3L accumulation in lipotoxic environments may lead to impaired insulin signalling, and what could possibly be the mechanisms linking mitophagy to insulin resistance, which will be thoroughly described in detail in Chapter III.

Nevertheless, research on the effects of mitophagy on insulin resistance and T2D is still an emerging field, and its role and molecular mechanisms (Figure 1.2) in these pathological processes require further *in vivo* experimentation.

1.8 BNIP3L

1.8.1 Bcl-2 family proteins

The B-cell lymphoma 2 (Bcl-2) family proteins are well-described regulators of apoptosis and cell death, containing one or more Bcl-2 homology (BH) domains (BH1-4) (244–246). These BH domains allow interaction among other family members and also indicate their pro- or anti-apoptotic functions. Among the four BH domains, BH3 is the only one conserved in the Bcl-2 family, and is essential for either their pro-apoptotic activity or for heterodimerization with anti-apoptosis proteins (Figure 1.6) (247, 248). Another important characteristic of the Bcl-2 family proteins is the presence of an additional transmembrane domain (TM) in the majority of the members, which allow their integration especially in the mitochondria, but also in other organelles such as the endoplasmic reticulum, nuclear envelope and lysosomes (249–251).

Figure 1.6. Bcl2-family proteins members and domains.

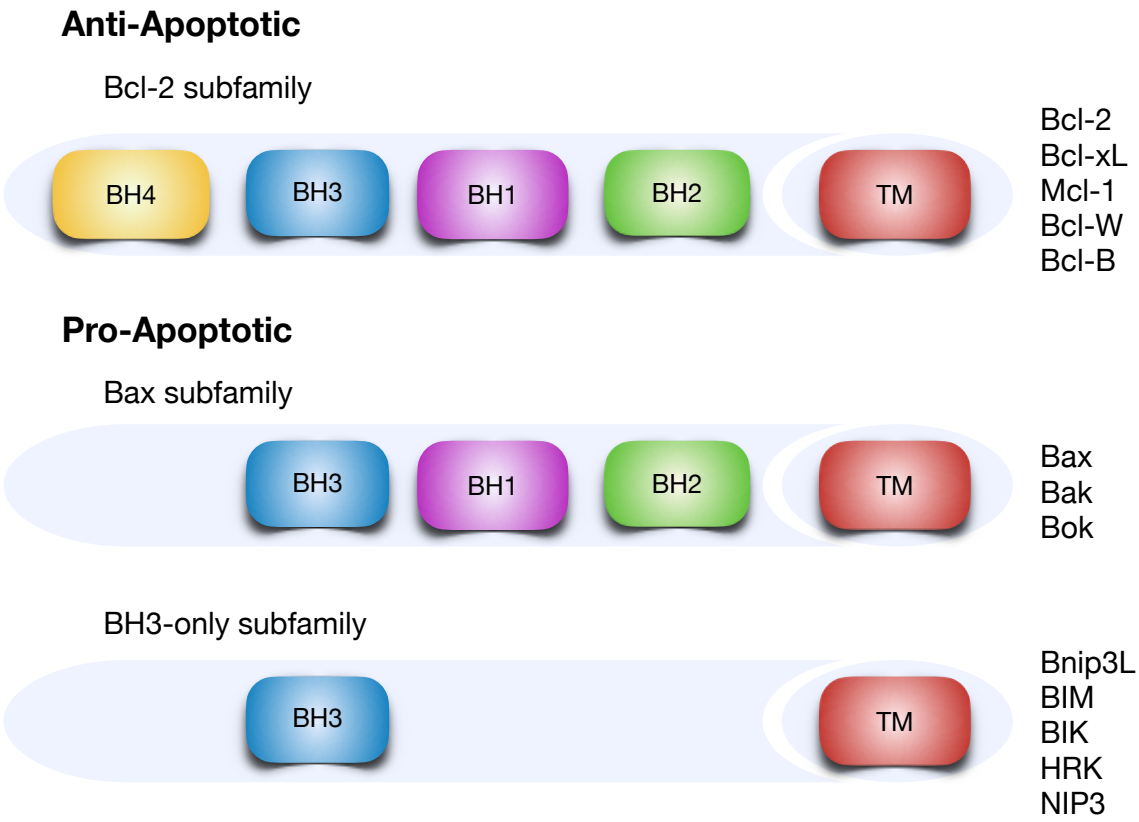

Two major groups, anti-apoptotic and pro-apoptotic representative members of each subfamily of the Bcl2-family protein members and their domains are shown. BCL2 homology domain (BH), and transmembrane domain (TM).

The 25 human Bcl-2 family members are categorized into three subfamilies based on their function. The first subfamily (Bcl-2 subfamily) includes anti-apoptotic proteins (Bcl-2, Bcl-Xl, Bcl-W, Mcl-1, Bfl-1/A1, Bcl2L12) (245) and contain four BH domains (BH1-BH4) (Figure 1.5). Additionally, they all share a BH4 domain, crucial for their anti-apoptotic activities, such as inhibition of Bax/Bak activation (252–254). The second subfamily is the pro-apoptotic effectors Bax and Bak subfamily (Figure 1.6), which contains BH1-BH3 domains, including a transmembrane domain (TM), and have the ability to cause mitochondrial pore formation (255, 256). Finally, the pro-apoptotic BH3-only subfamily (Bnip3L/Nix, BIM, BIK, HRK, Bnip3/NIP3, Spike, Noxa, BAD, BID, PUMA, BMF, MAP-1) possesses only a BH3 domain, and some members have a TM domain (Figure 1.6) (257).

The BH3-only proteins integrate signals from different pro-death stimuli, actively binding to- and inactivating anti-apoptotic Bcl-2 family proteins, via Bax/Bak activation (258, 259). Once activated, Bax/Bak regulates mitochondrial outer membrane permeabilization (MOMP) and generates pores that allow for the release of large apoptogenic proteins such as cytochrome C (260–262). Furthermore, other studies demonstrated that BH3-only peptides derived from BH3-domain-containing proteins could induce cytochrome c release from the mitochondria (263). These peptides were categorized as Bak "activators" (BID and BIM) directly binding and activating BAK and inducing mitochondrial cytochrome c release, and "sensitizers" (PUMA, BAD, HRK, BIK, BMF and NOXA), indirectly activating BAK without inducing cytochrome c release from the mitochondria (263, 264).

1.8.2 BNIP3L discovery and domains

Since the discovery of the first member (Bnip3; formerly Nip3) of the BH3-only family proteins in 1994 by Chinnadurai's group (265), many other protein members of this family were discovered. In 1999, Greenberg's group at the University of Manitoba (266) identified BNIP3L as a homolog of the E1B 19K/Bcl-2 binding and protein Nip3, hence Bnip3-Like protein (BNIP3L), also known as Nix. BNIP3L is expressed as a 48 kDa protein; however, the gene encodes a 23.8 kDa, suggestive that it undergoes homodimerization (266). Human BNIP3L has approximately 56% amino acid identity as human Bnip3, and 97% amino acid identity as murine BNIP3L (266, 267). As Bnip3, BNIP3L is an atypical BH3-only member and has a TM domain (Figure 1.7)

(268). Typically, heterodimerization of Bcl-2 homologues and Bcl-2/Bcl-xL is mediated by the BH3 domain, granting its proapoptotic effects; however, the BH3 domain is dispensable for BNIP3L pro-apoptotic activity, instead, it relies on the TM domain for that purpose (269). Furthermore, the deletion of the TM domain may cause mislocalization of BNIP3L to the cytoplasm resulting in its inability to induce cell death. BNIP3L also possesses a LIR motif on its N-terminal part exposed to the cytoplasm, becoming a typical autophagy receptor mediating mitochondria recruitment to autophagosomes through interaction with Atg8 family proteins (270). Additionally, a short linear motif (SLiM) has recently been identified in the cytoplasmatic domain of BNIP3L (271), which is essential to mediate mitochondrial clearance.

Figure 1.7. Domain map of BNIP3L.

The BNIP3L/Nix protein structure includes the following domains represented in the diagram: LC3-interacting region (LIR), essential short linear motif (SLiM), BCL2 homology domain (BH3), and transmembrane domain (TM).

1.8.3 Genetic models

In 2002, Yussman et al. (272) were the first to express BNIP3L in mouse hearts using alpha myosin heavy chain (α-MHC) transgenic promoter. In this initial study, α-MHC-BNIP3L mice were normal after birth, only until BNIP3L was overexpressed, and then they failed to thrive, dying at 7 to 8 days of age. The cause of death was due to substantial cardiomyocyte apoptosis, as well as dilated and hypo-contractile left ventricles (272).

Gerald Dorn's group, in 2007, Diwan et al. (273) generated a critical BNIP3L knockout (*BNIP3L*$^{-/-}$) mouse model that allowed understanding of its critical phenotypic role in hematopoiesis. The *BNIP3L* gene in mice was deleted using a germ-line deletion of BNIP3L by flanking exons 4 to 6a with loxP sites, later bred to mice expressing Cre recombinase (273). The BNIP3L$^{-/-}$ mice survived a minimum of 18 months (72 weeks of age), presenting modest growth

retardation compared to WT animals. The most striking observations were the spleen enlargement, around 80% bigger than WT at eight weeks of age; however, that was the only organ abnormality observed (273). Importantly, BNIP3L$^{-/-}$ mice presented reticulocytosis, erythroblastosis, and reduced apoptosis during erythrocyte maturation; therefore, BNIP3L appears to be critical for erythrocyte production and maintenance of hematological homeostasis (273). In 2008, Sandoval et al. (274) further determined the role of BNIP3L in erythroid maturation by generating a BNIP3L$^{-/-}$ mice using embryonic stem (ES) cells with gene trapping insertion targeting the BNIP3L locus between exons 3 and 4. Their study mechanistically concluded that the BNIP3L-dependent loss of mitochondrial membrane potential was an important step for targeting the mitochondria into autophagosomes for clearance during erythroid maturation, and interference with this may result in impaired erythroid maturation and anemia (274).

Based on previous reported roles of BNIP3L becoming upregulated in cardiac hypertrophy (272, 275), it was thought that ablation of BNIP3L would be protective of ventricular remodeling and heart-failure in chronic pressure overload. In fact, after long-term observation, at 60 weeks, the germ-line *BNIP3L* knockout mice developed cardiac enlargement with decreased left ventricular contractility compared to WT (273, 276). However, using a cardiac specific Nkx2-5 *BNIP3L*-/- model of selective cardiomyocyte deletion of BNIP3L was protective of pressure overload hypertrophy response, which further confirmed BNIP3L's essential function during cardiomyocyte apoptosis as a major determinant of adverse remodeling in pathological hypertrophies (277). In follow-up studies by Gerald Dorn's group in 2010, they used a conditional tetracycline cardiac *BNIP3L* suppression system, where they observed that cardiomyocyte apoptosis and cardiomyopathy were more prevalent and severe after neonatal BNIP3L expression than in adult (276).

1.8.4 Physiological role

BNIP3L is localized to the outer mitochondrial membrane and promotes various effects on the mitochondria, such as regulating apoptosis, necrosis, autophagy, mitophagy, and cancer (278, 279). Therefore, it has an emerging role in physiological health. BNIP3L's function has been highly studied in the heart, where it has been demonstrated to be involved in pathological remodeling events that lead to heart failure (280, 281) and necrotic- or apoptotic-induced cell death

(266, 282). Recent studies posit that the different subcellular locations of BNIP3L play different roles in these events. For instance, BNIP3L targeted to the ER/SR activates necrosis, whereas BNIP3L targeted to the mitochondria induces apoptosis (283, 284). Even though the precise mechanisms are not well understood, BNIP3L is preferentially localized to the SR during pressure overload in induced cardiac remodeling (284). Recent studies from our group identified a novel regulator of BNIP3L, microRNA-133a (miR-133a), as an important mechanism to control mitochondrial function and insulin sensitivity via repression of BNIP3L expression (243). Furthermore, Mughal et al. (285), in a follow-up study, demonstrated that myocardin, an important transcriptional co-activator required for cardiovascular development, highly upregulates miR-133a. However, loss of myocardin resulted in BNIP3L accumulation, which lead to mPTP and necrosis in the heart (285).

BNIP3L was originally identified for its pro-apoptotic role in cell death but later has been shown to critically induce mitophagy during erythrocyte maturation (274, 279, 286). During erythroid differentiation, GATA1 possibly induces BNIP3L; however, FOXO3 may also contribute. FOXO3 activity has been shown to be increased by starvation in myocytes, binding to BNIP3L and Bnip3 promoters, consequently increasing their expression and mediating autophagy via elevated LC3 lipidation (287). Additionally, FOXO3 expression, nuclear localization and transcriptional levels increased during erythroid differentiation (288, 289). In a murine BNIP3L-deficient model, these detrimental effects were confirmed, where these animals presented with defects in erythroid development, moderate anemia, reticulocytosis, and elevated splenic erythropoiesis (273, 274, 286). Furthermore, BNIP3L was identified as a selective mitochondrial autophagy receptor, which binds to LC3/GABARAB proteins through its LIR domain and enhanced by BNIP3L phosphorylation at Ser34 and Ser35 (290). Ablation of this interaction has also been shown to impair mitochondrial clearance in maturing murine reticulocyte (270). Interestingly, BNIP3L-mediated mitochondria clearance was shown to be independent of LC3/GABARAP interaction (270), suggesting the presence of an autophagy-independent pathway for programmed mitochondrial clearance in red blood cells (291, 292). More recent studies have further extended BNIP3L-mediated mitophagy as an important regulator of mitochondrial quality and functional integrity of platelets and their lifespan (293).

1.8.5 Role of BNIP3L in disease

BNIP3L can potentially cause disease, either through stress-induced BNIP3L overexpression or impairment of it, which can both ultimately lead to mitochondrial dysfunction and cell death (294). In the previous sections, BNIP3L's major roles in hematopoiesis and in the heart, where BNIP3L expression is lethal in perinatal cardiomyopathy in mice, while its deficiency may be protective of pressure overload, have been described (294). In the last decade, BNIP3L has become a focus of study in many other different disease models, such as diabetes. Heterozygous loss-of-function of pancreatic duodenal homeobox (PDX1), an important transcriptional factor during pancreatic development, is linked to type 2 diabetes (295, 296). In Pdx1 heterozygous mice, BNIP3L's inactivation rescued programmed cell death, beta-cell mass, insulin secretion and glucose tolerance (297). More recently, Humpton et al. (298) showed that the oncogene KRAS induces BNIP3L expression and its selective mitophagy machinery that restricts glucose flux to the mitochondria and enhances redox capacity in pancreatic ductal adenocarcinoma cells; however, loss of BNIP3L could restore functional mitochondria and decrease tumor proliferation in glucose-limited conditions. Among other cancers, such as glioblastoma, notably the most aggressive brain tumor, BNIP3L-induced mitophagy acts as a key survival mechanism (299). Jung et al. demonstrated that inhibition of BNIP3L could prevent mitochondrial ROS clearance and stem cell maintenance, resulting in suppression of glioblastoma in both *in vitro* and *in vivo* studies (299). Therefore, the BNIP3L-induced mitophagy pathway may represent a key therapeutic target for various diseases, including but not limited to cardiomyopathies, diabetes, and cancer. In our studies, we hypothesize that BNIP3L may be possibly targeted as a therapeutic approach modulated by PRKA signalling, which is described further in Chapter III.

1.9 PRKA Signalling in Muscle

1.9.1 Promotion and inhibition of muscle differentiation

cAMPs are important second messengers that are ubiquitously expressed and control various biological processes (300). An extracellular ligand binds to a G protein-coupled receptor (GPCR), such as β2-adrenergic receptors (β2-ARs), activating adenylyl cyclase (AC), subsequently raising and activating cAMP signalling in the skeletal muscle (301). Furthermore, adenylyl cyclase, along with phosphodiesterase (PDE) families of enzymes, tightly control cAMP generation and degradation [reviewed in (302, 303)]. Among cAMP's various effectors, the most common downstream effector is the cAMP-dependent protein kinase A, or simply PRKA (304). PRKA is a heterotetramer protein composed of two regulatory (PRKA-R) and two catalytic subunits (PRKA-C), with distinct physical and biological properties, such as a serine/threonine kinase that phosphorylates various downstream substrates (Figure 1.8); therefore, it is an essential regulator of many cellular signalling events (305, 306), such as muscle differentiation (307). A-kinase anchoring proteins (AKAPs) further contribute to cAMP-PRKA signalling specificity by binding AKAPs to PRKA-R subunits (308).

Figure 1.8. cAMP-PRKA/PKA signalling cascade activation.

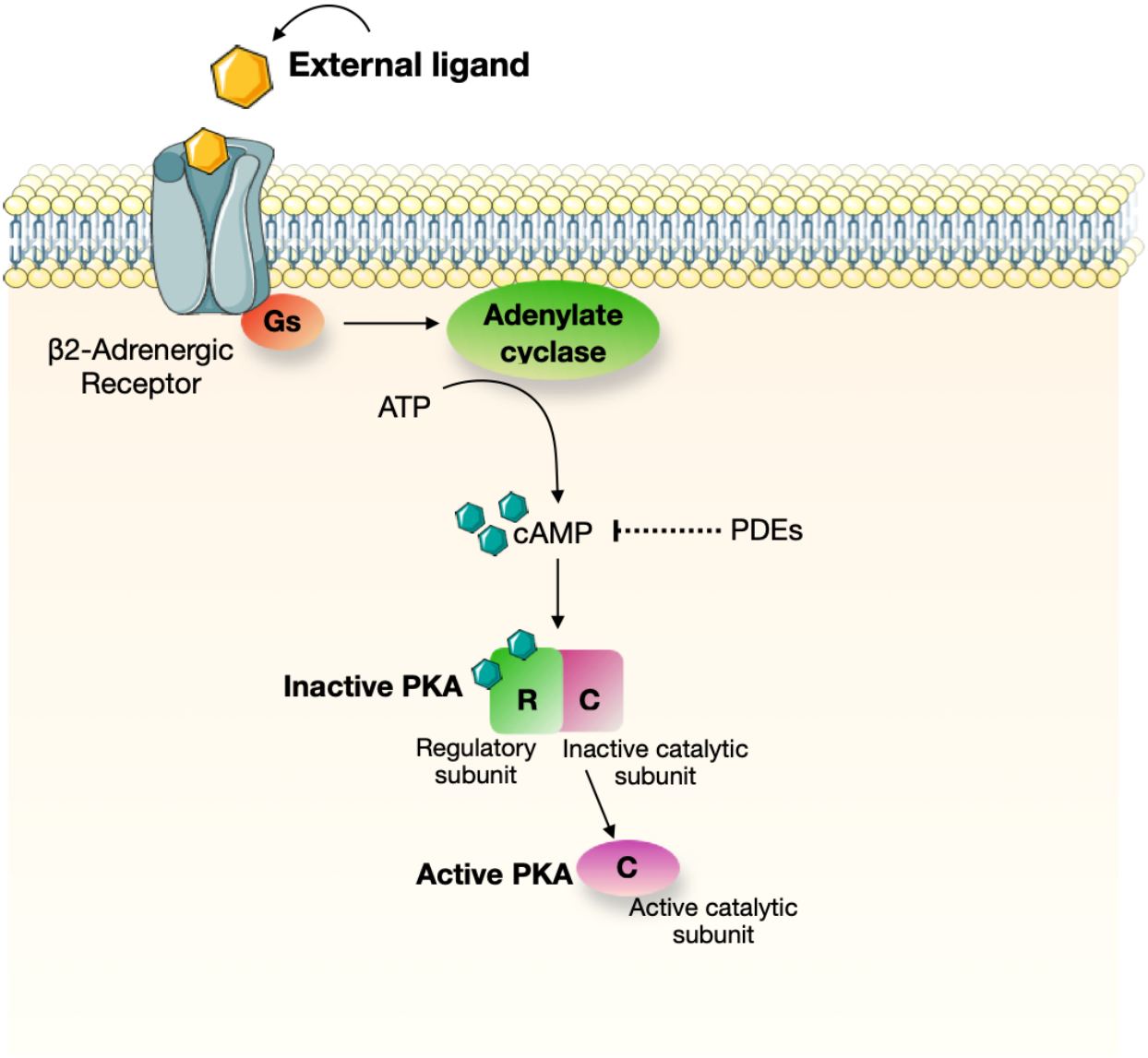

External ligand binds to G protein-coupled receptors and activates adenylyl cyclases. cAMP concentration is limited by phosphodiesterases (PDEs). Following stimulation of cAMP synthesis, the second messenger binds to the regulatory subunits and releases the catalytic subunits to phosphorylate target substrates, resulting in PRKA/PKA activation.

The precise molecular mechanism by which cAMP signalling regulates growth and muscle-sparing responses is not fully known; however, *in vivo* evidence suggests that it is in partly due to inhibition of muscle proteolysis (309, 310). Indeed, it was found that catecholamines play an inhibitory role in skeletal muscle proteolysis, most likely mediated by β_2-adrenergic receptors and cAMP signalling pathways (309, 310). Recent studies also demonstrated that β_2-adrenergic agonists might reduce muscle atrophy by inhibiting one of the major intracellular protein degradation pathways in skeletal muscle, the ubiquitin-proteasome system (311, 312). The cAMP/Akt pathway mediates this effect (311, 313, 314) via phosphorylation of FOXO3a and suppression of two ubiquitin E3- ligases involved in muscle atrophy, which are atrogin-1/MAFbx and MuRF1 (315–318). Furthermore, cAMP levels in muscle can be increased after treatment with PDE inhibitors, supporting the notion that the cAMP/PRKA pathway is the regulatory mechanism to prevent excessive skeletal muscle protein breakdown and atrophy (319).

The skeletal muscle has an excellent ability for functional adaptation, repair and regeneration (320). Once the muscle is damaged, precursor or satellite cells are activated to restore normal muscle structure and function; cAMP has been shown to play an important role in the regeneration in rodent models of necrotic injury (321) and Duchenne's muscle dystrophy (322). Myogenic cell differentiation and transcription activation in muscle are highly regulated by muscle-specific basic helix-loop-helix (bHLH) protein members such as Myf-5 and MyoD, as briefly described in previous sections of Chapter I (323). There are two transcription regulatory factor families responsible for regulating muscle-specific gene expression and differentiation, the muscle regulatory factors (MRFs) and the myocyte enhancer factors 2 (MEF2s) (324, 325). The MRFs (MyoD, Myf5, myogenin, and MRF4) bind to the regulatory regions of most muscle-specific genes (326); however, high levels of cAMP and PRKA have been shown to inhibit myogenic cell differentiation by repressing Myf-5 and MyoD (307). Furthermore, the MEF2 family of transcription factors (MEF2A to -D) are essential in regulating skeletal muscle differentiation (327, 328). Recent studies further revealed that PRKA specifically phosphorylates MEF2D, resulting in repression of its transactivation properties in differentiating myocytes, may also represent a PRKA-dependent myogenic repression mechanism (329).

1.9.2 AKAPS in Muscle (mAKAP)

When cAMP binds to PRKA-R subunits, it allows dissociation of PRKA-C subunits, and the latter is diffused across different compartments within the cell to phosphorylate target proteins (320). In skeletal myofibers, AKAPs compartmentalize cAMP production and PRKA activity in different subcellular locations (330). The most predominant isoforms expressed in skeletal muscle are AKAP15 (AKAP7) (331), AKAP-100/mAKAP (AKAP6) (332), Yotiao (AKAP9) (333), D-AKAP1 (AKAP1) (334) and D-AKAP2 (AKAP10) (335, 336), and myospryn (CMYA5) (337), respectively localizing PRKA to excitation-contraction coupling sites, sarcoplasmic reticulum, neuromuscular junction, mitochondria, nucleus, and costameres. Notably, in a mouse model of Duchenne's muscular dystrophy, the cAMP microdomains (338) and PRKA activity are reduced (339). This is partially a consequence of disrupted expression and myospryn's localization, which is important for interaction with costameres in the normal muscle (339).

1.9.3 Phosphodiesterase IV

PDEs are classified into 11 major families (PDE1-11), where PDE4 is the predominant member in skeletal muscle coordinating attenuation of cAMP effects (340, 341). PDE4A–PDE4D is highly specific for cAMP degradation; however, inhibition of PDE4 results in the accumulation of intracellular cAMP and, subsequently, activation of PRKA. In rodent models of diabetes (342), sepsis (343), and denervation (319), pharmacological inhibition of PDEs reduced muscle proteolysis and atrophy. Furthermore, manipulation of PDE4 activity has been demonstrated in many studies using selective inhibitors in clinical treatment against inflammatory processes such as psoriasis, psoriatic arthritis, and COPD [reviewed in (344)]. Despite its clinical relevance, PDE4 inhibitor treatment should be considered with caution, as Pde4 knockout mice present with exercise intolerance and myofiber damage after downhill running challenge (345). Additionally, there is a need for a more thorough histological and functional investigation of the PDE knockout phenotype in skeletal muscle as there is very little genetic information about specific PDE isoforms in skeletal muscle.

Recent findings suggest promising use of PDE4 inhibitors for treating metabolic disorders, such as diabetes (65). Rodent studies of T2D mouse model treated with PDE4 inhibitor Roflumilast presented elevated levels of GLP-1 boosting insulin secretion, accompanied by glucose-lowering

effects by reducing HbA1c by 50% (65). Given its promising anti-diabetic effects in mice, the selective PDE4-inhibitor TAK-648 compound was clinically tested for dose prediction of HbA1c lowering properties in humans for T2D treatment (346). In 2019, Muo et al. conducted an exploratory study where eight overweight adults with prediabetes received Roflumilast (Daliresp, Daxas) for 6 weeks, an FDA-approved PDE4 inhibitor to treat COPD (347). Despite their limited sample size due to insufficient recruitment of individuals that met the study's criteria, they concluded that Roflumilast improved insulin sensitivity most likely via increased skeletal muscle fat oxidation and weight loss, and/or via activation of incretin effects (GLP-1) (347). Furthermore, in other published Roflumilast trials with insulin resistant individuals, roflumilast induced 2 kg weight loss reduction over 3 months, along with a 0.79% reduction in HbA1c in newly diagnosed T2D patients (64, 348).

Even though PDE4 inhibitors represent a very attractive option for the treatment of T2D, mild unwanted symptoms are observed followed selective inhibition of PDE4, such as nausea, emesis, and gastrointestinal perturbations (349, 350). Therefore, further studies on the efficacy to minimize adverse effects are needed to the development of more innovative drugs.

1.9.4 Clenbuterol

Clenbuterol is an adrenergic agonist that preferentially activates the β_2-adrenergic receptor. Originally used as a bronchodilator for asthma therapy, clenbuterol has a pronounced effect on skeletal muscle (351). At the cellular level, clenbuterol can stimulate total protein synthesis (352, 353) and translational efficiency (354) as well as reduce proteolysis in rodent models (355). Clenbuterol has been demonstrated to induce muscle hypertrophy and enhance metabolism in healthy skeletal muscle and prevent disease-induced muscle atrophy associated with denervation and cancer-induced cachexia (319, 351). By activating the β_2-adrenergic receptor, clenbuterol stimulates down-stream cAMP-protein kinase A (PRKA) signalling, which induces expression of genes involved in the hypertrophy response (356). However, the metabolic phenotype observed with clenbuterol therapy remains largely unknown.

1.10 Summary

The present literature review identified a plethora of studies that identify mechanisms of insulin resistance in muscle. Additionally, it outlines important differences in insulin signalling and the development of insulin resistance in the major insulin target tissues (Figure 1.3, 1.4, 1.5). Normal insulin functioning is essential for skeletal muscle's energy expenditure and glucose metabolism. However, disruption of INSR-IRS-1-PI3K-Akt axis compromises normal insulin action in the muscle and leads to insulin resistance. Similarly, in adipose and liver tissue, disruption of the insulin signalling IRS-PI3K-Akt axis leads to severe glucose intolerance and insulin resistance.

Previous studies in both humans and rodents have established that lipid-induced insulin resistance in hepatic and skeletal muscle tissue are both dependent on the DAG-PKC axis, resulting in the phosphorylation of either IRS1 or IRS2 (104). Like the muscle and liver, adipose tissue insulin resistance plays an important role in the development of T2D (358). Studies have suggested that a disproportionate secretion of pro- and anti-inflammatory adipokines coupled with a reduction in lipolysis is concurrent with insulin resistance in adipose tissue. Specifically, impaired insulin suppression of lipolysis in adipose tissue leads to increased circulating plasma fatty acid and uptake by liver and muscle tissue leading to lipotoxic intracellular environments. These cascades ultimately prevent the translocation of GLUT4 receptors to the membrane surface of skeletal muscles and adipose tissue.

In addition, other factors, including metabolic inflexibility, mitochondrial dysfunction, mitophagy, and ER stress have all been linked to the pathogenesis of insulin resistance (Figure 1.2). As previously described, metabolic inflexibility is the inability to switch fuel sources that can consequently increase lipid levels and contribute to insulin resistance. Mitochondrial dysfunction, meanwhile, describes an increase in ROS that induces oxidative damage to the mitochondria, leading to insulin resistance. Furthermore, induced oxidative damage elicits a mitophagy response to remove damaged mitochondria, while lysosomal recruitment to mitochondria can activate MTOR-RPS6KB signalling to inhibit IRS1 (Figure 1.2). Taken as a whole, these mechanisms providing compelling evidence to the central role of lipid toxicity in insulin resistance and the downstream mechanisms are indeed intricate and interconnected. Interestingly, mitophagy genes, such as BNIP3L, Bnip3, and Fundc1, have also been associated with lipid metabolism.

CHAPTER II: Thesis Rationale and Specific Aims

An abundance of human and animal data have implicated impaired mitochondrial function as a proximal event in the development of metabolic complications associated with T2D. However, the precise cellular mechanisms linking mitochondrial dysfunction to muscle insulin resistance have historically been challenging. Lipotoxicity contributes to accumulation of myocyte diacylglycerides leading to activation of detrimental PKC signalling, which directly impairs insulin signalling, and mitochondrial impairment have been shown to be associated with muscle insulin resistance. Interestingly, mitophagy genes, such as BNIP3L, have also been linked to lipid metabolism. BNIP3L is an outer mitochondrial pro-apoptotic protein that plays an important role serving as a mitochondrial autophagy receptor and an indispensable regulator of erythropoiesis. Recent studies from our group demonstrated that BNIP3L is elevated in response to lipid-induced stress leading to mitochondrial dysfunction and impaired insulin stimulated glucose uptake (Figure 2.1). However, the precise mechanisms of BNIP3L activation of such responses are not entirely known.

Figure 2.1. BNIP3L-induced mitochondrial dysfunction and insulin resistance.

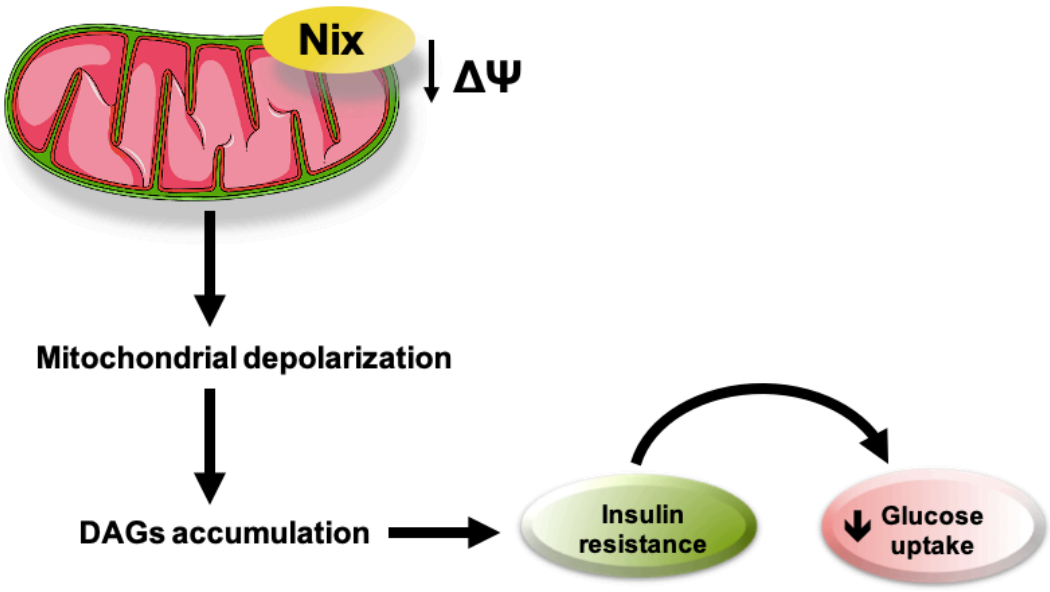

Proposed schematic showing that BNIP3L/Nix when targeted to the mitochondria leads to mitochondrial depolarization and diacylglycerol accumulation, resulting in impaired muscle insulin signalling and decreased insulin stimulated glucose uptake.

Therefore, the central hypothesis of my thesis is that "inhibition of BNIP3L/Nix function will improve mitochondrial function and insulin signaling in the skeletal muscle following diet-induced lipotoxicity". The purpose of my study is to investigate the notion that inhibition of BNIP3L function will improve mitochondrial function and insulin signalling in the skeletal muscle. This would highly contribute to the field of muscle cell biology, with the ultimate goal to characterize the molecular mechanisms underlying mitochondrial dysfunction during insulin resistance; in hopes of identifying an attractive therapeutic approach to circumvent the mitochondrial defects characteristic of insulin resistance. Figure 2.2 depicts the theoretical framework for the proposed mechanisms and signalling pathways involved.

Figure 2.2. Proposed mechanism of BNIP3L-induced mitochondrial dysfunction and muscle insulin resistance.

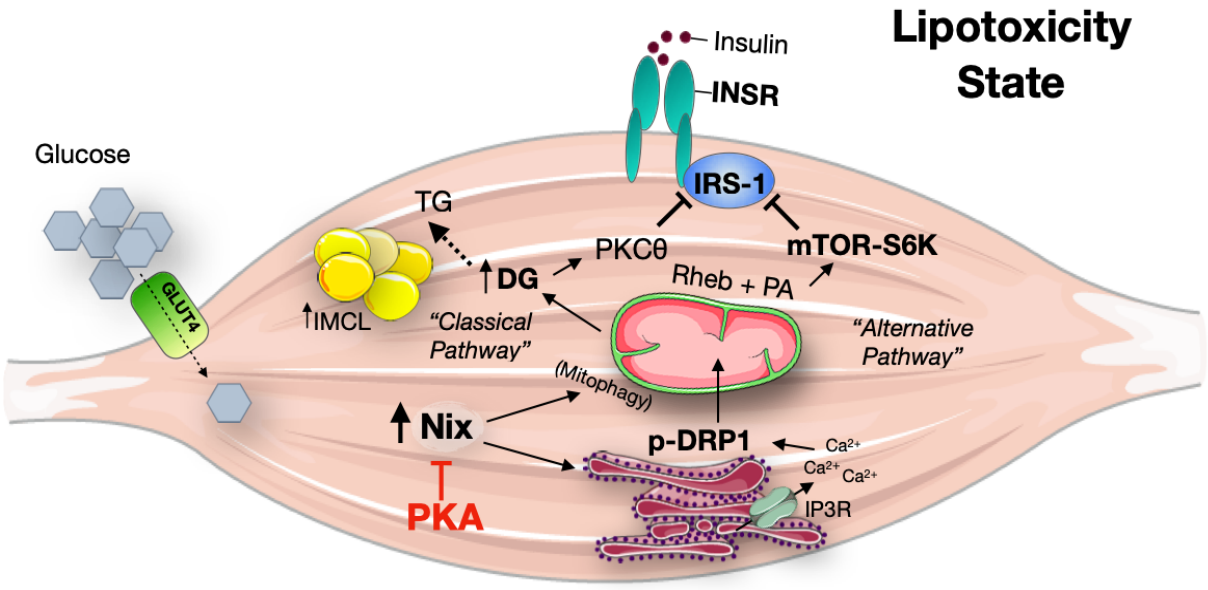

Based on the literature and our data, we propose that DAGs activate a classical pathway that leads to insulin resistance, and BNIP3L/Nix is activating an alternative pathway. In this classical pathway, DAGs accumulate and activate PKC theta and inhibit IRS1. Alternatively, DAGs also allow increased BNIP3L/Nix mitochondrial accumulation, which through its ER calcium mechanism activates DRP1 leading to mitophagy, with concurrent recruitment of Rheb GTPases and activation of MTOR-RPS6KB/mTOR-S6K in a PA dependent manner - ultimately resulting in impaired insulin-stimulated glucose uptake in the myocyte. However, we demonstrated that these BNIP3L/Nix-induced molecular defects could be averted via targeting BNIP3L/Nix through PRKA/PKA.

To achieve this purpose, my objective was to test the central hypothesis, where I first established baseline mechanistic understanding of how mitochondrial dysfunction may be playing a direct role on muscle insulin signalling, and addressed these specific hypotheses that are reported in the published comprehensive manuscript in Chapter III of this thesis:

1) BNIP3L expression alters mitochondrial morphology, mitophagy, and impairs insulin signalling.

2) PRKA phosphorylation of BNIP3L in the transmembrane domain regulates BNIP3L function.

3) YWHAB/14-3-3β regulates the subcellular localization and function of BNIP3L.

4) BNIP3L induces insulin resistance via MTOR-RPS6KB.

In this study, using a series of gain and loss-of-function approaches in rodent and human myotubes, I evaluated the role of BNIP3L accumulation and its impact on the mitochondria and elucidated the mechanisms by which BNIP3L regulates mitochondrial fission and mitophagy. I further evaluated the mechanisms by which BNIP3L-induced mitophagy impacts myotube insulin signalling. Furthermore, I identified a novel phosphorylation residue within BNIP3L, activated by PRKA, that serves to prevent BNIP3L-induced mitochondrial dysfunction and restore insulin sensitivity in cultured myotubes. Once phosphorylated, I found that BNIP3L interacts with YWHA molecular chaperones, which translocate BNIP3L from the mitochondria to the cytosol, therefore blunting BNIP3L function.

CHAPTER III: Manuscript

BNIP3L/Nix-induced mitochondrial fission, mitophagy, and impaired myocyte glucose uptake are abrogated by PRKA/PKA phosphorylation.

Simone C. da Silva Rosa[1,7,8], Matthew D. Martens[1,7,8], Jared T. Field[1,7,8], Lucas Nguyen[8], Stephanie M. Kereliuk[2,7,8], Yan Hai[8], Donald Chapman[8], William Diehl-Jones[3,8,9], Michel Aliani[5], Adrian R. West[3,8], James Thliveris[1], Saeid Ghavami[1], Christof Rampitsch[10], Vernon W. Dolinsky[2,7,8], and Joseph W. Gordon[1,6,7,8*].

Departments of Human Anatomy and Cell Science[1], University of Manitoba, Winnipeg, Canada.

Pharmacology and Therapeutics[2], University of Manitoba, Winnipeg, Canada.

Physiology and Pathophysiology[3], University of Manitoba, Winnipeg, Canada.

Biological Science[4], University of Manitoba, Winnipeg, Canada.

Human Nutritional Science[5], University of Manitoba, Winnipeg, Canada.

College of Nursing[6], University of Manitoba, Winnipeg, Canada.

The Diabetes Research Envisioned and Accomplished in Manitoba (DREAM) Theme[7].

Children's Hospital Research Institute of Manitoba (CHRIM)[8].

Faculty of Health Disciplines[9], Athabasca University, Edmonton, Canada.

Agriculture and Agrifood Canada[10], Morden, Manitoba Canada.

Running title: Phosphorylation of BNIP3L attenuates myocyte mitophagy.

Key words: insulin signaling, mitochondria, mitophagy, MTOR, muscle, BNIP3L, PRKA.

Author contribution:

SCdSR: Wrote and conceptualized manuscript, created figures, designed experiments, data analysis, Image J analysis and interpretation, cell culture, drug treatment, transfection, immunoblot, immunoprecipitation (IP), cell fractionation, fluorescent microscopy (epifluorescence and immunofluorescence), animal tissue protein sample preparation.

MDM: Assisted with fluorescent microscopy (Figure 3.1: C-D, H-N; Figure 3.4: L; Figure 3.5: H; Supplemental Figure 3.1: B, D). Assisted with developing immunoblot (Figure 3.1: G).

JTF: Assisted with fluorescent microscopy (Figure 3.1: A-B; Figure 3.2: H).

LN: Transfection and Co-IP (Figure 3.5: B, D). Transfection and fluorescent microscopy (Figure 3.4: K; Supplemental Figure 4: C).

SMK: Isolated soleus tissue from the insulin resistant rodent model used in (Figure 3.2: A; Figure 3.3: K; Supplemental Figure 3.2: B).

YH: Assisted with Co-IP (Figure 3.5: C) and cellular fractionation (Figure 3.5: A, E).

DC: In vitro kinase assay (Figure 3.3: A-B, H). Gene expression array (Supplemental Table 3.6). Assisted with phosphatidic acid assay (Figure 3.6: F). Assisted with soleus tissue preparation used in (Figure 3.2: A; Figure 3.3: K; Supplemental Figure 3.2: B) and in metabolomics and gene expression array (Supplemental Table: 3.1-3.6).

WDJ: Reviewed and edited manuscript.

MA: LC-MS metabolomics (Supplemental Table: 3.1-3.6).

ARW: Provided FRET imaging equipment used in (Figure 3.2: J; Figure 3.6: G).

JT: Assisted with electron microscopy imaging (Figure 3.4: G).

SG: Provided antibodies and technical expertise on autophagy (Supplemental Figure 3.2: A-B).

CR: Mass-spectrometry (Figure 3.3: C-G).

VWD: Generated diet-induced insulin resistant rodent model used in (Figure 3.2: A; Figure 3.3: K; Supplemental Figure 3.2: B) and in metabolomics and gene expression array (Supplemental Table: 3.1-3.6). Supervision and financial support of SMK.

JWG*: Generation of Myc-BNIP3L-S212A and Myc-BNIP3L-S212D constructs. Bioinformatics (Figure 3.3: A-B, H). Phospho-peptide mapping (Figure 3.3: C-G). Advisor and corresponding author: conceptualized and wrote manuscript.

3.1 Abstract

Lipotoxicity is a form of cellular stress caused by the accumulation of lipids resulting in mitochondrial dysfunction and insulin resistance in muscle. Previously, we demonstrated that the mitophagy receptor BNIP3L/Nix is responsive to lipotoxicity and accumulates in response to a high-fat (HF) feeding. To provide a better understanding of this observation, we undertook gene expression array and shot-gun metabolomics studies in soleus muscle from rodents on an HF diet. Interestingly, we observed a modest reduction in several autophagy-related genes. Moreover, we observed alterations in the fatty acyl composition of cardiolipins and phosphatidic acids. Given the previously reported roles of these phospholipids and BNIP3L in mitochondrial dynamics, we investigated aberrant mitochondrial turnover as a mechanism of impaired myocyte insulin signaling. In a series of gain-of-function and loss-of-function experiments in rodent and human myotubes, we demonstrate that BNIP3L accumulation triggers mitochondrial depolarization, calcium-dependent activation of DNM1L/DRP1, and mitophagy. In addition, BNIP3L can inhibit insulin signaling through activation of MTOR-RPS6KB/p70S6 kinase inhibition of IRS1, which is contingent on phosphatidic acids and RHEB. Finally, we demonstrate that BNIP3L-induced mitophagy and impaired glucose uptake can be reversed by direct phosphorylation of BNIP3L by PRKA/PKA, leading to the translocation of BNIP3L from the mitochondria and sarcoplasmic reticulum to the cytosol. These findings provide insight into the role of BNIP3L, mitochondrial turnover, and impaired myocyte insulin signaling during an overfed state when overall autophagy-related gene expression is reduced. Furthermore, our data suggest a mechanism by which exercise or pharmacological activation of PRKA may overcome myocyte insulin resistance.

3.2 Introduction

Skeletal muscle insulin resistance is one of the earliest detectable perturbations in the natural progression of type 2 diabetes, as muscle insulin resistance often precedes and may contribute to hepatic steatosis, as well as adipocyte and beta cell dysfunction [reviewed in (359–361)]. Although the cellular mechanisms responsible for muscle insulin resistance have been historically challenging to uncover, and are likely unique from the mechanisms responsible for insulin resistance in other tissues, ectopic lipid accumulation and mitochondrial dysfunction appear to be key factors contributing to the development of muscle insulin resistance in humans and in rodent models of obesity and type 2 diabetes (359–361). However, the exact nature of this mitochondrial defect, and how mitochondrial dysfunction impacts insulin signaling and glucose uptake in muscle, remain poorly understood.

Lipotoxicity is a form of cellular stress caused by the accumulation of lipid intermediates, contributing to the onset of insulin resistance (359, 361, 362). Lipid infusion studies in humans, and high-fat feeding in rodents have demonstrated that muscle tissue rapidly accumulates diacylglycerols, ceramides, and triglycerides in response to these lipid exposures (359, 361). Accumulation of diacylglycerols activate novel PRKC/PKC signaling, including PRKCD/PKCδ and PRKCQ/PKCθ (363–367). Importantly, PRKCQ/PKCθ has been shown in both human and rodent studies to phosphorylate and inhibit the IRS1 (insulin receptor substrate 1) to prevent insulin-mediated AKT2 activation and SLC2A4/GLUT4-dependent glucose uptake, where a key residue involved in human IRS1 inhibition is Ser1101 (368). This pathway may protect myocytes from metabolic stress, by preventing further influx of glucose and/or lipids (369).

Macroautophagy/autophagy is a lysosomal degradation pathway that functions in organelle and protein quality control. During cellular stress, increased levels of autophagy permit cells to adapt to changing nutritional and energy demands through catabolism (370–374). Although originally described as a cellular response to starvation, autophagy also protects against insulin resistance in fed animals (375). Acute exercise induces autophagy in skeletal muscle, while transgenic mice harboring a BCL2 mutant preventing autophagy induction display decreased exercise tolerance and altered glucose metabolism during acute exercise (375). Furthermore, exercise fails to protect these mice from high fat diet-induced insulin resistance (375). More recent

evidence suggests that autophagy can be selectively targeted to specific cellular structures, such as mitochondria, and mitochondrial proteins that contain an LC3 interacting region (LIR) can serve as selective mitochondrial autophagy receptors (i.e., mitophagy receptors) (376, 377). A recent study has demonstrated that a skeletal muscle restricted deletion of a hypoxia-inducible mitophagy receptor, called FUNDC1, blunts the mitophagy response and protects against high fat feeding-induced insulin resistance at the expense of exercise tolerance, suggesting that mitophagy may be a contributing factor in muscle insulin resistance. However, FUNDC1 is hypoxia-inducible and has not been shown to be activated by lipotoxicity; thus, other mitophagy receptors may serve to trigger selective autophagy of dysfunctional mitochondria in a fed lipotoxic state when generalized autophagy is inhibited (378, 379).

Mitochondrial quality control also involves dynamic fission and fusion events that serve to compartmentalize dysfunctional or depolarized mitochondrial fragments that can be targeted for autophagic degradation (377, 380). Mitochondrial fission and fusion are regulated by a family of GTPases, where DNM1L/DRP1 initiates mitochondrial fission, and MFN1 (mitofusin 1), MFN2, and OPA1 regulate fusion (377, 380). Moreover, lipotoxicity-induced muscle insulin resistance has been associated with mitochondrial fission and activation of DNM1L (381). Interestingly, phospholipids such as phosphatidic acid and cardiolipin, regulate mitochondrial fission and fusion, where cardiolipin facilitates fusion through and interaction with OPA1, and mitochondrial phosphatidic acids interact with DNM1L (382–384). In muscle, phosphatidic acids also regulate MTOR signaling during times of growth (385). MTOR signaling potently inhibits autophagy in a fed state, and is involved in a negative-feedback pathway that limits glucose uptake through MTOR-RPS6KB (p70S6 kinase)-mediated phosphorylation of IRS1 (386, 387). However, it remains to be determined how these interconnected signaling pathways contribute to muscle insulin resistance.

Previously, we described a lipotoxicity-activated signaling pathway leading to increased expression of the mitophagy receptor BNIP3L/Nix (388). This conserved pathway responds to elevated diacylglycerols by activating PRKCD which inhibits the expression of microRNA-133a, a negative regulator of BNIP3L expression. Furthermore, we established that BNIP3L expression is elevated in muscle tissue of rodents fed a high fat diet (HF) (388).

3.3 Experimental Overview and Rationale

In order to further explore the role of BNIP3L and mitochondrial dysfunction associated with muscle insulin resistance, we undertook an unbiased gene expression array and a shot-gun metabolomics screen in soleus muscle from rodents on a low fat (LF) or HF diet. We observed a decrease in the most abundant tetralinoleoyl-cardiolipin species and an increase in phosphatidic acids, concurrent with increased BNIP3L expression, suggesting altered mitochondrial dynamics and/or mitophagy contribute to muscle insulin resistance. Using two myocyte cell lines, and human myotubes differentiated from induced pluripotent stem cells (iPSCs), we mechanistically determined that BNIP3L accumulation triggers calcium-dependent activation of DNM1L and mitophagy. In addition, BNIP3L expression can impair insulin signaling in myotubes through MTOR-dependent inhibition of IRS1. Finally, we demonstrate that BNIP3L-induced mitophagy and impaired insulin signaling can be reversed by direct phosphorylation of BNIP3L by PRKA/PKA, leading to the translocation of BNIP3L from the mitochondria and sarcoplasmic reticulum to the cytosol. These findings are consistent with a model whereby BNIP3L responds to myocyte lipotoxicity in order to clear damaged mitochondria through receptor-mediated mitophagy and protect the myocyte against nutrient storage stress by activating MTOR-dependent desensitization of insulin signaling. In-depth analysis and evidence to support these claims are presented and described in the following results sections.

3.4 Results

3.4.1 Metabolomics and gene expression screen

Numerous lipid species were elevated in soleus muscle with HF feeding, including diacylglycerols, ceramides, and triglycerides **(Table 3.1 and Table S3.1-3.6)**. Interestingly, we also observed alterations in the composition of cardiolipin. Cardiolipin is normally found in the inner mitochondrial membrane and uniquely contains four acyl chains, where the tetra-linoleoyl (18:2) cardiolipin is the most abundant species. Interestingly, we observed a reduction in this species of cardiolipin with HF feeding **(Table 3.1)**. We also observed an increase in numerous phosphatidic acid species **(Table 3.1)**. To further explore the relationship between lipotoxicity and skeletal muscle autophagy, we performed a PCR-based array on soleus muscle from rats fed a LF or HF diet. We observed a modest reduction in several autophagy-related genes including Beclin-1, ATG3, -5, -12 and Atp6v1g2 in HF fed animals **(Table 3.1 and Table S3.1-3.6)**. These observations suggested that global autophagy-related gene expression is reduced in soleus muscle during a high fat diet.

Table 3.1. Representative metabolites and mRNAs altered by HF feedings.

Metabolite		Fold Change
Triacylglyceride		
	TG(22:3/22:6/22:6)	474
	TG(21:0/22:0/22:3)	225
	TG(20:0/22:0/22:6)	252
Diacylglyceride		
	DG(22:3/22:6)	315
	DG(22:2/24:1)	685
	DG(20:5/22:4)	380,753
	DG(20:4/22:6)	6177
	DG(20:1/18:0)	389
	DG(20:0/22:1)	209
	DG(18:4/22:6)	500
	DG(16:0/18:0)	8408
Ceramides		
	Ceramide (d18:1/26:0)	205
	Cer(t18:0/16:0)	5830
	Cer(d18:2/20:1)	298
	Cer(d18:2/14:0)	283
	Cer(d16:2/20:1)	122,962
Cardiolipins (CL)		
	CL(18:2/18:2/18:2/18:2)	0.003
Phosphatidic acids (PA)		
	PA(20:0/22:6)	19,843
	PA(20:0/18:2)	510
	PA(20:3/21:0)	518
	PA(19:0/20:0)	12,389
Genes		Fold Change
	Atg12	0.82
	Atg3	0.86
	Atg5	0.73
	Atp6v1g2	0.39
	Becn1	0.84
	Cs	0.80
	Mb	0.48
	Myh1	0.38
	Ppargc1a	0.65

3.4.2 BNIP3L expression alters mitochondrial morphology, mitophagy, and impairs insulin signaling

Given our previous findings that BNIP3L is induced in this rodent model (388), and that phospholipids have been implicated in both mitochondrial dynamics and MTOR signaling, we investigated the role of BNIP3L in regulating aspects of mitochondrial quality control following exposure to lipotoxicity. To begin, we expressed BNIP3L in C2C12 myoblasts and monitored mitochondrial morphology using a mitochondrial-targeted Emerald fluorophore (Mito-Emerald). In control cells we observed predominately elongated mitochondria; however, in cells expressing BNIP3L we observed a decrease in elongated mitochondria and increases in mitochondria with an intermediate or 'fissioned' morphology and increases in overt mitochondrial fragmentation with a more pronounced perinuclear distribution **(Figure 3.1A,B)**. In addition, expression of BNIP3L in both C2C12 and L6 myoblasts resulted in a significant decrease in mitochondrial membrane potential, determined by TMRM staining **(Figure 3.1C,D)**. Previously, we demonstrated that BNIP3L-induced mitochondrial depolarization in cardiomyocytes was due to ER/SR-dependent calcium release and subsequent mitochondrial permeability transition (389). Thus, we examined both steady-state ER/SR and mitochondrial calcium content in cells expressing BNIP3L using organelle-targeted calcium biosensors called GECOs (390–392). We observed that BNIP3L expression reduced steady-state ER/SR calcium and increased steady-state mitochondrial calcium **(Figure 3.1E,F)**. Furthermore, treatment of C2C12 cells with an IP3-receptor blocker (2APB) prevented BNIP3L-induced mitochondrial depolarization **(Figure S3.1A)**. Previous work has identified that the mitochondrial fission protein DNM1L is activated by PPP3CA/calcineurin, a calcium-calmodulin dependent phosphatase (393). Thus, we determined if BNIP3L-induced ER/SR calcium release could result in DNM1L dephosphorylation at a known PPP3CA site (mouse Ser643; human Ser637). In C2C12 cells expressing BNIP3L, we observed a reduction in Ser643 phosphorylation, compared to control cells **(Figure 3.1G)**. As mitochondrial fission and loss of membrane potential are important precursor events leading to mitochondrial autophagy, we evaluated mitophagy using a mitochondrial matrix-targeted pH biosensor called Mito-pHRed (394). BNIP3L expression in L6 and C2C12 myoblasts and myotubes increased Mito-pHRed fluorescence **(Figure 3.1H,J)**. As positive and negative controls, we expressed PRKN/Parkin and Mito-pHRed and observed increased fluorescence, while expression of a dominant-negative ATG5 prevented BNIP3L-induced Mito-pHRed activation **(Figure S3.1B,C)**. BNIP3L expression also

increased the number of GFP-LC3 puncta and the formation of LC3-II **(Figure S3.1D-F)**, and increased the colocalization of LysoTracker Red and Mito-Emerald **(Figure S3.1G)** and LAMP1 and TOMM20 by immunofluorescence **(Figure S3.2A)**. Moreover, BNIP3L-induced Mito-pHRed activation was prevented by a dominant-negative DNM1L, the mitochondrial fission inhibitor mdivi-1, and the lysosomal inhibitor bafilomycin A_1 **(Figure 3.1K,L)**.

To further delineate the role of BNIP3L as a mitophagy receptor at the mitochondria and as a regulator of calcium release at the ER/SR in our models, we utilized organelle-targeted BNIP3L constructs, as described previously (389). Interestingly, mitochondrial targeted BNIP3L constructs, using either the monoamine oxidase-B (BNIP3L-MaoB) or the *Listeria* ActA (BNIP3L-ActA) targeting domains, had little to no effect on Mito-pHRed activation; whereas, ER/SR targeted BNIP3L using the CYB5 (cytochrome b5; BNIP3L-CYB5) targeting domain had a similar effect to wild-type BNIP3L **(Figure 3.1M)**. In addition, we observed that both BNIP3L and BNIP3L-CYB5-induced Mito-pHRed activation was prevented with the IP3-receptor blocker 2APB **(Figure 3.1N)**. Finally, we observed that BNIP3L expression led to enhanced phosphorylation of IRS1 using the phospho-specific Ser1101 antibody and prevented downstream AKT(Ser473) phosphorylation **(Figure 3.1O)**. In addition, BNIP3L expression prevented insulin-stimulated glucose uptake, determined by 2NBDG fluorescence **(Figure 3.1P)**. Collectively, our findings suggest that in addition to its role as a mitophagy receptor, BNIP3L regulates mitochondrial fission through its effects on ER/SR calcium, and is also a regulator of insulin signaling.

Next, we confirmed that BNIP3L expression is elevated in soleus muscle of rats fed a HF diet compared to those fed a LF diet, concurrent with decreased phosphorylation of DNM1L **(Figure 3.2A)**. We also observed that SQSTM1 levels increased with HF feeding and LC3-II levels decreased, suggesting that autophagy in soleus muscle is inhibited by this diet **(Figure S3.2B)**.

Figure 3.1. BNIP3L regulates mitochondrial dynamics and mitophagy.

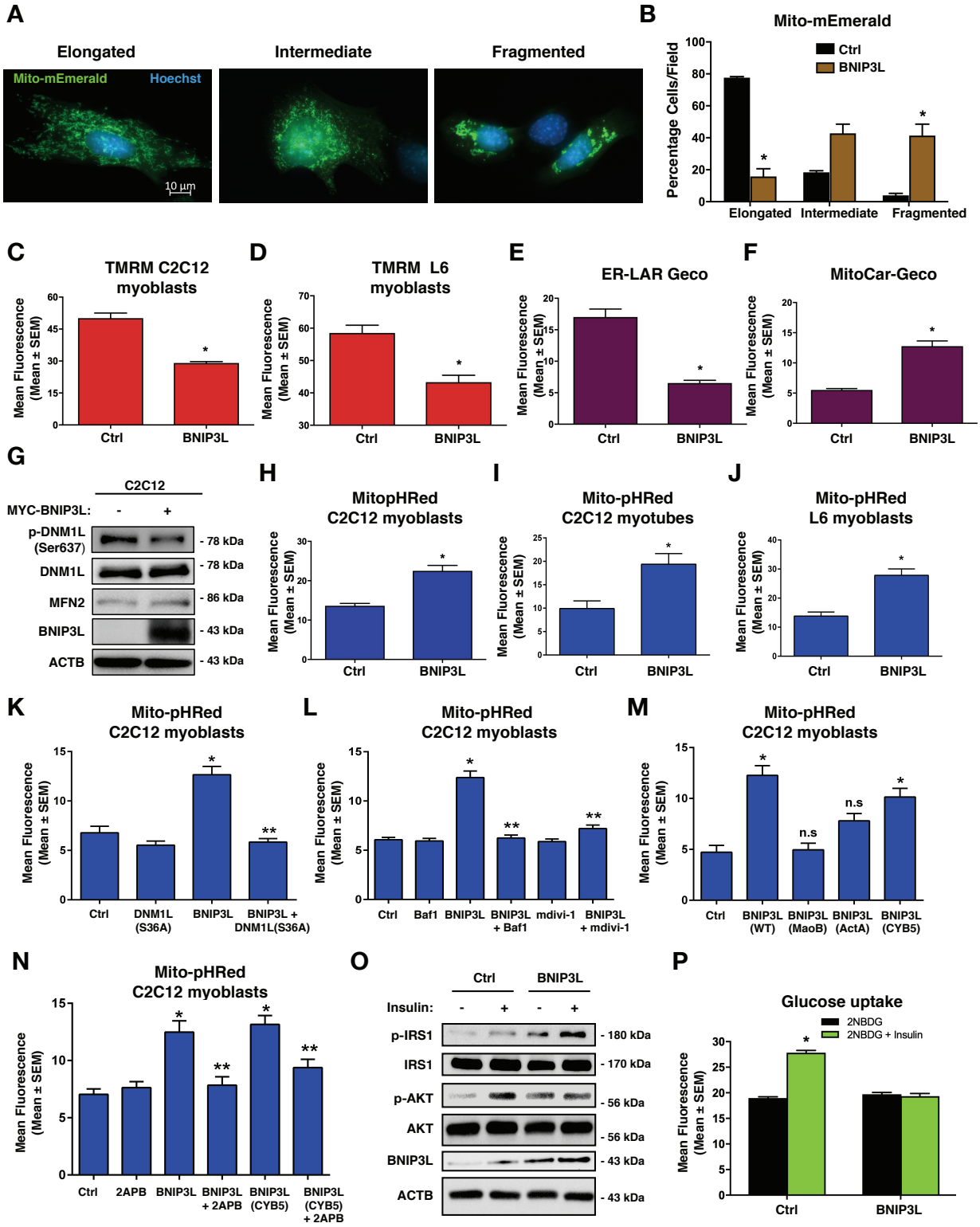

Figure 3.1. BNIP3L regulates mitochondrial dynamics and mitophagy. (**A-B**) C2C12 myoblast cells were transfected with Mito-mEmerald to assess mitochondrial morphology (left). Quantification of C2C12 myoblast cells transfected with BNIP3L or empty vector control (right). (**C-D**) Quantification of C2C12 myoblast cells (**C**) or L6 myoblasts (**D**) transfected with BNIP3L or an empty vector control; stained with TMRM. (**E**) Quantification of C2C12 myoblasts transfected with ER-LAR-GECO, BNIP3L, or an empty vector control. (**F**) Quantification of C2C12 myoblasts transfected with Mito-CAR-GECO, BNIP3L, or an empty vector control. (**G**) C2C12 cells were transfected with BNIP3L or empty vector. Protein extracts were analyzed as indicated. (**H-J**) Quantification of (**H**) C2C12 myoblasts, (**I**) C2C12 myotubes, and (**J**) L6 myoblasts cells transfected with BNIP3L, Mito-pHRed, or an empty vector control. (**K**) C2C12 cells were transfected with Mito-pHRed, BNIP3L, a dominant negative DNM1L/Drp1 (S36A), or an empty vector control and quantified. (**L**) C2C12 cells were transfected with Mito-pHRed, BNIP3L, or an empty vector control. Cells were treated with Bafilomycin (6 nM, 3 h) or with the mitochondrial fission inhibitor (mdivi-1, 20 μM, 1 h). (**M**) Quantification of C2C12 myoblast cells transfected with Mito-pHRed, BNIP3L, mitochondrial targeted BNIP3L fusion constructs BNIP3L-MaoB or BNIP3L-ActA, the ER/SR targeted BNIP3L construct BNIP3L-CYB5, or an empty vector control. (**N**) C2C12 myoblast cells were transfected with Mito-pHRed, BNIP3L, BNIP3L-CYB5, or an empty vector control. Cells were treated with 2-aminoethoxydiphenyl borate (2APB 10 μM, 1 h), or DMSO as control vehicle and quantified. (**O**) L6 myotubes were transfected with BNIP3L or empty vector followed by 15 min of insulin stimulation (10 nM). Protein extracts were analyzed as indicated. (**P**) L6 myotubes were transfected with BNIP3L or an empty vector control. Insulin stimulated glucose uptake (10 nM) was determined by 2NBDG fluorescence and quantified. Data are represented as mean ± S.E.M. *$P < 0.05$ compared with control, while **$P < 0.05$ compared with treatment, determined by 1-way or 2-way ANOVA.

Figure 3.2. Knockdown of BNIP3L improves mitochondrial function and insulin sensitivity in response to prolonged palmitate exposure.

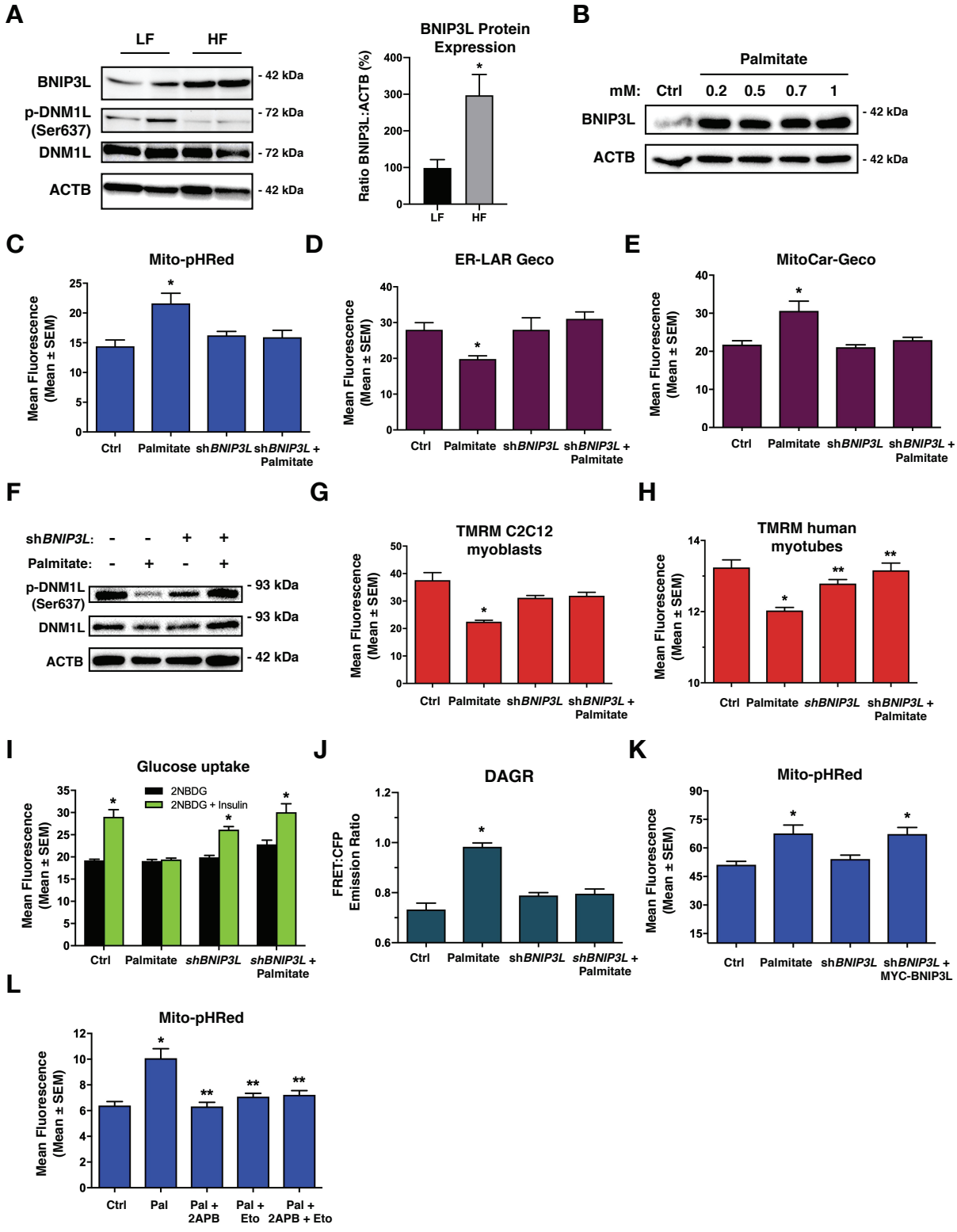

Figure 3.2. Knockdown of BNIP3L improves mitochondrial function and insulin sensitivity. (**A**) Western blot analysis of rat soleus muscle exposed to high fat (HF) or low fat (LF) diet for 12-weeks (left). Quantification of BNIP3L expression relative to actin (n=4)(right). (**B**) C2C12 myoblast cells were treated overnight with increasing doses of palmitate conjugated to 2% albumin in low-glucose media. Protein extracts were analyzed as indicated. (**C**) C2C12 myoblast cells were transfected with Mito-pHRed, sh*BNIP3L*, or a scrambled control shRNA. Cells were treated overnight with palmitate (200 μM). (**D**) Quantification of C2C12 myoblasts transfected with ER-LAR-GECO and treated as in (**C**). (**E**) Quantification of C2C12 myoblast cells transfected with Mito-CAR-GECO and treated as in (**C**). (**F**) C2C12 myoblast cells were transfected with sh*BNIP3L* or a scrambled control shRNA, followed by palmitate treatment as described in (**C**). Protein extracts were analyzed as indicated. (**G**) C2C12 myoblast and (**H**) human myotube cells were transfected with sh*BNIP3L* or a control shRNA. Cells were treated overnight with palmitate as in (**C**), stained for TMRM and quantified. (**I**) L6 myotubes were transfected with sh*BNIP3L* or a control shRNA. Cells were treated overnight with palmitate as in (**C**). Insulin stimulated glucose uptake (10 nM) was determined by 2NBDG fluorescence and quantified. (**J**) C2C12 myoblast cells as transfected as in (**H**), along with DAGR, a diacylglycerol biosensor. Cells were analyzed by using the emission ratio of YFP:CFP (FRET Ratio). (**K**) Quantification of C2C12 myoblast cells transfected as in (**H**), along with MYC-BNIP3Land treated as in (**C**). (**L**) C2C12 cells were transfected with Mito-pHRed. Cells were pre-treated overnight with etomoxir (100 μM) and palmitate, as described in (**C**), followed by co-treatment with 2APB (10 μM, 2 h) or DMSO as control vehicle and quantified. Data are represented as mean ± S.E.M. *$P < 0.05$ compared with control, while **$P < 0.05$ compared with treatment, determined by t-test, 1-way or 2-way ANOVA.

Interestingly, other markers of mitophagy, such as BNIP3, BCL2L13, FUNDC1, and RHEB, were unchanged or modestly decreased in HF fed rodents, while FKBP8/Fkbp38 and PRKN were increased **(Figure S3.2B)**. We also evaluated if PRKN activation could be downstream of BNIP3L induction, but BNIP3L expression failed to promote the mitochondrial localization of PRKN-YFP **(Figure S3.2C)**. In culture, we used palmitate treatment to induce lipotoxicity and performed a dose-response in C2C12 cells. BNIP3L expression was increased by 0.2 mM palmitate and plateaued at higher concentrations **(Figure 3.2B)**. Palmitate treatment also increased the number of GFP-LC3 puncta in C2C12 cells **(Figure S3.1E)**. Furthermore, palmitate treatment increased Mito-pHRed fluorescence, which was inhibited by knock-down of BNIP3L (sh*BNIP3L*)**(Figure 3.2C)**. Knock-down of BNIP3L also prevented palmitate-induced ER/SR calcium release and mitochondrial calcium accumulation **(Figure 3.2D,E)**, which were also blocked by 2APB treatment **(Figure S3.2D,E)**. Furthermore, palmitate treatment decreased DNM1L phosphorylation at the PPP3CA regulated residue and led to mitochondrial fission, which were restored by sh*BNIP3L* **(Figure 3.2F, Figure S3.2F)**. In addition, BNIP3L knock-down prevented palmitate-induced mitochondrial depolarization in both C2C12 cells and iPSC-derived human myotubes **(Figure 3.2G,H)**, and restored insulin-stimulated glucose uptake following palmitate exposure **(Figure 3.2I)**. Using a diacylglycerol biosensor called DAGR (395), we observed that palmitate treatment increased FRET emission, which was reversed by BNIP3L knock-down **(Figure 3.2J)**, suggesting a connection between mitochondrial function and diacylglycerol accumulation. To test the specificity of sh*BNIP3L*, we treated C2C12 myoblasts with palmitate and observed an increase in Mito-pHRed fluorescence, which was prevented when cells expressed sh*BNIP3L*, but was restored by co-expression of a MYC-tagged BNIP3L (MYC-BNIP3L)**(Figure 3.2K)**. Finally, we observed that palmitate-induced mitophagy was prevented by 2APB and with etomoxir, an inhibitor of mitochondrial fatty acid uptake through carnitine palmitoyltransferase-1 **(Figure 3.2L)**, consistent with the notion that fatty acid-induced mitochondrial overload may be important trigger for mitophagy.

3.4.3 Identification and characterization of a novel PRKA phosphorylation site in the transmembrane domain of BNIP3L

Next, we explored whether BNIP3L function was directly regulated by cellular signaling pathways to modulate mitophagy and insulin signaling. *In silico* analysis of the BNIP3L amino acid sequence identified a conserved PRKA consensus motif within the carboxy-terminus of the transmembrane domain **(Figure 3.3A,B)**, which is Serine-212 (Ser212) in human BNIP3L. We engineered synthetic peptides spanning the BNIP3L transmembrane domain and subjected them to *in vitro* kinase reaction with the catalytic subunit of PRKA and analyzed peptides by ion trap mass spectrometry. In the absence of kinase, single ion monitoring (SIM) scans displayed a predominant peak at m/z of 857.28 (z=2+)**(Figure 3.3C)**. Following kinase incubation, this peak shifted by m/z of 40 (897.78, z=2+), corresponding to the addition of a phosphate (PO_3) to the peptide (Mass = 80.00 Da)**(Figure 3.3D)**. However, when Ser212 was mutated to a neutral alanine (S212A) this m/z shift was eliminated **(Figure 3.3E)**. Next, we analyzed the MS^2 spectra produced by collision-induced dissociation (CID) of the precursor ion with m/z = 897.78 (z=2+). CID of the phospho-peptide yielded a product-ion with m/z of 848.67 (delta = 49.11), consistent with the neutral loss of phosphorylation (98/2 = 49; **Figure 3.3F**). We also evaluated if our BNIP3L peptide could be phosphorylated at more than one site; however, we did not detect an m/z shift equivalent to 160 Da **(Figure 3.3G)**. We modeled the BNIP3L structure using the Phyre^2 engine **(Figure 3.3H**). Using known 3D motifs, Phyre^2 predicted that Ser212 was exposed within the transmembrane domain, and likely well-positioned for kinase recognition.

Next, we used a custom antibody designed to specifically detect phosphorylated Ser212 of BNIP3L (p-BNIP3L). Following treatment of C2C12 cells with forskolin (FSK) or a cAMP analog, we detected a band that aligned with transfected MYC-tagged BNIP3L, which migrates slightly above the 43-kDa molecular mass marker **(Figure 3.3I and Figure S3.3A)**. However, when Ser212 was mutated to a neutral alanine, this band was lost **(Figure 3.3I)**. While investigating the endogenous expression of p-BNIP3L, we observed a notable cell-type specific pattern by western blot. BNIP3L has a predicted molecular weight of 26-kDa, but has been observed to migrate on SDS-PAGE as a 40-kDa monomer, and an 80-kDa dimer (388, 396, 397). In both C2C12 and L6 myoblasts, the dominant p-BNIP3L band migrated close to the predicted weight of BNIP3L **(Figure S3.3B-D)**. This band was also sensitive to H89 treatment and was substantially reduced in cells expressing an shRNA targeting *BNIP3L* **(Figure S3.3C,D)**.

However, in the human rhabdomyosarcomal cell lines (RH30 and A204), the p-BNIP3L antibody detected multiple bands spanning 40-80-kDa, while in human iPSC-derived myoblasts the dominant band migrated at the predicted dimer weight **(Figure S3.3B)**. These observations suggest that BNIP3L is likely exposed to other post-translational modifications, and that these modifications occur in a cell-type or species-specific manner. Next, to validate if we could modulate PRKA-induced Bnip3L phosphorylation pharmacologically, we performed a series of time-courses experiments with pharmacological agents known to activate PRKA signaling in muscle. We used the adrenergic agonist clenbuterol and the PDE4 (phosphodiesterase 4) inhibitor (PDE4i) cilomilast. Both of these agents increased p-BNIP3L expression peaking at 2 h and returning to control levels by 12-18 h **(Figure 3.3J and Figure S3.3E)**, and we confirmed they activated PRKA in C2C12 myoblasts **(Figure S3.4A,B)**. In addition, expression of PRKA and treatment of C2C12 cells with clenbuterol prevented BNIP3L-induced mitochondrial depolarization **(Figure S3.4C)**. Lastly, we probed soleus muscle extracts from rodents fed a LF or HF diet. In rodent muscle we observed three dominant p-BNIP3L bands; a predicted 26-kDa, a 52-kDa dimer band, and a 40-kDa band that aligned with monomeric BNIP3L. The 40-kDa band is likely more detectable in muscle tissue as total BNIP3L expression is much greater in muscle tissue compared to C2C12 and L6 myoblasts. In addition, we observed that the 26-kDa band and the dimer band were reduced with HF feeding **(Figure 3.3K)**, while the 40-kDa band more closely followed monomeric BNIP3L expression. Based on the positioning of the phospho-residue within the transmembrane domain of BNIP3L, we hypothesized that Ser212 is an inhibitory phosphorylation site.

Figure 3.3. PRKA phosphorylates BNIP3L at Ser212.

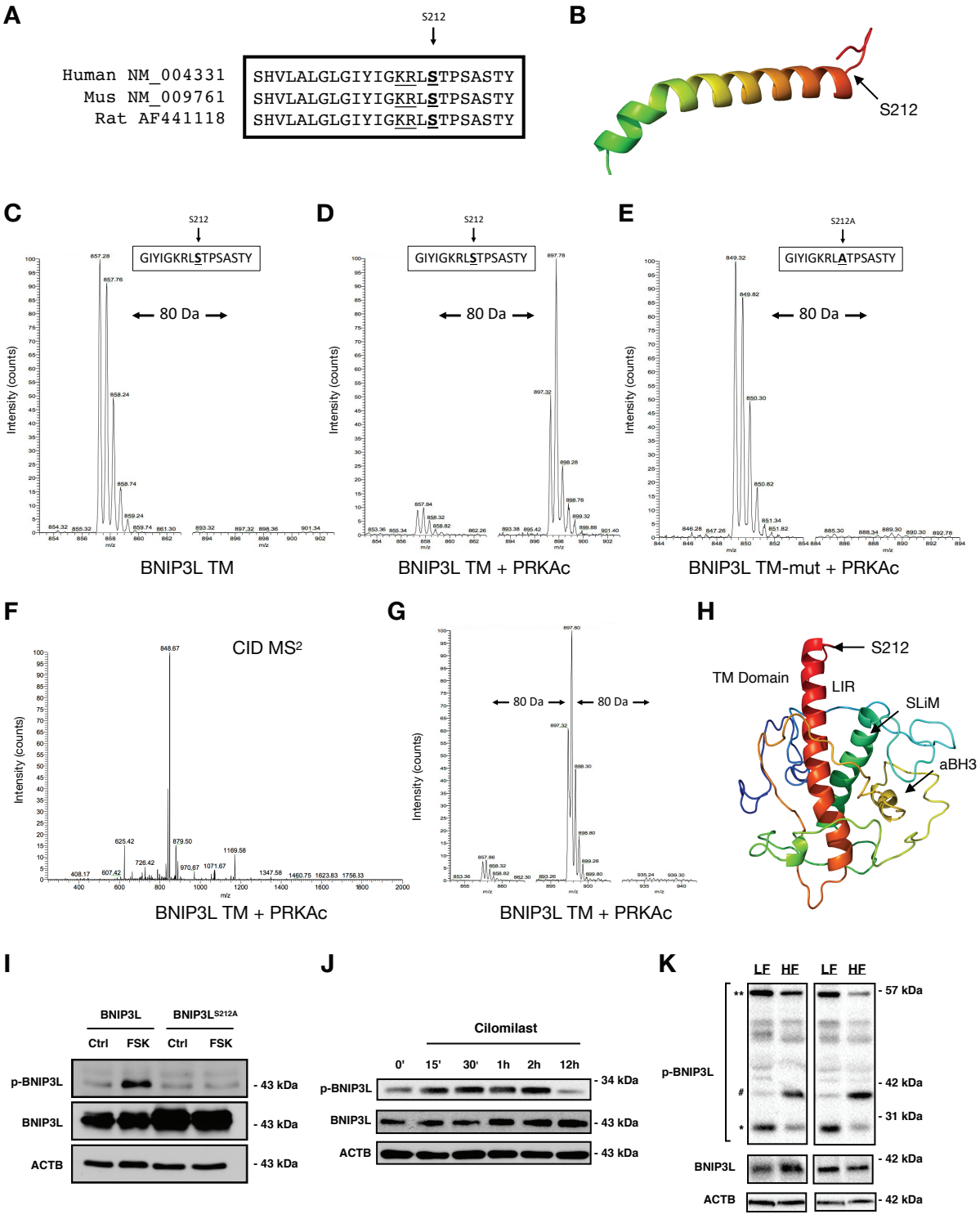

Figure 3.3. PRKA phosphorylates BNIP3L at Ser212. (**A**) Amino acid sequence alignment for human, mouse and rat BNIP3L. (**B**) Schematic BNIP3L transmembrane domain and the location of Ser212. (**C**) SIM scan of the wild-type peptide spanning the PRKA site of BNIP3L. The unphosphorylated peptide has 857.28 m/z (z=2+). (**D**) Putative phosphorylation showing an increased m/z of 40 that corresponds to PO_3 (M=80.00 Da). (**E**) SIM scan of mutated peptide (S212A) incubated with kinase, as in (**D**). (**F**) MS^2 spectra following collision-induced dissociation of the precursor ion in (D, m/z=897.78). A neutral loss of 49 m/z confirms phosphorylation. (**G**) SIM scanning showing BNIP3L peptide is not phosphorylated at two residues within the peptide. (**H**) BNIP3L structure modeled using Phyre2 engine. (**I**) 3T3 cells were transfected with wild type BNIP3L or a BNIP3L mutant where Ser212 is converted to alanine (S212A) and treated with 10 μM forskolin for 2 h. Protein extracts were immunoblotted, as indicated. (**J**) C2C12 myoblast cells were treated with 10 μM cilomilast or vehicle for multiple time points. Protein extracts were immunoblotted, as indicated. (**K**) p-BNIP3L is decreased as total BNIP3L increases in soleus muscle of rodents treated with high fat (HF) or low fat (LF) diet for 12-weeks. *predicted molecular weight, **predicted dimer weight, $^{\#}$aligned with total BNIP3L.

Figure 3.4. Clenbuterol and cilomilast inhibit palmitate-induced mitochondrial defects.

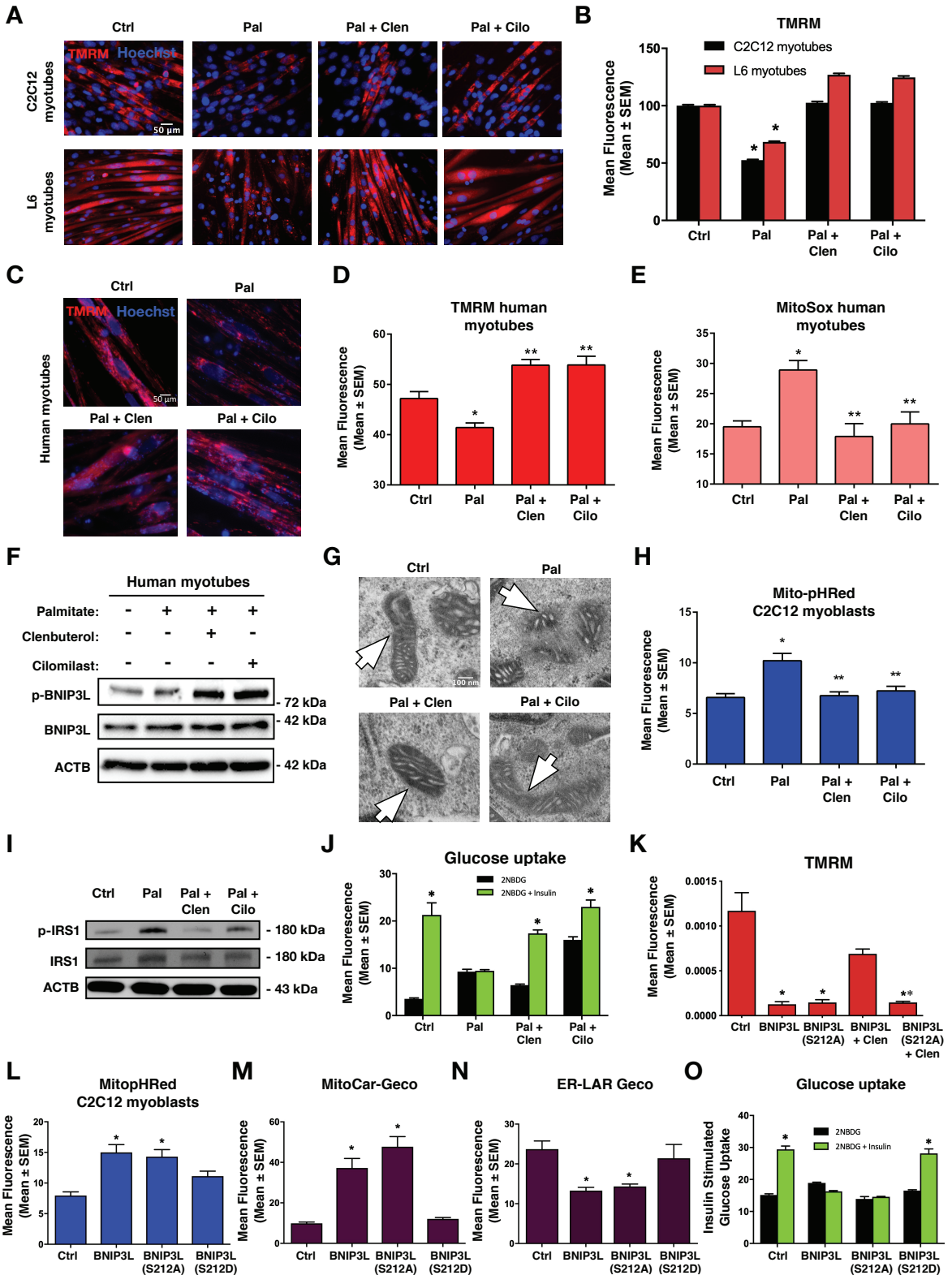

Figure 3.4. Clenbuterol and cilomilast inhibit palmitate-induced mitochondrial defects. (**A**) 5-day differentiated C2C12 myotubes and L6 myotubes were treated overnight with palmitate (200 μM) conjugated to 2% albumin in low glucose media. Control cells were treated with 2% albumin alone. Myotubes were treated with clenbuterol (500 nM, 2 h), cilomilast (10 μM, 2 h) or DMSO control vehicle and stained with TMRM (red) and Hoechst (blue) and imaged by standard fluorescence microscopy. (**B**) Quantification of (**A**). (**C**) 7-day differentiated human myotubes were treated and stained as in (**A**). (**D**) Quantification of (**C**). (**E**) 7-day differentiated human myotubes were stained with MitoSOX and quantified. (**F**) 7-day differentiated human myotubes were treated as in (**A**). Protein extracts were immunoblotted, as indicated. (**G**) C2C12 myoblast cells were treated as in (**A**) and imaged via electron microscopy. Mitochondria are indicated by arrows. (**H**) C2C12 myoblasts were transfected with Mito-pHRed and treated as in (**A**). (**I**) L6 myotube were treated as in (**A**) and protein extracts were immunoblotted, as indicated. (**J**) Insulin stimulated glucose uptake (10 nM) was determined by 2NBDG fluorescence in treated L6 myotubes and quantified. (**K**) C2C12 myoblast cells were transfected with BNIP3L wild type and BNIP3L^{S212A} followed by clenbuterol treatment (500 nM, 2 h). Cells were stained with TMRM and imaged by standard fluorescence microscopy. (**L-N**) C2C12 myoblasts cells were transfected with BNIP3L, BNIP3L^{S212A}, or BNIP3L^{S212D} with Mito-pHRed (**l**), Mito-Car-Geco (**M**), and ER-Lar-Geco (**N**). (**O**) L6 myotubes cells were transfected with BNIP3L, BNIP3L^{S212A}, or BNIP3L^{S212D}. Insulin stimulated uptake (10 nM) was determined by 2NBDG fluorescence and quantified. Data are represented as mean ± S.E.M. *P < 0.05 compared with control, while **P < 0.05 compared with treatment, determined by 1-way or 2-way ANOVA.

Next, we performed a series of experiments to evaluate if clenbuterol and cilomilast could inhibit palmitate-induced mitochondrial defects. In both C2C12 and L6 myotubes, clenbuterol and cilomilast reversed palmitate-induced mitochondrial depolarization **(Figure 3.4A,B)**. We also evaluated human iPSC-derived myotubes and observed similar rescue of TMRM and mitoSOX staining with clenbuterol and cilomilast treatment **(Figure 3.4C-E)**. In addition, we confirmed that clenbuterol and cilomilast increase p-BNIP3L expression in human myotubes **(Figure 3.4F)**. Clenbuterol and cilomilast also prevented palmitate-induced alterations in mitochondrial morphology, mitophagy, insulin signaling, and insulin-stimulated glucose uptake **(Figure 3.4G-J)**. Using TMRM as an indicator of BNIP3L activity, we observed that clenbuterol reversed BNIP3L-induced mitochondrial depolarization, but not when Ser212 was mutated to alanine (S212A; **Figure 3.4K**). In addition, we generated a Ser212 phospho-mimetic mutation (S212D) and compared the effects of this construct to wild-type BNIP3L and the $BNIP3L^{S212A}$ mutant. When transfected into C2C12 cells, wild-type BNIP3L and $BNIP3L^{S212A}$ induced mitophagy, increased mitochondrial calcium, reduced ER/SR calcium, and inhibited insulin-stimulated glucose uptake **(Figure 3.4L-O).** However, the $BNIP3L^{S212D}$ mutant did not significantly impact these end-points. Collectively, these findings suggest that clenbuterol and cilomilast treatment leads to PRKA -induced phosphorylation of BNIP3L at Ser212, and this phosphorylation site is inhibitory and can modulate BNIP3L-induced mitophagy, calcium homeostasis, and impaired glucose uptake.

3.4.4 YWHAB/14-3-3β regulates the subcellular localization and function of BNIP3L

To determine how PRKA phosphorylation of Ser212 leads to inhibition of BNIP3L-induced mitophagy and impaired insulin signaling, we undertook cell fractionation experiments to determine the cellular localization of p-BNIP3L. Although the majority of BNIP3L localized to the mitochondria and ER/SR in C2C12 myoblasts, p-BNIP3L was exclusively localized in the cytosolic fraction **(Figure 3.5A)**. Moreover, our *In silico* analysis of BNIP3L predicted that Ser212 lies within a conserved interacting domain of the molecular chaperone family YWHA/14-3-3, which identify the sequence RSxpSxP (BNIP3L: KRLpSTP) and are commonly found within PRKA and CAMK2A/CaMK-II phospho-motifs. Thus, we evaluated whether YWHA proteins could translocate BNIP3L from the mitochondria and/or ER/SR upon PRKA phosphorylation.

First, we performed co-immunoprecipitation of BNIP3L with YWHAB. We chose this YWHA family member as it has been shown to interact with other BCL2 proteins (398–400), and YWHAB expression was altered in our gene expression screen of insulin resistant soleus muscle (not shown). We expressed MYC-tagged BNIP3L and HA-tagged YWHAB in 293T cells. Shown in **Figure 3.5B**, we detected HA-YWHAB following immunoprecipitation with a MYC antibody. Furthermore, when transfected C2C12 cells were treated with clenbuterol prior to co-immunoprecipitation, the interaction between BNIP3L and YWHAB was enhanced **(Figure 3.5C)**. In a complementary experiment, we expressed HA- YWHAB with either wild-type BNIP3L, BNIP3L^{S212A}, or BNIP3L^{S212D} and subjected extracts to co-immunoprecipitation. We observed that the interaction between BNIP3L and YWHAB was enhanced when Ser212 was mutated to aspartic acid (BNIP3L^{S212D})**(Figure 3.5D)**. Next, we expressed BNIP3L with and without HA-YWHAB and treated with clenbuterol, and subjected extracts to sub-cellular fractionation. We observed that expression of HA-YWHAB and treatment with clenbuterol reduced the expression of BNIP3L in the mitochondrial and ER/SR fractions, with a corresponding increase in BNIP3L in the cytosolic fraction, and no change in total BNIP3L expression **(Figure 3.5E)**. Finally, we evaluated if YWHAB could counteract the effects of BNIP3L on mitochondria and insulin signaling. Shown in **Figure 3.5F**, and **3.5G**, co-expression of YWHAB with BNIP3L prevented ER/SR calcium release and mitochondrial calcium accumulation. In addition, YWHAB blocked BNIP3L-induced Mito-pHRed activation **(Figure 3.5H)**, prevented BNIP3L-induced IRS1 phosphorylation **(Figure 3.5I)**, and restored insulin-stimulated glucose uptake **(Figure 3.5J)**.

3.4.5 BNIP3L activates MTOR-RPS6KB, a negative regulator of insulin signaling

Previous studies have demonstrated that Ser1101 is phosphorylated by both novel PRKC isoforms and MTOR-RPS6KB to inhibit insulin signaling (367, 368, 386). Interestingly, both of these pathways are activated by lipid intermediates, diacylglycerols and phosphatidic acids, respectively, which were elevated in our metabolomics screen of insulin resistant muscle. To investigated how BNIP3L might activate MTOR-RPS6KB signaling, we expressed BNIP3L in C2C12 cells and evaluated activation of MTOR-RPS6KB by phosphorylation at Thr389 by phospho-specific antibody. BNIP3L expression increased MTOR-RPS6KB phosphorylation, which was prevented by treatment with the MTORC1 inhibitor rapamycin **(Figure 3.6A)**. In

addition, palmitate treatment increased MTOR-RPS6KB phosphorylation, which was attenuated in cells expressing sh*BNIP3L* **(Figure 3.6B)**. Furthermore, BNIP3L-induced MTOR-RPS6KB phosphorylation was inhibited by clenbuterol and cilomilast treatment **(Figure 3.6C)**, and prevented by treatment with the mitochondrial fission inhibitor mdivi-1 **(Figure 3.6D)**, collectively suggesting that BNIP3L is both necessary and sufficient to activate MTOR-RPS6KB phosphorylation in C2C12 cells.

As phosphatidic acids have been implicated as important regulators of MTOR signaling in muscle, we used 1-butanol, a primary alcohol which inhibits phospholipase-D catalyzed phosphatidic acid production, in C2C12 cells expressing BNIP3L. Shown in **Figure 3.6E**, BNIP3L-induced MTOR-RPS6KB phosphorylation was completely prevented in the presence of 1-butanol. To determine if BNIP3L activates MTOR signaling by directly influencing phosphatidic acids production, we expressed BNIP3L in C2C12 cells and evaluated phosphatidic acids content using a commercially available assay. Interestingly, phosphatidic acid content remained unchanged in cells expressing BNIP3L **(Figure 3.6F)**, as did diacylglycerol signaling **(Figure 3.6G)**, suggesting that BNIP3L alone does not alter lipid intermediate accumulation in the absence of an ectopic lipid source.

The conversion of phosphatidylcholine into phosphatidic acid involves the enzymatic function of PLD1 (phospholipase D1), which has been shown to be an important regulator of MTOR activation (385). However, the mitochondrial-targeted PLD6 (phospholipase D family member 6) which converts cardiolipin to phosphatidic acid has been shown to modulate mitochondrial dynamics (384). Moreover, the activation of MTORC1 has been previously shown to be dependent upon lysosomal GTPases, such as RHEB, which can activate mitophagy in a BNIP3L-dependent manner (401). Thus, we knocked-down both PLD6 and RHEB and determined the effect on BNIP3L-induced MTOR-RPS6KB activation. Shown in **Figure 3.6H**, siRNAs targeting RHEB and PLD6 reduced BNIP3L-dependent phosphorylation of MTOR-RPS6KB. In addition, knockdown of PLD6 also reduced the endogenous expression of both total MTOR-RPS6KB and RHEB, suggesting this phospholipase regulates multiple aspects of this pathway. Next, we expressed both BNIP3L and RHEB and observed Mito-pHRed activation **(Figure 3.6I)**. The addition of RHEB to BNIP3L enhanced Mito-pHRed fluorescence; however, when Ser212 of BNIP3L was mutated to a phospho-mimetic aspartic acid (S212D) or the mitochondrial-targeting transmembrane domain of BNIP3L was deleted (ΔTM), Mito-pHRed fluorescence was returned

to control levels. Collectively, these findings suggest that BNIP3L can modulate RHEB-dependent activation of MTOR-RPS6KB, and this pathway has substantial crosstalk with PLD6-dependent production of phosphatidic acid.

Figure 3.5. p-BNIP3L interacts with YWHAB proteins to determine subcellular location.

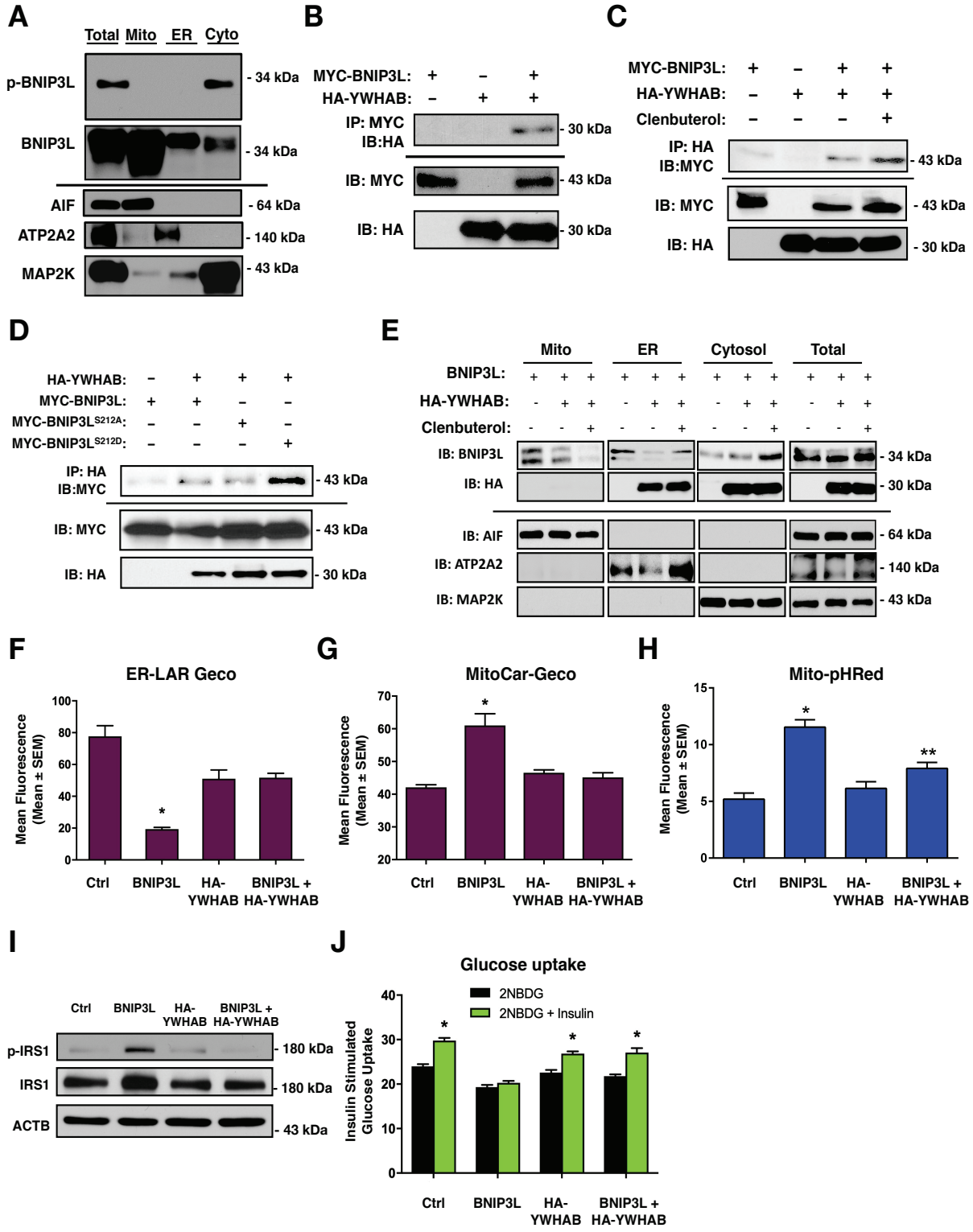

Figure 3.5. p-BNIP3L interacts with YWHAB proteins to determine subcellular location. (**A**) C2C12 myoblasts were subjected to subcellular fractionation. Protein extracts were immunoblotted for p-BNIP3L and total BNIP3L, as indicated. (**B**) 293T cells were transfected with MYC-BNIP3L or HA-YWHAB. Extracts were immunoprecipitated (IP) with a MYC antibody and immunoblotted (IB), as indicated. (**C**) C2C12 myoblasts were transfected as in (**B**) and treated with clenbuterol (500 nM, 2 h). Extracts were immunoprecipitated (IP) with HA antibody and immunoblotted (IB), as indicated. (**D**) C2C12 myoblasts were transfected with HA-YWHAB, MYC-BNIP3L, MYC-BNIP3L^{S212A} or MYC-BNIP3L^{S212D}. Extracts were immunoprecipitated (IP) with HA antibody and immunoblotted (IB), as indicated. (**E**) C2C12 myoblasts were transfected with either MYC-BNIP3L or HA-YWHAB, followed by clenbuterol treatment (500 nM, 2 h). Extracts were fractioned and protein extracts were immunoblotted, as indicated. (**F**) C2C12 myoblasts cells were transfected with BNIP3L wild type, HA-YWHAB, and ER-Lar-Geco. (**G**) C2C12 myoblasts cells were transfected with BNIP3L wild type, HA-YWHAB, and mitoCar-Geco. (**H**) C2C12 myoblasts cells were transfected with BNIP3L wild type, HA-YWHAB, and Mito-pHRed. (**I-J**) L6 myotubes were transfected with BNIP3L wild type, HA-YWHAB. Proteins were immunoblotted as indicated (**I**) and insulin stimulated glucose uptake (10 nM) was determined by 2NBDG fluorescence and quantified (**J**). Data are represented as mean ± S.E.M. *P < 0.05 compared with control, while **P < 0.05 compared with treatment, determined by 1-way or 2-way ANOVA.

Figure 3.6. BNIP3L-induced MTOR-RPS6KB activation.

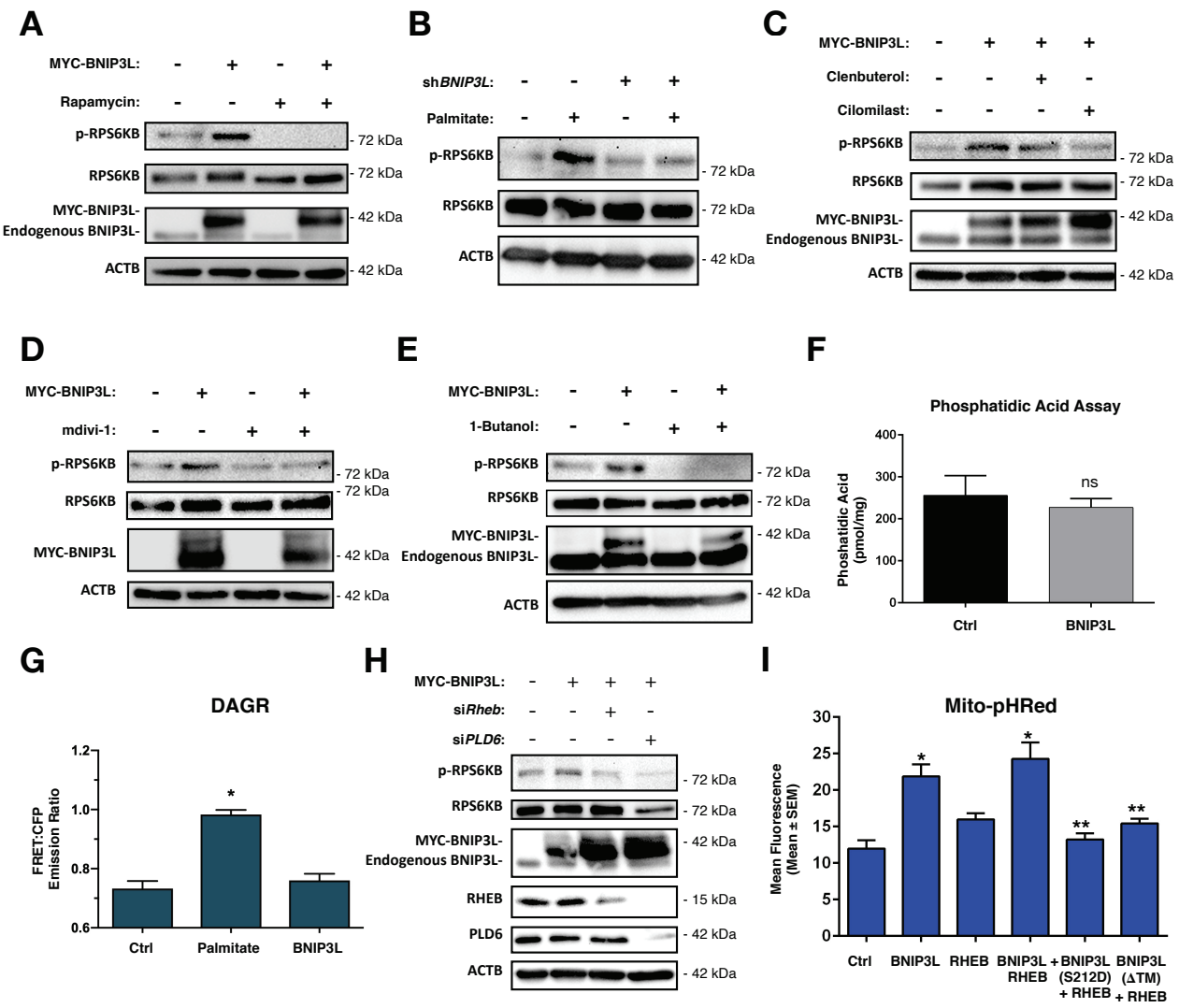

Figure 3.6. BNIP3L-induced MTOR-RPS6KB activation. (**A**) C2C12 myoblast cells transfected with MYC-BNIP3L or an empty vector control. Cells were treated with Rapamycin (500 nM, 1 h) or DMSO as vehicle control. Proteins were immunoblotted as indicated. (**B**) C2C12 myoblast cells transfected with sh*BNIP3L*, or a scramble control shRNA, and treated overnight with palmitate (200 μM) conjugated to 2% albumin in low-glucose media. Proteins were immunoblotted as indicated. (**C**) C2C12 myoblast cells were transfected as in (**A**), and were treated with clenbuterol (500 nM), cilomilast (10 μM) or vehicle for 2 h. Proteins were immunoblotted as indicated. (**D**) C2C12 myoblast cells were transfected as in (**A**). Cells were treated with mdivi-1 (20 μM) or vehicle for 1 h. Proteins were immunoblotted as indicated. (**E**) C2C12 myoblast cells were transfected as in (**A**) and treated with 1-butanol (1%) for 30 min. Proteins were immunoblotted as indicated. (**F**) C2C12 myoblast cells were transfected as in (**A**), followed by phosphatidic acid assay and quantification. (**G**) C2C12 myoblast cells were transfected as in (**A**), along with the diacylglycerol biosensor DAGR. Cells were treated overnight with palmitate and analyzed by FRET imaging. (**H**) C2C12 myoblast cells were transfected with MYC-BNIP3L, si*RHEB*, si*PLD6*. Proteins were immunoblotted as indicated. (**I**) C2C12 myoblast cells were transfected with MYC-BNIP3L, RHEB, MYC-BNIP3L^{S212D}, MYC-BNIP3L-ΔTM, along with Mito-pHRed. Cells were imaged by standard fluorescence and quantified. Data are represented as mean ± S.E.M. *P < 0.05 compared with control, while **P < 0.05 compared with treatment, determined by 1-way or 2-way ANOVA.

3.5 Discussion

Mitochondrial dysfunction has been implicated in insulin resistance and diabetic complications in numerous cell types, although the precise nature of this defect, and consequences resulting from it, are not fully defined in muscle. Utilizing two independent myoblast cell lines, a rodent model, and human iPSC-derived myotubes, we characterized a novel pathway initiated by lipotoxicity resulting in BNIP3L-induced mitochondrial fission, depolarization, mitophagy, and MTOR-RPS6KB dependent desensitization of IRS1. Interestingly, we also observed crosstalk between phospholipid metabolism and BNIP3L-induced IRS1 inhibition, where phosphatidic acids are critical modulators of this pathway. Furthermore, this work identifies a novel PRKA phosphorylation site within the BNIP3L transmembrane domain that serves to translocate BNIP3L from both the mitochondria and ER/SR membranes and inhibit mitochondrial perturbations and MTOR-RPS6KB activation.

Previous work has identified that the calcium-calmodulin dependent phosphatase, PPP3CA, activates the mitochondrial fission initiator DNM1L (393). Furthermore, muscle-specific DNM1L deletion in mice results in changes in mitochondrial volume and altered mitochondrial calcium handling (402). In addition, we have previously demonstrated in cardiomyocytes that BNIP3L modulates ER/SR calcium to control mitochondrial permeability transition (389). We extend these findings in the present work and demonstrate that BNIP3L-induced ER/SR calcium release activates DNM1L and mitophagy. These observations suggest that in addition to its role as a mitophagy receptor, BNIP3L modulates mitochondrial turn-over through ER/SR localization and activation of mitochondrial fission. Moreover, in a lipotoxic environment, knockdown of BNIP3L prevents mitochondrial depolarization, mitophagy, DNM1L activation, and restores insulin-stimulated glucose uptake. However, in the present study, it was not possible to delineate which aspect of BNIP3L-induced mitochondrial dysfunction (i.e. Fission vs depolarization vs mitophagy) directly led to MTOR-RPS6KB activation. It is likely that other post-translational modifications of BNIP3L operate to distinguish mitochondrial depolarization from the induction of mitophagy. For example, previous studies have shown that BNIP3L can be phosphorylated at Serine-34 and -35 to enhance the interaction with LC3 proteins (290). However, additional evidence suggests that muscle-specific deletion of the mitophagy receptor Fundc1

protects against HF feeding induced insulin resistance (403), suggesting that the mitophagy response may directly impact the sensitivity to insulin. Furthermore, BNIP3L and FUNDC1 cooperatively regulate mitophagy during cardiac progenitor differentiation (404). It is also interesting that the BNIP3L homolog BNIP3 is upregulated during myoblast differentiation to protect against oxidative stress, while BNIP3 and SQSTM1 are increased in muscle during starvation (405). Interestingly, we observed that following HF feeding BNIP3L expression was most highly induced in soleus muscle compared to other mitophagy receptors. Collectively, these findings suggest that mitophagy receptors may be induced in a stimulus-specific manner to control mitochondrial quality in muscle.

In this report, we provide detailed mass spectrometry analysis of BNIP3L and identify a novel PRKA phosphorylation site within the transmembrane domain. This phospho-acceptor residue serves to inhibit BNIP3L function by promoting the interaction with YWHAB and translocating BNIP3L away from the mitochondria and ER/SR. Using both adrenergic agonists and PDE4 inhibitors, we demonstrate that the function of BNIP3L can be pharmacologically manipulated to modulate myotube mitophagy and the response to insulin. These observations are consistent with previous work demonstrating the glucose lowering effects of the PDE4i roflumilast (406) and suggest an additional peripheral mechanism of action of these agents.

One of the most intriguing observations of the present study is the crosstalk between BNIP3L, mitochondrial dynamics, phospholipid metabolism, and MTOR signaling. Phosphatidic acids are a direct activator for MTORC1 both *in vitro* and *in vivo* (407). Phosphatidic acids bind directly to the FKBP12-rapamycin binding domain of MTOR, and compete with the inhibitor FKBP8 (i.e. FKBP38) to activate MTORC1 (408). The regulation of MTORC1 also involves recruitment to the lysosomal membranes and activation by small GTPases, such as RHEB, which also compete with FKBP8 (409). Interestingly, stimulation of mitochondrial oxidative phosphorylation results in BNIP3L-dependent recruitment of RHEB to the mitochondria and selective mitochondrial autophagy (401, 410). Our findings suggest crosstalk between these complex signaling pathways operates during myocyte lipotoxicity, and identifies BNIP3L as a regulator of MTOR-RPS6KB through RHEB, but contingent on the availability of phosphatidic acids. This notion is consistent with our metabolomics screen, that identified reduced muscle cardiolipin and increased phosphatidic acids content, while our mechanistic cell culture data demonstrate that knockdown of the mitochondrial PLD6 prevents BNIP3L induced MTOR-

RPS6KB activation. While the precise relationship between lipotoxicity-induced mitochondrial overload and the regulation of mitochondrial dynamics by phospholipids requires further investigation to more fully define, the activation of MTOR-RPS6KB and the phosphorylation of IRS1 at Ser-1101 during lipotoxicity suggests an important mechanism linking mitochondrial dysfunction to impaired insulin-stimulated glucose uptake. These observations are consistent with a model whereby BNIP3L responds to lipid-induced mitochondria overload and protects the myocyte against nutrient storage stress by activating MTOR-RPS6KB and IRS1 phosphorylation. However, this model requires further validation using *in vivo* models, particularly in the context of the heterogenous nature of skeletal muscle fibers.

In summary, these studies document a novel signaling cascade triggered by lipotoxicity and converging on BNIP3L-dependent mitochondrial regulation leading to desensitization of insulin receptor signaling. Furthermore, PRKA activation downstream of adrenergic signaling inhibits BNIP3L function and restores insulin signaling, suggesting a mechanism by which exercise or pharmacological modulation of PRKA may overcome myocyte insulin resistance.

3.6 Materials/Methods

3.6.1 Plasmids

MYC-tagged BNIP3L (Myc-Nix), BNIP3L-CYB5 (Nix-CytoB5), BNIP3L-MaoB (Nix-MaoB), BNIP3L-ActA (Nix-ActA), BNIP3L-ΔTM (Nix-delta TM) plasmids (Addgene, 100795, 100756, 100757, 100758, and 100755; deposited by Joseph Gordon) were described previously [(389)]. The MYC-tagged BNIP3L^{S212A} and BNIP3L^{S212D} were generated using a Q5 site directed mutagenesis kit (New England Biolabs, E0554S). The lentiviral sh*BNIP3L* (Addgene, 100770; deposited by Joseph Gordon) was generated by ligating oligonucleotides containing the targeting sequence 5'-CAGTTCCTGGGTGGAGCTA-3' into pLKO.1-puro (Addgene, 8453; deposited by Bob Weinberg). The mitochondrial (CMV-mitoCAR-GECO1) and endoplasmic reticulum (CMV-ER-LAR-GECO1) targeted calcium biosensors were gifts from Robert Campbell (Addgene, 46022 and 61244; deposited by Robert Campbell) (390, 391). The sh*BNIP3L* (17469; deposited by Wafik El-Deiry) (411), mEmerald-Mito-7 and mCherry-Mito-7 (54160 and 55102; deposited by Michael Davidson) (412, 413), pPHT- PRKA (60936; deposited by Anne Marie Quinn) [(414)], DAGR (14865; deposited by Alexandra Newton) (395), GW1-Mito-pHRed (31474; deposited by Gary Yellen) (394) and pcDNA3-FLAG-RHEB (19996; deposited by Fuyuhiko Tamanoi) (415) plasmids were purchased from Addgene.

3.6.2 Cell culture and transfections

C2C12 (ATCC, CRL-1772) and L6 (ATCC, CRL-1458) cell lines were maintained in Dulbecco's modified Eagle's medium (DMEM; HyClone, SH3002201), containing penicillin- streptomycin (HyClone, SV30010), and 10% fetal bovine serum (HyClone, SH3039603) at 37°C and 5% CO_2. All cells were transfected using JetPrime Polyplus reagent as per the manufacturer's instructions (Polyplus, 114-15) (388). The *RHEB* (19744) and the *PLD6* (194908) siRNA were purchased from Dharmacon, and the scrambled siRNA control (sc-37007) and control lentivirus (sc-108080) were purchased from Santa Cruz Biotechnology. C2C12 and L6 were differentiated by re-feeding confluent cells in 2% fetal bovine serum for to 2–5 days. Human skeletal myoblasts derived from induced pluripotent stem cells were obtained from Cellular Dynamics (iCell SKM-301-020-001-

PT). iCell Skeletal Myoblasts were cultured in maintenance medium as per manufacturer's protocol and differentiated for 5-7 days. Palmitate (Sigma, P9767) was conjugated to 2% albumin (BSA; Sigma, A7030) in low-glucose media (DMEM; HyClone, SH3002101) and treatments were performed as described previously [(388)]. Clenbuterol (C5423), cilomilast (SML0733), roflumilast (SML1099), 8-Br-cAMP (B7880), H89-dihydrochloride hydrate (B1427), 2-aminoethoxydipheny borate (2APB) (D9754), Mdivi-1 (MO199), etomoxir (E1905), rapamycin (553210), and bafilomycin A_1 (B1793) were purchased from Sigma. Butanol-1 (8399) and forskolin (BP25205) were purchased from Fisher Scientific.

3.6.3 Immunoblotting and immunoprecipitation

Protein samples were extracted using a RIPA lysis buffer system containing protease and phosphatase inhibitors (Santa Cruz, SC-24948A). Subcellular organelle fractionation was performed using a Mitochondrial Isolation Kit (Qiagen Qproteome, 37612) and a Nuclear/Cytosolic Isolation Kit (Pierce, PI78833) [(416)]. Protein determination was performed using a Bio-Rad protein assay kit (Bio-Rad, 5000006) and proteins were separated by reducing SDS-PAGE and transferred to a PVDF membrane (Roche, 03010040001) (388, 389, 416–418). Immunoblotting was carried out using the following antibodies for analysis: BNIP3L/Nix (Cell Signaling Technology [CST], 12396), MYC-Tag (Cell Signaling Technology [CST], 2278), HA-Tag (Cell Signaling Technology [CST],3724), phospho-RPS6KB/p70 S6 Kinase Thr389 (Cell Signaling Technology [CST], 9205), RPS6KB/p70 S6 Kinase (Cell Signaling Technology [CST], 9202), phospho-IRS1 Ser-1101 (Cell Signaling Technology [CST], 2385), IRS1 (ProteinTech, 17509-1-AP), AKT (ProteinTech, 60203-2-Ig), phospho-AKT S473 (ProteinTech, 66444-1-Ig), phospho-DNM1L/DRP1 Ser637 (Cell Signaling Technology [CST], 4867), DNM1L/DRP1-D6C7 (Cell Signaling Technology [CST],8570), RHEB E1G1R (Cell Signaling Technology [CST],13879), PLD6 (Invitrogen, PA5-71510), BCL2L13 (ProteinTech, 16612-1-AP), PRKN/Parkin (PRK8; Cell Signaling Technology [CST], 4211), BNIP3 (Cell Signaling Technology [CST], 3769), FKBP8 (ThermoFisher, PA5-47513), FUNDC1 (Aviva Systems Biology, ARP53280_P050), LC3B (Sigma, L7543), SQSTM1/p62 (Cell Signaling Technology [CST], 39749), AIF (Cell Signaling Technology [CST], 5318), MAP2K/MEK (Cell Signaling Technology [CST], 8727), ATP2A2/SERCA2 (Cell Signaling Technology [CST], 9580), and

ACTB/actin (Santa Cruz Biotechology, sc-1616). Primary antibodies were made as per manufacturer's protocol at a range of 1:1000 dilution. To detect the rodent phospho-BNIP3L/Nix, a custom rabbit polyclonal antibody was generated by Abgent using the following peptide sequence IGKRL(pS)TPSAS conjugated to adjuvant. Appropriate horseradish peroxidase-conjugated secondary antibody (Jackson ImmunoResearch Laboratories, 711-035-152) was used in a 1:5000 dilution in combination with chemiluminescence to visualize bands using film or a BioRad imager (Mississauga, ON, Canada). Image Lab Software offered by BioRad imager was used to ensure linear exposure.

3.6.4 Fluorescent staining

MitoSOX (Molecular Probes, M36008), MitoTracker Red CMXRos (Cell Signaling Technology, 9082), LysoTracker Red (Invitrogen, L7526), TMRM (Biotium, 70017) and Hoechst 33342 (Sigma, B2261) staining were described previously (388, 389, 416, 419–421). Insulin- (Sigma, I0516) stimulated glucose uptake assay was measured as previously described using the fluorescent D-glucose analog 2NBDG (Invitrogen, N13195) [30]. Microscopy was performed on an Olympus IX70 inverted microscope (Toronto, ON, Canada) with QImaging Retiga SRV Fast 1394 camera (Surrey, BC, Canada) using NIS Elements AR 3.0 software (Nikon Instruments Inc., Melville, NY, USA), or a Zeiss Axiovert 200 inverted microscope fitted with a Calibri 7 LED Light Source and Axiocam 702 mono camera (Pleasanton, USA) (389, 416). Quantification, scale bars, background subtract, and processing were done on Fiji (ImageJ) and Zen 2.3 Pro software.

3.6.5 Transmission electron microscopy (TEM)

TEM imaging was performed according to a protocol described previously (419–421). Briefly, C2C12 cells myoblasts were seeded in 100-mm plates. Cells were collected using trypsin. Cells were centrifuged three times (1500×g, 5 min) and then fixed (3% glutaraldehyde in 0.1 M Sorensen's phosphate buffer [Na_2HPO_4, KH_2PO_4 in distilled water, pH 7.3]; Fisher Scientific, 7558-80-7, 7778-77-0 respectively) for 3 h at room temperature. Cells were treated with a post-fixation step using 1% osmium tetroxide in 0.1 M Sorensen's phosphate buffer (pH 7.3) for 2 h at room temperature, followed by an alcohol dehydration series before embedding in Epon (EMbed

812; Electron Microscopy Sciences, 14900). TEM was performed with a Philips CM10, at 80 kV, on ultra-thin sections (100 nM on 200 mesh grids; Electron Microscopy Sciences, G200CU). Cells were stained with uranyl acetate and counterstained with lead citrate.

3.6.6 Phosphatidic acid assay

To quantitatively measure phosphatidic acid (PA) *in vitro*, a PA assay kit was purchased from PicoProbe™ (BioVision, K748-100). Protein extractions and fluorometric analysis were performed as per manufacture's protocol.

3.6.7 High-fat diet animal model

All procedures in this study were approved by the Animal Care Committee of the University of Manitoba, which adheres to the principles for biomedical research involving animals developed by the Council for International Organizations of Medical Sciences. Male Sprague-Dawley rats were weaned at 3 weeks of age and randomly assigned to a LF diet (10% fat; Research Diets, D12450B) or HF diet (45% fat; Research Diets, D12451), both containing sucrose, for 12 weeks, as previously described (388, 422). To analyze insulin-responsive signalling pathways, offspring were fasted for 4 h, followed by human insulin administration injected intraperitoneally (1 mU kg–1), and the tissues were collected 15 min after the injection, as previously described (422). The method of sacrifice was via anaesthesia by intraperitoneal injection of a sodium pentobarbital overdose (422). Soleus muscle tissues were collected and analyzed for metabolomics; muscle lipids were extracted using a lipid soluble extraction technique as previously described (423), in duplicate and stored at -80°C until further analysis. Muscle lipid extracts were reconstituted with 100 µl of 80% acetonitrile prepared in deionized water prior to analysis. Metabolomics analysis was performed on a 1290 Infinity Agilent high-performance liquid chromatography (HPLC) system coupled to a 6538 UHD Agilent Accurate Q-TOF LC/MS equipped with a dual electrospray ionization source, as previously described (388, 422)(N= 6). PCR-based gene expression arrays were purchased from SA Biosciences (Qiagen)(samples were pooled from 5 animals per condition).

3.6.8 In vitro *kinase assay and phospho-peptide mapping*

Synthetic peptides (GeneScript) were resuspended in ultrapure water as per manufacture's protocol at a concentration of 1 mg/ml. These peptides were used as the substrate in a PRKA kinase assay kit (New England Biolabs, P6000S) according to the manufacturer's instructions, with the exception that [32P]-ATP was replaced with fresh molecular biology grade ATP (SignalChem, A50-09). The Kemptide substrate (LRRASLG; Enzo Life Sciences, P-107) was used as a positive control in each assay. Before mass spectrometry analysis, kinase assays were prepared using C18 ZipTips (Millipore, ZTC18S096). Samples in 50% acetonitrile and 0.1% formic acid were introduced into a linear ion-trap mass spectrometer (LTQ XL; ThermoFisher, San Jose, CA, USA) via static nanoflow, using a glass capillary emitter (PicoTip; New Objective, Woburn, MA, USA), as described previously (388).

3.6.9 Statistics

Data are presented as mean ± standard error of the mean (S.E.M.). Differences between groups in imaging experiments with only 2 conditions were analyzed using an unpaired t-tests, where * indicates $P < 0.05$ compared with control. Experiments with 4 or more conditions were analyzed using a 1-way ANOVA or 2-way ANOVA, with Tukey's test for multiple comparison, where * indicates $P < 0.05$ compared with control, and ** indicates $P < 0.05$ compared with treatment. All statistical analysis were performed using GraphPad Prism 6 software. Regarding the arrays and metabolomics, both were presented in a semi-quantitative manner, therefore no statistics were done; however, changes greater than 2-fold were deemed to be relevant. Moreover, samples where the metabolic entity was below the level of detection were omitted from the analysis, unless otherwise noted in the reported manuscript in this Chapter.

3.7 Acknowledgements

This work was support by the Natural Science and Engineering Research Council (NSERC) Canada, through Discovery Grants to JWG and ARW. Seed funding was provided by the Children's Hospital Research Institute of Manitoba, the DREAM research theme, and the Manitoba Centre for Nursing and Health Research. V.W.D is supported by CIHR and is the Allen

Rouse Basic Scientist of the Manitoba Medical Services Foundation. J.W.G., A.R.W., and V.W.D are members of the DEVOTION Research Cluster. S.C.d.S.R. is supported by a University of Manitoba Graduate Studentship, J.T.F. is supported by an Alexander Graham Bell studentship from NSERC Canada, and M.D.M. and S.M.K. are supported by a studentship from the Children's Hospital Foundation of Manitoba and Research Manitoba. We wish to thank Drs. Christine Doucette and Grant Hatch for helpful discussions on the manuscript.

3.8 Supplemental Figures for Manuscript

Figure S3.1. BNIP3L and mitochondrial autophagy.

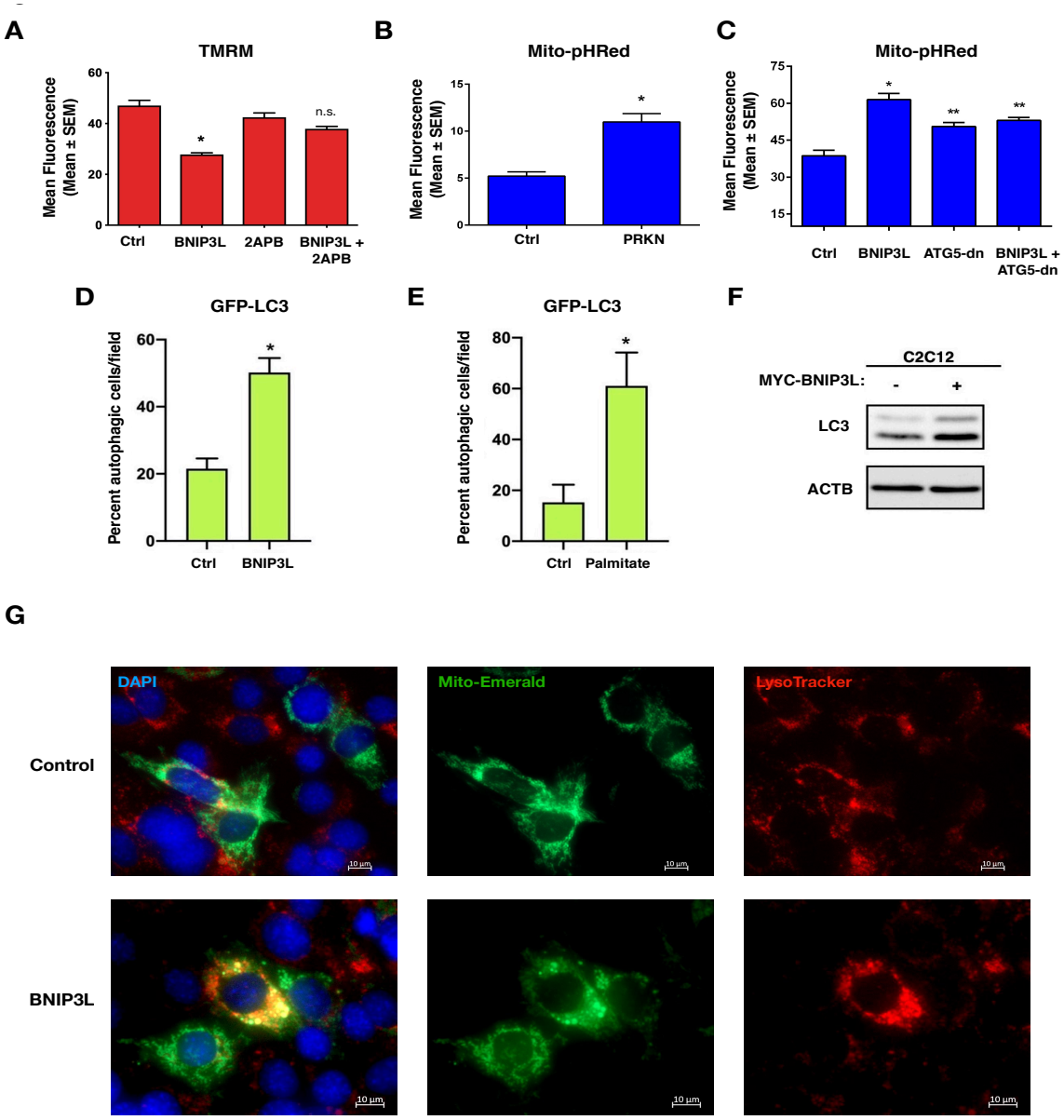

Figure S3.1. BNIP3L and mitochondrial autophagy. (**A**) C2C12 myoblast cells were transfected with MYC-BNIP3L or an empty vector. Cells were treated with 2-aminoethoxydiphenyl borate (2APB 10 μM, 1 h), or DMSO as a vehicle control. Cells were stained for TMRM and quantified. (**B**) C2C12 myoblasts cells were transfected with HA-PRKN or an empty vector, along with the mitophagy biosensor Mito-pHRed. (**C**) C2C12 myoblast cells were transfected MYC-BNIP3L, a dominant-negative ATG5, or an empty vector, along with Mito-pHRed. (**D**) C2C12 cells were transfected with GFP-LC3, MYC-BNIP3L or empty vector control, and dsRED to identify transfected cells. Cells were imaged by standard microscopy and quantified. (**E**) C2C12 cells were transfected with GFP-LC3 and treated overnight with palmitate. Cells were imaged and quantified as in (**D**). (**F**) C2C12 cells were transfected with empty vector or MYC-BNIP3L. Extracts were subjected to western blots, as indicated. (**G**) C2C12 cells were transfected with BNIP3L or empty vector, along with Mito-Emerald, and stained with LysoTracker Red. Data are represented as mean ± S.E.M. *P < 0.05 compared with control, while **P < 0.05 compared with treatment, determined by T-Test or 1-way ANOVA, where appropriate.

Figure S3.2. BNIP3L and other mitophagy markers.

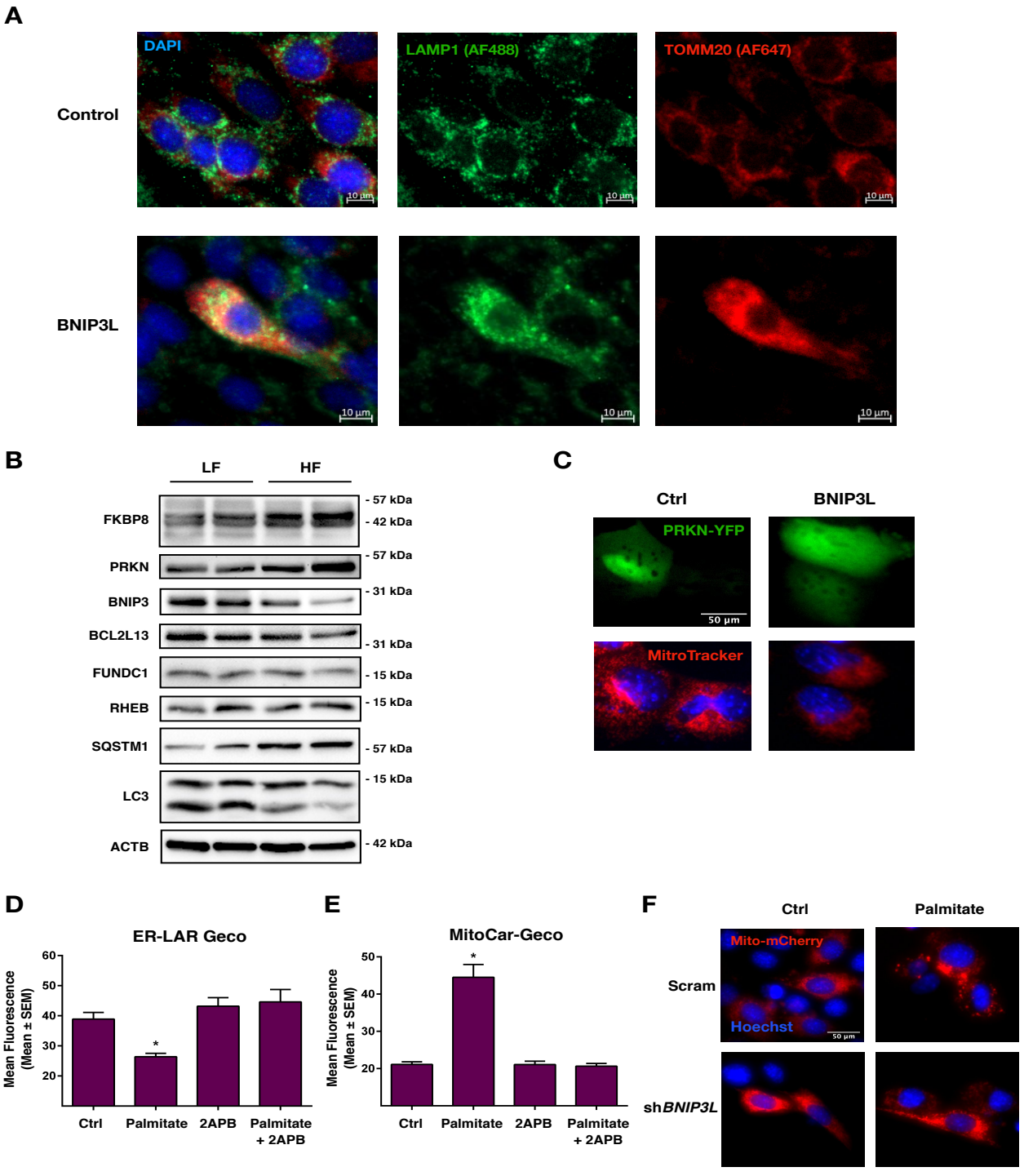

Figure S3.2. BNIP3L and other mitophagy markers. (**A**) C2C12 cells were transfected with BNIP3L or empty vector, fixed, permeabilized and subjected to immunofluorescence with antibodies targeting LAMP1 (green) or TOMM20 (red). (**B**) Western blot analysis of rat soleus muscle (n=2) exposed to high fat (HF) or low fat (LF) diet for 12-weeks. Protein extracts were analyzed as indicated. (**C**) C2C12 myoblasts cells were transfected with MYC-BNIP3L or an empty vector, along with fluorescent protein YFP-PRKN. Cells were stained with MitoTracker and Hoechst and imaged by standard fluorescence microscopy. (**D-E**) C2C12 myoblasts cells were transfected with ER-Lar-Geco (**D**) or MitoCar-Geco (**E**) and an empty vector, followed by overnight treatment with palmitate conjugated to 2% albumin in low glucose media. Control cells were treated with 2% albumin alone. Following palmitate treatment cells were treated with 2APB. (**F**) C2C12 myoblasts were transfected with sh*BNIP3L*, or a scrambled control sh*RNA*, along with Mito-mCherry. Cells were treated overnight with palmitate conjugated to 2% albumin in low-glucose media. Control cells were treated with 2% albumin alone. Cells were stained with Hoechst and imaged by standard fluorescence microscopy. Data are represented as mean ± S.E.M. *P < 0.05 compared with control, while **P < 0.05 compared with treatment, determined by 1-way ANOVA.

Figure S3.3. PRKA Phosphorylation of BNIP3L.

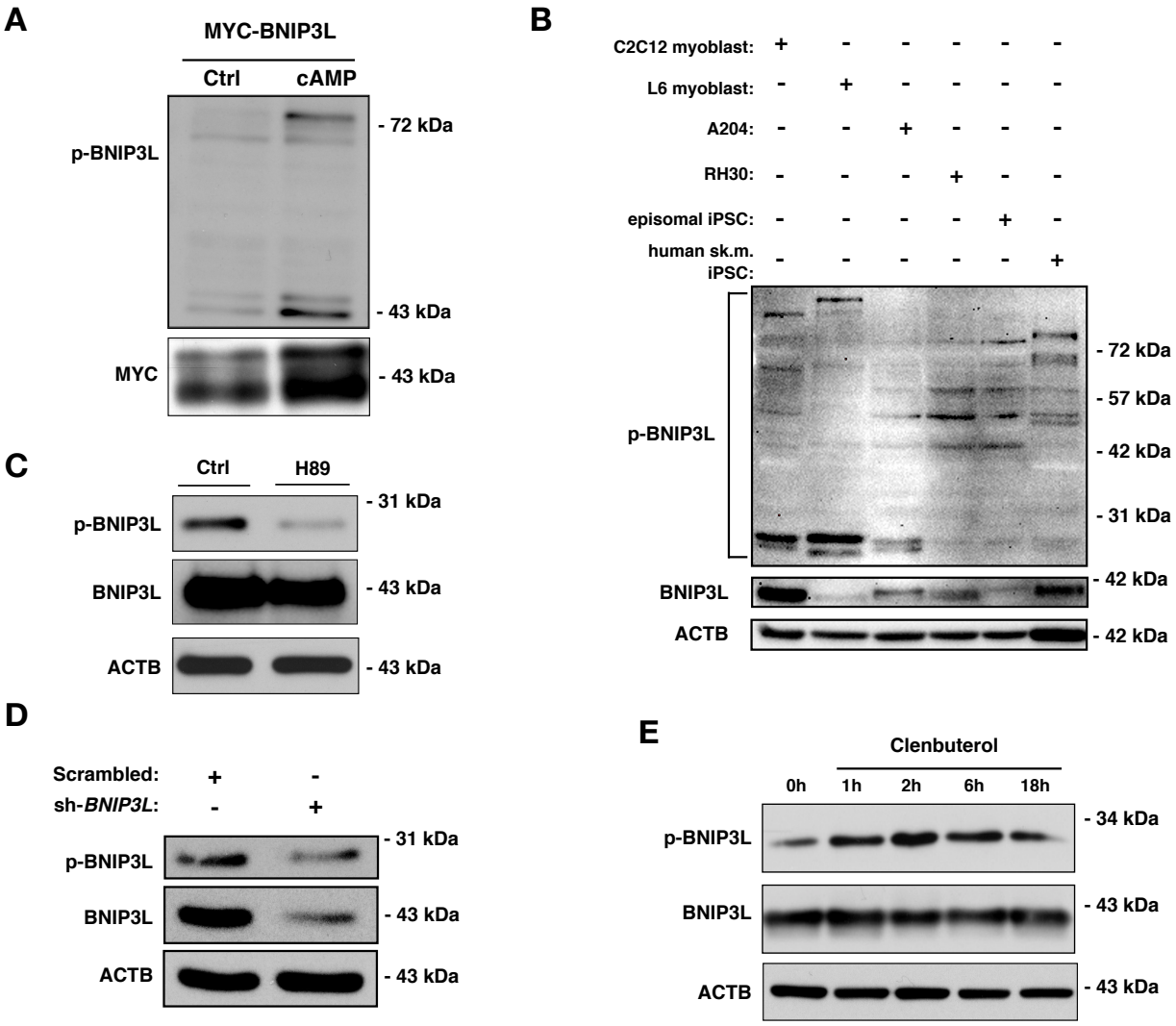

Figure S3.3. PRKA Phosphorylation of BNIP3L. (**A**) C2C12 myoblast cells were transfected with MYC-BNIP3L or an empty vector and treated with c-AMP analogue (1 mM, 1 h) or vehicle control. Protein extracts were immunoblotted, as indicated. (**B**) Protein extract of multiple cell lines (as indicated) were immunoblotted for endogenous p-BNIP3L. (**C**) C2C12 myoblast cells were treated with PRKA inhibitor, H89 (10 μM, 1 h) or vehicle control. Protein extracts were immunoblotted, as indicated. (**D**) C2C12 myoblasts were transfected with sh*BNIP3L*, or a scrambled control sh*RNA*. Protein extracts were immunoblotted, as indicated. (**E**) C2C12 myoblast cells were treated with 500 nM clenbuterol or vehicle for multiple time points. Protein extracts were immunoblotted, as indicated.

Figure 3.4. PRKA activation in C2C12 cells.

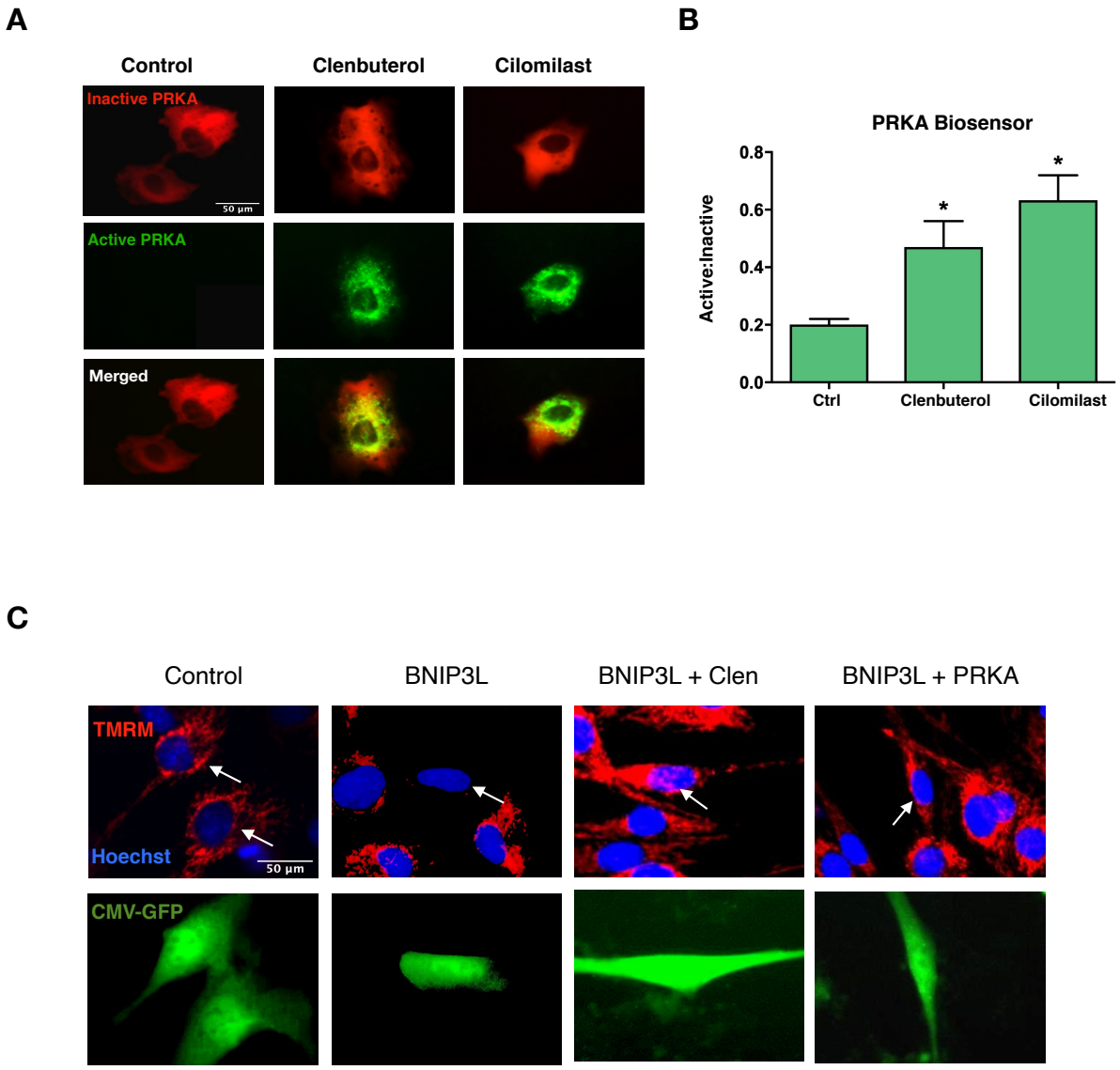

Figure S3.4. PRKA activation in C2C12 cells. (**A**) C2C12 myoblast cells were transfected with PRKA biosensor (pPHT-PRKA), and treated with clenbuterol (500 nM), cilomilast (10 μM) or vehicle for 2 h. Cells were imaged by standard fluorescence microscopy. (**B**) Quantification of fluorescent images in (**A**) by measuring the ratio of green (active) to red (inactive) fluorescent signal. (**C**) C2C12 myoblast cells were transfected with BNIP3L, PRKA or CMV-GFP as a control. Cells were treated with clenbuterol (500 nM, 2 h) or a vehicle control. Cells were stained for TMRM and Hoechst and imaged by standard fluorescence. Red active or inactive mitochondria are indicated by arrows. Data are represented as mean ± S.E.M. *$P < 0.05$ compared with control, determined by 1-way ANOVA.

Table S3.1. Metabolomics table for selected muscle triglycerides.

TG	HF diet (Fold of Control)
TG(22:3/22:6/22:6)	474.16094524
TG(21:0/22:0/22:3)	225.30109372
TG(20:0/22:0/22:6)	252.24362556
TG(13:0/18:3/22:2)	0.73820095
TG(13:0/16:0/18:3)	0.00002156
TG(13:0/15:1/17:2)	12.42594972
TG(13:0/14:0/18:2)	15.80467647
TG(13:0/14:0/18:2)	0.03724308
TG(12:0/19:1/19:1)	0.00010212
TG(12:0/17:0/17:0)	0.00000017
TG(12:0/16:0/20:1)	0.00454675
TG(12:0/15:1/16:0)	0.09477939
TG(12:0/15:1/16:0)	226.25782085
TG(12:0/14:1/18:4)	451.47187440
TG(12:0/14:1/18:0)	0.03885087
TG(12:0/14:1/15:1)	303.10081212
TG(12:0/14:1/15:1)	5701844.90556225
TG(12:0/13:0/22:5)	27.28222775
TG(12:0/12:0/20:0)	215.98445754
TG(12:0/12:0/19:1)	14.43848324
TG(12:0/12:0/18:0)	16.99116745
TG(12:0/12:0/14:1)	378.78275633

Table S3.2. Metabolomics table for selected muscle diacylglycerides.

DG	HF diet (Fold of Control)
DG(O-16:0/18:1)	302.8633348
DG(22:3/22:6)	315.3130896
DG(22:3/22:2)	0.765006279
DG(22:2/24:1)	685.4931195
DG(22:2/24:0)	393.766622
DG(21:0/22:6)	271.0025641
DG(20:5/22:4)	380753.4087
DG(20:4/22:6)	6176.598903
DG(20:4/20:4)	16.2638058
DG(20:2/24:0)	0.021997727
DG(20:2/22:0)	0.643402435
DG(20:2/14:1)	244.0439805
DG(20:2/20:2)	16.8409959
DG(20:1/18:0)	388.6799158
DG(20:0/22:1)	208.6105653
DG(20:0/20:0)	0.3638602
DG(19:0/19:0)	12.66929387
DG(18:4/24:1)	255.600736
DG(18:4/22:6)	499.6432217
DG(18:2/18:1)	19.57482869
DG(18:1/24:1)	0.040373546
DG(17:0/17:0)	0.00292789
DG(16:1/16:1)	347.202625
DG(16:0/20:0)	306.2108676
DG(16:0/18:0)	8408.447173
DG(16:0/16:0)	346.1952462
DG(15:0/16:0)	0.046122772
DG(12:0/20:0)	9857.486705

Table S3.3. Metabolomics table for selected muscle ceramides.

Cer	HF diet (Fold of Control)
α-Galactosyl Ceramide	0.002657066
Lactosylceramide (d18:1/22:0)	16.50345981
GlcCer(d18:2/23:0)	7.268878339
GlcCer(d18:2/23:0)	3059839.875
GlcCer(d18:2/23:0)	2728569.373
GlcCer(d18:2/21:0)	557.2568299
GlcCer(d18:2/21:0)	12.48381689
GlcCer(d18:1/26:0)	4.72854E-07
GlcCer(d18:0/24:0)	3.28482E-06
GlcCer(d16:2/20:0)	19.35893404
GlcCer(d15:2/22:0)	0.409136853
GlcCer(d15:2/22:0)	328.6126366
GlcCer(d15:2/22:0)	34.65256394
GlcCer(d15:2/20:0)	8118.391671
GlcCer(d15:2/18:0)	293.9558449
GlcCer(d15:1/22:0)	15.98534449
GlcCer(d15:1/20:0)	371.4533676
GlcCer(d15:1/20:0)	324.6849811
GlcCer(d14:1/18:1)	348.5725632
Dihydroceramide C2	556.0446801
Ceramide (d18:1/26:0)	205.005966
Cer(t18:0/16:0)	5829.65025
Cer(t18:0/16:0)	14.57712641
Cer(t18:0/16:0)	216.174369
Cer(d18:2/23:0)	0.030951015
Cer(d18:2/20:1)	270.0500114
Cer(d18:2/20:1)	297.7411079
Cer(d18:2/20:1)	11.30894339
Cer(d18:2/18:1)	0.944696921
Cer(d18:2/14:0)	16.71667118
Cer(d18:2/14:0)	282.8826293
Cer(d18:1/22:1)	0.020334332
Cer(d18:1/20:0)	2.15693E-06
Cer(d18:1/16:0)	367.3849827
Cer(d18:1/16:0)	190.163429
Cer(d18:0/17:0)	225.1782813
Cer(d18:0/15:0)	828.6573179
Cer(d18:0/13:0)	6573251.966
Cer(d18:0/12:0)	117007904.1

Cer(d16:2/24:0)	213.6848341
Cer(d16:2/20:1)	122962.2496
Cer(d16:1/23:0)	271.2296103
Cer(d15:2/22:0)	0.803124732
Cer(d14:2/20:0)	423.0099666
Cer(d14:2/18:1)	0.028376394
Cer(d14:2/18:0)	10.79612912
Cer(d14:2/18:0)	1.51852E+11
Cer(d14:1/26:0)	450314.2601
Cer(d14:1/24:0)	15.3688333
Cer(d14:1/22:1)	298.2445388
Cer(d14:1/22:0)	509.2305146
C-6 NBD Ceramide	450.8602007
AV-Ceramide	283.9401451
PE-Cer(d16:1/23:0)	13621.34993
PE-Cer(d16:1/18:0)	14.52539596
PE-Cer(d14:1/25:0)	344.1520018
PE-Cer(d14:1/23:0)	10237.21749
CerP(d18:1/24:1)	140907.4644
CerP(d18:1/18:0)	273.3677637

Table S3.4. Metabolomics table for selected muscle cardiolipins.

CL	HF diet (Fold of Control)
CL(18:2/18:2/18:2/18:2)	0.002684369
CL(22:6/20:3/18:2/18:2)	ND in HF condition
CL(18:2/18:2/18:2/18:3)	ND in HF condition
CL(22:1/22:1/22:1/14:1)	ND in HF condition
CL(14:1/14:1/14:1/15:1)	ND in HF condition

Table S3.5. Metabolomics table for selected muscle phosphatidic acids.

PA	HF diet (Fold of Control)
PA(20:0/22:6)	19842.77007
PA(20:0/18:2)	509.6983175
PA(22:6/14:1)	0.05364954
PA(20:5/22:6)	0.000120273
PA(20:5/18:3)	245.1649605
PA(20:5/18:3)	13.27455068
PA(20:5/18:3)	0.526316154
PA(20:5/18:3)	300.8537298
PA(20:3/21:0)	518.1851107
PA(20:2/21:0)	296.0700657
PA(20:1/22:0)	243.7446545
PA(19:0/20:0)	12388.91034
PA(18:4/20:5)	12.8543701
PA(18:4/18:4)	314.6167207
PA(18:4/18:3)	0.072812107
PA(16:0/21:0)	366.4071164
PA(15:1/22:4)	335.3509184
PA(15:0/20:3)	206.8535602
PA(14:1/17:2)	0.708617217
PA(14:0/15:0)	4534.707717
PA(14:0/12:0)	257.1628321

Table S3.6. Gene expression array table for selected muscle genes.

Gene	HF diet (Fold of Control)
Atg12	0.82
Atg16l1	0.97
Atg3	0.86
Atg5	0.73
Atg7	1.13
Atp6v1g2	0.39
Bax	1.05
Bcl2	1.08
Bcl2a1	0.7
Bcl2l1	0.7
Bcl2l11	0.91
Becn1	0.84
Igf1	1.13
Igf1r	1.25
Tnf	0.69
Tnfrsf11b	0.69
Tnfrsf1a	0.94
Tpr53	1.32
Ulk1	1.03
Actb	1.08
Ldha	1.03
Cs	0.8
Foxo3	0.87
Hdac5	0.91
Mb	0.48
Mef2c	0.91
Mstn	1.51
Myf5	1.37
Myod1	1.25
Myog	0.89
Myh1	0.38
Myh2	0.04
Nfkb1	1.04
Pdk4	0.51
Pparg	0.85
Ppargc1a	0.65
Ppargc1b	0.98

Rhoa	0.97
Slc2a4	0.95
Tgfb1	1.19
Tnnc1	0.02
Tnni2	1.02
Tnnt1	0.02
Tnnt3	1.06
Fasn	0.18
Gys1	0.95
Hk2	0.8
Il6	0.58
Insr	0.89
Irs1	1.2
Irs2	0.96
Mtor	0.97
Slc27a1	0.66
Srebf1	1.14
Srebf2	1.17
Bnip3	0.84
Cox18	0.91
Cpt1b	0.82
Cpt2	0.78
Dnm1l	0.73
Fis1	0.82
Gpx1	0.51
Mfn1	0.74
Mfn2	0.86
Opa1	0.92
Taz	0.91
Timm44	0.96
Tomm40	1.02
Tomm22	0.94
Ucp2	1.11
Ucp3	0.8
Acly	0.48
Aldoa	1.01
Idh2	0.74
Mdh1	0.63
Mdh2	0.91

CHAPTER IV: Dissertation Discussion

4.1 General Discussion

The overall hypothesis of this thesis was that inhibition of BNIP3L function would improve mitochondrial function and insulin signaling in the skeletal muscle following diet-induced lipotoxicity. In this present study we demonstrated that BNIP3L responds to lipotoxicity in order to clear damaged mitochondria through mitophagy. In turn, it protects the myocyte against nutrient storage stress through desensitization of insulin signalling, via activation of mTOR-dependent phosphorylation of Ser-1101 of IRS1. BNIP3L induced ER calcium release with concurrent DRP1 activation, along with increased levels of mitophagy. As previously described in the literature review in Chapter I, DRP1 is an important mediator of mitochondrial fission and mitophagy, which can be activated by sustained increased in calcium levels (424). The latter has been reported to be elevated in cell culture under high glucose conditions, implicating a role for fission in the onset of insulin resistance and T2D (425).

It remains a widely debatable topic whether insulin resistance and beta-cell failure are part of the cause or consequence of T2D (426, 427). However, evidence from a 25-year prospective longitudinal follow-up study demonstrated that insulin resistance precedes the development of T2D and predicts its development (428). Moreover, in the skeletal muscle, insulin promotes glucose transport and disposal (429, 430), becoming the primary site of insulin resistance in offspring of parents with T2D (431). Furthermore, the skeletal muscle of these individuals present reduced glucose uptake and glycogen synthesis (431). This impaired glucose metabolism phenotype has been proposed to be a result of various defects, including decreased glucose transport, ATP production, and expression of genes involved in mitochondrial function (162, 432–434). Importantly, other cellular-extrinsic factors such as lipids, metabolites and cytokines have also been shown to fundamentally contribute to the development of insulin resistance (35).

In an overfed state, high levels of circulating fatty acids and ectopic lipid accumulation in muscle contribute to insulin resistance via the release of metabolites such as DAG and ceramides, which activate PKC signaling pathways (36). Downstream activation of PKC protein members results in increased serine and threonine phosphorylation of INSR and IRS proteins, ultimately

impairing insulin signaling (435–437). Moreover, lipid overload and decreased muscle oxidative capacity have been a theme of the investigation by various laboratories, where most have focused on carnitine palmitoyltransferase-1 (CPT-1) (438). CPT-1 is necessary to allow mitochondrial fatty acid uptake and has been found to be reduced in skeletal muscle of obese insulin resistance individuals (439). Despite some clues on the possible defects in skeletal muscle, further studies are needed to provide a clear answer of the causes of decreased skeletal muscle oxidative capacity. Therefore, various aspects of mitochondrial function in the regulation of peripheral insulin sensitivity are an emerging area of investigation, in particular how dysfunctional mitochondria, including mitophagy, may be impairing glucose disposal and leading to insulin resistance (34, 132, 440, 441).

There is accumulating evidence that excessive or aberrant mitophagy contributes to muscle insulin resistance *in vivo* and that genetically inhibiting mitophagy receptors, such as FUNDC1 in muscle, improves glucose tolerance (237). BNIP3L has been previously shown to cooperate with FUNDC1 (404), and our *in vivo* data suggest that Nix phosphorylation may be inhibited following HF feeding in soleus muscle. Collectively with our culture data, these observations support our conclusions that BNIP3L and an abnormal excessive mitophagy response impair muscle insulin signalling. Moreover, consistent with the results of Fu and colleagues (2018), who showed that deletion of the mitophagy receptor FUNDC1 protects against HF feeding (237), we observed that BNIP3L is the most abundantly elevated mitophagy receptor in soleus muscle followed by HF feeding. Regarding other mitophagy pathways, we only have a small amount of data to suggest that BNIP3L does not activate Parkin, but we observed that Parkin expression was increased following HF feeding in soleus muscle.

At the present study, we were not able to delineate how BNIP3L can induce mitochondrial depolarization, fission or mitophagy in specific. We attempted to target BNIP3L to different organelles, for instance, to the ER or the mitochondrial, and have also used various pharmacological and chemical inhibitors. However, it seems that inhibiting one aspect of BNIP3L function can impact multiple mitochondrial parameters, such as membrane potential, calcium, morphology and mitophagy activation. As of now, it is our hypothesis, these pathways are in parallel to one another and may have opposing effects on muscle insulin signaling. This is consistent with the work of others demonstrating that mitochondrial metabolism can be uncoupled from muscle insulin signaling (237, 442).

Regarding BNIP3L regulation of insulin signaling, our data suggest that BNIP3L inhibits insulin signaling through phosphorylation of IRS1 at Ser-1101, an inhibitory site. Phosphorylation of IRS1 Ser-1101 is highly associated with the emergence of insulin resistance and T2D (443). Tremblay and colleagues (2006) showed that RPS6KB directly phosphorylates IRS1 *in vitro* and also indicated that nutrient activation of RPS6KB results in insulin resistance in both humans and mice, partly due to activation of IRS1 Ser-1101 phosphorylation (154). Furthermore, we highlight a link between BNIP3L-induced mTOR-RPS6KB activation and the recruitment of small GTPases such as RHEB to the mitochondria to initiate mitophagy and later insulin resistance. This phenomenon was demonstrated to depend on phosphatidic acid availability, which is also an important modulator of mitochondrial dynamics (444). At this time, we do not have evidence that BNIP3L induces a permanent inhibition on IRS1; it is only in the presence of BNIP3L and lipotoxicity with elevated DAGs and PAs.

Using several inhibitors, and an shRNA targeting RHEB, our data implicate that the mTOR pathway and mitochondrial fission are playing a role in mitophagy and impaired insulin signaling. Previous reports have shown that BNIP3L serves to recruit RHEB to mitochondria to promote mitophagy under high oxidative phosphorylation conditions in myotubes (445), which is consistent with our RHEB knockdown data. In our studies, we have demonstrated that BNIP3L activates MTOR-RPS6KB; however, it is not clear the precise mechanisms. One possibility is that BNIP3L activates MTOR-RPS6KB in a GTPase-dependent manner via direct interaction. This hypothesis will be further confirmed via immunofluorescence technique to investigate BNIP3L and MTOR-RPS6KB interaction and lysosomal colocalization.

In a cellular model, we demonstrated that the mitochondrial phospholipase-D knockdown, an enzyme responsible for converting cardiolipin to phosphatidic acid, prevented BNIP3L-induced MTOR-RPS6KB activation. Conversely, phosphatidic acid phosphatases are also known to mediate phosphatidic acids conversion to diacylglycerol (DAG). Interestingly, DAGs have been previously reported to contribute to increasing fission while reducing fusion; via unknown mechanisms, independently of phosphatidic acids (446). However, our studies suggest that BNIP3L mediates this effect, as we see a positive correlation of BNIP3L and DAGs, concurrent with increased mitochondrial fission and mitophagy. Therefore, unlike previous reports, we propose that this effect is contingent on phosphatidic acid availability. A summary of these novel mechanisms is highlighted in Figure 4.1 below.

Figure 4.1. BNIP3L-induced mitochondrial dysfunction and muscle insulin resistance.

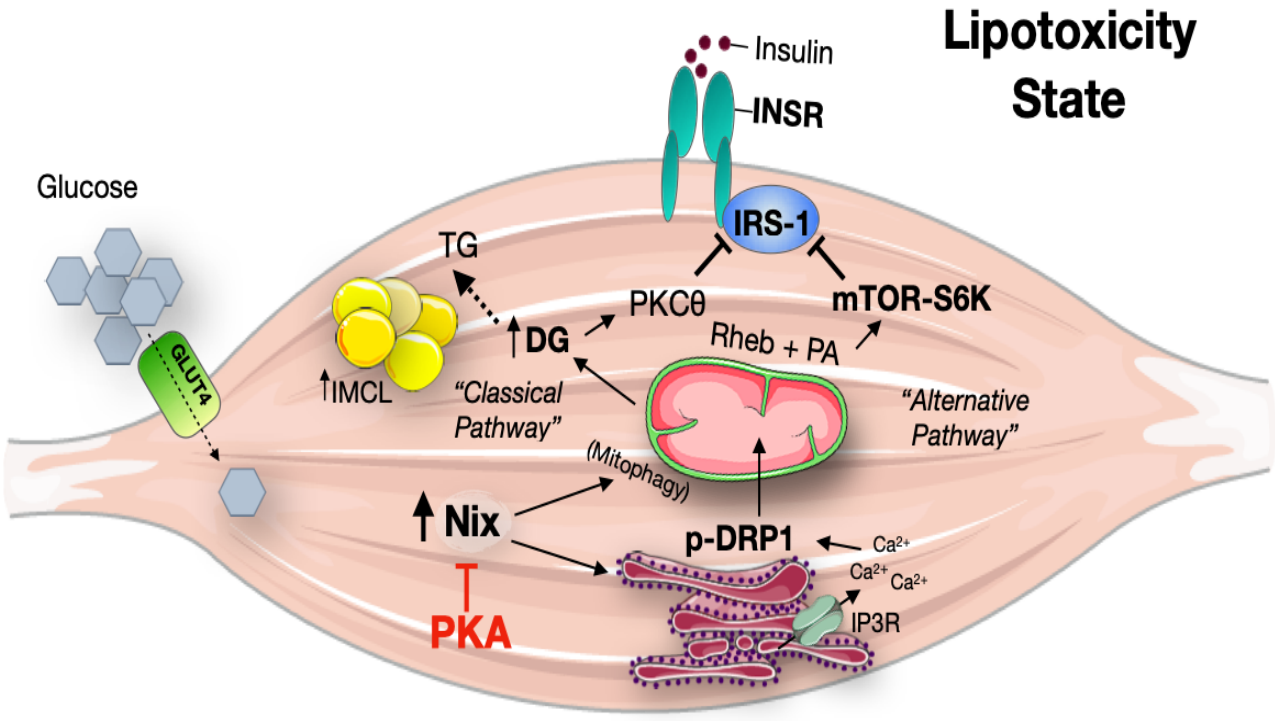

Based on the literature and our data, we propose that DAGs activate a classical pathway that leads to insulin resistance, and BNIP3L/Nix is activating an alternative pathway. In this classical pathway, DAGs accumulate and activate PKC theta and inhibit IRS1. Alternatively, DAGs also allow increased BNIP3L mitochondrial accumulation, which through its ER calcium mechanism activates DRP1 leading to mitophagy, with concurrent recruitment of RHEB GTPases and activation of MTOR-RPS6KB/mTOR-S6K in a PA dependent manner - ultimately resulting in impaired insulin-stimulated glucose uptake in the myocyte. However, we demonstrated that these BNIP3L/Nix-induced molecular defects could be averted via targeting BNIP3L/Nix through PRKA/PKA (Figure 4.2).

To our knowledge, our laboratory was the first to propose that the cell death gene BNIP3L, involved in the regulation of both apoptosis and necrosis (245), may be a key regulator of lipid-induced muscle insulin resistance, proposed by Mughal et al. in 2015 (243). Those preliminary observations laid the grounds for our current mechanistic discoveries of the possible mechanisms involved in this process. However, very little is known about how BNIP3L may impact insulin signaling in other tissues. One study by Fujimoto and colleagues (2010) demonstrates that beta-cell depletion of pancreatic duodenal homeobox (PDX1) resulted in increased BNIP3L (297). Their findings further confirmed that BNIP3L accumulation resulted in pancreatic beta-cell programmed cell death via concurrent activation of apoptotic and mitochondrial permeability transition-dependent necrotic pathways (297). Furthermore, both apoptosis and necrosis of beta cells are involved in diabetes progression, hence implicating a possible role of BNIP3L in mediating this molecular defect (447).

One of the limitations of our studies is that we mostly used culture-based models to test our central hypothesis. While these models are great for answering various mechanistic questions, they are not always indicative of translatability to *in vivo* models. We acknowledge the lack of animal-animal variability and depth regarding the variance in fiber type of skeletal muscle tissue, especially in its relation to whole-body glucose homeostasis. However, no animal model has been reported in the literature where BNIP3L has been specifically deleted in the skeletal muscle so it could be assessed its effect on mitochondrial energetics and insulin signaling.

Currently, our laboratory is developing a conditional muscle BNIP3L knockout mouse model to further address these intriguing questions. Preliminary data from our newly generated muscle-specific BNIP3L knockout mouse (unpublished) show that these animals display evidence of dysfunctional mitochondrial accumulation as a ragged red fiber phenotype (MERRF syndrome (or myoclonic epilepsy with ragged red fibers) (448), which is a mitochondrial disease. It is extremely rare, clumps of diseased mitochondria accumulate in the subsarcolemmal region of the muscle fiber and appear as "Ragged Red Fibers" when the muscle is stained with modified Gömöri trichrome stain. Besides this phenotype, the BNIP3L muscle-specific knockout mice are also more sensitive to exogenous insulin. Even though these investigations are still in the early stages, we hypothesize that we will be able to replicate our *in vitro* findings and further confirm the role of BNIP3L in insulin resistance in response to HF feeding.

In our *in vitro* studies, BNIP3L-induced mitophagy and impaired insulin signalling could be reversed by direct phosphorylation of BNIP3L at Serine 212 by PRKA activating agents, such as clenbuterol and phosphodiesterase-4 inhibitors (PDE4i). Our studies identified that upon phosphorylation, BNIP3L becomes highly susceptible to interact with molecular chaperones, such as YWHAB. The YWHA proteins are ubiquitously expressed, abundant in the brain (449). These proteins contain phosphoserine and threonine-dependent binding motifs (450, 451), where once phosphorylated, the YWHA proteins control subcellular translocation of various proteins to different organelles (452). Furthermore, other Bcl-2 family members, such as the pro-apoptotic BAD, once phosphorylated it physically interacts with YWHAB isoform, becoming inactive and no longer inducing cell death, resting at the cytosol (453). Similarly, our group was the first to demonstrate through this work that upon PRKA phosphorylation, BNIP3L binds to YWHAB, and it is translocated from the outer mitochondrial membrane and the ER to the cytosol, where it is inactive, improving mitochondrial function and muscle insulin signalling. Therefore, this novel target may represent a future therapeutic strategy to circumvent the mitochondrial defects observed in muscle insulin resistance, summarized in Figure 4.2.

Notably, in recent years, PRKA activating agents such as PDE4i have gained notoriety for their role in diabetes (454). Animal models (65) and human studies (346) have shown that PDE4i treatment promotes glucose-lowering and weight loss, likely via elevated GLP-1 levels, which contributes to promoting insulin secretion. Even though PDE4i seems an attractive therapy to treat T2D, little is known about its mechanisms and how it precisely averts the disease. In our culture-based investigations, we were able to elucidate a potential mechanism via which PDE4i treatment serves to induce PRKA inactivation of BNIP3L function, contributing to improved mitochondrial function and insulin signaling. Nonetheless, *in vivo* studies are necessary to further characterize the phenotype and role of BNIP3L function on muscle tissues of animals fed with a HF diet and treated with PDE4i. Additional details on how we will address this gap in our knowledge will be addressed in the next section of my discussion, under future directions.

Collectively, the data presented in this thesis emphasize that proper mitochondrial quality control is crucial for maintaining muscle homeostasis. Furthermore, disruption of mitochondrial quality control pathways, such as under lipotoxic stress, may lead to lipotoxic conditions whereby mitophagy becomes a maladaptive response to nutrient storage stress. Therefore, understanding BNIP3L's critical role in mitophagy and how it impairs muscle insulin signalling *in vitro* is

essential to further investigate and delineate its importance *in vivo* and in human studies, with the ultimate goal to avert the early onset of insulin resistance, characteristic of T2D.

Figure 4.2. Pharmacological inhibition of BNIP3L.

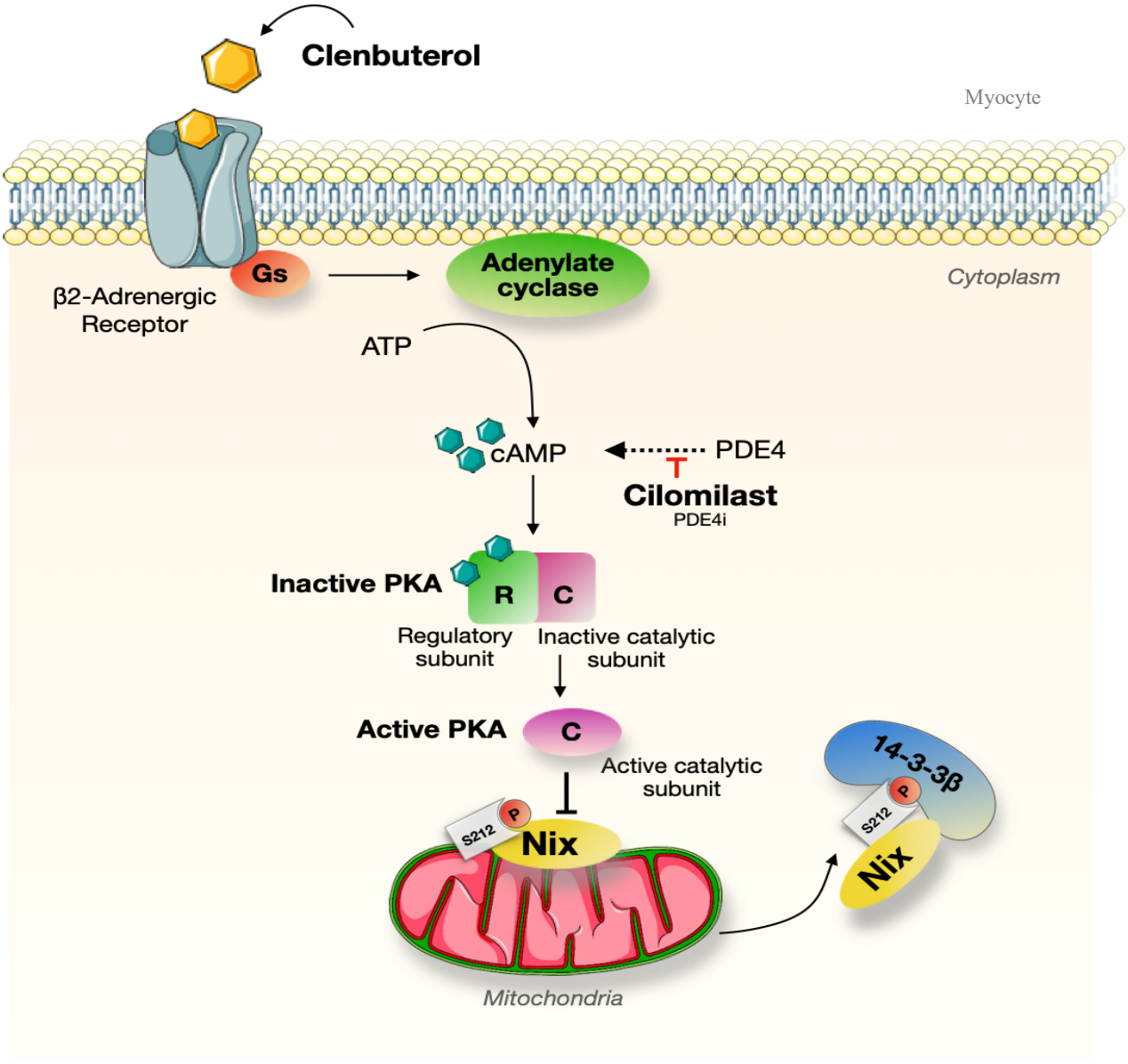

PRKA/PKA activating agents, clenbuterol and cilomilast, increase phosphorylation of BNIP3L/Nix at Serine 212 site. Upon phosphorylation, BNIP3L highly interacts with molecular chaperone YWHAB/14-3-3β, which translocate BNIP3L from mitochondria into the cytosol, improving mitochondrial dysfunction and preventing impairment of muscle insulin signalling.

4.2 Future Directions

As previously reviewed in Chapter I, BNIP3L has been extensively studied in model systems of pressure-overload cardiac remodeling and erythrocyte differentiation; however, less is known about the role of BNIP3L in insulin sensitivity. Evidence from my work is that BNIP3L can induce insulin resistance in myocyte cultures, and that PRKA can inhibit BNIP3L function, raising the possibility that pharmacological agents that target BNIP3L could be an innovative approach to reverse the adverse metabolic effects induced by BNIP3L.

I demonstrate that clenbuterol treatment restores mitochondrial function and insulin sensitivity when myotubes were cultured in a lipotoxic media. Although clenbuterol is not a safe drug to treat youth, it is a useful proof-of-concept drug, mimics some of the beneficial effects of exercise, and is a well characterized PRKA activator in myocyte cultures (351). Conversely, roflumilast, apremilast, and cilomilast have been used in human clinical trials (roflumilast and apremilast are FDA and Health Canada approved) and are inhibitors of the cardiac, skeletal, and smooth muscle-enriched phosphodiesterase-4 (i.e. PDE4is) and activate PRKA signalling in these tissues. Intended to be used as bronchodilators for asthma and COPD therapy, PDE4is have beneficial effects on the cardiovascular system and skeletal muscle leading to improved metabolism and weight loss (319). Thus, PDE4i therapy may represent a safe and effective way to improve early onset myocyte insulin resistance in youth. However, before attempts are made to target BNIP3L in human trials, it is vital to understand how PDE4i therapy regulates BNIP3L-induced insulin resistance and mitochondrial dysfunction in pre-clinical animal studies.

Therefore, the molecular framework laid in my thesis will support future investigations on the mechanistic role of BNIP3L-induced mitophagy and insulin resistance *in vivo*. Given my findings presented in Chapter III that BNIP3L is increased in response to lipotoxicity and contributes to mitophagy and myotube insulin resistance, and that BNIP3L can be pharmacologically modulated by PRKA activating agents, my central hypothesis is that by pharmacologically targeting BNIP3L we can prevent BNIP3L-induced mitochondrial dysfunction and insulin resistance in skeletal muscle *in vivo*. To evaluate this central hypothesis, I will use complementary approaches in animal models to accomplish the following aim:

To determine if targeting BNIP3L pharmacologically with PDE4i cilomilast can circumvent myocyte insulin resistance and mitochondrial derangements *in vivo*.

To achieve this, we will expose rodents to a LF diet (10% low fat) or a HFS diet (45% high fat and sucrose) for 12 weeks. At 15-weeks of age animals will be treated with PDE4i cilomilast (3mg/kg body weight daily) for 7, 14, and 21 days, while control animals will be treated with a vehicle control. At this dose, cilomilast prevented skeletal muscle atrophy elicited by denervation (319). Thus, this will be our starting dose; however, we will also perform dose-response analysis in control mice and evaluate BNIP3L phosphorylation as an end-point. We will use custom phospho-specific antibody designed to specifically recognize Serine-212 of BNIP3L (described in Chapter III) and evaluate BNIP3L phosphorylation in protein extracts made from these tissues, to determine if cilomilast treatment can restore BNIP3L phosphorylation in rodents exposed to HFS diet. In addition, we will perform glucose and insulin tolerance tests, exercise testing, and probe the insulin signalling pathway by western blot. We will also determine if cilomilast treatment can reduce BNIP3L content in isolated mitochondria from muscle tissue and determine mitochondrial oxygen consumption using a Seahorse metabolic flux analyzer. We predict that cilomilast treatment will serve to restore mitochondrial function, and reduce mitochondrial BNIP3L accumulation, concurrent with improvements in glucose tolerance, including insulin signalling, and exercise capacity.

These experiments will add the next logical extension to this work, whereby accurately understanding the causes of muscle insulin resistance at the molecular level *in vitro* and *in vivo*, we will be able to identify opportunities for clinical therapeutic exploitation. The anticipated project contributions are likely to advance knowledge of diabetes progression by providing novel pathways and targets for reversing early onset insulin resistance and mitochondrial dysfunction associated with exposure to a lipotoxic diet. Furthermore, the results of this future study will help us develop a therapeutic strategy to circumvent these adverse metabolic effects and minimize the burden of complications associated with type 2 diabetes in Canada.

4.3 Conclusion

In conclusion, during my PhD, I have investigated how BNIP3L, a mitophagy receptor, led to mitochondrial dysfunction and mitophagy in myocytes under lipotoxic conditions. This work's rationale was based on the fact that lipotoxicity and mitochondrial dysfunction play an interconnected role in myocyte insulin resistance and T2D; yet the precise molecular mechanisms are not fully understood. BNIP3L is a mitochondrial outer membrane protein involved in quality control, and it has been previously shown by our group to be responsive to lipid stress. In my study, I describe a novel mitophagy-driven pathway activated by BNIP3L that contributes to impaired insulin signalling in skeletal muscle.

The most significant observation that I made was that BNIP3L alters insulin sensitivity in the skeletal muscle and mitophagy plays an important role in this process. I found that BNIP3L-induced calcium release and mitophagy triggered insulin resistance through inhibitory phosphorylation of IRS1 by p70RPS6KB, contingent on phosphatidic acids availability. Furthermore, I identified a novel phosphorylation site of BNIP3L (Serine 212) at its transmembrane domain that can be activated by PRKA, which inhibited BNIP3L-induced mitochondrial dysfunction and insulin resistance. These findings allowed me to significantly contribute to the cellular biology field in the understanding of BNIP3L and its potential role in delaying or averting myocyte insulin resistance and T2D.

CHAPTER V: References

1. **Shadrin IY**, **Khodabukus A**, **Bursac N**. Striated Muscle Function, Regeneration, and Repair. *Cell Mol Life Sci CMLS* 73: 4175–4202, 2016. doi: 10.1007/s00018-016-2285-z.

2. **Brozovich FV**, **Nicholson CJ**, **Degen CV**, **Gao YZ**, **Aggarwal M**, **Morgan KG**. Mechanisms of Vascular Smooth Muscle Contraction and the Basis for Pharmacologic Treatment of Smooth Muscle Disorders. *Pharmacol Rev* 68: 476–532, 2016. doi: 10.1124/pr.115.010652.

3. **Jafri MS**. Models of Excitation–Contraction Coupling in Cardiac Ventricular Myocytes. *Methods Mol Biol Clifton NJ* 910: 309–335, 2012. doi: 10.1007/978-1-61779-965-5_14.

4. **Rassier DE**. Sarcomere mechanics in striated muscles: from molecules to sarcomeres to cells. *Am J Physiol-Cell Physiol* 313: C134–C145, 2017. doi: 10.1152/ajpcell.00050.2017.

5. **Henderson CA**, **Gomez CG**, **Novak SM**, **Mi-Mi L**, **Gregorio CC**. Overview of the Muscle Cytoskeleton. *Compr Physiol* 7: 891–944, 2017. doi: 10.1002/cphy.c160033.

6. **Gouspillou G**, **Hepple RT**. Editorial: Mitochondria in Skeletal Muscle Health, Aging and Diseases. *Front Physiol* 7, 2016. doi: 10.3389/fphys.2016.00446.

7. **Gan Z**, **Fu T**, **Kelly DP**, **Vega RB**. Skeletal muscle mitochondrial remodeling in exercise and diseases. *Cell Res* 28: 969–980, 2018. doi: 10.1038/s41422-018-0078-7.

8. **Glancy B**, **Hartnell LM**, **Malide D**, **Yu Z-X**, **Combs CA**, **Connelly PS**, **Subramaniam S**, **Balaban RS**. Mitochondrial reticulum for cellular energy distribution in muscle. *Nature* 523: 617–620, 2015. doi: 10.1038/nature14614.

9. **Relaix F**, **Rocancourt D**, **Mansouri A**, **Buckingham M**. A Pax3/Pax7-dependent population of skeletal muscle progenitor cells. *Nature* 435: 948–953, 2005. doi: 10.1038/nature03594.

10. **Kassar-Duchossoy L**, **Gayraud-Morel B**, **Gomès D**, **Rocancourt D**, **Buckingham M**, **Shinin V**, **Tajbakhsh S**. Mrf4 determines skeletal muscle identity in Myf5:Myod double-mutant mice. *Nature* 431: 466–471, 2004. doi: 10.1038/nature02876.

11. **Chal J**, **Pourquié O**. Making muscle: skeletal myogenesis in vivo and in vitro. *Development* 144: 2104–2122, 2017. doi: 10.1242/dev.151035.

12. **Schiaffino S**, **Reggiani C**. Fiber types in mammalian skeletal muscles. *Physiol Rev* 91: 1447–1531, 2011. doi: 10.1152/physrev.00031.2010.

13. **Chakkalakal JV**, **Kuang S**, **Buffelli M**, **Lichtman JW**, **Sanes JR**. MOUSE TRANSGENIC LINES THAT SELECTIVELY LABEL TYPE I, TYPE IIA AND

TYPES IIX+B SKELETAL MUSCLE FIBERS. *Genes N Y N 2000* 50: 50–58, 2012. doi: 10.1002/dvg.20794.

14. **Bassel-Duby R**, **Olson EN**. Signaling pathways in skeletal muscle remodeling. *Annu Rev Biochem* 75: 19–37, 2006. doi: 10.1146/annurev.biochem.75.103004.142622.

15. **Harridge SD**, **Bottinelli R**, **Canepari M**, **Pellegrino MA**, **Reggiani C**, **Esbjörnsson M**, **Saltin B**. Whole-muscle and single-fibre contractile properties and myosin heavy chain isoforms in humans. *Pflugers Arch* 432: 913–920, 1996. doi: 10.1007/s004240050215.

16. **McComas AJ**, **Thomas HC**. Fast and slow twitch muscles in man. *J Neurol Sci* 7: 301–307, 1968. doi: 10.1016/0022-510x(68)90150-0.

17. **Chen H**, **Vermulst M**, **Wang YE**, **Chomyn A**, **Prolla TA**, **McCaffery JM**, **Chan DC**. Mitochondrial fusion is required for mtDNA stability in skeletal muscle and tolerance of mtDNA mutations. *Cell* 141: 280–289, 2010. doi: 10.1016/j.cell.2010.02.026.

18. **Mishra P**, **Varuzhanyan G**, **Pham AH**, **Chan DC**. Mitochondrial dynamics is a distinguishing feature of skeletal muscle fiber types and regulates organellar compartmentalization. *Cell Metab* 22: 1033–1044, 2015. doi: 10.1016/j.cmet.2015.09.027.

19. **Gomes LC**, **Di Benedetto G**, **Scorrano L**. During autophagy mitochondria elongate, are spared from degradation and sustain cell viability. *Nat Cell Biol* 13: 589–598, 2011. doi: 10.1038/ncb2220.

20. **Talbot J**, **Maves L**. Skeletal muscle fiber type: using insights from muscle developmental biology to dissect targets for susceptibility and resistance to muscle disease. *Wiley Interdiscip Rev Dev Biol* 5: 518–534, 2016. doi: 10.1002/wdev.230.

21. **Albers PH**, **Pedersen AJT**, **Birk JB**, **Kristensen DE**, **Vind BF**, **Baba O**, **Nøhr J**, **Højlund K**, **Wojtaszewski JFP**. Human Muscle Fiber Type–Specific Insulin Signaling: Impact of Obesity and Type 2 Diabetes. *Diabetes* 64: 485–497, 2015. doi: 10.2337/db14-0590.

22. **Oberbach A**, **Bossenz Y**, **Lehmann S**, **Niebauer J**, **Adams V**, **Paschke R**, **Schön MR**, **Blüher M**, **Punkt K**. Altered Fiber Distribution and Fiber-Specific Glycolytic and Oxidative Enzyme Activity in Skeletal Muscle of Patients With Type 2 Diabetes. *Diabetes Care* 29: 895–900, 2006. doi: 10.2337/diacare.29.04.06.dc05-1854.

23. **Umek N**, **Horvat S**, **Cvetko E**, **Kreft M**, **Janáček J**, **Kubínová L**, **Stopar Pintarič T**, **Eržen I**. 3D analysis of capillary network in skeletal muscle of obese insulin-resistant mice. .

24. **Ferrannini E**, **Simonson DC**, **Katz LD**, **Reichard G**, **Bevilacqua S**, **Barrett EJ**, **Olsson M**, **DeFronzo RA**. The disposal of an oral glucose load in patients with non-insulin-dependent diabetes. *Metabolism* 37: 79–85, 1988. doi: 10.1016/0026-0495(88)90033-9.

25. **Hargreaves M**, **Spriet LL**. Skeletal muscle energy metabolism during exercise. *Nat Metab* 2: 817–828, 2020. doi: 10.1038/s42255-020-0251-4.

26. **Gowans GJ**, **Hardie DG**. AMPK: a cellular energy sensor primarily regulated by AMP. *Biochem Soc Trans* 42: 71–75, 2014. doi: 10.1042/BST20130244.

27. **Hayashi T**, **Hirshman MF**, **Fujii N**, **Habinowski SA**, **Witters LA**, **Goodyear LJ**. Metabolic stress and altered glucose transport: activation of AMP-activated protein kinase as a unifying coupling mechanism. *Diabetes* 49: 527–531, 2000. doi: 10.2337/diabetes.49.4.527.

28. **Kelley DE**. Skeletal muscle fat oxidation: timing and flexibility are everything. *J Clin Invest* 115: 1699–1702, 2005. doi: 10.1172/JCI25758.

29. **Ukropcova B**, **McNeil M**, **Sereda O**, **de Jonge L**, **Xie H**, **Bray GA**, **Smith SR**. Dynamic changes in fat oxidation in human primary myocytes mirror metabolic characteristics of the donor. *J Clin Invest* 115: 1934–1941, 2005. doi: 10.1172/JCI24332.

30. **Sears B**, **Perry M**. The role of fatty acids in insulin resistance. *Lipids Health Dis* 14, 2015. doi: 10.1186/s12944-015-0123-1.

31. **Karamitsos DT**. The story of insulin discovery. *Diabetes Res Clin Pract* 93: S2–S8, 2011. doi: 10.1016/S0168-8227(11)70007-9.

32. **Petersen MC**, **Shulman GI**. Mechanisms of Insulin Action and Insulin Resistance. *Physiol Rev* 98: 2133–2223, 2018. doi: 10.1152/physrev.00063.2017.

33. **Tokarz VL**, **MacDonald PE**, **Klip A**. The cell biology of systemic insulin function. .

34. **Ruegsegger GN**, **Creo AL**, **Cortes TM**, **Dasari S**, **Nair KS**. Altered mitochondrial function in insulin-deficient and insulin-resistant states. *J Clin Invest* 128: 3671–3681, [date unknown]. doi: 10.1172/JCI120843.

35. **Wilcox G**. Insulin and Insulin Resistance. *Clin Biochem Rev* 26: 19–39, 2005.

36. **Batista TM**, **Haider N**, **Kahn CR**. Defining the underlying defect in insulin action in type 2 diabetes. *Diabetologia* 64: 994–1006, 2021. doi: 10.1007/s00125-021-05415-5.

37. **Nadeau K**, **Dabelea D**. Epidemiology of type 2 diabetes in children and adolescents. *Endocr Res* 33: 35–58, 2008. doi: 10.1080/07435800802080138.

38. **DiMeglio LA**, **Evans-Molina C**, **Oram RA**. Type 1 diabetes. *Lancet Lond Engl* 391: 2449–2462, 2018. doi: 10.1016/S0140-6736(18)31320-5.

39. **Hull CM**, **Peakman M**, **Tree TIM**. Regulatory T cell dysfunction in type 1 diabetes: what's broken and how can we fix it? *Diabetologia* 60: 1839–1850, 2017. doi: 10.1007/s00125-017-4377-1.

40. **Gordon JW**, **Dolinsky VW**, **Mughal W**, **Gordon GRJ**, **McGavock J**. Targeting skeletal muscle mitochondria to prevent type 2 diabetes in youth. *Biochem Cell Biol Biochim Biol Cell* 93: 452–465, 2015. doi: 10.1139/bcb-2015-0012.

41. **Hesselink MKC**, **Schrauwen-Hinderling V**, **Schrauwen P**. Skeletal muscle mitochondria as a target to prevent or treat type 2 diabetes mellitus. *Nat Rev Endocrinol* 12: 633–645, 2016. doi: 10.1038/nrendo.2016.104.

42. **Muoio DM**. Metabolic inflexibility: when mitochondrial indecision leads to metabolic gridlock. *Cell* 159: 1253–1262, 2014. doi: 10.1016/j.cell.2014.11.034.

43. **Olokoba AB**, **Obateru OA**, **Olokoba LB**. Type 2 diabetes mellitus: a review of current trends. *Oman Med J* 27: 269–273, 2012. doi: 10.5001/omj.2012.68.

44. **Ader M**, **Bergman RN**. Insulin sensitivity in the intact organism. *Baillieres Clin Endocrinol Metab* 1: 879–910, 1987. doi: 10.1016/s0950-351x(87)80010-1.

45. **Pileggi CA**, **Parmar G**, **Harper M-E**. The lifecycle of skeletal muscle mitochondria in obesity. *Obes Rev* 22: e13164, 2021. doi: https://doi.org/10.1111/obr.13164.

46. **Simoneau JA**, **Colberg SR**, **Thaete FL**, **Kelley DE**. Skeletal muscle glycolytic and oxidative enzyme capacities are determinants of insulin sensitivity and muscle composition in obese women. *FASEB J Off Publ Fed Am Soc Exp Biol* 9: 273–278, 1995.

47. **Ritov VB**, **Menshikova EV**, **He J**, **Ferrell RE**, **Goodpaster BH**, **Kelley DE**. Deficiency of subsarcolemmal mitochondria in obesity and type 2 diabetes. *Diabetes* 54: 8–14, 2005. doi: 10.2337/diabetes.54.1.8.

48. **Holloway GP**, **Thrush AB**, **Heigenhauser GJF**, **Tandon NN**, **Dyck DJ**, **Bonen A**, **Spriet LL**. Skeletal muscle mitochondrial FAT/CD36 content and palmitate oxidation are not decreased in obese women. *Am J Physiol Endocrinol Metab* 292: E1782-1789, 2007. doi: 10.1152/ajpendo.00639.2006.

49. **Chomentowski P**, **Coen PM**, **Radiková Z**, **Goodpaster BH**, **Toledo FGS**. Skeletal muscle mitochondria in insulin resistance: differences in intermyofibrillar versus subsarcolemmal subpopulations and relationship to metabolic flexibility. *J Clin Endocrinol Metab* 96: 494–503, 2011. doi: 10.1210/jc.2010-0822.

50. **Dohm GL**, **Tapscott EB**, **Pories WJ**, **Dabbs DJ**, **Flickinger EG**, **Meelheim D**, **Fushiki T**, **Atkinson SM**, **Elton CW**, **Caro JF**. An in vitro human muscle preparation suitable for metabolic studies. Decreased insulin stimulation of glucose transport in muscle from morbidly obese and diabetic subjects. *J Clin Invest* 82: 486–494, 1988. doi: 10.1172/JCI113622.

51. **De Filippis E**, **Alvarez G**, **Berria R**, **Cusi K**, **Everman S**, **Meyer C**, **Mandarino LJ**. Insulin-resistant muscle is exercise resistant: evidence for reduced response of nuclear-encoded mitochondrial genes to exercise. *Am J Physiol Endocrinol Metab* 294: E607-614, 2008. doi: 10.1152/ajpendo.00729.2007.

52. **Coen PM**, **Hames KC**, **Leachman EM**, **DeLany JP**, **Ritov VB**, **Menshikova EV**, **Dubé JJ**, **Stefanovic-Racic M**, **Toledo FGS**, **Goodpaster BH**. Reduced skeletal muscle oxidative capacity and elevated ceramide but not diacylglycerol content in severe obesity. *Obes Silver Spring Md* 21: 2362–2371, 2013. doi: 10.1002/oby.20381.

53. **Koves TR**, **Ussher JR**, **Noland RC**, **Slentz D**, **Mosedale M**, **Ilkayeva O**, **Bain J**, **Stevens R**, **Dyck JRB**, **Newgard CB**, **Lopaschuk GD**, **Muoio DM**. Mitochondrial Overload and Incomplete Fatty Acid Oxidation Contribute to Skeletal Muscle Insulin Resistance. *Cell Metab* 7: 45–56, 2008. doi: 10.1016/j.cmet.2007.10.013.

54. **Egan B**, **Zierath JR**. Exercise metabolism and the molecular regulation of skeletal muscle adaptation. *Cell Metab* 17: 162–184, 2013. doi: 10.1016/j.cmet.2012.12.012.

55. **Tahrani AA**, **Bailey CJ**, **Del Prato S**, **Barnett AH**. Management of type 2 diabetes: new and future developments in treatment. *Lancet Lond Engl* 378: 182–197, 2011. doi: 10.1016/S0140-6736(11)60207-9.

56. **Diabetes Canada Clinical Practice Guidelines Expert Committee**, **Prebtani APH**, **Bajaj HS**, **Goldenberg R**, **Mullan Y**. Reducing the Risk of Developing Diabetes. *Can J Diabetes* 42 Suppl 1: S20–S26, 2018. doi: 10.1016/j.jcjd.2017.10.033.

57. **Inzucchi SE**, **Bergenstal RM**, **Buse JB**, **Diamant M**, **Ferrannini E**, **Nauck M**, **Peters AL**, **Tsapas A**, **Wender R**, **Matthews DR**. Management of hyperglycemia in type 2 diabetes, 2015: a patient-centered approach: update to a position statement of the American Diabetes Association and the European Association for the Study of Diabetes. *Diabetes Care* 38: 140–149, 2015. doi: 10.2337/dc14-2441.

58. IDF diabetes atlas - Home [Online]. [date unknown]. http://www.diabetesatlas.org/ [20 Apr. 2018].

59. **Kahn SE**, **Cooper ME**, **Del Prato S**. Pathophysiology and treatment of type 2 diabetes: perspectives on the past, present, and future. *Lancet Lond Engl* 383: 1068–1083, 2014. doi: 10.1016/S0140-6736(13)62154-6.

60. **Quianzon CCL**, **Cheikh IE**. History of current non-insulin medications for diabetes mellitus. *J Community Hosp Intern Med Perspect* 2, 2012. doi: 10.3402/jchimp.v2i3.19081.

61. **American Diabetes Association**. Standards of Medical Care in Diabetes-2018 Abridged for Primary Care Providers. *Clin Diabetes Publ Am Diabetes Assoc* 36: 14–37, 2018. doi: 10.2337/cd17-0119.

62. **Brunetti L**, **Kalabalik J**. Management of type-2 diabetes mellitus in adults: focus on individualizing non-insulin therapies. *P T Peer-Rev J Formul Manag* 37: 687–696, 2012.

63. **Fonseca VA**. New developments in diabetes management: medications of the 21st century. *Clin Ther* 36: 477–484, 2014. doi: 10.1016/j.clinthera.2014.01.018.

64. **Wouters EFM**, **Bredenbröker D**, **Teichmann P**, **Brose M**, **Rabe KF**, **Fabbri LM**, **Göke B**. Effect of the phosphodiesterase 4 inhibitor roflumilast on glucose metabolism in patients with treatment-naive, newly diagnosed type 2 diabetes mellitus. *J Clin Endocrinol Metab* 97: E1720-1725, 2012. doi: 10.1210/jc.2011-2886.

65. **Vollert S**, **Kaessner N**, **Heuser A**, **Hanauer G**, **Dieckmann A**, **Knaack D**, **Kley HP**, **Beume R**, **Weiss-Haljiti C**. The glucose-lowering effects of the PDE4 inhibitors roflumilast and roflumilast-N-oxide in db/db mice. *Diabetologia* 55: 2779–2788, 2012. doi: 10.1007/s00125-012-2632-z.

66. **Calverley PMA**, **Rabe KF**, **Goehring U-M**, **Kristiansen S**, **Fabbri LM**, **Martinez FJ**, **M2-124 and M2-125 study groups**. Roflumilast in symptomatic chronic obstructive pulmonary disease: two randomised clinical trials. *Lancet Lond Engl* 374: 685–694, 2009. doi: 10.1016/S0140-6736(09)61255-1.

67. **Fabbri LM**, **Calverley PMA**, **Izquierdo-Alonso JL**, **Bundschuh DS**, **Brose M**, **Martinez FJ**, **Rabe KF**, **M2-127 and M2-128 study groups**. Roflumilast in moderate-to-severe chronic obstructive pulmonary disease treated with longacting bronchodilators: two randomised clinical trials. *Lancet Lond Engl* 374: 695–703, 2009. doi: 10.1016/S0140-6736(09)61252-6.

68. **Möllmann J**, **Kahles F**, **Lebherz C**, **Kappel B**, **Baeck C**, **Tacke F**, **Werner C**, **Federici M**, **Marx N**, **Lehrke M**. The PDE4 inhibitor roflumilast reduces weight gain by increasing energy expenditure and leads to improved glucose metabolism. *Diabetes Obes Metab* 19: 496–508, 2017. doi: 10.1111/dom.12839.

69. **Ward CW**, **Lawrence MC**. Landmarks in Insulin Research. *Front Endocrinol* 2, 2011. doi: 10.3389/fendo.2011.00076.

70. **House PDR**, **Weidemann MJ**. Characterization of an [125I]-Insulin binding plasma membrane fraction from rat liver. *Biochem Biophys Res Commun* 41: 541–548, 1970. doi: 10.1016/0006-291X(70)90046-X.

71. **De Meyts P**. Insulin and its receptor: structure, function and evolution. *BioEssays News Rev Mol Cell Dev Biol* 26: 1351–1362, 2004. doi: 10.1002/bies.20151.

72. **Czech MP**. The nature and regulation of the insulin receptor: structure and function. *Annu Rev Physiol* 47: 357–381, 1985. doi: 10.1146/annurev.ph.47.030185.002041.

73. **Mosthaf L**, **Grako K**, **Dull TJ**, **Coussens L**, **Ullrich A**, **McClain DA**. Functionally distinct insulin receptors generated by tissue-specific alternative splicing. *EMBO J* 9: 2409–2413, 1990.

74. **Moller DE**, **Yokota A**, **Caro JF**, **Flier JS**. Tissue-specific expression of two alternatively spliced insulin receptor mRNAs in man. *Mol Endocrinol Baltim Md* 3: 1263–1269, 1989. doi: 10.1210/mend-3-8-1263.

75. **Wei L**, **Hubbard SR**, **Hendrickson WA**, **Ellis L**. Expression, Characterization, and Crystallization of the Catalytic Core of the Human Insulin Receptor Protein-tyrosine Kinase Domain. *J Biol Chem* 270: 8122–8130, 1995. doi: 10.1074/jbc.270.14.8122.

76. **Youngren JF**. Regulation of insulin receptor function. *Cell Mol Life Sci* 64: 873–891, 2007. doi: 10.1007/s00018-007-6359-9.

77. **Bedinger DH**, **Adams SH**. Metabolic, anabolic, and mitogenic insulin responses: A tissue-specific perspective for insulin receptor activators. *Mol Cell Endocrinol* 415: 143–156, 2015. doi: 10.1016/j.mce.2015.08.013.

78. **Hubbard SR**. The Insulin Receptor: Both a Prototypical and Atypical Receptor Tyrosine Kinase. *Cold Spring Harb Perspect Biol* 5: a008946, 2013. doi: 10.1101/cshperspect.a008946.

79. **Hsu PP**, **Kang SA**, **Rameseder J**, **Zhang Y**, **Ottina KA**, **Lim D**, **Peterson TR**, **Choi Y**, **Gray NS**, **Yaffe MB**, **Marto JA**, **Sabatini DM**. The mTOR-Regulated Phosphoproteome Reveals a Mechanism of mTORC1-Mediated Inhibition of Growth Factor Signaling. *Science* 332: 1317–1322, 2011. doi: 10.1126/science.1199498.

80. **Mahadev K**, **Motoshima H**, **Wu X**, **Ruddy JM**, **Arnold RS**, **Cheng G**, **Lambeth JD**, **Goldstein BJ**. The NAD(P)H Oxidase Homolog Nox4 Modulates Insulin-Stimulated Generation of H2O2 and Plays an Integral Role in Insulin Signal Transduction. *Mol Cell Biol* 24: 1844–1854, 2004. doi: 10.1128/MCB.24.5.1844-1854.2004.

81. **Araki E**, **Lipes MA**, **Patti M-E**, **Brüning JC**, **Haag Iii B**, **Johnson RS**, **Kahn CR**. Alternative pathway of insulin signalling in mice with targeted disruption of the IRS-1 gene. *Nature* 372: 186–190, 1994. doi: 10.1038/372186a0.

82. **Sun XJ**, **Rothenberg P**, **Kahn CR**, **Backer JM**, **Araki E**, **Wilden PA**, **Cahill DA**, **Goldstein BJ**, **White MF**. Structure of the insulin receptor substrate IRS-1 defines a unique signal transduction protein. *Nature* 352: 73–77, 1991. doi: 10.1038/352073a0.

83. **White MF**, **White MF**. Mechanisms of Insulin Action. In: *Atlas of Diabetes: Fourth Edition*, edited by Skyler J. Springer US, p. 19–38.

84. **Brachmann SM**, **Ueki K**, **Engelman JA**, **Kahn RC**, **Cantley LC**. Phosphoinositide 3-Kinase Catalytic Subunit Deletion and Regulatory Subunit Deletion Have Opposite Effects on Insulin Sensitivity in Mice. *Mol Cell Biol* 25: 1596–1607, 2005. doi: 10.1128/MCB.25.5.1596-1607.2005.

85. **Cheatham B**, **Vlahos CJ**, **Cheatham L**, **Wang L**, **Kahn' CR**. Phosphatidylinositol 3-Kinase Activation Is Required for Insulin Stimulation of pp7O S6 Kinase, DNA Synthesis, and Glucose Transporter Translocation. 14: 10, 1994.

86. **Hodakoski C**, **Hopkins BD**, **Barrows D**, **Mense SM**, **Keniry M**, **Anderson KE**, **Kern PA**, **Hawkins PT**, **Stephens LR**, **Parsons R**. Regulation of PTEN inhibition by the

pleckstrin homology domain of P-REX2 during insulin signaling and glucose homeostasis. *Proc Natl Acad Sci* 111: 155–160, 2014. doi: 10.1073/pnas.1213773111.

87. **Stephens L**, **Anderson K**, **Stokoe D**, **Erdjument-Bromage H**, **Painter GF**, **Holmes AB**, **Gaffney PRJ**, **Reese CB**, **McCormick F**, **Tempst P**, **Coadwell J**, **Hawkins PT**. Protein Kinase B Kinases That Mediate Phosphatidylinositol 3,4,5-Trisphosphate-Dependent Activation of Protein Kinase B. *Science* 279: 710–714, 1998. doi: 10.1126/science.279.5351.710.

88. **Sarbassov DD**, **Guertin DA**, **Ali SM**, **Sabatini DM**. Phosphorylation and Regulation of Akt/PKB by the Rictor-mTOR Complex. *Science* 307: 1098–1101, 2005. doi: 10.1126/science.1106148.

89. **Leto D**, **Saltiel AR**. Regulation of glucose transport by insulin: traffic control of GLUT4. *Nat Rev Mol Cell Biol* 13: 383–396, 2012. doi: 10.1038/nrm3351.

90. **Yu Y**, **Yoon S-O**, **Poulogiannis G**, **Yang Q**, **Ma XM**, **Villén J**, **Kubica N**, **Hoffman GR**, **Cantley LC**, **Gygi SP**, **Blenis J**. Phosphoproteomic Analysis Identifies Grb10 as an mTORC1 Substrate That Negatively Regulates Insulin Signaling. *Science* 332: 1322–1326, 2011. doi: 10.1126/science.1199484.

91. **DeFronzo RA**, **Tripathy D**. Skeletal Muscle Insulin Resistance Is the Primary Defect in Type 2 Diabetes. *Diabetes Care* 32: S157–S163, 2009. doi: 10.2337/dc09-S302.

92. **Shulman GI**, **Rothman DL**, **Jue T**, **Stein P**, **DeFronzo RA**, **Shulman RG**. Quantitation of muscle glycogen synthesis in normal subjects and subjects with non-insulin-dependent diabetes by 13C nuclear magnetic resonance spectroscopy. *N Engl J Med* 322: 223–228, 1990. doi: 10.1056/NEJM199001253220403.

93. **Thiebaud D**, **Jacot E**, **Defronzo RA**, **Maeder E**, **Jequier E**, **Felber J-P**. The Effect of Graded Doses of Insulin on Total Glucose Uptake, Glucose Oxidation, and Glucose Storage in Man. *Diabetes* 31: 957–963, 1982. doi: 10.2337/diacare.31.11.957.

94. **Boucher J**, **Kleinridders A**, **Kahn CR**. Insulin Receptor Signaling in Normal and Insulin-Resistant States. *Cold Spring Harb Perspect Biol* 6: a009191, 2014. doi: 10.1101/cshperspect.a009191.

95. **Taniguchi CM**, **Emanuelli B**, **Kahn CR**. Critical nodes in signalling pathways: insights into insulin action. *Nat Rev Mol Cell Biol* 7: 85, 2006. doi: 10.1038/nrm1837.

96. **Pederson TM**, **Kramer DL**, **Rondinone CM**. Serine/Threonine Phosphorylation of IRS-1 Triggers Its Degradation: Possible Regulation by Tyrosine Phosphorylation. *Diabetes* 50: 24–31, 2001. doi: 10.2337/diabetes.50.1.24.

97. **Higaki Y**, **Wojtaszewski JF**, **Hirshman MF**, **Withers DJ**, **Towery H**, **White MF**, **Goodyear LJ**. Insulin receptor substrate-2 is not necessary for insulin- and exercise-stimulated glucose transport in skeletal muscle. *J Biol Chem* 274: 20791–20795, 1999. doi: 10.1074/jbc.274.30.20791.

98. **Gao X**, **Lowry PR**, **Zhou X**, **Depry C**, **Wei Z**, **Wong GW**, **Zhang J**. PI3K/Akt signaling requires spatial compartmentalization in plasma membrane microdomains. *Proc Natl Acad Sci U S A* 108: 14509–14514, 2011. doi: 10.1073/pnas.1019386108.

99. **Cho H**, **Mu J**, **Kim JK**, **Thorvaldsen JL**, **Chu Q**, **Crenshaw EB**, **Kaestner KH**, **Bartolomei MS**, **Shulman GI**, **Birnbaum MJ**. Insulin Resistance and a Diabetes Mellitus-Like Syndrome in Mice Lacking the Protein Kinase Akt2 (PKBβ). *Science* 292: 1728–1731, 2001. doi: 10.1126/science.292.5522.1728.

100. **Cho H**, **Thorvaldsen JL**, **Chu Q**, **Feng F**, **Birnbaum MJ**. Akt1/PKBα Is Required for Normal Growth but Dispensable for Maintenance of Glucose Homeostasis in Mice. *J Biol Chem* 276: 38349–38352, 2001. doi: 10.1074/jbc.C100462200.

101. **Hausdorff SF**, **Fingar DC**, **Morioka K**, **Garza LA**, **Whiteman EL**, **Summers SA**, **Birnbaum MJ**. Identification of Wortmannin-sensitive Targets in 3T3-L1 Adipocytes: DISSOCIATION OF INSULIN-STIMULATED GLUCOSE UPTAKE AND GLUT4 TRANSLOCATION. *J Biol Chem* 274: 24677–24684, 1999. doi: 10.1074/jbc.274.35.24677.

102. **Gonzalez E**, **McGraw TE**. Insulin-modulated Akt subcellular localization determines Akt isoform-specific signaling. *Proc Natl Acad Sci* 106: 7004–7009, 2009. doi: 10.1073/pnas.0901933106.

103. **Zeigerer A**, **McBrayer MK**, **McGraw TE**. Insulin Stimulation of GLUT4 Exocytosis, but Not Its Inhibition of Endocytosis, Is Dependent on RabGAP AS160. *Mol Biol Cell* 15: 4406–4415, 2004. doi: 10.1091/mbc.E04-04-0333.

104. **Wu H**, **Wang Y**, **Li W**, **Chen H**, **Du L**, **Liu D**, **Wang X**, **Xu T**, **Liu L**, **Chen Q**. Deficiency of mitophagy receptor FUNDC1 impairs mitochondrial quality and aggravates dietary-induced obesity and metabolic syndrome. *Autophagy* 15: 1882–1898, 2019. doi: 10.1080/15548627.2019.1596482.

105. **Sylow L**, **Jensen TE**, **Kleinert M**, **Højlund K**, **Kiens B**, **Wojtaszewski J**, **Prats C**, **Schjerling P**, **Richter EA**. Rac1 Signaling Is Required for Insulin-Stimulated Glucose Uptake and Is Dysregulated in Insulin-Resistant Murine and Human Skeletal Muscle. *Diabetes* 62: 1865–1875, 2013. doi: 10.2337/db12-1148.

106. **Mehran AE**, **Templeman NM**, **Brigidi GS**, **Lim GE**, **Chu K-Y**, **Hu X**, **Botezelli JD**, **Asadi A**, **Hoffman BG**, **Kieffer TJ**, **Bamji SX**, **Clee SM**, **Johnson JD**. Hyperinsulinemia Drives Diet-Induced Obesity Independently of Brain Insulin Production. *Cell Metab* 16: 723–737, 2012. doi: 10.1016/j.cmet.2012.10.019.

107. **Templeman NM**, **Clee SM**, **Johnson JD**. Suppression of hyperinsulinaemia in growing female mice provides long-term protection against obesity. *Diabetologia* 58: 2392–2402, 2015. doi: 10.1007/s00125-015-3676-7.

108. **Kahn BB**, **Flier JS**. Obesity and insulin resistance. *J Clin Invest* 106: 473–481, 2000.

109. **Erion DM**, **Shulman GI**. Diacylglycerol-mediated insulin resistance. *Nat Med* 16: 400–402, 2010. doi: 10.1038/nm0410-400.

110. **Samuel VT**, **Shulman GI**. The pathogenesis of insulin resistance: integrating signaling pathways and substrate flux. *J Clin Invest* 126: 12–22, 2016. doi: 10.1172/JCI77812.

111. **Chavez JA**, **Summers SA**. Characterizing the effects of saturated fatty acids on insulin signaling and ceramide and diacylglycerol accumulation in 3T3-L1 adipocytes and C2C12 myotubes. *Arch Biochem Biophys* 419: 101–109, 2003. doi: 10.1016/j.abb.2003.08.020.

112. **Itani SI**, **Ruderman NB**, **Schmieder F**, **Boden G**. Lipid-induced insulin resistance in human muscle is associated with changes in diacylglycerol, protein kinase C, and IkappaB-alpha. *Diabetes* 51: 2005–2011, 2002. doi: 10.2337/diabetes.51.7.2005.

113. **Montell E**, **Turini M**, **Marotta M**, **Roberts M**, **Noé V**, **Ciudad CJ**, **Macé K**, **Gómez-Foix AM**. DAG accumulation from saturated fatty acids desensitizes insulin stimulation of glucose uptake in muscle cells. *Am J Physiol Endocrinol Metab* 280: E229-237, 2001. doi: 10.1152/ajpendo.2001.280.2.E229.

114. **Marchesini G**, **Brizi M**, **Morselli-Labate AM**, **Bianchi G**, **Bugianesi E**, **McCullough AJ**, **Forlani G**, **Melchionda N**. Association of nonalcoholic fatty liver disease with insulin resistance. *Am J Med* 107: 450–455, 1999. doi: 10.1016/S0002-9343(99)00271-5.

115. **Morigny P**, **Houssier M**, **Mouisel E**, **Langin D**. Adipocyte lipolysis and insulin resistance. *Biochimie* 125: 259–266, 2016. doi: 10.1016/j.biochi.2015.10.024.

116. **Goodpaster BH**, **Sparks LM**. Metabolic Flexibility in Health and Disease. *Cell Metab* 25: 1027–1036, 2017. doi: 10.1016/j.cmet.2017.04.015.

117. **Rahimi Y**, **Camporez J-PG**, **Petersen MC**, **Pesta D**, **Perry RJ**, **Jurczak MJ**, **Cline GW**, **Shulman GI**. Genetic activation of pyruvate dehydrogenase alters oxidative substrate selection to induce skeletal muscle insulin resistance. *Proc Natl Acad Sci U S A* 111: 16508–16513, 2014. doi: 10.1073/pnas.1419104111.

118. **Morino K**, **Petersen KF**, **Shulman GI**. Molecular Mechanisms of Insulin Resistance in Humans and Their Potential Links With Mitochondrial Dysfunction. *Diabetes* 55: S9–S15, 2006. doi: 10.2337/db06-S002.

119. **Summers SA**, **Nelson DH**. A Role for Sphingolipids in Producing the Common Features of Type 2 Diabetes, Metabolic Syndrome X, and Cushing's Syndrome. *Diabetes* 54: 591–602, 2005. doi: 10.2337/diabetes.54.3.591.

120. **Corpeleijn E**, **Saris WHM**, **Blaak EE**. Metabolic flexibility in the development of insulin resistance and type 2 diabetes: effects of lifestyle. *Obes Rev* 10: 178–193, 2009. doi: 10.1111/j.1467-789X.2008.00544.x.

121. **San-Millán I**, **Brooks GA**. Assessment of Metabolic Flexibility by Means of Measuring Blood Lactate, Fat, and Carbohydrate Oxidation Responses to Exercise in Professional

Endurance Athletes and Less-Fit Individuals. *Sports Med* 48: 467–479, 2018. doi: 10.1007/s40279-017-0751-x.

122. **Gaster M**. Metabolic flexibility is conserved in diabetic myotubes. *J Lipid Res* 48: 207–217, 2007. doi: 10.1194/jlr.M600319-JLR200.

123. **Gaster M**, **Rustan AC**, **Aas V**, **Beck-Nielsen H**. Reduced lipid oxidation in skeletal muscle from type 2 diabetic subjects may be of genetic origin: evidence from cultured myotubes. *Diabetes* 53: 542–548, 2004. doi: 10.2337/diabetes.53.3.542.

124. **Villalobos-Labra R**, **Subiabre M**, **Toledo F**, **Pardo F**, **Sobrevia L**. Endoplasmic reticulum stress and development of insulin resistance in adipose, skeletal, liver, and foetoplacental tissue in diabesity. *Mol Aspects Med* 66: 49–61, 2019. doi: 10.1016/j.mam.2018.11.001.

125. **White SA**, **Zhang LS**, **Pasula DJ**, **Yang YHC**, **Luciani DS**. Bax and Bak jointly control survival and dampen the early unfolded protein response in pancreatic β-cells under glucolipotoxic stress. *Sci Rep* 10, 2020. doi: 10.1038/s41598-020-67755-3.

126. **Vincenz-Donnelly L**, **Hipp MS**. The endoplasmic reticulum: A hub of protein quality control in health and disease. *Free Radic Biol Med* 108: 383–393, 2017. doi: 10.1016/j.freeradbiomed.2017.03.031.

127. **Adams CJ**, **Kopp MC**, **Larburu N**, **Nowak PR**, **Ali MMU**. Structure and Molecular Mechanism of ER Stress Signaling by the Unfolded Protein Response Signal Activator IRE1. *Front Mol Biosci* 6: 11, 2019. doi: 10.3389/fmolb.2019.00011.

128. **Aguirre V**, **Uchida T**, **Yenush L**, **Davis R**, **White MF**. The c-Jun NH2-terminal Kinase Promotes Insulin Resistance during Association with Insulin Receptor Substrate-1 and Phosphorylation of Ser307. *J Biol Chem* 275: 9047–9054, 2000. doi: 10.1074/jbc.275.12.9047.

129. **Solinas G**, **Becattini B**. JNK at the crossroad of obesity, insulin resistance, and cell stress response. *Mol Metab* 6: 174–184, 2016. doi: 10.1016/j.molmet.2016.12.001.

130. **Ohoka N**, **Yoshii S**, **Hattori T**, **Onozaki K**, **Hayashi H**. TRB3, a novel ER stress-inducible gene, is induced via ATF4–CHOP pathway and is involved in cell death. *EMBO J* 24: 1243–1255, 2005. doi: 10.1038/sj.emboj.7600596.

131. **Ozcan L**, **Cristina de Souza J**, **Harari AA**, **Backs J**, **Olson EN**, **Tabas I**. Activation of Calcium/Calmodulin-Dependent Protein Kinase II in Obesity Mediates Suppression of Hepatic Insulin Signaling. *Cell Metab* 18: 803–815, 2013. doi: 10.1016/j.cmet.2013.10.011.

132. **Sergi D**, **Naumovski N**, **Heilbronn LK**, **Abeywardena M**, **O'Callaghan N**, **Lionetti L**, **Luscombe-Marsh N**. Mitochondrial (Dys)function and Insulin Resistance: From Pathophysiological Molecular Mechanisms to the Impact of Diet. *Front Physiol* 10, 2019. doi: 10.3389/fphys.2019.00532.

133. **Kim Jeong-a**, **Wei Yongzhong**, **Sowers James R.** Role of Mitochondrial Dysfunction in Insulin Resistance. *Circ Res* 102: 401–414, 2008. doi: 10.1161/CIRCRESAHA.107.165472.

134. **Lowell BB**, **Shulman GI**. Mitochondrial dysfunction and type 2 diabetes. *Science* 307: 384–387, 2005. doi: 10.1126/science.1104343.

135. **Jheng H-F**, **Tsai P-J**, **Guo S-M**, **Kuo L-H**, **Chang C-S**, **Su I-J**, **Chang C-R**, **Tsai Y-S**. Mitochondrial Fission Contributes to Mitochondrial Dysfunction and Insulin Resistance in Skeletal Muscle. *Mol Cell Biol* 32: 309–319, 2012. doi: 10.1128/MCB.05603-11.

136. **Schieber M**, **Chandel NS**. ROS Function in Redox Signaling and Oxidative Stress. *Curr Biol* 24: R453–R462, 2014. doi: 10.1016/j.cub.2014.03.034.

137. **Wei X**, **Qi Y**, **Zhang X**, **Qiu Q**, **Gu X**, **Tao C**, **Huang D**, **Zhang Y**. Cadmium induces mitophagy through ROS-mediated PINK1/Parkin pathway. *Toxicol Mech Methods* 24: 504–511, 2014. doi: 10.3109/15376516.2014.943444.

138. **Montgomery MK**, **Turner N**. Mitochondrial dysfunction and insulin resistance: an update. *Endocr Connect* 4: R1–R15, 2014. doi: 10.1530/EC-14-0092.

139. **Garvey WT**, **Maianu L**, **Zhu JH**, **Brechtel-Hook G**, **Wallace P**, **Baron AD**. Evidence for defects in the trafficking and translocation of GLUT4 glucose transporters in skeletal muscle as a cause of human insulin resistance. 1998.

140. **Abdul-Ghani MA**, **DeFronzo RA**. Pathogenesis of Insulin Resistance in Skeletal Muscle. *BioMed Res. Int.*: 2010.

141. **Randle PJ**, **Garland PB**, **Hales CN**, **Newsholme EA**. The glucose fatty-acid cycle. Its role in insulin sensitivity and the metabolic disturbances of diabetes mellitus. *Lancet Lond Engl* 1: 785–789, 1963.

142. **Gassaway BM**, **Petersen MC**, **Surovtseva YV**, **Barber KW**, **Sheetz JB**, **Aerni HR**, **Merkel JS**, **Samuel VT**, **Shulman GI**, **Rinehart J**. PKCε contributes to lipid-induced insulin resistance through cross talk with p70S6K and through previously unknown regulators of insulin signaling. *Proc Natl Acad Sci* 115: E8996–E9005, 2018. doi: 10.1073/pnas.1804379115.

143. **Muoio DM**, **Newgard CB**. Molecular and metabolic mechanisms of insulin resistance and β-cell failure in type 2 diabetes. *Nat Rev Mol Cell Biol* 9: 193–205, 2008. doi: 10.1038/nrm2327.

144. **Shulman GI**. Cellular mechanisms of insulin resistance. *J Clin Invest* 106: 171–176, 2000. doi: 10.1172/JCI10583.

145. **Yu C**, **Chen Y**, **Cline GW**, **Zhang D**, **Zong H**, **Wang Y**, **Bergeron R**, **Kim JK**, **Cushman SW**, **Cooney GJ**, **Atcheson B**, **White MF**, **Kraegen EW**, **Shulman GI**. Mechanism by which fatty acids inhibit insulin activation of insulin receptor substrate-1 (IRS-1)-

associated phosphatidylinositol 3-kinase activity in muscle. *J Biol Chem* 277: 50230–50236, 2002. doi: 10.1074/jbc.M200958200.

146. **Szendroedi J**, **Yoshimura T**, **Phielix E**, **Koliaki C**, **Marcucci M**, **Zhang D**, **Jelenik T**, **Müller J**, **Herder C**, **Nowotny P**, **Shulman GI**, **Roden M**. Role of diacylglycerol activation of PKCθ in lipid-induced muscle insulin resistance in humans. *Proc Natl Acad Sci U S A* 111: 9597–9602, 2014. doi: 10.1073/pnas.1409229111.

147. **Perreault L**, **Newsom SA**, **Strauss A**, **Kerege A**, **Kahn DE**, **Harrison KA**, **Snell-Bergeon JK**, **Nemkov T**, **D'Alessandro A**, **Jackman MR**, **MacLean PS**, **Bergman BC**. Intracellular localization of diacylglycerols and sphingolipids influences insulin sensitivity and mitochondrial function in human skeletal muscle. *JCI Insight* 3, 2018. doi: 10.1172/jci.insight.96805.

148. **Daemen S**, **Gemmink A**, **Brouwers B**, **Meex RCR**, **Huntjens PR**, **Schaart G**, **Moonen-Kornips E**, **Jörgensen J**, **Hoeks J**, **Schrauwen P**, **Hesselink MKC**. Distinct lipid droplet characteristics and distribution unmask the apparent contradiction of the athlete's paradox. *Mol Metab* 17: 71–81, 2018. doi: 10.1016/j.molmet.2018.08.004.

149. **Felig P**, **Wahren J**, **Hendler R**, **Brundin T**. Splanchnic glucose and amino acid metabolism in obesity. *J Clin Invest* 53: 582–590, 1974. doi: 10.1172/JCI107593.

150. **Krebs M**, **Krssak M**, **Bernroider E**, **Anderwald C**, **Brehm A**, **Meyerspeer M**, **Nowotny P**, **Roth E**, **Waldhäusl W**, **Roden M**. Mechanism of amino acid-induced skeletal muscle insulin resistance in humans. *Diabetes* 51: 599–605, 2002. doi: 10.2337/diabetes.51.3.599.

151. **Um SH**, **D'Alessio D**, **Thomas G**. Nutrient overload, insulin resistance, and ribosomal protein S6 kinase 1, S6K1. *Cell Metab* 3: 393–402, 2006. doi: 10.1016/j.cmet.2006.05.003.

152. **Zhou M**, **Shao J**, **Wu C-Y**, **Shu L**, **Dong W**, **Liu Y**, **Chen M**, **Wynn RM**, **Wang J**, **Wang J**, **Gui W-J**, **Qi X**, **Lusis AJ**, **Li Z**, **Wang W**, **Ning G**, **Yang X**, **Chuang DT**, **Wang Y**, **Sun H**. Targeting BCAA Catabolism to Treat Obesity-Associated Insulin Resistance. *Diabetes* 68: 1730–1746, 2019. doi: 10.2337/db18-0927.

153. **Sun H**, **Wang Y**. A new branch connecting thermogenesis and diabetes. *Nat Metab* 1: 845–846, 2019. doi: 10.1038/s42255-019-0112-1.

154. **Tremblay F**, **Brûlé S**, **Hee Um S**, **Li Y**, **Masuda K**, **Roden M**, **Sun XJ**, **Krebs M**, **Polakiewicz RD**, **Thomas G**, **Marette A**. Identification of IRS-1 Ser-1101 as a target of S6K1 in nutrient- and obesity-induced insulin resistance. *Proc Natl Acad Sci U S A* 104: 14056–14061, 2007. doi: 10.1073/pnas.0706517104.

155. **Rudich A**, **Tirosh A**, **Potashnik R**, **Hemi R**, **Kanety H**, **Bashan N**. Prolonged oxidative stress impairs insulin-induced GLUT4 translocation in 3T3-L1 adipocytes. *Diabetes* 47: 1562–1569, 1998. doi: 10.2337/diabetes.47.10.1562.

156. **Hurrle S**, **Hsu WH**. The etiology of oxidative stress in insulin resistance. *Biomed J* 40: 257–262, 2017. doi: 10.1016/j.bj.2017.06.007.

157. **Loh K**, **Deng H**, **Fukushima A**, **Cai X**, **Boivin B**, **Galic S**, **Bruce C**, **Shields BJ**, **Skiba B**, **Ooms LM**, **Stepto N**, **Wu B**, **Mitchell CA**, **Tonks NK**, **Watt MJ**, **Febbraio MA**, **Crack PJ**, **Andrikopoulos S**, **Tiganis T**. Reactive oxygen species enhance insulin sensitivity. *Cell Metab* 10: 260–272, 2009. doi: 10.1016/j.cmet.2009.08.009.

158. **Anderson EJ**, **Lustig ME**, **Boyle KE**, **Woodlief TL**, **Kane DA**, **Lin C-T**, **Price JW**, **Kang L**, **Rabinovitch PS**, **Szeto HH**, **Houmard JA**, **Cortright RN**, **Wasserman DH**, **Neufer PD**. Mitochondrial H2O2 emission and cellular redox state link excess fat intake to insulin resistance in both rodents and humans. *J Clin Invest* 119: 573–581, 2009. doi: 10.1172/JCI37048.

159. **Song F**, **Jia W**, **Yao Y**, **Hu Y**, **Lei L**, **Lin J**, **Sun X**, **Liu L**. Oxidative stress, antioxidant status and DNA damage in patients with impaired glucose regulation and newly diagnosed Type 2 diabetes. *Clin Sci* 112: 599–606, 2007. doi: 10.1042/CS20060323.

160. **Lee H-Y**, **Lee JS**, **Alves T**, **Ladiges W**, **Rabinovitch PS**, **Jurczak MJ**, **Choi CS**, **Shulman GI**, **Samuel VT**. Mitochondrial-Targeted Catalase Protects Against High-Fat Diet–Induced Muscle Insulin Resistance by Decreasing Intramuscular Lipid Accumulation. *Diabetes* 66: 2072–2081, 2017. doi: 10.2337/db16-1334.

161. **Mootha VK**, **Lindgren CM**, **Eriksson K-F**, **Subramanian A**, **Sihag S**, **Lehar J**, **Puigserver P**, **Carlsson E**, **Ridderstråle M**, **Laurila E**, **Houstis N**, **Daly MJ**, **Patterson N**, **Mesirov JP**, **Golub TR**, **Tamayo P**, **Spiegelman B**, **Lander ES**, **Hirschhorn JN**, **Altshuler D**, **Groop LC**. PGC-1α-responsive genes involved in oxidative phosphorylation are coordinately downregulated in human diabetes. *Nat Genet* 34: 267–273, 2003. doi: 10.1038/ng1180.

162. **Patti ME**, **Butte AJ**, **Crunkhorn S**, **Cusi K**, **Berria R**, **Kashyap S**, **Miyazaki Y**, **Kohane I**, **Costello M**, **Saccone R**, **Landaker EJ**, **Goldfine AB**, **Mun E**, **DeFronzo R**, **Finlayson J**, **Kahn CR**, **Mandarino LJ**. Coordinated reduction of genes of oxidative metabolism in humans with insulin resistance and diabetes: Potential role of PGC1 and NRF1. *Proc Natl Acad Sci* 100: 8466–8471, 2003. doi: 10.1073/pnas.1032913100.

163. **Chow LS**, **Mashek DG**, **Wang Q**, **Shepherd SO**, **Goodpaster BH**, **Dubé JJ**. Effect of acute physiological free fatty acid elevation in the context of hyperinsulinemia on fiber type-specific IMCL accumulation. *J Appl Physiol* 123: 71–78, 2017. doi: 10.1152/japplphysiol.00209.2017.

164. **Mugabo Y**, **Lim GE**. Scaffold Proteins: From Coordinating Signaling Pathways to Metabolic Regulation. *Endocrinology* 159: 3615–3630, 2018. doi: 10.1210/en.2018-00705.

165. **Dong XC**, **Copps KD**, **Guo S**, **Li Y**, **Kollipara R**, **DePinho RA**, **White MF**. Inactivation of Hepatic Foxo1 by Insulin Signaling Is Required for Adaptive Nutrient Homeostasis and

Endocrine Growth Regulation. *Cell Metab* 8: 65–76, 2008. doi: 10.1016/j.cmet.2008.06.006.

166. **Lu M**, **Wan M**, **Leavens KF**, **Chu Q**, **Monks BR**, **Fernandez S**, **Ahima RS**, **Ueki K**, **Kahn CR**, **Birnbaum MJ**. Insulin regulates liver metabolism in vivo in the absence of hepatic Akt and Foxo1. *Nat Med* 18: 388–395, 2012. doi: 10.1038/nm.2686.

167. **Tikhanovich I**, **Cox J**, **Weinman S**. FOXO Transcription Factors in Liver Function and Disease. *J Gastroenterol Hepatol* 28: 125–131, 2013. doi: 10.1111/jgh.12021.

168. **Zhao X**, **Gan L**, **Pan H**, **Kan D**, **Majeski M**, **Adam SA**, **Unterman TG**. Multiple elements regulate nuclear/cytoplasmic shuttling of FOXO1: characterization of phosphorylation- and 14-3-3-dependent and -independent mechanisms. *Biochem J* 378: 839–849, 2004. doi: 10.1042/BJ20031450.

169. **Matsumoto M**, **Pocai A**, **Rossetti L**, **DePinho RA**, **Accili D**. Impaired Regulation of Hepatic Glucose Production in Mice Lacking the Forkhead Transcription Factor Foxo1 in Liver. *Cell Metab* 6: 208–216, 2007. doi: 10.1016/j.cmet.2007.08.006.

170. **Schwarz J-M**, **Clearfield M**, **Mulligan K**. Conversion of Sugar to Fat: Is Hepatic de Novo Lipogenesis Leading to Metabolic Syndrome and Associated Chronic Diseases? *J Am Osteopath Assoc* 117: 520–527, 2017. doi: 10.7556/jaoa.2017.102.

171. **Li S**, **Brown MS**, **Goldstein JL**. Bifurcation of insulin signaling pathway in rat liver: mTORC1 required for stimulation of lipogenesis, but not inhibition of gluconeogenesis. *Proc Natl Acad Sci* 107: 3441–3446, 2010. doi: 10.1073/pnas.0914798107.

172. **Wu Y**, **Pan Q**, **Yan H**, **Zhang K**, **Guo X**, **Xu Z**, **Yang W**, **Qi Y**, **Guo CA**, **Hornsby C**, **Zhang L**, **Zhou A**, **Li L**, **Chen Y**, **Zhang W**, **Sun Y**, **Zheng H**, **Wondisford F**, **He L**, **Guo S**. Novel Mechanism of Foxo1 Phosphorylation in Glucagon Signaling in Control of Glucose Homeostasis. *Diabetes* 67: 2167–2182, 2018. doi: 10.2337/db18-0674.

173. **Czech MP**. Insulin action and resistance in obesity and type 2 diabetes. *Nat Med* 23: 804–814, 2017. doi: 10.1038/nm.4350.

174. **Qu S**, **Altomonte J**, **Perdomo G**, **He J**, **Fan Y**, **Kamagate A**, **Meseck M**, **Dong HH**. Aberrant Forkhead box O1 function is associated with impaired hepatic metabolism. *Endocrinology* 147: 5641–5652, 2006. doi: 10.1210/en.2006-0541.

175. **O-Sullivan I**, **Zhang W**, **Wasserman DH**, **Liew CW**, **Liu J**, **Paik J**, **DePinho RA**, **Stolz DB**, **Kahn CR**, **Schwartz MW**, **Unterman TG**. FoxO1 integrates direct and indirect effects of insulin on hepatic glucose production and glucose utilization. *Nat Commun* 6: 1–15, 2015. doi: 10.1038/ncomms8079.

176. **Besse-Patin A**, **Jeromson S**, **Levesque-Damphousse P**, **Secco B**, **Laplante M**, **Estall JL**. PGC1A regulates the IRS1:IRS2 ratio during fasting to influence hepatic metabolism downstream of insulin. *Proc Natl Acad Sci U S A* 116: 4285–4290, 2019. doi: 10.1073/pnas.1815150116.

177. **Besse-Patin A**, **Léveillé M**, **Oropeza D**, **Nguyen BN**, **Prat A**, **Estall JL**. Estrogen Signals Through Peroxisome Proliferator-Activated Receptor-γ Coactivator 1α to Reduce Oxidative Damage Associated With Diet-Induced Fatty Liver Disease. *Gastroenterology* 152: 243–256, 2017. doi: 10.1053/j.gastro.2016.09.017.

178. **Biddinger SB**, **Hernandez-Ono A**, **Rask-Madsen C**, **Haas JT**, **Alemán JO**, **Suzuki R**, **Scapa EF**, **Agarwal C**, **Carey MC**, **Stephanopoulos G**, **Cohen DE**, **King GL**, **Ginsberg HN**, **Kahn CR**. Hepatic Insulin Resistance Is Sufficient to Produce Dyslipidemia and Susceptibility to Atherosclerosis. *Cell Metab* 7: 125–134, 2008. doi: 10.1016/j.cmet.2007.11.013.

179. **Manning BD**, **Toker A**. AKT/PKB Signaling: Navigating the Network. *Cell* 169: 381–405, 2017. doi: 10.1016/j.cell.2017.04.001.

180. **Donnelly KL**, **Smith CI**, **Schwarzenberg SJ**, **Jessurun J**, **Boldt MD**, **Parks EJ**. Sources of fatty acids stored in liver and secreted via lipoproteins in patients with nonalcoholic fatty liver disease. *J Clin Invest* 115: 1343–1351, 2005. doi: 10.1172/JCI23621.

181. **Akhtar DH**, **Iqbal U**, **Vazquez-Montesino LM**, **Dennis BB**, **Ahmed A**. Pathogenesis of Insulin Resistance and Atherogenic Dyslipidemia in Nonalcoholic Fatty Liver Disease. *J Clin Transl Hepatol* 7: 362–370, 2019. doi: 10.14218/JCTH.2019.00028.

182. **Xia JY**, **Holland WL**, **Kusminski CM**, **Sun K**, **Sharma AX**, **Pearson MJ**, **Sifuentes AJ**, **McDonald JG**, **Gordillo R**, **Scherer PE**. Targeted Induction of Ceramide Degradation Leads to Improved Systemic Metabolism and Reduced Hepatic Steatosis. *Cell Metab* 22: 266–278, 2015. doi: 10.1016/j.cmet.2015.06.007.

183. **Jelenik T**, **Kaul K**, **Séquaris G**, **Flögel U**, **Phielix E**, **Kotzka J**, **Knebel B**, **Fahlbusch P**, **Hörbelt T**, **Lehr S**, **Reinbeck AL**, **Müller-Wieland D**, **Esposito I**, **Shulman GI**, **Szendroedi J**, **Roden M**. Mechanisms of Insulin Resistance in Primary and Secondary Nonalcoholic Fatty Liver. *Diabetes* 66: 2241–2253, 2017. doi: 10.2337/db16-1147.

184. **Su Z**, **Nie Y**, **Huang X**, **Zhu Y**, **Feng B**, **Tang L**, **Zheng G**. Mitophagy in Hepatic Insulin Resistance: Therapeutic Potential and Concerns. *Front Pharmacol* 10, 2019. doi: 10.3389/fphar.2019.01193.

185. **Wu W**, **Xu H**, **Wang Z**, **Mao Y**, **Yuan L**, **Luo W**, **Cui Z**, **Cui T**, **Wang XL**, **Shen YH**. PINK1-Parkin-Mediated Mitophagy Protects Mitochondrial Integrity and Prevents Metabolic Stress-Induced Endothelial Injury. *PLoS ONE* 10, 2015. doi: 10.1371/journal.pone.0132499.

186. **Nguyen TN**, **Padman BS**, **Lazarou M**. Deciphering the Molecular Signals of PINK1/Parkin Mitophagy. *Trends Cell Biol* 26: 733–744, 2016. doi: 10.1016/j.tcb.2016.05.008.

187. **Wang H**, **Ni H-M**, **Chao X**, **Ma X**, **Rodriguez YA**, **Chavan H**, **Wang S**, **Krishnamurthy P**, **Dobrowsky R**, **Xu D-X**, **Jaeschke H**, **Ding W-X**. Double deletion of PINK1 and

Parkin impairs hepatic mitophagy and exacerbates acetaminophen-induced liver injury in mice. *Redox Biol* 22: 101148, 2019. doi: 10.1016/j.redox.2019.101148.

188. **Kershaw EE**, **Flier JS**. Adipose tissue as an endocrine organ. *J Clin Endocrinol Metab* 89: 2548–2556, 2004. doi: 10.1210/jc.2004-0395.

189. **Scherer PE**. Adipose Tissue: From Lipid Storage Compartment to Endocrine Organ. *Diabetes* 55: 1537–1545, 2006. doi: 10.2337/db06-0263.

190. **Jung UJ**, **Choi M-S**. Obesity and Its Metabolic Complications: The Role of Adipokines and the Relationship between Obesity, Inflammation, Insulin Resistance, Dyslipidemia and Nonalcoholic Fatty Liver Disease. *Int J Mol Sci* 15: 6184–6223, 2014. doi: 10.3390/ijms15046184.

191. **Perry RJ**, **Camporez J-PG**, **Kursawe R**, **Titchenell PM**, **Zhang D**, **Perry CJ**, **Jurczak MJ**, **Abudukadier A**, **Han MS**, **Zhang X-M**, **Ruan H-B**, **Yang X**, **Caprio S**, **Kaech SM**, **Sul HS**, **Birnbaum MJ**, **Davis RJ**, **Cline GW**, **Petersen KF**, **Shulman GI**. Hepatic Acetyl CoA Links Adipose Tissue Inflammation to Hepatic Insulin Resistance and Type 2 Diabetes. *Cell* 160: 745–758, 2015. doi: 10.1016/j.cell.2015.01.012.

192. **Chadt A**, **Immisch A**, **Wendt C de**, **Springer C**, **Zhou Z**, **Stermann T**, **Holman GD**, **Loffing-Cueni D**, **Loffing J**, **Joost H-G**, **Al-Hasani H**. Deletion of Both Rab-GTPase–Activating Proteins TBC14KO and TBC1D4 in Mice Eliminates Insulin- and AICAR-Stimulated Glucose Transport. Diabetes 2015;64:746–759. *Diabetes* 64: 1492–1492, 2015. doi: 10.2337/db15-er04.

193. **Jaworski K**, **Sarkadi-Nagy E**, **Duncan RE**, **Ahmadian M**, **Sul HS**. Regulation of Triglyceride Metabolism.IV. Hormonal regulation of lipolysis in adipose tissue. *Am J Physiol-Gastrointest Liver Physiol* 293: G1–G4, 2007. doi: 10.1152/ajpgi.00554.2006.

194. **Skurk T**, **Alberti-Huber C**, **Herder C**, **Hauner H**. Relationship between adipocyte size and adipokine expression and secretion. *J Clin Endocrinol Metab* 92: 1023–1033, 2007. doi: 10.1210/jc.2006-1055.

195. **Wu L**, **Derynck R**. Essential role of TGF-beta signaling in glucose-induced cell hypertrophy. *Dev Cell* 17: 35–48, 2009. doi: 10.1016/j.devcel.2009.05.010.

196. **Ghaben AL**, **Scherer PE**. Adipogenesis and metabolic health. *Nat Rev Mol Cell Biol* 20: 242–258, 2019. doi: 10.1038/s41580-018-0093-z.

197. **Soehnlein O**, **Zernecke A**, **Eriksson EE**, **Rothfuchs AG**, **Pham CT**, **Herwald H**, **Bidzhekov K**, **Rottenberg ME**, **Weber C**, **Lindbom L**. Neutrophil secretion products pave the way for inflammatory monocytes. *Blood* 112: 1461–1471, 2008. doi: 10.1182/blood-2008-02-139634.

198. **Kany S**, **Vollrath JT**, **Relja B**. Cytokines in Inflammatory Disease. *Int J Mol Sci* 20, 2019. doi: 10.3390/ijms20236008.

199. **De M**. Potential Role of TNF-alpha in the Pathogenesis of Insulin Resistance and Type 2 Diabetes. *Trends Endocrinol. Metab. TEM* 11 Trends Endocrinol Metab: 2000.

200. **Rui L**, **Aguirre V**, **Kim JK**, **Shulman GI**, **Lee A**, **Corbould A**, **Dunaif A**, **White MF**. Insulin/IGF-1 and TNF-α stimulate phosphorylation of IRS-1 at inhibitory Ser307 via distinct pathways. *J Clin Invest* 107: 181, 2001. doi: 10.1172/JCI10934.

201. **Breznik JA**, **Naidoo A**, **Foley KP**, **Schulz C**, **Lau TC**, **Loukov D**, **Sloboda DM**, **Bowdish DME**, **Schertzer JD**. TNF, but not hyperinsulinemia or hyperglycemia, is a key driver of obesity-induced monocytosis revealing that inflammatory monocytes correlate with insulin in obese male mice. *Physiol Rep* 6, 2018. doi: 10.14814/phy2.13937.

202. **Liu L**, **Feng D**, **Chen G**, **Chen M**, **Zheng Q**, **Song P**, **Ma Q**, **Zhu C**, **Wang R**, **Qi W**, **Huang L**, **Xue P**, **Li B**, **Wang X**, **Jin H**, **Wang J**, **Yang F**, **Liu P**, **Zhu Y**, **Sui S**, **Chen Q**. Mitochondrial outer-membrane protein FUNDC1 mediates hypoxia-induced mitophagy in mammalian cells. *Nat Cell Biol* 14: 177–185, 2012. doi: 10.1038/ncb2422.

203. **Feng Y**, **He D**, **Yao Z**, **Klionsky DJ**. The machinery of macroautophagy. *Cell Res* 24: 24–41, 2014. doi: 10.1038/cr.2013.168.

204. **He C**, **Klionsky DJ**. Regulation mechanisms and signaling pathways of autophagy. *Annu Rev Genet* 43: 67–93, 2009. doi: 10.1146/annurev-genet-102808-114910.

205. **Kroemer G**, **Mariño G**, **Levine B**. Autophagy and the integrated stress response. *Mol Cell* 40: 280–293, 2010. doi: 10.1016/j.molcel.2010.09.023.

206. **Mizushima N**. A brief history of autophagy from cell biology to physiology and disease. *Nat Cell Biol* 20: 521–527, 2018. doi: 10.1038/s41556-018-0092-5.

207. **Mizushima N**, **Levine B**. Autophagy in mammalian development and differentiation. *Nat Cell Biol* 12: 823–830, 2010. doi: 10.1038/ncb0910-823.

208. **Badadani M**. Autophagy Mechanism, Regulation, Functions, and Disorders. *ISRN Cell Biol.* 2012 Hindawi: e927064, 2012.

209. **Yang Z**, **Klionsky DJ**. Eaten alive: a history of macroautophagy. *Nat Cell Biol* 12: 814–822, 2010. doi: 10.1038/ncb0910-814.

210. **Yamamoto S**, **Kuramoto K**, **Wang N**, **Situ X**, **Priyadarshini M**, **Zhang W**, **Cordoba-Chacon J**, **Layden BT**, **He C**. Autophagy Differentially Regulates Insulin Production and Insulin Sensitivity. *Cell Rep* 23: 3286–3299, 2018. doi: 10.1016/j.celrep.2018.05.032.

211. **Rocha M**, **Apostolova N**, **Diaz-Rua R**, **Muntane J**, **Victor VM**. Mitochondria and T2D: Role of Autophagy, ER Stress, and Inflammasome. .

212. **Pattingre S**, **Tassa A**, **Qu X**, **Garuti R**, **Liang XH**, **Mizushima N**, **Packer M**, **Schneider MD**, **Levine B**. Bcl-2 Antiapoptotic Proteins Inhibit Beclin 1-Dependent Autophagy. *Cell* 122: 927–939, 2005. doi: 10.1016/j.cell.2005.07.002.

213. **Jamart C**, **Naslain D**, **Gilson H**, **Francaux M**. Higher activation of autophagy in skeletal muscle of mice during endurance exercise in the fasted state. *Am J Physiol-Endocrinol Metab* 305: E964–E974, 2013. doi: 10.1152/ajpendo.00270.2013.

214. **He C**, **Bassik MC**, **Moresi V**, **Sun K**, **Wei Y**, **Zou Z**, **An Z**, **Loh J**, **Fisher J**, **Sun Q**, **Korsmeyer S**, **Packer M**, **May HI**, **Hill JA**, **Virgin HW**, **Gilpin C**, **Xiao G**, **Bassel-Duby R**, **Scherer PE**, **Levine B**. Exercise-induced BCL2-regulated autophagy is required for muscle glucose homeostasis. *Nature* 481: 511–515, 2012. doi: 10.1038/nature10758.

215. **Palikaras K**, **Lionaki E**, **Tavernarakis N**. Mechanisms of mitophagy in cellular homeostasis, physiology and pathology. *Nat Cell Biol* 20: 1013–1022, 2018. doi: 10.1038/s41556-018-0176-2.

216. **Yu SB**, **Pekkurnaz G**. Mechanisms Orchestrating Mitochondrial Dynamics for Energy Homeostasis. *J Mol Biol* 430: 3922–3941, 2018. doi: 10.1016/j.jmb.2018.07.027.

217. **Westermann B**. Bioenergetic role of mitochondrial fusion and fission. *Biochim Biophys Acta BBA - Bioenerg* 1817: 1833–1838, 2012. doi: 10.1016/j.bbabio.2012.02.033.

218. **Youle RJ**, **Karbowski M**. Mitochondrial fission in apoptosis. *Nat Rev Mol Cell Biol* 6: 657–663, 2005. doi: 10.1038/nrm1697.

219. **Ding W-X**, **Yin X-M**. Mitophagy: mechanisms, pathophysiological roles, and analysis. *Biol Chem* 393: 547–564, 2012. doi: 10.1515/hsz-2012-0119.

220. **Youle RJ**, **Bliek AM van der**. Mitochondrial Fission, Fusion, and Stress. *Science* 337: 1062–1065, 2012. doi: 10.1126/science.1219855.

221. **Lin H-Y**, **Weng S-W**, **Chang Y-H**, **Su Y-J**, **Chang C-M**, **Tsai C-J**, **Shen F-C**, **Chuang J-H**, **Lin T-K**, **Liou C-W**, **Lin C-Y**, **Wang P-W**. The Causal Role of Mitochondrial Dynamics in Regulating Insulin Resistance in Diabetes: Link through Mitochondrial Reactive Oxygen Species. *Oxid. Med. Cell. Longev.* 2018 Hindawi: e7514383, 2018.

222. **Lionetti L**, **Mollica MP**, **Donizzetti I**, **Gifuni G**, **Sica R**, **Pignalosa A**, **Cavaliere G**, **Gaita M**, **Filippo CD**, **Zorzano A**, **Putti R**. High-Lard and High-Fish-Oil Diets Differ in Their Effects on Function and Dynamic Behaviour of Rat Hepatic Mitochondria. *PLOS ONE* 9: e92753, 2014. doi: 10.1371/journal.pone.0092753.

223. **Xia M**, **Zhang Y**, **Jin K**, **Lu Z**, **Zeng Z**, **Xiong W**. Communication between mitochondria and other organelles: a brand-new perspective on mitochondria in cancer. *Cell Biosci* 9: 27, 2019. doi: 10.1186/s13578-019-0289-8.

224. **Tubbs E**, **Chanon S**, **Robert M**, **Bendridi N**, **Bidaux G**, **Chauvin M-A**, **Ji-Cao J**, **Durand C**, **Gauvrit-Ramette D**, **Vidal H**, **Lefai E**, **Rieusset J**. Disruption of Mitochondria-Associated Endoplasmic Reticulum Membrane (MAM) Integrity Contributes to Muscle Insulin Resistance in Mice and Humans. *Diabetes* 67: 636–650, 2018. doi: 10.2337/db17-0316.

225. **Theurey P**, **Rieusset J**. Mitochondria-Associated Membranes Response to Nutrient Availability and Role in Metabolic Diseases. *Trends Endocrinol Metab* 28: 32–45, 2017. doi: 10.1016/j.tem.2016.09.002.

226. **Tubbs E**, **Theurey P**, **Vial G**, **Bendridi N**, **Bravard A**, **Chauvin M-A**, **Ji-Cao J**, **Zoulim F**, **Bartosch B**, **Ovize M**, **Vidal H**, **Rieusset J**. Mitochondria-Associated Endoplasmic Reticulum Membrane (MAM) Integrity Is Required for Insulin Signaling and Is Implicated in Hepatic Insulin Resistance. *Diabetes* 63: 3279–3294, 2014. doi: 10.2337/db13-1751.

227. **Arruda AP**, **Pers BM**, **Parlakgül G**, **Güney E**, **Inouye K**, **Hotamisligil GS**. Chronic enrichment of hepatic endoplasmic reticulum–mitochondria contact leads to mitochondrial dysfunction in obesity. *Nat Med* 20: 1427–1435, 2014. doi: 10.1038/nm.3735.

228. **Taddeo EP**, **Laker RC**, **Breen DS**, **Akhtar YN**, **Kenwood BM**, **Liao JA**, **Zhang M**, **Fazakerley DJ**, **Tomsig JL**, **Harris TE**, **Keller SR**, **Chow JD**, **Lynch KR**, **Chokki M**, **Molkentin JD**, **Turner N**, **James DE**, **Yan Z**, **Hoehn KL**. Opening of the mitochondrial permeability transition pore links mitochondrial dysfunction to insulin resistance in skeletal muscle. *Mol Metab* 3: 124–134, 2014. doi: 10.1016/j.molmet.2013.11.003.

229. **Tsuchiya Y**, **Hatakeyama H**, **Emoto N**, **Wagatsuma F**, **Matsushita S**, **Kanzaki M**. Palmitate-induced Down-regulation of Sortilin and Impaired GLUT4 Trafficking in C2C12 Myotubes. *J Biol Chem* 285: 34371–34381, 2010. doi: 10.1074/jbc.M110.128520.

230. **Rovira-Llopis S**, **Bañuls C**, **Diaz-Morales N**, **Hernandez-Mijares A**, **Rocha M**, **Victor VM**. Mitochondrial dynamics in type 2 diabetes: Pathophysiological implications. *Redox Biol* 11: 637–645, 2017. doi: 10.1016/j.redox.2017.01.013.

231. **Xiao B**, **Goh J-Y**, **Xiao L**, **Xian H**, **Lim K-L**, **Liou Y-C**. Reactive oxygen species trigger Parkin/PINK1 pathway-dependent mitophagy by inducing mitochondrial recruitment of Parkin. *J Biol Chem* 292: 16697–16708, 2017. doi: 10.1074/jbc.M117.787739.

232. **Chan NC**, **Salazar AM**, **Pham AH**, **Sweredoski MJ**, **Kolawa NJ**, **Graham RLJ**, **Hess S**, **Chan DC**. Broad activation of the ubiquitin-proteasome system by Parkin is critical for mitophagy. *Hum Mol Genet* 20: 1726–1737, 2011. doi: 10.1093/hmg/ddr048.

233. **Ordureau A**, **Paulo JA**, **Zhang W**, **Ahfeldt T**, **Zhang J**, **Cohn EF**, **Hou Z**, **Heo J-M**, **Rubin LL**, **Sidhu SS**, **Gygi SP**, **Harper JW**. Dynamics of PARKIN-Dependent Mitochondrial Ubiquitylation in Induced Neurons and Model Systems Revealed by Digital Snapshot Proteomics. *Mol Cell* 70: 211-227.e8, 2018. doi: 10.1016/j.molcel.2018.03.012.

234. **Sarraf SA**, **Raman M**, **Guarani-Pereira V**, **Sowa ME**, **Huttlin EL**, **Gygi SP**, **Harper JW**. Landscape of the PARKIN-dependent ubiquitylome in response to mitochondrial depolarization. *Nature* 496: 372–376, 2013. doi: 10.1038/nature12043.

235. **Bhansali S**, **Bhansali A**, **Walia R**, **Saikia UN**, **Dhawan V**. Alterations in Mitochondrial Oxidative Stress and Mitophagy in Subjects with Prediabetes and Type 2 Diabetes Mellitus. *Front Endocrinol* 8: 347, 2017. doi: 10.3389/fendo.2017.00347.

236. **Gatica D**, **Lahiri V**, **Klionsky DJ**. Cargo recognition and degradation by selective autophagy. *Nat Cell Biol* 20: 233–242, 2018. doi: 10.1038/s41556-018-0037-z.

237. **Fu T**, **Xu Z**, **Liu L**, **Guo Q**, **Wu H**, **Liang X**, **Zhou D**, **Xiao L**, **Liu L**, **Liu Y**, **Zhu M-S**, **Chen Q**, **Gan Z**. Mitophagy Directs Muscle-Adipose Crosstalk to Alleviate Dietary Obesity. *Cell Rep* 23: 1357–1372, 2018. doi: 10.1016/j.celrep.2018.03.127.

238. **Glick D**, **Zhang W**, **Beaton M**, **Marsboom G**, **Gruber M**, **Simon MC**, **Hart J**, **Dorn GW**, **Brady MJ**, **Macleod KF**. BNip3 Regulates Mitochondrial Function and Lipid Metabolism in the Liver. *Mol Cell Biol* 32: 2570–2584, 2012. doi: 10.1128/MCB.00167-12.

239. **Moreira OC**, **Estébanez B**, **Martínez-Florez S**, **de Paz JA**, **Cuevas MJ**, **González-Gallego J**. Mitochondrial Function and Mitophagy in the Elderly: Effects of Exercise. *Oxid Med Cell Longev* 2017, 2017. doi: 10.1155/2017/2012798.

240. **Chao X**, **Wang H**, **Jaeschke H**, **Ding W-X**. Role and mechanisms of autophagy in acetaminophen-induced liver injury. *Liver Int Off J Int Assoc Study Liver* 38: 1363–1374, 2018. doi: 10.1111/liv.13866.

241. **Li W**, **Li Y**, **Siraj S**, **Jin H**, **Fan Y**, **Yang X**, **Huang X**, **Wang X**, **Wang J**, **Liu L**, **Du L**, **Chen Q**. FUN14 Domain-Containing 1-Mediated Mitophagy Suppresses Hepatocarcinogenesis by Inhibition of Inflammasome Activation in Mice. *Hepatol Baltim Md* 69: 604–621, 2019. doi: 10.1002/hep.30191.

242. **Williams JA**, **Ding W-X**. A Mechanistic Review of Mitophagy and Its Role in Protection against Alcoholic Liver Disease. *Biomolecules* 5: 2619–2642, 2015. doi: 10.3390/biom5042619.

243. **Mughal W**, **Nguyen L**, **Pustylnik S**, **da Silva Rosa SC**, **Piotrowski S**, **Chapman D**, **Du M**, **Alli NS**, **Grigull J**, **Halayko AJ**, **Aliani M**, **Topham MK**, **Epand RM**, **Hatch GM**, **Pereira TJ**, **Kereliuk S**, **McDermott JC**, **Rampitsch C**, **Dolinsky VW**, **Gordon JW**. A conserved MADS-box phosphorylation motif regulates differentiation and mitochondrial function in skeletal, cardiac, and smooth muscle cells. *Cell Death Dis* 6: e1944, 2015. doi: 10.1038/cddis.2015.306.

244. **Cory S**, **Adams JM**. The Bcl2 family: regulators of the cellular life-or-death switch | Nature Reviews Cancer. *Nat Rev Cancer* 2: 647–656, 2002. doi: 10.1038/nrc883.

245. **Lomonosova E**, **Chinnadurai G**. BH3-only proteins in apoptosis and beyond: an overview. *Oncogene* 27 Suppl 1: S2-19, 2008. doi: 10.1038/onc.2009.39.

246. **Sato T**, **Irie S**, **Krajewski S**, **Reed JC**. Cloning and sequencing of a cDNA encoding the rat Bcl-2 protein. *Gene* 140: 291–292, 1994. doi: 10.1016/0378-1119(94)90561-4.

247. **Chittenden T**, **Flemington C**, **Houghton AB**, **Ebb RG**, **Gallo GJ**, **Elangovan B**, **Chinnadurai G**, **Lutz RJ**. A conserved domain in Bak, distinct from BH1 and BH2, mediates cell death and protein binding functions. *EMBO J* 14: 5589–5596, 1995.

248. **Boyd JM**, **Gallo GJ**, **Elangovan B**, **Houghton AB**, **Malstrom S**, **Avery BJ**, **Ebb RG**, **Subramanian T**, **Chittenden T**, **Lutz RJ**. Bik, a novel death-inducing protein shares a distinct sequence motif with Bcl-2 family proteins and interacts with viral and cellular survival-promoting proteins. *Oncogene* 11: 1921–1928, 1995.

249. **Goping IS**, **Gross A**, **Lavoie JN**, **Nguyen M**, **Jemmerson R**, **Roth K**, **Korsmeyer SJ**, **Shore GC**. Regulated Targeting of BAX to Mitochondria. *J Cell Biol* 143: 207–215, 1998.

250. **Krajewski S**, **Tanaka S**, **Takayama S**, **Schibler MJ**, **Fenton W**, **Reed JC**. Investigation of the subcellular distribution of the bcl-2 oncoprotein: residence in the nuclear envelope, endoplasmic reticulum, and outer mitochondrial membranes. *Cancer Res* 53: 4701–4714, 1993.

251. **Nguyen M**, **Millar DG**, **Yong VW**, **Korsmeyer SJ**, **Shore GC**. Targeting of Bcl-2 to the mitochondrial outer membrane by a COOH-terminal signal anchor sequence. *J Biol Chem* 268: 25265–25268, 1993.

252. **Huang DC**, **Adams JM**, **Cory S**. The conserved N-terminal BH4 domain of Bcl-2 homologues is essential for inhibition of apoptosis and interaction with CED-4. *EMBO J* 17: 1029–1039, 1998. doi: 10.1093/emboj/17.4.1029.

253. **Shimizu S**, **Konishi A**, **Kodama T**, **Tsujimoto Y**. BH4 domain of antiapoptotic Bcl-2 family members closes voltage-dependent anion channel and inhibits apoptotic mitochondrial changes and cell death. *Proc Natl Acad Sci U S A* 97: 3100–3105, 2000. doi: 10.1073/pnas.97.7.3100.

254. **Sugioka R**, **Shimizu S**, **Funatsu T**, **Tamagawa H**, **Sawa Y**, **Kawakami T**, **Tsujimoto Y**. BH4-domain peptide from Bcl-xL exerts anti-apoptotic activity in vivo. *Oncogene* 22: 8432–8440, 2003. doi: 10.1038/sj.onc.1207180.

255. **Gross A**, **Jockel J**, **Wei MC**, **Korsmeyer SJ**. Enforced dimerization of BAX results in its translocation, mitochondrial dysfunction and apoptosis. *EMBO J* 17: 3878–3885, 1998. doi: 10.1093/emboj/17.14.3878.

256. **Wei MC**, **Lindsten T**, **Mootha VK**, **Weiler S**, **Gross A**, **Ashiya M**, **Thompson CB**, **Korsmeyer SJ**. tBID, a membrane-targeted death ligand, oligomerizes BAK to release cytochrome c. *Genes Dev* 14: 2060–2071, 2000.

257. **Karch Jason**, **Molkentin Jeffery D.** Regulated Necrotic Cell Death. *Circ Res* 116: 1800–1809, 2015. doi: 10.1161/CIRCRESAHA.116.305421.

258. **Youle RJ**, **Strasser A**. The BCL-2 protein family: opposing activities that mediate cell death. *Nat Rev Mol Cell Biol* 9: 47–59, 2008. doi: 10.1038/nrm2308.

259. **O'Neill KL**, **Huang K**, **Zhang J**, **Chen Y**, **Luo X**. Inactivation of prosurvival Bcl-2 proteins activates Bax/Bak through the outer mitochondrial membrane. *Genes Dev* 30: 973–988, 2016. doi: 10.1101/gad.276725.115.

260. **Korsmeyer SJ**, **Wei MC**, **Saito M**, **Weiler S**, **Oh KJ**, **Schlesinger PH**. Pro-apoptotic cascade activates BID, which oligomerizes BAK or BAX into pores that result in the release of cytochrome c. *Cell Death Differ* 7: 1166–1173, 2000. doi: 10.1038/sj.cdd.4400783.

261. **Wolter KG**, **Hsu Y-T**, **Smith CL**, **Nechushtan A**, **Xi X-G**, **Youle RJ**. Movement of Bax from the Cytosol to Mitochondria during Apoptosis. *J Cell Biol* 139: 1281–1292, 1997. doi: 10.1083/jcb.139.5.1281.

262. **O'Neill KL**, **Huang K**, **Zhang J**, **Chen Y**, **Luo X**. Inactivation of prosurvival Bcl-2 proteins activates Bax/Bak through the outer mitochondrial membrane. *Genes Dev* 30: 973–988, 2016. doi: 10.1101/gad.276725.115.

263. **Letai A**, **Bassik MC**, **Walensky LD**, **Sorcinelli MD**, **Weiler S**, **Korsmeyer SJ**. Distinct BH3 domains either sensitize or activate mitochondrial apoptosis, serving as prototype cancer therapeutics. *Cancer Cell* 2: 183–192, 2002. doi: 10.1016/s1535-6108(02)00127-7.

264. **Certo M**, **Del Gaizo Moore V**, **Nishino M**, **Wei G**, **Korsmeyer S**, **Armstrong SA**, **Letai A**. Mitochondria primed by death signals determine cellular addiction to antiapoptotic BCL-2 family members. *Cancer Cell* 9: 351–365, 2006. doi: 10.1016/j.ccr.2006.03.027.

265. **Boyd JM**, **Malstrom S**, **Subramanian T**, **Venkatesh LK**, **Schaeper U**, **Elangovan B**, **D'Sa-Eipper C**, **Chinnadurai G**. Adenovirus E1B 19 kDa and Bcl-2 proteins interact with a common set of cellular proteins. *Cell* 79: 341–351, 1994. doi: 10.1016/0092-8674(94)90202-x.

266. **Chen G**, **Cizeau J**, **Velde CV**, **Park JH**, **Bozek G**, **Bolton J**, **Shi L**, **Dubik D**, **Greenberg A**. Nix and Nip3 Form a Subfamily of Pro-apoptotic Mitochondrial Proteins. *J Biol Chem* 274: 7–10, 1999. doi: 10.1074/jbc.274.1.7.

267. **Zhang J**, **Ney PA**. Mechanisms and Biology of B-Cell Leukemia/Lymphoma 2/Adenovirus E1B Interacting Protein 3 and Nip-Like Protein X. *Antioxid Redox Signal* 14: 1959–1969, 2011. doi: 10.1089/ars.2010.3772.

268. **Imazu T**, **Shimizu S**, **Tagami S**, **Matsushima M**, **Nakamura Y**, **Miki T**, **Okuyama A**, **Tsujimoto Y**. Bcl-2/E1B 19 kDa-interacting protein 3-like protein (Bnip3L) interacts with bcl-2/Bcl-xL and induces apoptosis by altering mitochondrial membrane permeability. *Oncogene* 18: 4523–4529, 1999. doi: 10.1038/sj.onc.1202722.

269. **Ray R**, **Chen G**, **Vande Velde C**, **Cizeau J**, **Park JH**, **Reed JC**, **Gietz RD**, **Greenberg AH**. BNIP3 heterodimerizes with Bcl-2/Bcl-X(L) and induces cell death independent of a Bcl-2 homology 3 (BH3) domain at both mitochondrial and nonmitochondrial sites. *J Biol Chem* 275: 1439–1448, 2000. doi: 10.1074/jbc.275.2.1439.

270. **Novak I**, **Kirkin V**, **McEwan DG**, **Zhang J**, **Wild P**, **Rozenknop A**, **Rogov V**, **Löhr F**, **Popovic D**, **Occhipinti A**, **Reichert AS**, **Terzic J**, **Dötsch V**, **Ney PA**, **Dikic I**. Nix is a selective autophagy receptor for mitochondrial clearance. *EMBO Rep* 11: 45–51, 2010. doi: 10.1038/embor.2009.256.

271. **Zhang J**, **Loyd MR**, **Randall MS**, **Waddell MB**, **Kriwacki RW**, **Ney PA**. A short linear motif in BNIP3L (NIX) mediates mitochondrial clearance in reticulocytes. *Autophagy* 8: 1325–1332, 2012. doi: 10.4161/auto.20764.

272. **Yussman MG**, **Toyokawa T**, **Odley A**, **Lynch RA**, **Wu G**, **Colbert MC**, **Aronow BJ**, **Lorenz JN**, **Dorn GW**. Mitochondrial death protein Nix is induced in cardiac hypertrophy and triggers apoptotic cardiomyopathy. *Nat Med* 8: 725–730, 2002. doi: 10.1038/nm719.

273. **Diwan A**, **Koesters AG**, **Odley AM**, **Pushkaran S**, **Baines CP**, **Spike BT**, **Daria D**, **Jegga AG**, **Geiger H**, **Aronow BJ**, **Molkentin JD**, **Macleod KF**, **Kalfa TA**, **Dorn GW**. Unrestrained erythroblast development in Nix−/− mice reveals a mechanism for apoptotic modulation of erythropoiesis. *Proc Natl Acad Sci* 104: 6794–6799, 2007. doi: 10.1073/pnas.0610666104.

274. **Sandoval H**, **Thiagarajan P**, **Dasgupta SK**, **Schumacher A**, **Prchal JT**, **Chen M**, **Wang J**. Essential role for Nix in autophagic maturation of erythroid cells. *Nature* 454: 232–235, 2008. doi: 10.1038/nature07006.

275. **Gálvez AS**, **Brunskill EW**, **Marreez Y**, **Benner BJ**, **Regula KM**, **Kirschenbaum LA**, **Dorn GW**. Distinct pathways regulate proapoptotic Nix and BNip3 in cardiac stress. *J Biol Chem* 281: 1442–1448, 2006. doi: 10.1074/jbc.M509056200.

276. **Dorn GW**. Mitochondrial pruning by Nix and BNip3: an essential function for cardiac-expressed death factors. *J Cardiovasc Transl Res* 3: 374–383, 2010. doi: 10.1007/s12265-010-9174-x.

277. **Diwan A**, **Wansapura J**, **Syed FM**, **Matkovich SJ**, **Lorenz JN**, **Dorn GW**. Nix-mediated apoptosis links myocardial fibrosis, cardiac remodeling, and hypertrophy decompensation. *Circulation* 117: 396–404, 2008. doi: 10.1161/CIRCULATIONAHA.107.727073.

278. **Warren CFA**, **Wong-Brown MW**, **Bowden NA**. BCL-2 family isoforms in apoptosis and cancer. *Cell Death Dis* 10, 2019. doi: 10.1038/s41419-019-1407-6.

279. **Zhang J**, **Ney PA**. Role of BNIP3 and NIX in cell death, autophagy, and mitophagy. *Cell Death Differ* 16: 939–946, 2009. doi: 10.1038/cdd.2009.16.

280. **Dorn GW**, **Kirshenbaum LA**. Cardiac reanimation: targeting cardiomyocyte death by BNIP3 and NIX/BNIP3L. *Oncogene* 27 Suppl 1: S158-167, 2008. doi: 10.1038/onc.2009.53.

281. **Dorn GW**. Nix Nought Nothing: fairy tale or real deal. *J Mol Cell Cardiol* 51: 497–500, 2011. doi: 10.1016/j.yjmcc.2010.09.011.

282. **Vande Velde C**, **Cizeau J**, **Dubik D**, **Alimonti J**, **Brown T**, **Israels S**, **Hakem R**, **Greenberg AH**. BNIP3 and Genetic Control of Necrosis-Like Cell Death through the Mitochondrial Permeability Transition Pore. *Mol Cell Biol* 20: 5454–5468, 2000.

283. **Chen Y**, **Lewis W**, **Diwan A**, **Cheng EH-Y**, **Matkovich SJ**, **Dorn GW**. Dual autonomous mitochondrial cell death pathways are activated by Nix/BNip3L and induce cardiomyopathy. *Proc Natl Acad Sci U S A* 107: 9035–9042, 2010. doi: 10.1073/pnas.0914013107.

284. **Diwan A**, **Matkovich SJ**, **Yuan Q**, **Zhao W**, **Yatani A**, **Brown JH**, **Molkentin JD**, **Kranias EG**, **Dorn GW**. Endoplasmic reticulum–mitochondria crosstalk in NIX-mediated murine cell death. *J Clin Invest* 119: 203–212, 2009. doi: 10.1172/JCI36445.

285. **Mughal W**, **Martens M**, **Field J**, **Chapman D**, **Huang J**, **Rattan S**, **Hai Y**, **Cheung KG**, **Kereliuk S**, **West AR**, **Cole LK**, **Hatch GM**, **Diehl-Jones W**, **Keijzer R**, **Dolinsky VW**, **Dixon IM**, **Parmacek MS**, **Gordon JW**. Myocardin regulates mitochondrial calcium homeostasis and prevents permeability transition. *Cell Death Differ* 25: 1732–1748, 2018. doi: 10.1038/s41418-018-0073-z.

286. **Schweers RL**, **Zhang J**, **Randall MS**, **Loyd MR**, **Li W**, **Dorsey FC**, **Kundu M**, **Opferman JT**, **Cleveland JL**, **Miller JL**, **Ney PA**. NIX is required for programmed mitochondrial clearance during reticulocyte maturation. *Proc Natl Acad Sci U S A* 104: 19500–19505, 2007. doi: 10.1073/pnas.0708818104.

287. **Mammucari C**, **Milan G**, **Romanello V**, **Masiero E**, **Rudolf R**, **Del Piccolo P**, **Burden SJ**, **Di Lisi R**, **Sandri C**, **Zhao J**, **Goldberg AL**, **Schiaffino S**, **Sandri M**. FoxO3 controls autophagy in skeletal muscle in vivo. *Cell Metab* 6: 458–471, 2007. doi: 10.1016/j.cmet.2007.11.001.

288. **Bakker WJ**, **Blázquez-Domingo M**, **Kolbus A**, **Besooyen J**, **Steinlein P**, **Beug H**, **Coffer PJ**, **Löwenberg B**, **von Lindern M**, **van Dijk TB**. FoxO3a regulates erythroid differentiation and induces BTG1, an activator of protein arginine methyl transferase 1. *J Cell Biol* 164: 175–184, 2004. doi: 10.1083/jcb.200307056.

289. **Marinkovic D**, **Zhang X**, **Yalcin S**, **Luciano JP**, **Brugnara C**, **Huber T**, **Ghaffari S**. Foxo3 is required for the regulation of oxidative stress in erythropoiesis. *J Clin Invest* 117: 2133–2144, 2007. doi: 10.1172/JCI31807.

290. **Rogov VV**, **Suzuki H**, **Marinković M**, **Lang V**, **Kato R**, **Kawasaki M**, **Buljubašić M**, **Šprung M**, **Rogova N**, **Wakatsuki S**, **Hamacher-Brady A**, **Dötsch V**, **Dikic I**, **Brady NR**, **Novak I**. Phosphorylation of the mitochondrial autophagy receptor Nix enhances its interaction with LC3 proteins. *Sci Rep* 7: 1131, 2017. doi: 10.1038/s41598-017-01258-6.

291. **Matsui M**, **Yamamoto A**, **Kuma A**, **Ohsumi Y**, **Mizushima N**. Organelle degradation during the lens and erythroid differentiation is independent of autophagy. *Biochem Biophys Res Commun* 339: 485–489, 2006. doi: 10.1016/j.bbrc.2005.11.044.

292. **Zhang J**, **Randall MS**, **Loyd MR**, **Dorsey FC**, **Kundu M**, **Cleveland JL**, **Ney PA**. Mitochondrial clearance is regulated by Atg7-dependent and -independent mechanisms during reticulocyte maturation. *Blood* 114: 157–164, 2009. doi: 10.1182/blood-2008-04-151639.

293. **Zhang W**, **Ma Q**, **Siraj S**, **Ney PA**, **Liu J**, **Liao X**, **Yuan Y**, **Li W**, **Liu L**, **Chen Q**. Nix-mediated mitophagy regulates platelet activation and life span. *Blood Adv* 3: 2342–2354, 2019. doi: 10.1182/bloodadvances.2019032334.

294. **Ney PA**. Mitochondrial autophagy: Origins, significance, and role of BNIP3 and NIX. *Biochim Biophys Acta* 1853: 2775–2783, 2015. doi: 10.1016/j.bbamcr.2015.02.022.

295. **Stoffers DA**, **Stanojevic V**, **Habener JF**. Insulin promoter factor-1 gene mutation linked to early-onset type 2 diabetes mellitus directs expression of a dominant negative isoprotein. *J Clin Invest* 102: 232–241, 1998. doi: 10.1172/JCI2242.

296. **Macfarlane WM**, **Frayling TM**, **Ellard S**, **Evans JC**, **Allen LI**, **Bulman MP**, **Ayres S**, **Shepherd M**, **Clark P**, **Millward A**, **Demaine A**, **Wilkin T**, **Docherty K**, **Hattersley AT**. Missense mutations in the insulin promoter factor-1 gene predispose to type 2 diabetes. *J Clin Invest* 104: R33-39, 1999. doi: 10.1172/JCI7449.

297. **Fujimoto K**, **Ford EL**, **Tran H**, **Wice BM**, **Crosby SD**, **Dorn GW**, **Polonsky KS**. Loss of Nix in Pdx1-deficient mice prevents apoptotic and necrotic β cell death and diabetes. *J Clin Invest* 120: 4031–4039, 2010. doi: 10.1172/JCI44011.

298. **Humpton TJ**, **Alagesan B**, **DeNicola GM**, **Lu D**, **Yordanov GN**, **Leonhardt CS**, **Yao MA**, **Alagesan P**, **Zaatari MN**, **Park Y**, **Skepper JN**, **Macleod KF**, **Perez-Mancera PA**, **Murphy MP**, **Evan GI**, **Vousden KH**, **Tuveson DA**. Oncogenic Kras induces Nix-mediated mitophagy to promote pancreatic cancer. *Cancer Discov* 9: 1268–1287, 2019. doi: 10.1158/2159-8290.CD-18-1409.

299. **Jung J**, **Zhang Y**, **Celiku O**, **Zhang W**, **Song H**, **Williams BJ**, **Giles AJ**, **Rich JN**, **Abounader R**, **Gilbert MR**, **Park DM**. Mitochondrial NIX Promotes Tumor Survival in the Hypoxic Niche of Glioblastoma. *Cancer Res* 79: 5218–5232, 2019. doi: 10.1158/0008-5472.CAN-19-0198.

300. **Taskén K**, **Aandahl EM**. Localized effects of cAMP mediated by distinct routes of protein kinase A. *Physiol Rev* 84: 137–167, 2004. doi: 10.1152/physrev.00021.2003.

301. **Liggett SB**, **Raymond JR**. Pharmacology and molecular biology of adrenergic receptors. *Baillieres Clin Endocrinol Metab* 7: 279–306, 1993. doi: 10.1016/s0950-351x(05)80178-8.

302. **Soderling SH**, **Beavo JA**. Regulation of cAMP and cGMP signaling: new phosphodiesterases and new functions. *Curr Opin Cell Biol* 12: 174–179, 2000. doi: 10.1016/s0955-0674(99)00073-3.

303. **Sunahara RK**, **Dessauer CW**, **Gilman AG**. Complexity and diversity of mammalian adenylyl cyclases. *Annu Rev Pharmacol Toxicol* 36: 461–480, 1996. doi: 10.1146/annurev.pa.36.040196.002333.

304. **Fischer EH**, **Krebs EG**. Conversion of phosphorylase b to phosphorylase a in muscle extracts. *J Biol Chem* 216: 121–132, 1955.

305. **Skalhegg BS**, **Tasken K**. Specificity in the cAMP/PKA signaling pathway. Differential expression,regulation, and subcellular localization of subunits of PKA. *Front Biosci J Virtual Libr* 5: D678-693, 2000. doi: 10.2741/skalhegg.

306. **Taskén K**, **Skålhegg BS**, **Taskén KA**, **Solberg R**, **Knutsen HK**, **Levy FO**, **Sandberg M**, **Orstavik S**, **Larsen T**, **Johansen AK**, **Vang T**, **Schrader HP**, **Reinton NT**, **Torgersen KM**, **Hansson V**, **Jahnsen T**. Structure, function, and regulation of human cAMP-dependent protein kinases. *Adv Second Messenger Phosphoprotein Res* 31: 191–204, 1997. doi: 10.1016/s1040-7952(97)80019-5.

307. **Winter B**, **Braun T**, **Arnold HH**. cAMP-dependent protein kinase represses myogenic differentiation and the activity of the muscle-specific helix-loop-helix transcription factors Myf-5 and MyoD. *J Biol Chem* 268: 9869–9878, 1993.

308. **Scott JD**, **Stofko RE**, **McDonald JR**, **Comer JD**, **Vitalis EA**, **Mangili JA**. Type II regulatory subunit dimerization determines the subcellular localization of the cAMP-dependent protein kinase. *J Biol Chem* 265: 21561–21566, 1990.

309. **Navegantes LC**, **Resano NM**, **Migliorini RH**, **Kettelhut IC**. Effect of guanethidine-induced adrenergic blockade on the different proteolytic systems in rat skeletal muscle. *Am J Physiol* 277: E883-889, 1999. doi: 10.1152/ajpendo.1999.277.5.E883.

310. **Navegantes LC**, **Resano NM**, **Migliorini RH**, **Kettelhut IC**. Role of adrenoceptors and cAMP on the catecholamine-induced inhibition of proteolysis in rat skeletal muscle. *Am J Physiol Endocrinol Metab* 279: E663-668, 2000. doi: 10.1152/ajpendo.2000.279.3.E663.

311. **Gonçalves DAP**, **Silveira WA**, **Lira EC**, **Graça FA**, **Paula-Gomes S**, **Zanon NM**, **Kettelhut IC**, **Navegantes LCC**. Clenbuterol suppresses proteasomal and lysosomal proteolysis and atrophy-related genes in denervated rat soleus muscles independently of Akt. *Am J Physiol Endocrinol Metab* 302: E123-133, 2012. doi: 10.1152/ajpendo.00188.2011.

312. **Yimlamai T**, **Dodd SL**, **Borst SE**, **Park S**. Clenbuterol induces muscle-specific attenuation of atrophy through effects on the ubiquitin-proteasome pathway. *J Appl Physiol Bethesda Md 1985* 99: 71–80, 2005. doi: 10.1152/japplphysiol.00448.2004.

313. **Gonçalves DAP**, **Lira EC**, **Baviera AM**, **Cao P**, **Zanon NM**, **Arany Z**, **Bedard N**, **Tanksale P**, **Wing SS**, **Lecker SH**, **Kettelhut IC**, **Navegantes LCC**. Mechanisms involved in 3',5'-cyclic adenosine monophosphate-mediated inhibition of the ubiquitin-proteasome system in skeletal muscle. *Endocrinology* 150: 5395–5404, 2009. doi: 10.1210/en.2009-0428.

314. **Kline WO**, **Panaro FJ**, **Yang H**, **Bodine SC**. Rapamycin inhibits the growth and muscle-sparing effects of clenbuterol. *J Appl Physiol Bethesda Md 1985* 102: 740–747, 2007. doi: 10.1152/japplphysiol.00873.2006.

315. **Bodine SC**, **Latres E**, **Baumhueter S**, **Lai VK**, **Nunez L**, **Clarke BA**, **Poueymirou WT**, **Panaro FJ**, **Na E**, **Dharmarajan K**, **Pan ZQ**, **Valenzuela DM**, **DeChiara TM**, **Stitt TN**,

Yancopoulos GD, **Glass DJ**. Identification of ubiquitin ligases required for skeletal muscle atrophy. *Science* 294: 1704–1708, 2001. doi: 10.1126/science.1065874.

316. **Centner T**, **Yano J**, **Kimura E**, **McElhinny AS**, **Pelin K**, **Witt CC**, **Bang ML**, **Trombitas K**, **Granzier H**, **Gregorio CC**, **Sorimachi H**, **Labeit S**. Identification of muscle specific ring finger proteins as potential regulators of the titin kinase domain. *J Mol Biol* 306: 717–726, 2001. doi: 10.1006/jmbi.2001.4448.

317. **Lecker SH**, **Jagoe RT**, **Gilbert A**, **Gomes M**, **Baracos V**, **Bailey J**, **Price SR**, **Mitch WE**, **Goldberg AL**. Multiple types of skeletal muscle atrophy involve a common program of changes in gene expression. *FASEB J Off Publ Fed Am Soc Exp Biol* 18: 39–51, 2004. doi: 10.1096/fj.03-0610com.

318. **Sandri M**, **Sandri C**, **Gilbert A**, **Skurk C**, **Calabria E**, **Picard A**, **Walsh K**, **Schiaffino S**, **Lecker SH**, **Goldberg AL**. Foxo transcription factors induce the atrophy-related ubiquitin ligase atrogin-1 and cause skeletal muscle atrophy. *Cell* 117: 399–412, 2004. doi: 10.1016/s0092-8674(04)00400-3.

319. **Hinkle RT**, **Dolan E**, **Cody DB**, **Bauer MB**, **Isfort RJ**. Phosphodiesterase 4 inhibition reduces skeletal muscle atrophy. *Muscle Nerve* 32: 775–781, 2005. doi: 10.1002/mus.20416.

320. **Berdeaux R**, **Stewart R**. cAMP signaling in skeletal muscle adaptation: hypertrophy, metabolism, and regeneration. *Am J Physiol - Endocrinol Metab* 303: E1–E17, 2012. doi: 10.1152/ajpendo.00555.2011.

321. **Beitzel F**, **Gregorevic P**, **Ryall JG**, **Plant DR**, **Sillence MN**, **Lynch GS**. Beta2-adrenoceptor agonist fenoterol enhances functional repair of regenerating rat skeletal muscle after injury. *J Appl Physiol Bethesda Md 1985* 96: 1385–1392, 2004. doi: 10.1152/japplphysiol.01081.2003.

322. **Harcourt LJ**, **Schertzer JD**, **Ryall JG**, **Lynch GS**. Low dose formoterol administration improves muscle function in dystrophic mdx mice without increasing fatigue. *Neuromuscul Disord NMD* 17: 47–55, 2007. doi: 10.1016/j.nmd.2006.08.012.

323. **Hamamori Y**, **Wu HY**, **Sartorelli V**, **Kedes L**. The basic domain of myogenic basic helix-loop-helix (bHLH) proteins is the novel target for direct inhibition by another bHLH protein, Twist. *Mol Cell Biol* 17: 6563–6573, 1997.

324. **Black BL**, **Olson EN**. Transcriptional control of muscle development by myocyte enhancer factor-2 (MEF2) proteins. *Annu Rev Cell Dev Biol* 14: 167–196, 1998. doi: 10.1146/annurev.cellbio.14.1.167.

325. **Pownall ME**, **Gustafsson MK**, **Emerson CP**. Myogenic regulatory factors and the specification of muscle progenitors in vertebrate embryos. *Annu Rev Cell Dev Biol* 18: 747–783, 2002. doi: 10.1146/annurev.cellbio.18.012502.105758.

326. **Olson EN**. MyoD family: a paradigm for development? *Genes Dev* 4: 1454–1461, 1990. doi: 10.1101/gad.4.9.1454.

327. **Naya FJ**, **Olson E**. MEF2: a transcriptional target for signaling pathways controlling skeletal muscle growth and differentiation. *Curr Opin Cell Biol* 11: 683–688, 1999. doi: 10.1016/s0955-0674(99)00036-8.

328. **Ornatsky OI**, **Andreucci JJ**, **McDermott JC**. A Dominant-Negative Form of Transcription Factor MEF2 Inhibits Myogenesis. *J Biol Chem* 272: 33271–33278, 1997. doi: 10.1074/jbc.272.52.33271.

329. **Du M**, **Perry RLS**, **Nowacki NB**, **Gordon JW**, **Salma J**, **Zhao J**, **Aziz A**, **Chan J**, **Siu KWM**, **McDermott JC**. Protein kinase A represses skeletal myogenesis by targeting myocyte enhancer factor 2D. *Mol Cell Biol* 28: 2952–2970, 2008. doi: 10.1128/MCB.00248-08.

330. **Rababa'h A**, **Singh S**, **Suryavanshi SV**, **Altarabsheh SE**, **Deo SV**, **McConnell BK**. Compartmentalization Role of A-Kinase Anchoring Proteins (AKAPs) in Mediating Protein Kinase A (PKA) Signaling and Cardiomyocyte Hypertrophy. *Int J Mol Sci* 16: 218–229, 2014. doi: 10.3390/ijms16010218.

331. **Gray PC**, **Tibbs VC**, **Catterall WA**, **Murphy BJ**. Identification of a 15-kDa cAMP-dependent protein kinase-anchoring protein associated with skeletal muscle L-type calcium channels. *J Biol Chem* 272: 6297–6302, 1997. doi: 10.1074/jbc.272.10.6297.

332. **McCartney S**, **Little BM**, **Langeberg LK**, **Scott JD**. Cloning and characterization of A-kinase anchor protein 100 (AKAP100). A protein that targets A-kinase to the sarcoplasmic reticulum. *J Biol Chem* 270: 9327–9333, 1995. doi: 10.1074/jbc.270.16.9327.

333. **Lin JW**, **Wyszynski M**, **Madhavan R**, **Sealock R**, **Kim JU**, **Sheng M**. Yotiao, a Novel Protein of Neuromuscular Junction and Brain That Interacts with Specific Splice Variants of NMDA Receptor Subunit NR1. *J Neurosci* 18: 2017–2027, 1998. doi: 10.1523/JNEUROSCI.18-06-02017.1998.

334. **Huang LJ**, **Durick K**, **Weiner JA**, **Chun J**, **Taylor SS**. Identification of a novel protein kinase A anchoring protein that binds both type I and type II regulatory subunits. *J Biol Chem* 272: 8057–8064, 1997. doi: 10.1074/jbc.272.12.8057.

335. **Burns-Hamuro LL**, **Barraclough DM**, **Taylor SS**. Identification and functional analysis of dual-specific A kinase-anchoring protein-2. *Methods Enzymol* 390: 354–374, 2004. doi: 10.1016/S0076-6879(04)90022-5.

336. **Huang LJ**, **Durick K**, **Weiner JA**, **Chun J**, **Taylor SS**. D-AKAP2, a novel protein kinase A anchoring protein with a putative RGS domain. *Proc Natl Acad Sci U S A* 94: 11184–11189, 1997. doi: 10.1073/pnas.94.21.11184.

337. **Reynolds JG**, **McCalmon SA**, **Tomczyk T**, **Naya FJ**. IDENTIFICATION AND MAPPING OF PROTEIN KINASE A BINDING SITES IN THE COSTAMERIC

PROTEIN MYOSPRYN. *Biochim Biophys Acta* 1773: 891–902, 2007. doi: 10.1016/j.bbamcr.2007.04.004.

338. **Röder IV**, **Lissandron V**, **Martin J**, **Petersen Y**, **Di Benedetto G**, **Zaccolo M**, **Rudolf R**. PKA microdomain organisation and cAMP handling in healthy and dystrophic muscle in vivo. *Cell Signal* 21: 819–826, 2009. doi: 10.1016/j.cellsig.2009.01.029.

339. **Reynolds JG**, **McCalmon SA**, **Donaghey JA**, **Naya FJ**. Deregulated protein kinase A signaling and myospryn expression in muscular dystrophy. *J Biol Chem* 283: 8070–8074, 2008. doi: 10.1074/jbc.C700221200.

340. **Bloom TJ**. Cyclic nucleotide phosphodiesterase isozymes expressed in mouse skeletal muscle. *Can J Physiol Pharmacol* 80: 1132–1135, 2002. doi: 10.1139/y02-149.

341. **Omori K**, **Kotera J**. Overview of PDEs and their regulation. *Circ Res* 100: 309–327, 2007. doi: 10.1161/01.RES.0000256354.95791.f1.

342. **Baviera AM**, **Zanon NM**, **Carvalho Navegantes LC**, **Migliorini RH**, **do Carmo Kettelhut I**. Pentoxifylline inhibits Ca2+-dependent and ATP proteasome-dependent proteolysis in skeletal muscle from acutely diabetic rats. *Am J Physiol Endocrinol Metab* 292: E702-708, 2007. doi: 10.1152/ajpendo.00147.2006.

343. **Lira EC**, **Graca FA**, **Goncalves DAP**, **Zanon NM**, **Baviera AM**, **Strindberg L**, **Lönnroth P**, **Migliorini RH**, **Kettelhut IC**, **Navegantes LCC**. Cyclic adenosine monophosphate-phosphodiesterase inhibitors reduce skeletal muscle protein catabolism in septic rats. *Shock Augusta Ga* 27: 687–694, 2007. doi: 10.1097/SHK.0b013e31802e43a6.

344. **Li H**, **Zuo J**, **Tang W**. Phosphodiesterase-4 Inhibitors for the Treatment of Inflammatory Diseases. *Front Pharmacol* 9, 2018. doi: 10.3389/fphar.2018.01048.

345. **Bellinger AM**, **Reiken S**, **Dura M**, **Murphy PW**, **Deng S-X**, **Landry DW**, **Nieman D**, **Lehnart SE**, **Samaru M**, **LaCampagne A**, **Marks AR**. Remodeling of ryanodine receptor complex causes “leaky” channels: a molecular mechanism for decreased exercise capacity. *Proc Natl Acad Sci U S A* 105: 2198–2202, 2008. doi: 10.1073/pnas.0711074105.

346. **Plock N**, **Vollert S**, **Mayer M**, **Hanauer G**, **Lahu G**. Pharmacokinetic/Pharmacodynamic Modeling of the PDE4 Inhibitor TAK-648 in Type 2 Diabetes: Early Translational Approaches for Human Dose Prediction. *Clin Transl Sci* 10: 185–193, 2017. doi: 10.1111/cts.12436.

347. **Muo IM**, **MacDonald SD**, **Madan R**, **Park S-J**, **Gharib AM**, **Martinez PE**, **Walter MF**, **Yang SB**, **Rodante JA**, **Courville AB**, **Walter PJ**, **Cai H**, **Glicksman M**, **Guerrieri GM**, **Ben-Dor RR**, **Ouwerkerk R**, **Mao S**, **Chung JH**. Early effects of roflumilast on insulin sensitivity in adults with prediabetes and overweight/obesity involve age-associated fat mass loss – results of an exploratory study. *Diabetes Metab Syndr Obes Targets Ther* 12: 743–759, 2019. doi: 10.2147/DMSO.S182953.

348. **Jensterle M**, **Kocjan T**, **Janez A**. Phosphodiesterase 4 inhibition as a potential new therapeutic target in obese women with polycystic ovary syndrome. *J Clin Endocrinol Metab* 99: E1476-1481, 2014. doi: 10.1210/jc.2014-1430.

349. **Dietsch GN**, **Dipalma CR**, **Eyre RJ**, **Pham TQ**, **Poole KM**, **Pefaur NB**, **Welch WD**, **Trueblood E**, **Kerns WD**, **Kanaly ST**. Characterization of the inflammatory response to a highly selective PDE4 inhibitor in the rat and the identification of biomarkers that correlate with toxicity. *Toxicol Pathol* 34: 39–51, 2006. doi: 10.1080/01926230500385549.

350. **Kumar N**, **Goldminz AM**, **Kim N**, **Gottlieb AB**. Phosphodiesterase 4-targeted treatments for autoimmune diseases. *BMC Med* 11: 96, 2013. doi: 10.1186/1741-7015-11-96.

351. **Ruas JL**, **White JP**, **Rao RR**, **Kleiner S**, **Brannan KT**, **Harrison BC**, **Greene NP**, **Wu J**, **Estall JL**, **Irving BA**, **Lanza IR**, **Rasbach KA**, **Okutsu M**, **Nair KS**, **Yan Z**, **Leinwand LA**, **Spiegelman BM**. A PGC-1α Isoform Induced by Resistance Training Regulates Skeletal Muscle Hypertrophy. *Cell* 151: 1319–1331, 2012. doi: 10.1016/j.cell.2012.10.050.

352. **Emery PW**, **Rothwell NJ**, **Stock MJ**, **Winter PD**. Chronic effects of beta 2-adrenergic agonists on body composition and protein synthesis in the rat. *Biosci Rep* 4: 83–91, 1984. doi: 10.1007/BF01120827.

353. **Maltin CA**, **Hay SM**, **Delday MI**, **Lobley GE**, **Reeds PJ**. The action of the beta-agonist clenbuterol on protein metabolism in innervated and denervated phasic muscles. *Biochem J* 261: 965–971, 1989. doi: 10.1042/bj2610965.

354. **Maltin CA**, **Hay SM**, **McMillan DN**, **Delday MI**. Tissue specific responses to clenbuterol; temporal changes in protein metabolism of striated muscle and visceral tissues from rats. *Growth Regul* 2: 161–166, 1992.

355. **Benson DW**, **Foley-Nelson T**, **Chance WT**, **Zhang FS**, **James JH**, **Fischer JE**. Decreased myofibrillar protein breakdown following treatment with clenbuterol. *J Surg Res* 50: 1–5, 1991. doi: 10.1016/0022-4804(91)90002-4.

356. **Sato S**, **Shirato K**, **Mitsuhashi R**, **Inoue D**, **Kizaki T**, **Ohno H**, **Tachiyashiki K**, **Imaizumi K**. Intracellular β2-adrenergic receptor signaling specificity in mouse skeletal muscle in response to single-dose β2-agonist clenbuterol treatment and acute exercise. *J Physiol Sci* 63: 211–218, 2013. doi: 10.1007/s12576-013-0253-z.

357. **Samuel VT**, **Liu Z-X**, **Qu X**, **Elder BD**, **Bilz S**, **Befroy D**, **Romanelli AJ**, **Shulman GI**. Mechanism of Hepatic Insulin Resistance in Non-alcoholic Fatty Liver Disease. *J Biol Chem* 279: 32345–32353, 2004. doi: 10.1074/jbc.M313478200.

358. **Goedeke L**, **Perry RJ**, **Shulman GI**. Emerging Pharmacological Targets for the Treatment of Nonalcoholic Fatty Liver Disease, Insulin Resistance, and Type 2 Diabetes. *Annu Rev Pharmacol Toxicol* 59: 65–87, 2019. doi: 10.1146/annurev-pharmtox-010716-104727.

359. **Gordon JW**, **Dolinsky VW**, **Mughal W**, **Gordon GRJ**, **McGavock J**. Targeting skeletal muscle mitochondria to prevent type 2 diabetes in youth. .

360. **Hesselink MKC**, **Schrauwen-Hinderling V**, **Schrauwen P**. Skeletal muscle mitochondria as a target to prevent or treat type 2 diabetes mellitus. *Nat Rev Endocrinol* 12: 633–645, 2016. doi: 10.1038/nrendo.2016.104.

361. **Samuel VT**, **Shulman GI**. The pathogenesis of insulin resistance: integrating signaling pathways and substrate flux. *J Clin Invest* 126: 12–22, 2016. doi: 10.1172/JCI77812.

362. **Erion DM**, **Shulman GI**. Diacylglycerol-mediated insulin resistance. *Nat Med* 16: 400–402, 2010. doi: 10.1038/nm0410-400.

363. **Schenk S**, **Horowitz JF**. Acute exercise increases triglyceride synthesis in skeletal muscle and prevents fatty acid-induced insulin resistance. *J Clin Invest* 117: 1690–1698, 2007. doi: 10.1172/JCI30566.

364. **Yang G**, **Badeanlou L**, **Bielawski J**, **Roberts AJ**, **Hannun YA**, **Samad F**. Central role of ceramide biosynthesis in body weight regulation, energy metabolism, and the metabolic syndrome. *Am J Physiol Endocrinol Metab* 297: E211-224, 2009. doi: 10.1152/ajpendo.91014.2008.

365. **Yu C**, **Chen Y**, **Cline GW**, **Zhang D**, **Zong H**, **Wang Y**, **Bergeron R**, **Kim JK**, **Cushman SW**, **Cooney GJ**, **Atcheson B**, **White MF**, **Kraegen EW**, **Shulman GI**. Mechanism by which fatty acids inhibit insulin activation of insulin receptor substrate-1 (IRS-1)-associated phosphatidylinositol 3-kinase activity in muscle. *J Biol Chem* 277: 50230–50236, 2002. doi: 10.1074/jbc.M200958200.

366. **Itani SI**, **Ruderman NB**, **Schmieder F**, **Boden G**. Lipid-induced insulin resistance in human muscle is associated with changes in diacylglycerol, protein kinase C, and IkappaB-alpha. *Diabetes* 51: 2005–2011, 2002.

367. **Szendroedi J**, **Yoshimura T**, **Phielix E**, **Koliaki C**, **Marcucci M**, **Zhang D**, **Jelenik T**, **Müller J**, **Herder C**, **Nowotny P**, **Shulman GI**, **Roden M**. Role of diacylglycerol activation of PKCθ in lipid-induced muscle insulin resistance in humans. *Proc Natl Acad Sci U S A* 111: 9597–9602, 2014. doi: 10.1073/pnas.1409229111.

368. **Li Y**, **Soos TJ**, **Li X**, **Wu J**, **Degennaro M**, **Sun X**, **Littman DR**, **Birnbaum MJ**, **Polakiewicz RD**. Protein kinase C Theta inhibits insulin signaling by phosphorylating IRS1 at Ser(1101). *J Biol Chem* 279: 45304–45307, 2004. doi: 10.1074/jbc.C400186200.

369. **Saltiel AR**. Insulin Resistance in the Defense against Obesity. *Cell Metab* 15: 798–804, 2012.

370. **Mizushima N**, **Levine B**. Autophagy in mammalian development and differentiation. *Nat Cell Biol* 12: 823–830, 2010. doi: 10.1038/ncb0910-823.

371. **Kroemer G**, **Mariño G**, **Levine B**. Autophagy and the integrated stress response. *Mol Cell* 40: 280–293, 2010. doi: 10.1016/j.molcel.2010.09.023.

372. **Feng Y**, **He D**, **Yao Z**, **Klionsky DJ**. The machinery of macroautophagy. *Cell Res* 24: 24–41, 2014. doi: 10.1038/cr.2013.168.

373. **He C**, **Klionsky DJ**. Regulation Mechanisms and Signaling Pathways of Autophagy. *Annu Rev Genet* 43: 67–93, 2009.

374. **Mizushima N**. A brief history of autophagy from cell biology to physiology and disease. *Nat Cell Biol* 20: 521–527, 2018. doi: 10.1038/s41556-018-0092-5.

375. **He C**, **Bassik MC**, **Moresi V**, **Sun K**, **Wei Y**, **Zou Z**, **An Z**, **Loh J**, **Fisher J**, **Sun Q**, **Korsmeyer S**, **Packer M**, **May HI**, **Hill JA**, **Virgin HW**, **Gilpin C**, **Xiao G**, **Bassel-Duby R**, **Scherer PE**, **Levine B**. Exercise-induced BCL2-regulated autophagy is required for muscle glucose homeostasis. *Nature* 481: 511–515, 2012.

376. **Villa E**, **Marchetti S**, **Ricci J-E**. No Parkin Zone: Mitophagy without Parkin. *Trends Cell Biol* 28: 882–895, 2018. doi: 10.1016/j.tcb.2018.07.004.

377. **Palikaras K**, **Lionaki E**, **Tavernarakis N**. Mechanisms of mitophagy in cellular homeostasis, physiology and pathology. *Nat Cell Biol* 20: 1013–1022, 2018. doi: 10.1038/s41556-018-0176-2.

378. **Liu L**, **Feng D**, **Chen G**, **Chen M**, **Zheng Q**, **Song P**, **Ma Q**, **Zhu C**, **Wang R**, **Qi W**, **Huang L**, **Xue P**, **Li B**, **Wang X**, **Jin H**, **Wang J**, **Yang F**, **Liu P**, **Zhu Y**, **Sui S**, **Chen Q**. Mitochondrial outer-membrane protein FUNDC1 mediates hypoxia-induced mitophagy in mammalian cells. *Nat Cell Biol* 14: 177–185, 2012. doi: 10.1038/ncb2422.

379. **Wu W**, **Lin C**, **Wu K**, **Jiang L**, **Wang X**, **Li W**, **Zhuang H**, **Zhang X**, **Chen H**, **Li S**, **Yang Y**, **Lu Y**, **Wang J**, **Zhu R**, **Zhang L**, **Sui S**, **Tan N**, **Zhao B**, **Zhang J**, **Li L**, **Feng D**. FUNDC1 regulates mitochondrial dynamics at the ER–mitochondrial contact site under hypoxic conditions. *EMBO J* 35: 1368–1384, 2016. doi: 10.15252/embj.201593102.

380. **Eisner V**, **Picard M**, **Hajnóczky G**. Mitochondrial dynamics in adaptive and maladaptive cellular stress responses. *Nat Cell Biol* 20: 755–765, 2018. doi: 10.1038/s41556-018-0133-0.

381. **Jheng H-F**, **Tsai P-J**, **Guo S-M**, **Kuo L-H**, **Chang C-S**, **Su I-J**, **Chang C-R**, **Tsai Y-S**. Mitochondrial fission contributes to mitochondrial dysfunction and insulin resistance in skeletal muscle. *Mol Cell Biol* 32: 309–319, 2012. doi: 10.1128/MCB.05603-11.

382. **Kameoka S**, **Adachi Y**, **Okamoto K**, **Iijima M**, **Sesaki H**. Phosphatidic Acid and Cardiolipin Coordinate Mitochondrial Dynamics. *Trends Cell Biol* 28: 67–76, 2018. doi: 10.1016/j.tcb.2017.08.011.

383. **Adachi Y**, **Iijima M**, **Sesaki H**. An unstructured loop that is critical for interactions of the stalk domain of Drp1 with saturated phosphatidic acid. *Small GTPases* 9: 472–479, 2018. doi: 10.1080/21541248.2017.1321614.

384. **Adachi Y**, **Itoh K**, **Yamada T**, **Cerveny KL**, **Suzuki TL**, **Macdonald P**, **Frohman MA**, **Ramachandran R**, **Iijima M**, **Sesaki H**. Coincident Phosphatidic Acid Interaction Restrains Drp1 in Mitochondrial Division. *Mol Cell* 63: 1034–1043, 2016. doi: 10.1016/j.molcel.2016.08.013.

385. **Hornberger TA**, **Chu WK**, **Mak YW**, **Hsiung JW**, **Huang SA**, **Chien S**. The role of phospholipase D and phosphatidic acid in the mechanical activation of mTOR signaling in skeletal muscle. *Proc Natl Acad Sci U S A* 103: 4741–4746, 2006. doi: 10.1073/pnas.0600678103.

386. **Tremblay F**, **Brûlé S**, **Hee Um S**, **Li Y**, **Masuda K**, **Roden M**, **Sun XJ**, **Krebs M**, **Polakiewicz RD**, **Thomas G**, **Marette A**. Identification of IRS-1 Ser-1101 as a target of S6K1 in nutrient- and obesity-induced insulin resistance. *Proc Natl Acad Sci U S A* 104: 14056–14061, 2007. doi: 10.1073/pnas.0706517104.

387. **Wang EY**, **Biala AK**, **Gordon JW**, **Kirshenbaum LA**. Autophagy in the heart: too much of a good thing? *J Cardiovasc Pharmacol* 60: 110–117, 2012. doi: 10.1097/FJC.0b013e31824cc427.

388. **Mughal W**, **Nguyen L**, **Pustylnik S**, **da Silva Rosa SC**, **Piotrowski S**, **Chapman D**, **Du M**, **Alli NS**, **Grigull J**, **Halayko AJ**, **Aliani M**, **Topham MK**, **Epand RM**, **Hatch GM**, **Pereira TJ**, **Kereliuk S**, **McDermott JC**, **Rampitsch C**, **Dolinsky VW**, **Gordon JW**. A conserved MADS-box phosphorylation motif regulates differentiation and mitochondrial function in skeletal, cardiac, and smooth muscle cells. *Cell Death Dis* 6: e1944, 2015. doi: 10.1038/cddis.2015.306.

389. **Mughal W**, **Martens M**, **Field J**, **Chapman D**, **Huang J**, **Rattan S**, **Hai Y**, **Cheung KG**, **Kereliuk S**, **West AR**, **Cole LK**, **Hatch GM**, **Diehl-Jones W**, **Keijzer R**, **Dolinsky VW**, **Dixon IM**, **Parmacek MS**, **Gordon JW**. Myocardin regulates mitochondrial calcium homeostasis and prevents permeability transition. *Cell Death Differ* 25: 1732–1748, 2018. doi: 10.1038/s41418-018-0073-z.

390. **Wu J**, **Prole DL**, **Shen Y**, **Lin Z**, **Gnanasekaran A**, **Liu Y**, **Chen L**, **Zhou H**, **Chen SRW**, **Usachev YM**, **Taylor CW**, **Campbell RE**. Red fluorescent genetically encoded Ca 2+indicators for use in mitochondria and endoplasmic reticulum. *Biochem J* 464: 13–22, 2014.

391. **Wu J**, **Liu L**, **Matsuda T**, **Zhao Y**, **Rebane A**, **Drobizhev M**, **Chang Y-F**, **Araki S**, **Arai Y**, **March K**, **Hughes TE**, **Sagou K**, **Miyata T**, **Nagai T**, **Li W**, **Campbell RE**. Improved Orange and Red Ca 2+Indicators and Photophysical Considerations for Optogenetic Applications. *ACS Chem Neurosci* 4: 963–972, 2013.

392. **Zhao Y**, **Araki S**, **Wu J**, **Teramoto T**, **Chang YF**, **Nakano M**, **Abdelfattah AS**, **Fujiwara M**, **Ishihara T**, **Nagai T**, **Campbell RE**. An Expanded Palette of Genetically Encoded Ca2+ Indicators. *Sci N Y NY* 333: 1888–1891, 2011.

393. **Cribbs JT**, **Strack S**. Reversible phosphorylation of Drp1 by cyclic AMP-dependent protein kinase and calcineurin regulates mitochondrial fission and cell death. *EMBO Rep* 8: 939–944, 2007. doi: 10.1038/sj.embor.7401062.

394. **Tantama M**, **Hung YP**, **Yellen G**. Imaging intracellular pH in live cells with a genetically encoded red fluorescent protein sensor. *J Am Chem Soc* 133: 10034–10037, 2011. doi: 10.1021/ja202902d.

395. **Violin JD**, **Zhang J**, **Tsien RY**, **Newton AC**. A genetically encoded fluorescent reporter reveals oscillatory phosphorylation by protein kinase C. *J Cell Biol* 161: 899–909, 2003. doi: 10.1083/jcb.200302125.

396. **Chen G**, **Cizeau J**, **Vande Velde C**, **Park JH**, **Bozek G**, **Bolton J**, **Shi L**, **Dubik D**, **Greenberg A**. Nix and Nip3 form a subfamily of pro-apoptotic mitochondrial proteins. *J Biol Chem* 274: 7–10, 1999.

397. **Yussman MG**, **Toyokawa T**, **Odley A**, **Lynch RA**, **Wu G**, **Colbert MC**, **Aronow BJ**, **Lorenz JN**, **Dorn GW**. Mitochondrial death protein Nix is induced in cardiac hypertrophy and triggers apoptotic cardiomyopathy. .

398. **Hsu SY**, **Kaipia A**, **Zhu L**, **Hsueh AJ**. Interference of BAD (Bcl-xL/Bcl-2-associated death promoter)-induced apoptosis in mammalian cells by 14-3-3 isoforms and P11. *Mol Endocrinol Baltim Md* 11: 1858–1867, 1997. doi: 10.1210/mend.11.12.0023.

399. **Konishi Y**, **Lehtinen M**, **Donovan N**, **Bonni A**. Cdc2 phosphorylation of BAD links the cell cycle to the cell death machinery. *Mol Cell* 9: 1005–1016, 2002.

400. **Zha J**, **Harada H**, **Yang E**, **Jockel J**, **Korsmeyer SJ**. Serine Phosphorylation of Death Agonist BAD in Response to Survival Factor Results in Binding to 14-3-3 Not BCL-XL. *Cell* 87: 619–628, 1996. doi: 10.1016/S0092-8674(00)81382-3.

401. **Melser S**, **Chatelain EH**, **Lavie J**, **Mahfouf W**, **Jose C**, **Obre E**, **Goorden S**, **Priault M**, **Elgersma Y**, **Rezvani HR**, **Rossignol R**, **Bénard G**. Rheb regulates mitophagy induced by mitochondrial energetic status. *Cell Metab* 17: 719–730, 2013. doi: 10.1016/j.cmet.2013.03.014.

402. **Favaro G**, **Romanello V**, **Varanita T**, **Andrea Desbats M**, **Morbidoni V**, **Tezze C**, **Albiero M**, **Canato M**, **Gherardi G**, **De Stefani D**, **Mammucari C**, **Blaauw B**, **Boncompagni S**, **Protasi F**, **Reggiani C**, **Scorrano L**, **Salviati L**, **Sandri M**. DRP1-mediated mitochondrial shape controls calcium homeostasis and muscle mass. *Nat Commun* 10: 2576, 2019. doi: 10.1038/s41467-019-10226-9.

403. **Fu T**, **Xu Z**, **Liu L**, **Guo Q**, **Wu H**, **Liang X**, **Zhou D**, **Xiao L**, **Liu L**, **Liu Y**, **Zhu M-S**, **Chen Q**, **Gan Z**. Mitophagy Directs Muscle-Adipose Crosstalk to Alleviate Dietary Obesity. *Cell Rep* 23: 1357–1372, 2018. doi: 10.1016/j.celrep.2018.03.127.

404. **Lampert MA**, **Orogo AM**, **Najor RH**, **Hammerling BC**, **Leon LJ**, **Wang BJ**, **Kim T**, **Sussman MA**, **Gustafsson ÅB**. BNIP3L/NIX and FUNDC1-mediated mitophagy is required for mitochondrial network remodeling during cardiac progenitor cell differentiation. *Autophagy* 15: 1182–1198, 2019. doi: 10.1080/15548627.2019.1580095.

405. **Bujak AL**, **Crane JD**, **Lally JS**, **Ford RJ**, **Kang SJ**, **Rebalka IA**, **Green AE**, **Kemp BE**, **Hawke TJ**, **Schertzer JD**, **Steinberg GR**. AMPK activation of muscle autophagy prevents fasting-induced hypoglycemia and myopathy during aging. *Cell Metab* 21: 883–890, 2015. doi: 10.1016/j.cmet.2015.05.016.

406. **Vollert S**, **Kaessner N**, **Heuser A**, **Hanauer G**, **Dieckmann A**, **Knaack D**, **Kley HP**, **Beume R**, **Weiss-Haljiti C**. The glucose-lowering effects of the PDE4 inhibitors roflumilast and roflumilast-N-oxide in db/db mice. *Diabetologia* 55: 2779–2788, 2012. doi: 10.1007/s00125-012-2632-z.

407. **Fang Y**, **Vilella-Bach M**, **Bachmann R**, **Flanigan A**, **Chen J**. Phosphatidic Acid-Mediated Mitogenic Activation of mTOR Signaling. *Science* 294: 1942–1945, 2001. doi: 10.1126/science.1066015.

408. **Yoon M-S**, **Sun Y**, **Arauz E**, **Jiang Y**, **Chen J**. Phosphatidic acid activates mammalian target of rapamycin complex 1 (mTORC1) kinase by displacing FK506 binding protein 38 (FKBP38) and exerting an allosteric effect. *J Biol Chem* 286: 29568–29574, 2011. doi: 10.1074/jbc.M111.262816.

409. **Bai X**, **Ma D**, **Liu A**, **Shen X**, **Wang QJ**, **Liu Y**, **Jiang Y**. Rheb activates mTOR by antagonizing its endogenous inhibitor, FKBP38. *Science* 318: 977–980, 2007. doi: 10.1126/science.1147379.

410. **Bhujabal Z**, **Birgisdottir ÅB**, **Sjøttem E**, **Brenne HB**, **Øvervatn A**, **Habisov S**, **Kirkin V**, **Lamark T**, **Johansen T**. FKBP8 recruits LC3A to mediate Parkin-independent mitophagy. *EMBO Rep* 18: 947–961, 2017. doi: 10.15252/embr.201643147.

411. **Fei P**, **Wang W**, **Kim S**, **Wang S**, **Burns TF**, **Sax JK**, **Buzzai M**, **Dicker DT**, **McKenna WG**, **Bernhard EJ**, **El-Deiry WS**. Bnip3L is induced by p53 under hypoxia, and its knockdown promotes tumor growth. *Cancer Cell* 6: 597–609, 2004.

412. **Olenych SG**, **Claxton NS**, **Ottenberg GK**, **Davidson MW**. The fluorescent protein color palette. *Curr Protoc Cell Biol* Chapter 21: Unit 21.5, 2007. doi: 10.1002/0471143030.cb2105s36.

413. **Planchon TA**, **Gao L**, **Milkie DE**, **Davidson MW**, **Galbraith JA**, **Galbraith CG**, **Betzig E**. Rapid three-dimensional isotropic imaging of living cells using Bessel beam plane illumination. *Nat Methods* 8: 417–423, 2011. doi: 10.1038/nmeth.1586.

414. **Ding Y**, **Li J**, **Enterina JR**, **Shen Y**, **Zhang I**, **Tewson PH**, **Mo GCH**, **Zhang J**, **Quinn AM**, **Hughes TE**, **Maysinger D**, **Alford SC**, **Zhang Y**, **Campbell RE**. Ratiometric biosensors based on dimerization-dependent fluorescent protein exchange. *Nat Methods* 12: 195–198, 2015. doi: 10.1038/nmeth.3261.

415. **Urano J**, **Sato T**, **Matsuo T**, **Otsubo Y**, **Yamamoto M**, **Tamanoi F**. Point mutations in TOR confer Rheb-independent growth in fission yeast and nutrient-independent mammalian TOR signaling in mammalian cells. *Proc Natl Acad Sci U S A* 104: 3514–3519, 2007. doi: 10.1073/pnas.0608510104.

416. **Field JT**, **Martens MD**, **Mughal W**, **Hai Y**, **Chapman D**, **Hatch GM**, **Ivanco TL**, **Diehl-Jones W**, **Gordon JW**. Misoprostol regulates Bnip3 repression and alternative splicing to control cellular calcium homeostasis during hypoxic stress. *Cell Death Discov* 5: 37, 2018. doi: 10.1038/s41420-018-0104-z.

417. **Pagiatakis C**, **Gordon JW**, **Ehyai S**, **Mcdermott JC**. A Novel RhoA/ROCK-CPI-17-MEF2C Signaling Pathway Regulates Vascular Smooth Muscle Cell Gene Expression. *J Biol Chem* 287: 8361–8370, 2012.

418. **Gordon JW**, **Pagiatakis C**, **Salma J**, **Du M**, **Andreucci JJ**, **Zhao J**, **Hou G**, **Perry RL**, **Dan Q**, **Courtman D**, **Bendeck MP**, **Mcdermott JC**. Protein kinase A-regulated assembly of a MEF2middle dotHDAC4 repressor complex controls c-Jun expression in vascular smooth muscle cells. *J Biol Chem* 284: 19027–19042, 2009.

419. **Alizadeh J**, **Zeki AA**, **Mirzaei N**, **Tewary S**, **Rezaei Moghadam A**, **Glogowska A**, **Nagakannan P**, **Eftekharpour E**, **Wiechec E**, **Gordon JW**, **Xu FY**, **Field JT**, **Yoneda KY**, **Kenyon NJ**, **Hashemi M**, **Hatch GM**, **Hombach-Klonisch S**, **Klonisch T**, **Ghavami S**. Mevalonate Cascade Inhibition by Simvastatin Induces the Intrinsic Apoptosis Pathway via Depletion of Isoprenoids in Tumor Cells. *Sci Rep* 7: 44841, 2017. doi: 10.1038/srep44841.

420. **Emami A**, **Shojaei S**, **da Silva Rosa SC**, **Aghaei M**, **Samiei E**, **Vosoughi AR**, **Kalantari F**, **Kawalec P**, **Thliveris J**, **Sharma P**, **Zeki AA**, **Akbari M**, **Gordon JW**, **Ghavami S**. Mechanisms of simvastatin myotoxicity: The role of autophagy flux inhibition. *Eur J Pharmacol* 862: 172616, 2019. doi: 10.1016/j.ejphar.2019.172616.

421. **Moghadam AR**, **da Silva Rosa SC**, **Samiei E**, **Alizadeh J**, **Field J**, **Kawalec P**, **Thliveris J**, **Akbari M**, **Ghavami S**, **Gordon JW**. Autophagy modulates temozolomide-induced cell death in alveolar Rhabdomyosarcoma cells. *Cell Death Discov* 4: 52, 2018. doi: 10.1038/s41420-018-0115-9.

422. **Pereira TJ**, **Fonseca MA**, **Campbell KE**, **Moyce BL**, **Cole LK**, **Hatch GM**, **Doucette CA**, **Klein J**, **Aliani M**, **Dolinsky VW**. Maternal obesity characterized by gestational diabetes increases the susceptibility of rat offspring to hepatic steatosis via a disrupted liver metabolome. .

423. **Folch J**, **Lees M**, **Sloane Stanley GH**. A simple method for the isolation and purification of total lipides from animal tissues. *J Biol Chem* 226: 497–509, 1957.

424. **Gandhi S**, **Perry CGR**. Mapping the role of mitochondrial DRP1 in skeletal muscle health: is too much and too little a bad thing? *J Physiol* 598: 3539–3540, 2020. doi: 10.1113/JP280316.

425. **Yu T**, **Robotham JL**, **Yoon Y**. Increased production of reactive oxygen species in hyperglycemic conditions requires dynamic change of mitochondrial morphology. *Proc Natl Acad Sci* 103: 2653–2658, 2006. doi: 10.1073/pnas.0511154103.

426. **Roden M**, **Shulman GI**. The integrative biology of type 2 diabetes. *Nature* 576: 51–60, 2019. doi: 10.1038/s41586-019-1797-8.

427. **Zaharia OP**, **Strassburger K**, **Strom A**, **Bönhof GJ**, **Karusheva Y**, **Antoniou S**, **Bódis K**, **Markgraf DF**, **Burkart V**, **Müssig K**, **Hwang J-H**, **Asplund O**, **Groop L**, **Ahlqvist E**, **Seissler J**, **Nawroth P**, **Kopf S**, **Schmid SM**, **Stumvoll M**, **Pfeiffer AFH**, **Kabisch S**, **Tselmin S**, **Häring HU**, **Ziegler D**, **Kuss O**, **Szendroedi J**, **Roden M**, **German Diabetes Study Group**. Risk of diabetes-associated diseases in subgroups of patients with recent-onset diabetes: a 5-year follow-up study. *Lancet Diabetes Endocrinol* 7: 684–694, 2019. doi: 10.1016/S2213-8587(19)30187-1.

428. **Martin BC**, **Warram JH**, **Krolewski AS**, **Bergman RN**, **Soeldner JS**, **Kahn CR**. Role of glucose and insulin resistance in development of type 2 diabetes mellitus: results of a 25-year follow-up study. *Lancet Lond Engl* 340: 925–929, 1992. doi: 10.1016/0140-6736(92)92814-v.

429. **Roy D**, **Perreault M**, **Marette A**. Insulin stimulation of glucose uptake in skeletal muscles and adipose tissues in vivo is NO dependent. *Am J Physiol-Endocrinol Metab* 274: E692–E699, 1998. doi: 10.1152/ajpendo.1998.274.4.E692.

430. **Sylow L**, **Tokarz VL**, **Richter EA**, **Klip A**. The many actions of insulin in skeletal muscle, the paramount tissue determining glycemia. *Cell Metab* 33: 758–780, 2021. doi: 10.1016/j.cmet.2021.03.020.

431. **Rothman DL**, **Magnusson I**, **Cline G**, **Gerard D**, **Kahn CR**, **Shulman RG**, **Shulman GI**. Decreased muscle glucose transport/phosphorylation is an early defect in the pathogenesis of non-insulin-dependent diabetes mellitus. *Proc Natl Acad Sci U S A* 92: 983–987, 1995. doi: 10.1073/pnas.92.4.983.

432. **Cline GW**, **Petersen KF**, **Krssak M**, **Shen J**, **Hundal RS**, **Trajanoski Z**, **Inzucchi S**, **Dresner A**, **Rothman DL**, **Shulman GI**. Impaired glucose transport as a cause of decreased insulin-stimulated muscle glycogen synthesis in type 2 diabetes. *N Engl J Med* 341: 240–246, 1999. doi: 10.1056/NEJM199907223410404.

433. **Mootha VK**, **Lindgren CM**, **Eriksson K-F**, **Subramanian A**, **Sihag S**, **Lehar J**, **Puigserver P**, **Carlsson E**, **Ridderstråle M**, **Laurila E**, **Houstis N**, **Daly MJ**, **Patterson N**, **Mesirov JP**, **Golub TR**, **Tamayo P**, **Spiegelman B**, **Lander ES**, **Hirschhorn JN**, **Altshuler D**, **Groop LC**. PGC-1alpha-responsive genes involved in oxidative phosphorylation are coordinately downregulated in human diabetes. *Nat Genet* 34: 267–273, 2003. doi: 10.1038/ng1180.

434. **Stump CS**, **Short KR**, **Bigelow ML**, **Schimke JM**, **Nair KS**. Effect of insulin on human skeletal muscle mitochondrial ATP production, protein synthesis, and mRNA transcripts. *Proc Natl Acad Sci U S A* 100: 7996–8001, 2003. doi: 10.1073/pnas.1332551100.

435. **Weigert C**, **Hennige AM**, **Brischmann T**, **Beck A**, **Moeschel K**, **Schaüble M**, **Brodbeck K**, **Häring H-U**, **Schleicher ED**, **Lehmann R**. The Phosphorylation of Ser318 of Insulin Receptor Substrate 1 Is Not per se Inhibitory in Skeletal Muscle Cells but Is Necessary to Trigger the Attenuation of the Insulin-stimulated Signal*. *J Biol Chem* 280: 37393–37399, 2005. doi: 10.1074/jbc.M506134200.

436. **Moeschel K**, **Beck A**, **Weigert C**, **Lammers R**, **Kalbacher H**, **Voelter W**, **Schleicher ED**, **Häring H-U**, **Lehmann R**. Protein Kinase C-ζ-induced Phosphorylation of Ser318 in Insulin Receptor Substrate-1 (IRS-1) Attenuates the Interaction with the Insulin Receptor and the Tyrosine Phosphorylation of IRS-1*. *J Biol Chem* 279: 25157–25163, 2004. doi: 10.1074/jbc.M402477200.

437. **Itani SI**, **Ruderman NB**, **Schmieder F**, **Boden G**. Lipid-Induced Insulin Resistance in Human Muscle Is Associated With Changes in Diacylglycerol, Protein Kinase C, and IκB-α. *Diabetes* 51: 2005–2011, 2002. doi: 10.2337/diabetes.51.7.2005.

438. **Schrauwen P**, **Hesselink MKC**. Oxidative Capacity, Lipotoxicity, and Mitochondrial Damage in Type 2 Diabetes. *Diabetes* 53: 1412–1417, 2004. doi: 10.2337/diabetes.53.6.1412.

439. **Simoneau J-A**, **Veerkamp JH**, **Turcotte LP**, **Kelley DE**. Markers of capacity to utilize fatty acids in human skeletal muscle: relation to insulin resistance and obesity and effects of weight loss. *FASEB J* 13: 2051–2060, 1999. doi: 10.1096/fasebj.13.14.2051.

440. **Kelley DE**, **He J**, **Menshikova EV**, **Ritov VB**. Dysfunction of Mitochondria in Human Skeletal Muscle in Type 2 Diabetes. *Diabetes* 51: 2944–2950, 2002. doi: 10.2337/diabetes.51.10.2944.

441. **Sivitz WI**, **Yorek MA**. Mitochondrial Dysfunction in Diabetes: From Molecular Mechanisms to Functional Significance and Therapeutic Opportunities. *Antioxid Redox Signal* 12: 537–577, 2010. doi: 10.1089/ars.2009.2531.

442. **Zechner C**, **Lai L**, **Zechner JF**, **Geng T**, **Yan Z**, **Rumsey JW**, **Collia D**, **Chen Z**, **Wozniak DF**, **Leone TC**, **Kelly DP**. Total skeletal muscle PGC-1 deficiency uncouples mitochondrial derangements from fiber type determination and insulin sensitivity. *Cell Metab* 12: 633–642, 2010. doi: 10.1016/j.cmet.2010.11.008.

443. **Copps KD**, **White MF**. Regulation of insulin sensitivity by serine/threonine phosphorylation of insulin receptor substrate proteins IRS1 and IRS2. *Diabetologia* 55: 2565–2582, 2012. doi: 10.1007/s00125-012-2644-8.

444. **Hornberger TA**, **Chu WK**, **Mak YW**, **Hsiung JW**, **Huang SA**, **Chien S**. The role of phospholipase D and phosphatidic acid in the mechanical activation of mTOR signaling in

skeletal muscle. *Proc Natl Acad Sci* 103: 4741–4746, 2006. doi: 10.1073/pnas.0600678103.

445. **Melser S**, **Chatelain EH**, **Lavie J**, **Mahfouf W**, **Jose C**, **Obre E**, **Goorden S**, **Priault M**, **Elgersma Y**, **Rezvani HR**, **Rossignol R**, **Bénard G**. Rheb regulates mitophagy induced by mitochondrial energetic status. *Cell Metab* 17: 719–730, 2013. doi: 10.1016/j.cmet.2013.03.014.

446. **Huang H**, **Gao Q**, **Peng X**, **Choi S-Y**, **Sarma K**, **Ren H**, **Morris AJ**, **Frohman MA**. piRNA-Associated Germline Nuage Formation and Spermatogenesis Require MitoPLD Profusogenic Mitochondrial-Surface Lipid Signaling. *Dev Cell* 20: 376–387, 2011. doi: 10.1016/j.devcel.2011.01.004.

447. **Cnop M**, **Welsh N**, **Jonas J-C**, **Jörns A**, **Lenzen S**, **Eizirik DL**. Mechanisms of Pancreatic β-Cell Death in Type 1 and Type 2 Diabetes: Many Differences, Few Similarities. *Diabetes* 54: S97–S107, 2005. doi: 10.2337/diabetes.54.suppl_2.S97.

448. **Chandra S**, **Issac T**, **Gayathri N**, **Gupta N**, **Abbas M**. A typical case of myoclonic epilepsy with ragged red fibers (MERRF) and the lessons learned. *J Postgrad Med* 61: 200–202, 2015. doi: 10.4103/0022-3859.150905.

449. **Boston PF**, **Jackson P**, **Thompson RJ**. Human 14-3-3 protein: radioimmunoassay, tissue distribution, and cerebrospinal fluid levels in patients with neurological disorders. *J Neurochem* 38: 1475–1482, 1982. doi: 10.1111/j.1471-4159.1982.tb07928.x.

450. **Rittinger K**, **Budman J**, **Xu J**, **Volinia S**, **Cantley LC**, **Smerdon SJ**, **Gamblin SJ**, **Yaffe MB**. Structural Analysis of 14-3-3 Phosphopeptide Complexes Identifies a Dual Role for the Nuclear Export Signal of 14-3-3 in Ligand Binding. *Mol Cell* 4: 153–166, 1999. doi: 10.1016/S1097-2765(00)80363-9.

451. **Yaffe MB**, **Rittinger K**, **Volinia S**, **Caron PR**, **Aitken A**, **Leffers H**, **Gamblin SJ**, **Smerdon SJ**, **Cantley LC**. The Structural Basis for 14-3-3:Phosphopeptide Binding Specificity. *Cell* 91: 961–971, 1997. doi: 10.1016/S0092-8674(00)80487-0.

452. **Dougherty MK**, **Morrison DK**. Unlocking the code of 14-3-3. *J Cell Sci* 117: 1875–1884, 2004. doi: 10.1242/jcs.01171.

453. **Zha J**, **Harada H**, **Yang E**, **Jockel J**, **Korsmeyer SJ**. Serine Phosphorylation of Death Agonist BAD in Response to Survival Factor Results in Binding to 14-3-3 Not BCL-XL. *Cell* 87: 619–628, 1996. doi: 10.1016/S0092-8674(00)81382-3.

454. **Kilanowska A**, **Ziółkowska A**. Role of Phosphodiesterase in the Biology and Pathology of Diabetes. *Int J Mol Sci* 21: 8244, 2020. doi: 10.3390/ijms21218244.